NTNU
Norwegian University of Science and Technology
Department of Marine Technology

M.Sc.THESIS

Title:	**Delivered:**
Installation of Offshore Wind Turbine	6. June 2011
	Availability:
	Confidential
Student:	**Number of pages:**
Amund Torgersrud & Atle Fossestøl	133

Abstract:

Ingenium AS is developing a new concept for transporting and installing fixed wind turbines, mainly jacket structures. As a part of the installation the jacket is lowered down to the seabed from a free hanging configuration, supported by a hydraulic frame.

This operation is analyzed by use of the computer program Orcaflex, where the structure is modeled as rigid.

Two critical scenarios are identified. In Scenario 1a the jacket is 10 m above seabed. Here, the jacket may collide with the support frame if the motions are sufficiently large. In Scenario 2a, the jacket is 3 m above seabed, and large motions may cause troubles under installation. Both these Scenarios are modeled and investigated by running response analyses in Orcaflex.

The effect of applying a passive heave compensation system is also investigated. Damping characteristics for the system are provided by Ingenium. By these damping characteristics, the heave compensation system is implemented in the Orcaflex models.

Contact between the support frame and the jacket legs may occur if the jacket motions are sufficiently large. The effect of applying a bumper system to reduce the stress in the jacket legs is investigated. This is done by attaching a bumper to the support frame in Scenario 1a, and use different materials with different contact stiffness for the bumper analysis.

All scenarios are run with different environmental conditions. A matrix which defines the different cases for each scenario with respect to load parameters is established. Modal analyses with different line length are performed to see what effect the line length has on the natural frequency of the system.

Keyword:

Ingenium
Wind Farm Installation
Jacket

Advisor:

Bernt J. Leira

Address:
NTNU
Department of Marine Technology
N-7491 Trondheim

Location
Marinteknisk Senter
O. Nielsens vei 10

Tel. +47 73 595501
Fax +47 73 595697

Master thesis, Spring 2011

for

Stud. Techn. Atle Fossestøl and Amund Torgersrud

Installation of Offshore Wind Turbine

Installasjon av Offshore Vindturbin

A particular barge concept for transport and installation of offshore wind-mills has been developed by the company Ingenium during the last year, see the figures below. The objective of the concept is that the installation process can be performed efficiently and at a low cost. Installation during relatively rough weather conditions should also be possible.

One of the critical phases of the operation is during release of the windmill from the barge and the transit to the seabed support frame.

The main objective of the master thesis is to consider the loading and forces that occur during this critical phase. The following input to the analysis will be provided by the company Ingenium: Motion characteristics (RAO) for the barge (for a specific draft), barge dimensions, downwards velocity and lifting height, dimensions and weight of the Jacket foundation, water depth (30m), wave directions and wave conditions (0,15,30 and 45 degrees, Hs=2m and 2.5m, wave periods 4s -12s), current velocity (2 knots) and wind velocity (12m/s)

The following subjects are to be examined in this thesis:

1. Describe the type of loads that will occur, the load modeling and the procedures for response analysis that are to be applied (i.e. static/dynamic, linear/nonlinear, etc.).

2. Critical phases during the installation process are identified. For two of these phases, response analyses are performed by application of the relevant computer program(s). Subsequently, a parameter study is to be performed. A matrix which defines the different cases (with respect to load parameters such as wave height/wave period/current/wind is to be establish based on discussion with the supervisor.

3. Potential other critical phases during the lowering of the jacket are also to be considered. In particular, the possibility that high dynamic amplification of the response may occur is to be focused upon. The natural frequency of the suspended pendulum system will change during the lowering due to varying line length, and the effect of this should be assessed.

4. The effect of applying a passive heave compensation system (PHC) between the lifting unit and the jacket structure is to be investigated. The damping characteristics which are required for this purpose are to be provided by Ingenium

5. Impacts between the jacket and the support frame may occur due to large jacket motions. The effect of applying a bumper system is to be studied.

The work-scope may prove to be larger than initially anticipated. Subject to approval from the supervisor, topics may be deleted from the list above or reduced in extent.

In the thesis the candidate shall present his personal contribution to the resolution of problems within the scope of the thesis work. Theories and conclusions should be based on mathematical derivations and/or logic reasoning identifying the various steps in the deduction. The candidate should utilise the existing possibilities for obtaining relevant literature.

The thesis should be organised in a rational manner to give a clear exposition of results, assessments, and conclusions. The text should be brief and to the point, with a clear language. Telegraphic language should be avoided.

The thesis shall contain the following elements: A text defining the scope, preface, list of contents, summary, main body of thesis, conclusions with recommendations for further work, list of symbols and acronyms, references and (optional) appendices. All figures, tables and equations shall be numerated.

The supervisor may require that the candidate, at an early stage of the work, presents a written plan for the completion of the work. The plan should include a budget for the use of computer and laboratory resources which will be charged to the department. Overruns shall be reported to the supervisor.

The original contribution of the candidate and material taken from other sources shall be clearly defined. Work from other sources shall be properly referenced using an acknowledged referencing system.

The thesis shall be submitted in 3 copies:

- Signed by the candidate
- The text defining the scope included
- In bound volume(s)
- Drawings and/or computer prints which cannot be bound should be organised in a separate folder.

Supervisor(s) : Professor Bernt J. Leira + + + Contact person at Ingenium: Jan Fosso

Start: January 17th, 2011 Deadline: June 14th, 2011

Trondheim, 17 January 2011

Bernt J. Leira

Preface

This is the Master Thesis for Amund Torgersrud and Atle Fossestøl, as a part of the Master of Science study at the Department of Marine Technology at NTNU. The Thesis is limited in time and work amount to correspond one semester (from January 15th to June 14th 2011). It is developed in collaboration with Ingenium AS and deals with a new project called WFIB.

Amund Torgersrud and Atle Fossestøl were given the opportunity to work with this project in their master thesis. To be a part of a new idea and help develop structures not yet realized is both challenging and exciting. Also to be a part of the meetings and conversations at Ingenium during this thesis was much appreciated.

At NTNU we would like to thank our supervisor Professor Bernt J. Leira for his expertise and advice during the master thesis. We never hesitated meeting him when we had problems, due to his open and pleasant approach.

We would also like to thank everybody at Ingenium for allowing us to work there and giving us both advice and help. To work in such a great workplace with so many helpful people made us very committed and dedicated to work. We would especially like to thank Senior Project Engineer Jan Fosso at Ingenium for, even in busy times, always being willing to help and guide us.

X _____
Amund Torgersrud

X _____
Atle Fossestøl

Summary

Ingenium AS is developing a new concept for transporting and installing fixed wind turbines, mainly jacket structures. As a part of the installation the jacket is lowered down to the seabed from a free-hanging configuration, supported by a hydraulic frame.

This operation is analyzed by use of the computer program Orcaflex, where the structure is modeled as rigid. Added mass and drag parameters that need to be specified are calculated according to DNV's recommended practice. The linear hydrodynamic damping is set to zero.

Two critical scenarios are identified. In Scenario 1a the jacket is 10 m above seabed. Here, the jacket may collide with the support frame if the motions are sufficiently large. In Scenario 2a, the jacket is 3 m above seabed, and large motions may cause trouble when installing. Both these Scenarios are modeled and investigated by running response analyses in Orcaflex. The jacket motions for the identified critical scenarios are too large to install. Wires or other systems that can keep the jacket in place are strictly necessary. In Scenario 1a, the jacket does not collide with the frame due to the strong current.

The effect of applying a passive heave compensation system is also investigated. Damping characteristics for the system are provided by Ingenium. By these damping characteristics, the heave compensation system is implemented in the Orcaflex models. Scenarios 1b and 2b are identical to 1a and 2a, the only difference is the heave compensation. Response analyses are performed to compare the results with Scenarios 1a and 2a. The heave compensation does not seem to work properly. This may be due to the low values of tangential drag and added mass as well as the zero hydrodynamic damping and small waterline area.

Contact between the support frame and the jacket legs may occur if the jacket motions are sufficiently large. The effect of applying a bumper system to reduce the stress in the jacket legs is investigated. This is done by attaching a bumper to the support frame in Scenario 1a, and use different materials with different contact stiffness for the bumper analysis. The contact stiffness is found from a simplified approach using Young's modulus. The scenario with a bumper system is called Scenario 3 and is run only for the worst cases from Scenario 1a. Response analyses are performed in Orcaflex and the von Mises stresses in one of the jacket legs are compared for different materials. The most proper stress distribution in the jacket leg was caused by Polypropylene, with E = 100 000 kPa.

All scenarios are run with different environmental conditions. A matrix which defines the different cases for each scenario with respect to load parameters is established. Modal analyses with different line length are performed to see what effect the line length has on the natural frequency of the system. A nearly linear relationship was discovered between the two parameters.

Contents

Figures

Tables

Symbols and Abbreviations

$(AI)_i$	[kg]	Added inertia moment when body fully submerged
$(DM)_i$	[kg]	Instantaneous displaced mass for flow in i-direction
a_r	[m/s^2]	Fluid particle acceleration relative to body
a_{ri}	[m/s^2]	Normal water particle acceleration relative to the body
a_w	[m/s^2]	Fluid particle acceleration relative to seabed
A	[m^2]	Area
A	[m]	Wave amplitude
A	[kg]	Added mass
A_1	[-]	Function for calculation of added mass
A_{330}	[kg]	Added mass for a flat plate
A_O	[m^2]	External cross section area
A_c	[m^2]	Contact area
A_i	[m^2]	Internal cross section area
A_i	[m^2]	Area in i-direction
A_{ji}	[kg]	Added mass for component nr. i,j
A_{kj}	[kg]	Added mass components nr. k,j
A_{mi}	[m^2]	Projected drag area moment for i-direction
A_n	[m]	Wave amplitude for wave component nr. n
A_p	[m^2]	Area of submerged part
b	[-]	Function in the JONSWAP wave spectrum
B_{cr}	[kg/s]	Critical damping
B_i	[kg/s]	Unit damping force in i-direction
B_{kj}	[kg/s]	Damping Force components nr. k,j
c	[N]	Specific damping
C	[m^2/s^2]	Constant in Bernoulli's equation
C	[rad/m]	Effective curvature vector
C	[Nms]	Torsional damping coefficient
C	[kg/s^2]	Stiffness
$\boldsymbol{C}$	[kg/s]	Damping matrix
$C(critical)$	[Nms]	Critical damping value
C_A	[-]	Added mass coefficient
C_D	[-]	Drag coefficient
C_{DS}	[-]	Drag coefficient dependent on surface roughness
C_{Di}	[-]	Drag coefficient in i-direction
C_{Dn}	[-]	Normal drag coefficient
C_{Dn}	[-]	Normal drag coefficient
C_{Dt}	[-]	Tangential drag coefficient
C_M	[-]	Mass coefficient
C_a	[-]	Added mass coefficient
C_a,	[-]	Added mass coefficient
C_{ai}	[-]	Added mass coefficient in i-direction
C_{kj}	[kg/s^2]	Unit damping force component nr. k,j
d	[m]	Penetration depth
d	[m]	Diameter

D	[m]	Diameter
D	[Nm^2]	Bending damping value
D_c	[Nm^2]	Bending critical damping value
e	[-]	Damping coefficient
$e(critical)$	[-]	Critical damping coefficient
$\mathbf{e_j}$	[-]	Unit *vector* s along x-,y-z and z-axis
E	[Pa]	Young's modulus
f		Random function
f	[Hz]	Wave frequency
f_m	[Hz]	Peak frequency in a spectrum
F		Random function
$\boldsymbol{F}$	[N]	Load vector
$F_{am,i}$	[N]	Added mass force in i-direction
$F_{am,k}$	[N]	Added mass force component nr. k
F_{base}	[N]	Base pressure force in drag theory
F_C	[N]	Total current force
$F_{damp,i}$	[N]	Damping force
$F_{damp,k}$	[N]	Linear damping force nr. k
F_{pot}	[N]	Drag force in the flow direction
F_R	[N]	Reaction force
$F_{stiff,k}$	[N]	Stiffness force component nr. k
$\boldsymbol{F_t}$	[N]	Load vector at time step t
F_w	[N]	Wave induced force on a strip
g	[m/s^2]	Acceleration of gravity
h	[m]	Water depth
h	[m]	Height
H_s	[m]	Significant wave height
$\boldsymbol{i}, \boldsymbol{j}, \boldsymbol{k}$	[-]	Unit vectors along the x-,y-and z-axis
I	[m^4]	Second moment of area
I_z	[m^4]	Rotational moment of inertia
J_1'	[-]	First derivative of Bessel function
J_α	[-]	Bessel function of first kind
k	[rad/m]	Wave number
k	[N]	Specified stiffness (tether)
k	[N/m]	Specified stiffness (spring/damper)
k_c	[N/m^3]	Normal contact stiffness
K	[Nm^2]	Torsional stiffness
$\mathbf{K}$	[kg/s^s]	Stiffness matrix
K_C	[-]	Keulegan Carpenter number
l	[m]	Length
L	[m]	Instantaneous length
L	[m]	Length of pendulum
L_0	[m]	Unstretched length
m	[-]	Coefficient based on published data
M	[Nm]	Bending moment
M	[kg]	Mass
$\boldsymbol{M}$	[kg]	Mass matrix

M_c	[Nm]	Moment due to current flow
$\boldsymbol{M_m}$	[Nm]	Munk moment vector
n	[-]	Coefficient based on published data
p	[Pa]	Pressure
P_O	[Pa]	External pressure
P_i	[Pa]	Internal pressure
PW	[-]	Wet portion
Q	[-]	Constant base-pressure coefficient
r	[m]	Cylinder radius
R	[m]	Radius
R_n	[-]	Reynolds number
$\boldsymbol{s}$	[m]	Motion vector of a point
S	[m^{2}s]	Wave spectrum
t	[N]	Tension
t	[s]	Time
t_t	[s]	Time at time step t
t_{t+1}	[s]	Time at time step t+1
T	[s]	Period
T_e	[N]	Effective tension
T_p	[s]	Peak period for a spectrum
T_w	[N]	Wall tension
T_z	[s]	Wave period, zero upcrossing period
T_0	[s]	Eigenperiod
T_{02}	[s]	Eigenperiod of Mode 2
T_{03}	[s]	Eigenperiod of Mode 3
T_{04}	[s]	Eigenperiod of Mode 4
T_{05}	[s]	Eigenperiod of Mode 5
u, v, w	[m/s]	Velocity components in x-,y- and z-direction
u_r	[m/s]	Fluid velocity relative to the body
$\boldsymbol{U}$	[m/s]	Velocity vector for incoming current
U_∞	[m/s]	Incident flow
v_c	[m/s]	Current velocity
$v_{current}$	[m/s]	Current velocity
v_m	[m/s]	Maximum wave velocity
v_{wind}	[m/s]	Wind velocity
V	[m/s]	Wind velocity
$\boldsymbol{V}$	[m/s]	Velocity vector
V_{ri}	[m/s]	Relative fluid velocity in i-direction
V_{rxy}	[m/s]	Relative fluid velocity in the x-y plane
w_{ri}	[rad/s]	Relative fluid angular velocity
$\dot{w}_{ri}$	[rad/s^2]	Angular water particle acceleration relative to the body (error 3.27)
w_{rxy}	[rad/s]	Relative angular velocity in the x-y plane
x, y, z	[m]	Cartesian coordinates
$\boldsymbol{X}$	[m]	Displacement vector
$\dot{\boldsymbol{X}}$	[m/s]	First order derivative of the displacement vector
$\ddot{\boldsymbol{X}}$	[m/s^2]	Second order derivative of the displacement vector

$\boldsymbol{X_t}$	[m]	Displacement at time step t
$\boldsymbol{\dot{X}_t}$	[m/s]	Velocity at time step t
$\boldsymbol{\ddot{X}_t}$	[m/s^2]	Acceleration at time step t
$\boldsymbol{X_{t+1}}$	[m]	Displacement at time step t+1
$\boldsymbol{\dot{X}_{t+1}}$	[m/s]	Velocity at time step t+1
Y_1'		First derivative of Bessel function
Y_α		Bessel function of second kind
$\boldsymbol{z}_k$	[m]	An approximation of $\boldsymbol{\Phi}$
$\boldsymbol{z}_{k+1}$	[m]	A better approximation of $\boldsymbol{\Phi}$
z_{seabed}	[m]	Distance from sea level to seabed

Greek symbols

α	[-]	Spectral energy parameter
α	[rad]	Angle
α	[rad]	Flow angle of attack
α_f	[-]	Algorithmic parameters
α_m	[-]	Algorithmic parameters
α_{wave}	[deg]	Incoming wave direction
β	[rad]	Angle of attack
γ	[-]	Peak enchantment factor in a spectrum
γ	[-]	Algorithmic parameters
Γ	[-]	Gamma function
Δ	[-]	Roughness parameter
Δt	[s]	Time interval
ε	[rad]	Phase Angle
ε	[-]	Strain
ε_n	[rad]	Phase angle for wave component nr. n
ζ	[m]	Wave elevation
$\eta_{1,2,3}$	[m]	Motion component in x-,y-,z-direction
$\eta_{4,5,6}$	[rad]	Angular motion about x-,y- and z-direction
θ	[rad]	Angle
λ	[-]	Expansion factor
λ	[-]	Target bending damping
λ	[-]	Function for added mass calculations
λ_R	[rad^2/s^2]	Rayleigh quotient
μ	[rad^2/s^2]	Shift value for eigenvalue solutions
ν	[-]	Poisson's ratio
ξ	[-]	Percentage of critical damping
π	[-]	The constant 3.14159…
ρ	[kg/m^3]	Density
$\sigma, \sigma_1, \sigma_2$	[-]	Standard deviation, width parameters in the JONSWAP spectrum
τ	[-]	Torque angle
ϕ	[m^2/s]	Velocity potential
$\boldsymbol{\Phi}$	[m]	Matrix of eigenvectors
ϕ_1	[m^2/s]	First order velocity potential

ϕ_2	[m^2/s]	Second order velocity potential
$\boldsymbol{\Phi_n}$	[m]	Vector of n eigenvectors
ω	[rad/s]	Wave frequency
ω	[rad/s]	Eigen frequency
ω_0	[rad/s]	Eigen frequency
ω_{k+1}	[rad/s]	A better approximation of the Eigen frequency
ω_n	[rad/s]	Wave frequency for wave component nr. n

Abbrevations

3D	Three Dimentional
6D	Six Dimentional
DOF	Degrees of Freedom
JONSWAP	Joint North Sea Wave Project
RAO	Response Amplitude Operator
DNV	Det Norske Veritas
SWL	Safe Working Load
KC	Keulegan-Carpenter
CoG	Center of Gravity
WFIB	Wind Farm Installation Barge

1 Introduction

"The Stone Age did not end for lack of stone, and the Oil Age will end long before the world runs out of oil." This is an expression often heard in the energy circles these days. The need of other ways to produce energy is becoming more important. One emerging way of producing energy is by wind turbines. Because of the higher winds out at sea, offshore wind turbines may well be the next big energy source.

In 2009 Ingenium launched a new project called WFIB (Wind Farm Installation Barge). With an increasing market in offshore wind turbines, Ingenium AS wanted to provide a fast and cost efficient way to install wind turbines. What Ingenium offered was doing analysis on the behavior of a jacket being lowered to the seabed from the WFIB. The project is still in an early stage with many exciting and challenging tasks ahead. To analyze the behavior of the jacket during lowering will give important information on how to optimize and perfect the WFIB. To find the critical scenarios and study how the different sea states will influence the operation is both a very important and necessary task. Also the implementation of a passive heave compensation system and bumpers are taken into account.

The analysis is done in Orcaflex. Orcaflex is a non-linear time domain, finite element software program principally used for the static and dynamic modeling of systems used in offshore construction environment. Microsoft Excel and MATLAB are used for calculating different variables to be implemented in Orcaflex. Marine technology literature, professors and employees of Ingenium provide valuable help and guidance.

This Master Thesis will deal with many different scenarios and sea states. The main focus will be to discuss and show results in the most comprehensible way. There will be additional emphasis on the more critical cases. Hopefully this thesis will give valuable information on the WFIB project and the further development.

The chapters are split into Theory, Orcaflex, Methods, Results, Discussion, Conclusion and recommendations for Further Work. In Theory the fundamental theory surrounding all the variables and calculations are considered. The Orcaflex chapter gives a brief introduction to Orcaflex and its features. In Methods the critical scenarios are defined and considered. The modeling of the system, environment, the different loads, tests and studies of the model and analysis are also explained. Further the different results are shown in Results. In Discussion the results are studied with respect to the environmental conditions. Finally a Conclusion is made together with Recommendations for Further work. For referencing and bibliography a numerical referencing system, ISO 690 is used.

2 Theory

2.1 Linear Motions of Rigid Floating Structures

The response of a structure in regular waves may be described with six degrees of freedom (DOF's). These DOF's are displacements along the axes of the 3D coordinate system, and the corresponding rotations. This is illustrated in Figure 1, and the name of the corresponding motions may be found in Table 1.

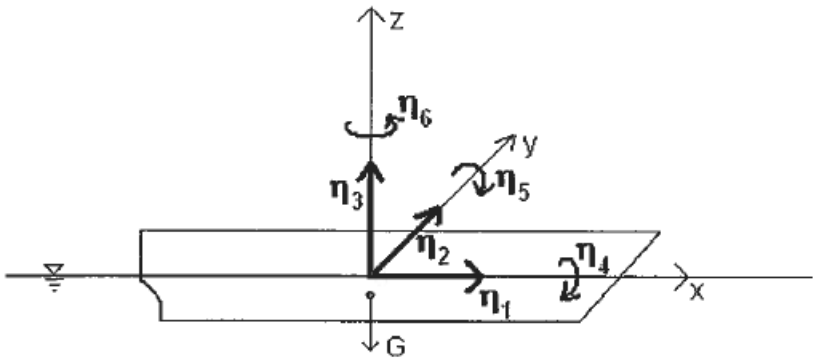

Figure 1 Linear Motions of Rigid Floating Structures

DOF	Name	Description
η_1	Surge	Translation in x-direction
η_2	Sway	Translation in y-direction
η_3	Heave	Translation in z-direction
η_4	Roll	Rotation about x-axis
η_5	Pitch	Rotation about y-axis
η_6	Yaw	Rotation about z-axis

Table 1 Linear Motions of Rigid Floating Structures

The linear motions on any floating rigid body can be described using the following equation:

$$\boldsymbol{s} = (\eta_1 + z\eta_5 - y\eta_6)\boldsymbol{i} + (\eta_2 - z\eta_4 + x\eta_6)\boldsymbol{j} + (\eta_3 + y\eta_4 - x\eta_5)\boldsymbol{k} \tag{2.1}$$

By assuming that the motions of the barge at any DOF can be described harmonically with the equation

$$\eta_i = |\eta_i| \cos(\omega t) \tag{2.2}$$

the motions at any point of the rigid floating structure can be obtained. The equation above will hold as long as the waves are linear and harmonic. (1)

2.2 Wave Theory

2.2.1 Potential Flow

Potential flow is often used to find velocities and accelerations in waves. The sea water is assumed incompressible, inviscid and the fluid is irrotational. The velocity is a vector defined as:

$$\boldsymbol{V}(x,y,z,t) = u(x,y,z,t)\boldsymbol{i} + v(x,y,z,t)\boldsymbol{j} + w(x,y,z,t)\boldsymbol{k} \tag{2.3}$$

where u, v and w are velocity components in x-, y- and z-direction. Mass conservation of a homogenous, incompressible fluid leads to:

$$\nabla \cdot \boldsymbol{V} = 0 \tag{2.4}$$

when having no vorticity:

$$curl\, \boldsymbol{V} = \nabla \times \boldsymbol{V} = 0 \tag{2.5}$$

With vector mathematics it is possible to show that if $\nabla \times \boldsymbol{V} = 0$, then $\boldsymbol{V}$ must be $\boldsymbol{V} = \nabla\phi$, where ϕ is a scalar function. ϕ(x,y,z,t) is the velocity potential. Inserting this into equation (2.4), Laplace equation is obtained:

$$\nabla^2\phi = 0 \tag{2.6}$$

The complete mathematical problem of finding a velocity potential of irrotational, incompressible fluid motion consists of the solution of the Laplace equation with relevant boundary conditions on the fluid.

The pressure p is found by using Bernoulli's equation:

$$p + \rho g z + \rho\frac{\partial\phi}{\partial t} + \frac{\rho}{2}\boldsymbol{V}\cdot\boldsymbol{V} = C \tag{2.7}$$

where ρ is the density, g is gravity, z is the vertical position and C is a constant (when including time dependence of C in the velocity potential). It is assumed that the only external force is gravity, z is the mean free-surface level (z=0) and C can be related to the atmospheric pressure. (1)

To find the velocity potential certain boundary conditions have to be satisfied.

2.2.1.1 Kinematic boundary condition

When following a fluid particle in space, the substantial derivative *DF/Dt* of a function *F(x,y,z,t)* express the rate of change with time of the function F. Mathematically it can be expressed:

$$\frac{DF}{Dt} = \frac{\partial F}{\partial t} + \boldsymbol{V}\cdot\nabla F \tag{2.8}$$

Where $\boldsymbol{V}$ is the fluid velocity at the point *(x,y,z)* at time *t*. The free surface is defined by:

$$z = \zeta(x,y,t) \tag{2.9}$$

where ζ is the wave elevation. The function *F(x,y,z,t)* is defined as:

$$F(x,y,z,t) = z - \zeta(x,y,t) = 0 \tag{2.10}$$

Observations show that a fluid particle on the free-surface always stays on the free-surface. This implies *DF/Dt=0*. Inserting the function *F(x,y,z,t)* into equation (2.8) shows that:

$$\frac{\partial \zeta}{\partial t} + \frac{\partial \phi}{\partial x}\frac{\partial \zeta}{\partial x} + \frac{\partial \phi}{\partial y}\frac{\partial \zeta}{\partial y} - \frac{\partial \phi}{\partial z} = 0 \tag{2.11}$$

on *z=ζ(x,y,t)*. (1)

2.2.1.2 Dynamic free-surface condition

The dynamic free-surface condition is the water pressure being equal to the constant atmospheric pressure p_0 on the free-surface. If $C=p_0/\rho$ Bernoulli's equation yields:

$$g\zeta + \frac{\partial \phi}{\partial t} + \frac{1}{2}\left(\left(\frac{\partial \phi}{\partial x}\right)^2 + \left(\frac{\partial \phi}{\partial y}\right)^2 + \left(\frac{\partial \phi}{\partial z}\right)^2\right) = 0 \tag{2.12}$$

When linearizing both the kinematic and the dynamic conditions with Taylor expansions, the following expressions are obtained. The dynamic condition now follows from the linearized Bernoulli's equation:

$$\frac{\partial \zeta}{\partial t} = \frac{\partial \phi}{\partial z} \; on \; z = 0 \; (kinematic) \tag{2.13}$$

$$g\zeta + \frac{\partial \phi}{\partial t} = 0 \; on \; z = 0 \; (dynamic \; condtion) \tag{2.14}$$

These equations can be combined to get a general free-surface condition:

$$\frac{\partial^2 \phi}{\partial t^2} + g\frac{\partial \phi}{\partial z} = 0 \tag{2.15}$$

If the velocity potential is oscillating harmonically in time with circular frequency ω, it can be written as:

$$\phi = f(z)\sin(kx - \omega t) \tag{2.16}$$

where $f(z)$ is some unknown function, k is the wave number and ω is the wave frequency.

$$-\omega^2\phi + g\frac{\partial \phi}{\partial z} = 0 \tag{2.17}$$

This is the combined free-surface condition. (1)

2.2.1.3 Statistical description of waves

The wave elevation of a long-crested irregular sea propagating along the positive x-axis can be written as the sum of a large number of wave components:

$$\zeta(x,t) = \sum_{n=1}^{N} A_n \cos(\omega_n t - k_n x + \varepsilon_n) \tag{2.18}$$

$$\frac{1}{2}{A_n}^2 = S(\omega_n)\Delta\omega \tag{2.19}$$

Where A_n, ω_n, k_n and ε_n respectively represent the wave amplitude, circular frequency, wave number and random phase angle of wave component *n*. The random phase angle is a number between 0 and 2π. The different amplitudes can be expressed by a wave spectrum, *S(ω)*. (1)

2.2.2 JONSWAP Spectra

JONSWAP (Joint North Sea Wave Project) is the most commonly used spectrum for marine operations in the North Sea. The spectrum is a result of a multinational measuring project in the south-eastern parts of the North Sea. The data is gathered from areas which are relatively shallow and close to land. A plot of the JONSWAP spectrum is presented in Figure 2.

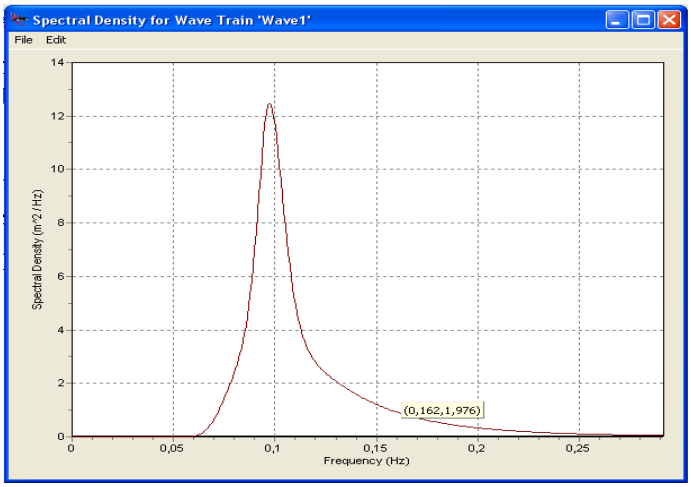

Figure 2 The JONSWAP Spectrum

The formula for the spectrum is:

$$S(f) = \frac{\alpha g^2}{16\pi^4} f^{-5} \exp\left(-\frac{5}{4}\left[\frac{f}{f_m}\right]^{-4}\right)\gamma^b \tag{2.20}$$

where g is the gravitational constant, $b = \exp\left(-\frac{1}{2}\sigma^{-2}\left[\frac{f}{f_m} - 1\right]^2\right)$, $\sigma = \sigma_1$ for $f \leq f_m$, $\sigma = \sigma_2$ for $f > f_m$, and the parameters γ, α, σ_1 and σ_2 are data items. f_m is the peak frequency, γ is the peak enchantment factor, σ_1 and σ_2 are the spectral width parameters, and α is the spectral energy parameter. (2)

Hasselmann with others has specified the following mean values for each of the parameters for the North Sea (2):

$$\bar{\gamma} = 3.3 \tag{2.21}$$

$$\sigma_1 = 0.07 \tag{2.22}$$

$$\sigma_2 = 0.09 \tag{2.23}$$

$$\alpha = 0.076\left(\frac{gx}{V^2}\right)^{-0.22} \tag{2.24}$$

$$f_m = \frac{1}{T_p} = 3.5\pi\left(\frac{g}{V}\right)\left(\frac{gx}{V^2}\right)^{-0.33} \tag{2.25}$$

where x is the free distance above sea level in which the wind travels, V is the wind velocity, T_p is the peak period and f_m the peak frequency.

2.3 Environmental Loads

In addition to the barge motions, the jacket is subjected to environmental loads. A response problem is often considered using linear potential theory. It is then convenient to split the problem into two subproblems, the diffraction- and radiation problems. This may be done since the superposition principle is valid for linear theory. The procedure is illustrated in Figure 3. (1)

The diffraction problem includes the external loads when the structure is restrained against movement. These loads are called excitation loads. The hydrodynamic excitation loads consists of wave induced drag forces and inertia loads. In addition, current and wind loads also need to be considered.

The radiation problem includes the forces generated by the structure when it is forced to oscillate harmonically. In this problem there are no incident waves. The forces generated are due to energy dissipation when the forced body motions generate waves, and consist of added mass, damping and restoring forces.

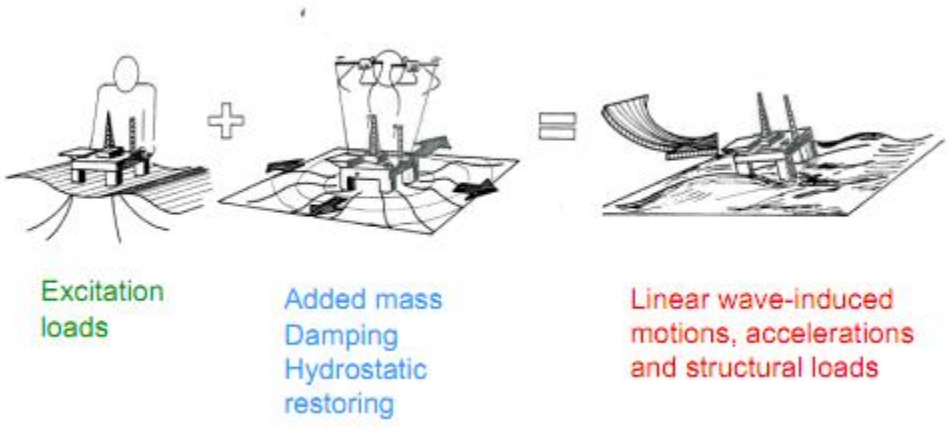

Figure 3 Superposition of Response Problems in Linear Potential Theory

2.3.1 Drag and Inertia Loads

Morison's equation calculates the wave induced force on a strip of a fixed cylinder and is given as follows:

$$dF_w = \rho\pi\frac{D^2}{4}C_M a + \frac{\rho}{2}C_D D|u|u \tag{2.26}$$

where dF_w is the wave force on one strip, ρ is the water density, D is the cylinder diameter, C_M and C_D are the mass and drag coefficients for the cylinder and u and a are the fluid velocity and acceleration respectively. (1)

An extended version of this equation may be used to calculate drag and inertia forces on a moving cylinder strip:

$$dF_w = \rho\pi\frac{D^2}{4}(a_w + C_a a_r) + \frac{\rho}{2}C_D D|u_r|u_r \tag{2.27}$$

Here, F_w is the wave force, C_a is the added mass coefficient for the cylinder. a_w and a_r are fluid particle accelerations relative to the seabed and the body, respectively. u_r is the fluid velocity relative to the body. (3)

The mass force-term now consists of two components. The Froude-Krylov component, proportional to the acceleration relative to the earth, and the added mass component, proportional to the acceleration relative to the body. By comparing this with the first equation, it is seen that C_M = 1 + C_a when the cylinder is fixed. This is the definition of the mass coefficient according to DNV's recommended practice (4).

2.3.2 Added Mass and Damping

The added mass force is from Faltinsen (1) given by:

$$F_{am,k} = -A_{kj}\frac{d^2\eta_j}{dt^2} \qquad k = 1{:}6, \qquad j = 1{:}6 \tag{2.28}$$

where $F_{am,k}$ is the added mass force in direction k, and η_j is the displacement or rotation of the body in direction j, with index notations as described in Table 1. A_{kj} is the added mass that causes a force in direction k, due to a displacement in direction j. For k = 1:3, $F_{am,k}$ are given as a force. For k = 4:6, $F_{am,k}$ represents a moment. Note that the dimensions of A_{kj} not always are given in [kg]. The minus sign indicates that the force is working in the opposite direction of the motion of the cylinder.

The hydrodynamic linear damping force is proportional to the velocity of the body motion, and is given by:

$$F_{damp,k} = -B_{kj}\frac{d\eta_j}{dt} \qquad k = 1{:}6, \qquad j = 1{:}6 \tag{2.29}$$

B_{kj} is the damping force when the velocity of the moving object equals 1. The index notations correspond to those given in Table 1. The minus sign indicates that the force is acting in the opposite direction of the cylinder motion. (1)

2.3.3 Restoring Forces

For a freely floating body, restoring forces will follow from hydrostatic- and mass considerations. These forces are due to change in buoyancy when the body undergoes translational and rotational displacements, and are given by the following equation:

$$F_{stiff,k} = -C_{kj}\eta_j \qquad k = 1{:}6, \qquad j = 1{:}6 \tag{2.30}$$

where $F_{stiff,k}$ is the stiffness force or moment acting in the opposite direction of the motion and C_{kj} is the restoring coefficient. For bodies with submerged volume that is symmetrical about the x-z plane, the only nonzero coefficients, C_{kj}, are for heave, roll and pitch. (1)

2.3.4 Current and Wind Loads

It is difficult to predict current and wind loads with sufficient accuracy, especially for 3-dimensional and turbulent incoming flow. Turbulence often occurs when interaction is present, that is for structures near the sea surface or structures in wake of other structures, which indeed are present for jackets. This chapter will briefly discuss the main current loads of slender structures. Wind loads may be estimated in the same manner as current loads for constant incoming velocity.

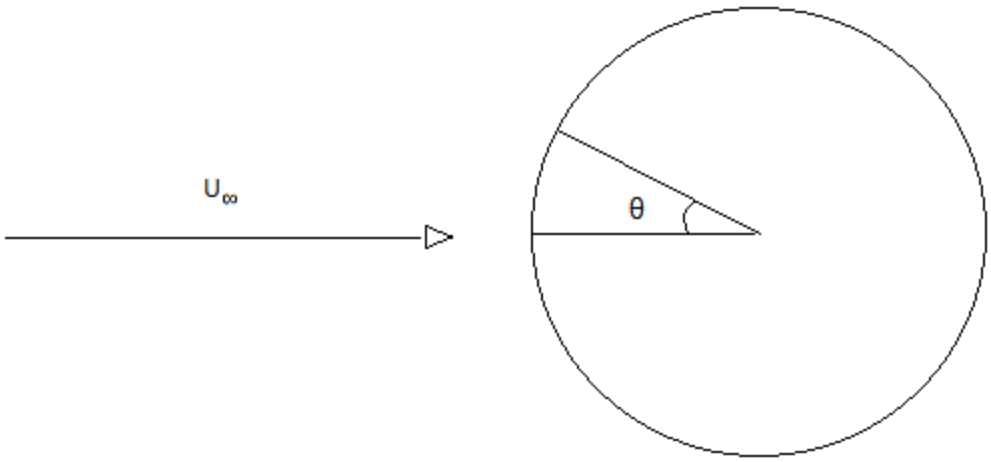

Figure 4 Circular Cylinder Subjected to Steady Flow

Figure 4 shows a circular cylinder subjected to steady incident flow. The major contribution to current forces comes from the changing pressure field around the cylinder. Shear forces are small compared to the pressure forces and may be neglected. (1)

Integrating the pressure forces over the field using non-separated potential theory, results in a drag force in the flow direction:

$$F_{pot} = \frac{1}{2}\rho {U_\infty}^2 \int_{-\pi/2}^{\pi/2} (1 - 4\,sin^2\theta)\cos(\theta)\, R d\theta \tag{2.31}$$

However, the average pressure distribution around a circular cylinder is strongly dependent on Reynolds number, Rn, due to viscous effects. To account for this, an additional term needs to be added to F_{pot} to get the total current force, F_C :

$$F_{base} = \frac{1}{2}\rho {U_\infty}^2 \int_{\frac{\pi}{2}}^{\frac{3\pi}{2}} Q\cos(\theta)\, R d\theta \tag{2.32}$$

where Q is a constant base-pressure coefficient. This gives the drag coefficient:

$$C_D = \frac{F_C}{\frac{1}{2}\rho {U_\infty}^2 D} = -(Q + \frac{1}{3}) \tag{2.33}$$

The total viscous drag force on the cylinder may then be calculated by:

$$F_c = \tfrac{1}{2}\, \rho {U_\infty}^2 \int_L C_D\ D\ dx\ \text{sinβ}|\text{sinβ}| \tag{2.34}$$

where β is the attack angle of the incoming velocity. The corresponding moment due to current flow, may be found by:

$$M_c = \frac{1}{2}\, \rho {U_\infty}^2 \int_L C_D\ D\ x dx\ \text{sinβ}|\text{sinβ}| \tag{2.35}$$

which would be zero for a circular cylinder subjected to transverse flow.

Slender bodies in near axial flow experience a destablishing moment called the Munk moment, different from the viscous drag moment. This should be added to the moment in Equation (2.35). The Munk moment may be derived from non-separated potential theory, and is given by:

$$\boldsymbol{M_m} = -\boldsymbol{U} \times [\sum_{i=1}^{3} U_i [\sum_{i=1}^{3} A_{ji} \mathbf{e_j}]] \tag{2.36}$$

where $\mathbf{e_j}$ are unit vectors unit vectors along x-, y- and z-axis, A_{ji} are the added mass and $\boldsymbol{U}$ is the velocity vector for incoming current. (1)

2.3.5 Forces from Second Order Effects

By using linear potential wave theory as described in chapter 2.2.1, the excitation forces obtained from pressure integration will be linear and oscillate with the frequency of the incident wave hitting the structure. However, if a second order velocity potential is used, the forces obtained from the pressure integration may oscillate with different frequencies than the incident wave frequency. This will of course affect the response of the structure.

Consider now, two incident wave components with amplitudes ζ_{a1} and ζ_{a2} and frequencies ω_1 and ω_2 of a sea state with spectrum $S(\omega)$. The second order velocity potential accurate to the second order for the two waves according to Faltinsen (1) is:

$$\phi = \phi_1 + \phi_2 = \phi_1{}^{(1)}(\omega_1) + \phi_1{}^{(2)}(\omega_2) + \phi_2(\omega_1, \omega_2) \tag{2.37}$$

where ${\phi_1}^{(1)}$ and ${\phi_1}^{(2)}$ are the first order velocity potentials for wave 1 and 2 respectively. ϕ_2 is the second order velocity potential involving a combined effect from the two incident waves. Bernoulli's equation gives the second order pressure distribution:

$$p = -\rho g z - \rho \frac{\partial \phi_1}{\partial t} - \rho \frac{\partial \phi_2}{\partial t} - \rho \frac{1}{2} \nabla \phi_1 \cdot \nabla \phi_1 \tag{2.38}$$

To investigate the features of the last second order term, the velocity component in x-direction is squared at x=0:

$$\left. \frac{\partial \phi_1}{\partial x} \right|_{x=0} = A_1 \cos(\omega_1 t + \varepsilon_1) + A_2 \cos(\omega_2 t + \varepsilon_2) \tag{2.39}$$

$$\begin{aligned} \left(\left. \frac{\partial \phi_1}{\partial x} \right|_{x=0} \right)^2 = & \frac{1}{2}({A_1}^2 + {A_2}^2) + \frac{1}{2}{A_1}^2 \cos[2(\omega_1 t + \varepsilon_1)] \\ & + \frac{1}{2}{A_2}^2 \cos[2(\omega_2 t + \varepsilon_2)] \\ & + A_1 A_2 \cos[(\omega_1 + \omega_2)t + \varepsilon_1 + \varepsilon_2] \\ & + A_1 A_2 \cos[(\omega_1 - \omega_2)t + \varepsilon_1 - \varepsilon_2] \end{aligned} \tag{2.40}$$

From Equation (2.40), one can see that the first order wave potential will cause forces that will oscillate with frequencies $\omega_1 + \omega_2$ and $\omega_1 - \omega_2$, as well as a constant mean force term when considering second order potential theory. These forces are in addition to the forces derived from the first order potential theory, and may be divided into (1):

- Mean force – a constant drift force independent on the frequencies
- Slow drift force – oscillates with a difference wave frequency, $\omega_1 - \omega_2$
- Sum frequency force – oscillates with a sum wave frequency, $\omega_1 + \omega_2$

2.4 Analysis Theory

When performing a dynamic response analysis of a multi DOF system, the equation of motion has to be solved. The equation of motion is obtained from Newton's 2nd law:

$$\boldsymbol{M\ddot{X} + C\dot{X} + KX = F} \tag{2.41}$$

Here, $\boldsymbol{M}$ is the mass matrix, $\boldsymbol{C}$ is the damping matrix and $\mathbf{K}$ is the stiffness matrix of the system. $\boldsymbol{X}$ is the displacement vector, and $\dot{\boldsymbol{X}}$ and $\ddot{\boldsymbol{X}}$ are the first and second order derivatives of the displacements, respectively. $\boldsymbol{F}$ is the load vector containing the external loads working on the system for each DOF.

This chapter gives a brief description of the methods used for analysis.

2.4.1 Time Domain Solutions

Different methods may be used to solve the dynamic equilibrium equation in the time domain. Two common principles that are widely used are numerical differentiation or numerical integration. Many methods are based on one of these principles. Two methods of numerical integration are briefly described below.

2.4.1.1 Explicit Integration using Forward Euler Method

The explicit integration schemes solve for the motions with a constant time step. The basis of the Forward Euler Method is to describe the displacements and velocities by a Taylor expansion using velocities and accelerations at the beginning of the time step, Δt, and neglecting higher order terms:

$$\boldsymbol{X_{t+1} = X_t + \dot{X}_t \Delta t} \tag{2.42}$$

$$\boldsymbol{\dot{X}_{t+1} = \dot{X}_t + \ddot{X}_t \Delta t} \tag{2.43}$$

The acceleration needs to be calculated at the beginning of each time step using the equation of motion. We then get the following expression for the acceleration:

$$\boldsymbol{\ddot{X}_t = \frac{F_t - C\dot{X}_t - KX_t}{M}} \tag{2.44}$$

These equations may then be solved explicitly with respect to the displacements, and the process may be repeated for each time step. (5)

2.4.1.2 Implicit Integration using The Generalized α-method

The principle for the implicit integration scheme is the same as for the explicit scheme, but here the velocities and accelerations are solved for at the end of each time step. There are many different methods for implicit integration, but here the generalized α-method is described. The basic form of this method is given by (6):

$$\boldsymbol{X_{t+1} = X_t + \dot{X}_t \Delta t + (\left(\frac{1}{2} - \beta\right)\ddot{X}_t + \beta \ddot{X}_{t+1})\Delta t^2} \tag{2.45}$$

$$\dot{\boldsymbol{X}}_{\boldsymbol{t+1}} = \dot{\boldsymbol{X}}_{\boldsymbol{t}} + \Delta t\left((1-\gamma)\ddot{\boldsymbol{X}}_{\boldsymbol{t}} + \boldsymbol{\gamma}\ddot{\boldsymbol{X}}_{\boldsymbol{t+1}}\right) \tag{2.46}$$

$$\boldsymbol{M}\ddot{\boldsymbol{X}}_{\boldsymbol{t+1-\alpha_m}} + \boldsymbol{C}\dot{\boldsymbol{X}}_{\boldsymbol{t+1-\alpha_f}} + \boldsymbol{K}\boldsymbol{X}_{\boldsymbol{t+1-\alpha_f}} = \boldsymbol{F}(t_{t+1-\alpha_f}) \tag{2.47}$$

where

$$\boldsymbol{X}_{\boldsymbol{t+1-\alpha_f}} = (1-\alpha_f)\boldsymbol{X}_{\boldsymbol{t+1}} + \alpha_f \boldsymbol{X}_{\boldsymbol{t}} \tag{2.48}$$

$$\dot{\boldsymbol{X}}_{\boldsymbol{t+1-\alpha_f}} = (1-\alpha_f)\dot{\boldsymbol{X}}_{\boldsymbol{t+1}} + \alpha_f \dot{\boldsymbol{X}}_{\boldsymbol{t}} \tag{2.49}$$

$$\ddot{\boldsymbol{X}}_{\boldsymbol{t+1-\alpha_m}} = (1-\alpha_m)\ddot{\boldsymbol{X}}_{\boldsymbol{t+1}} + \alpha_m \ddot{\boldsymbol{X}}_{\boldsymbol{t}} \tag{2.50}$$

$$t_{t+1-\alpha_f} = (1-\alpha_f)t_{t+1} + \alpha_f t_t \tag{2.51}$$

Here, α_f, α_m, β, and γ are algorithmic parameters. These equations give the motions at each time step implicitly. Since the parameters $\boldsymbol{X}_{\boldsymbol{t+1}}$ and $\dot{\boldsymbol{X}}_{\boldsymbol{t+1}}$ are unknown at the end of each time step, an iterative solution is required.

Even though each step requires more calculation than for an explicit procedure, the implicit method is often stable for much longer time steps. The latter scheme also has controllable numerical damping, which assures more stable convergence. This often implies that the implicit method is faster. (3)

2.4.2 Modal Analysis

Modal analysis is performed by solving the dynamic equation of motion by assuming that the system is oscillating harmonically. The goal is to find the eigenfrequencies and mode shapes of the oscillating system.

For undamped free oscillations the equation of motion and the corresponding oscillations becomes:

$$\boldsymbol{M}\ddot{\boldsymbol{X}} + \mathbf{K}\boldsymbol{X} = \mathbf{0} \tag{2.52}$$

$$\boldsymbol{X} = \boldsymbol{\Phi}\sin(\omega t) \tag{2.53}$$

provided that the harmonic assumption is valid. Here, $\boldsymbol{\Phi}$ is a matrix consisting of n eigenvectors (the mode shapes):

$$\boldsymbol{\Phi} = [\boldsymbol{\Phi_1}\ \boldsymbol{\Phi_2}\ \ \boldsymbol{\Phi_3}\ \ \ldots\ \boldsymbol{\Phi_n}\ ] \tag{2.54}$$

Each eigenvector, $\boldsymbol{\Phi_i}$, contains the maximum displacement at all degrees of freedom. In reality a system may be described by an infinite number of DOF's.

The equation of motion for the whole system may be written in the following manner:

$$(\boldsymbol{K} - \omega^2\mathbf{M})\boldsymbol{\Phi} = \mathbf{0} \tag{2.55}$$

The natural frequencies of the system are then given by solutions of the equation:

$$\det(\boldsymbol{K} - \omega^2 \mathbf{M}) = 0 \tag{2.56}$$

This is the analytical solution of the eigenvalue problem, given by Equation (2.56) (7). Computer methods are however based on numerical solutions. Two such methods are briefly presented here.

2.4.2.1 Vector Inverse Iteration

Vector iteration methods are particularly used when a limited number of eigenvalues are wanted. The inverse iteration method determines the smallest eigenvalue of the system. Assume that $\boldsymbol{z}_k$ is an approximation of $\boldsymbol{\Phi}$. Then a better approximation may be found by iteration using the eigenvalue equation for the smallest ω, where $\boldsymbol{z}_{k+1}$ is the better approximation of $\boldsymbol{\Phi}$:

$$\boldsymbol{K}\boldsymbol{z}_{k+1} = \boldsymbol{M}\boldsymbol{z}_k \tag{2.57}$$

The approximation of the corresponding eigenvalue may then be found by the Rayleigh quotient:

$$\omega^2{}_{k+1} = \lambda_{R,k+1} = \frac{\boldsymbol{z}^{\boldsymbol{T}}{}_{k+1}\boldsymbol{K}\boldsymbol{z}_{k+1}}{\boldsymbol{z}^{\boldsymbol{T}}{}_{k+1}\boldsymbol{M}\boldsymbol{z}_{k+1}} \tag{2.58}$$

where $\lambda_R$is the Rayleigh quotient. This iteration is performed until convergence is obtained. To get convergence the approximation vector $\boldsymbol{z}_{k+1}$ must be normalized before each step.

To get other eigenvalues as for example the second lowest, a shift, μ, can be introduced, slightly larger than the first eigenvalue. The new eigenvalues, $\bar{\lambda}$, are then given as:

$$\bar{\lambda} = \lambda - \mu \tag{2.59}$$

This results in a new coordinate system, as indicated in Figure 5. Inserted in the eigenvalue problem for the smallest eigenvalue, the iteration procedure becomes:

$$(\boldsymbol{K} - \mu\boldsymbol{M})\boldsymbol{z}_{k+1} = \boldsymbol{M}\boldsymbol{z}_k \tag{2.60}$$

The eigenvalue for the new system may now be found by the Rayleigh quotient, now given as:

$$\bar{\omega}^2{}_{k+1} = \bar{\lambda}_{R,k+1} = \frac{\boldsymbol{z}^{\boldsymbol{T}}{}_{k+1}(\boldsymbol{K} - \mu\boldsymbol{M})\boldsymbol{z}_{k+1}}{\boldsymbol{z}^{\boldsymbol{T}}{}_{k+1}\boldsymbol{M}\boldsymbol{z}_{k+1}} \tag{2.61}$$

When convergence is obtained for the eigenvalue, the second lowest eigenvalue is found by transforming the new eigenvalue back to the old system (7):

$$\lambda = \bar{\lambda} + \mu \tag{2.62}$$

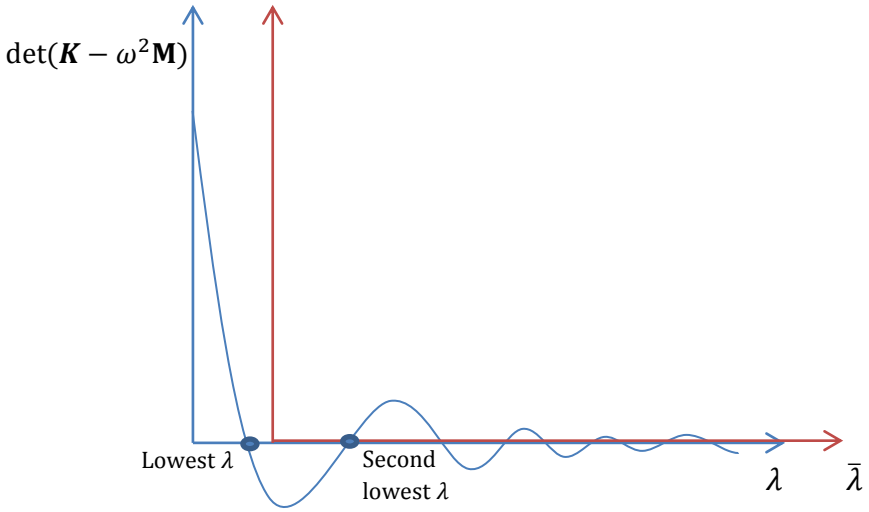

Figure 5 Vector Inverse Iteration With Shift

2.4.2.2 Lanczos Eigensolver Algorithm

While the method described above is a vector iteration method, the Lanczos method for solving eigenvalue problems is classified as a transformation method. The essence of this method is to transform a given symmetrical matrix into a reduced tridiagonal matrix, and then solve for the eigenvalues of the transformed matrix. The transformation to tridiagonal form is achieved via a recurrence relation that generates an orthogonal basis for certain Krylov subspaces. The drawback of this method is that the recurrence relation may be numerically unstable due to loss of orthogonality in the basis of Krylov subspaces. However, the method is well suited when dealing with large-space matrix eigenvalue problems. (8)

3 Orcaflex

3.1 System Modeling

This chapter describes some of the structure modeling options in Orcaflex, together with assumptions and limitations for the modeling techniques.

3.1.1 Buoys

A structure may be modeled as a 6D- or a 3D buoy. Both models are treated as rigid bodies. 6D buoys have 6 DOF's, 3 translational and 3 rotational. For a 3D buoy the rotational degrees of freedom are neglected, meaning that only the translational degrees of freedom are taken into account. (3)

To create a buoy in Orcaflex, the user must specify the geometry together with the mass distribution of the buoy. The input data form for a cylindrical 6D Buoy is shown in Figure 6. It is seen from the figure that the buoy also may be divided into a stack of cylinders with individual geometry.

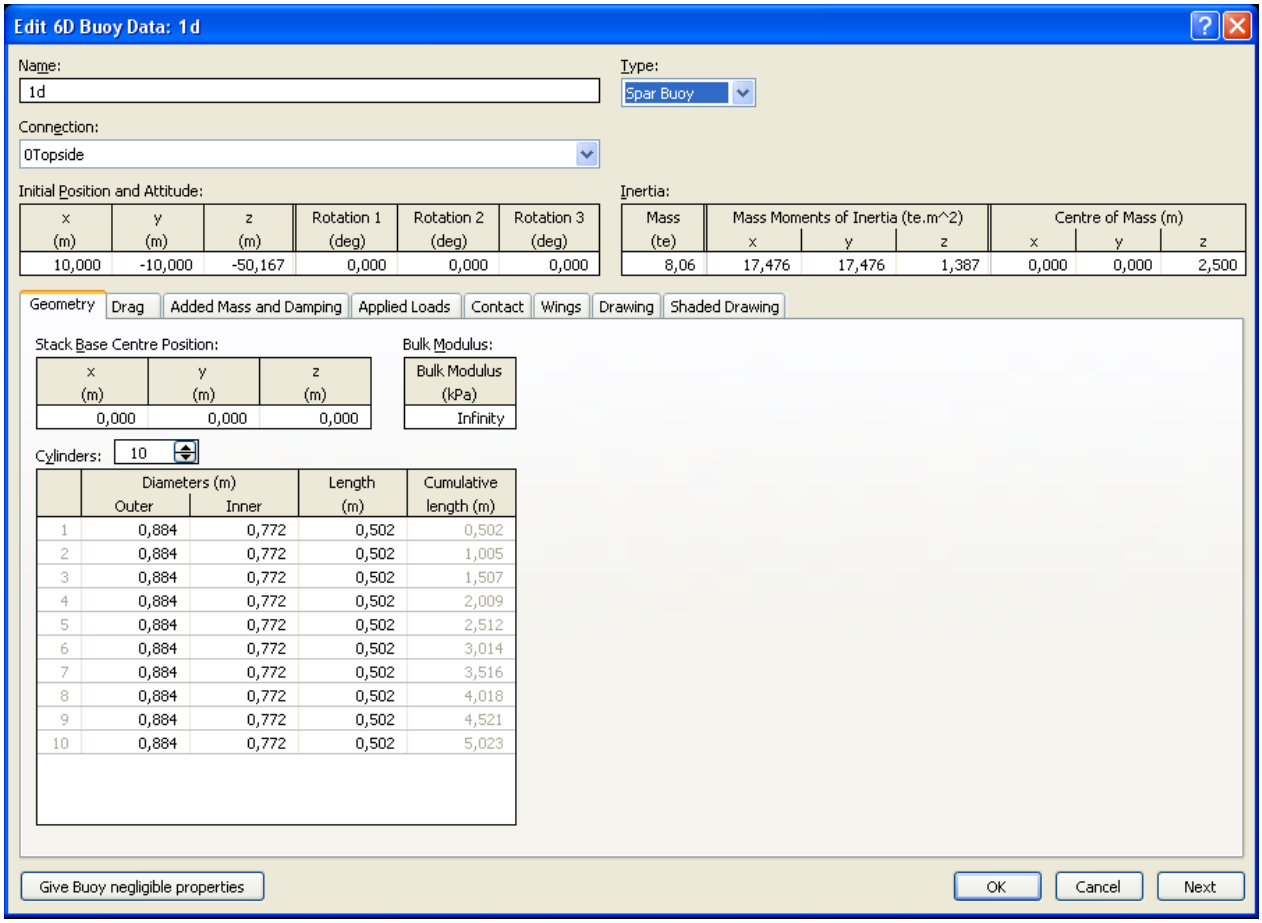

Figure 6 The Orcaflex Buoy Data Form

3.1.2 Vessels

A Vessel is another way of modeling a floating structure in Orcaflex. Vessels are also treated as rigid bodies with 6 DOF's. When creating a Vessel, the user must specify the mass distribution together with hydrodynamic coefficients to calculate the motions of the floating structure. However, if the motions of the vessel are known, the user may simply specify the given displacement RAOs (see Figure 7). The RAOs are given together with the RAO origin. If second order effects are wanted, load RAOs may be specified in a similar manner. (3)

The Vessel may be sketched by the user to get the exact geometry. Orcaflex then uses Equation (2.1) to calculate the motions on the rigid body structure relative to the RAO-origin.

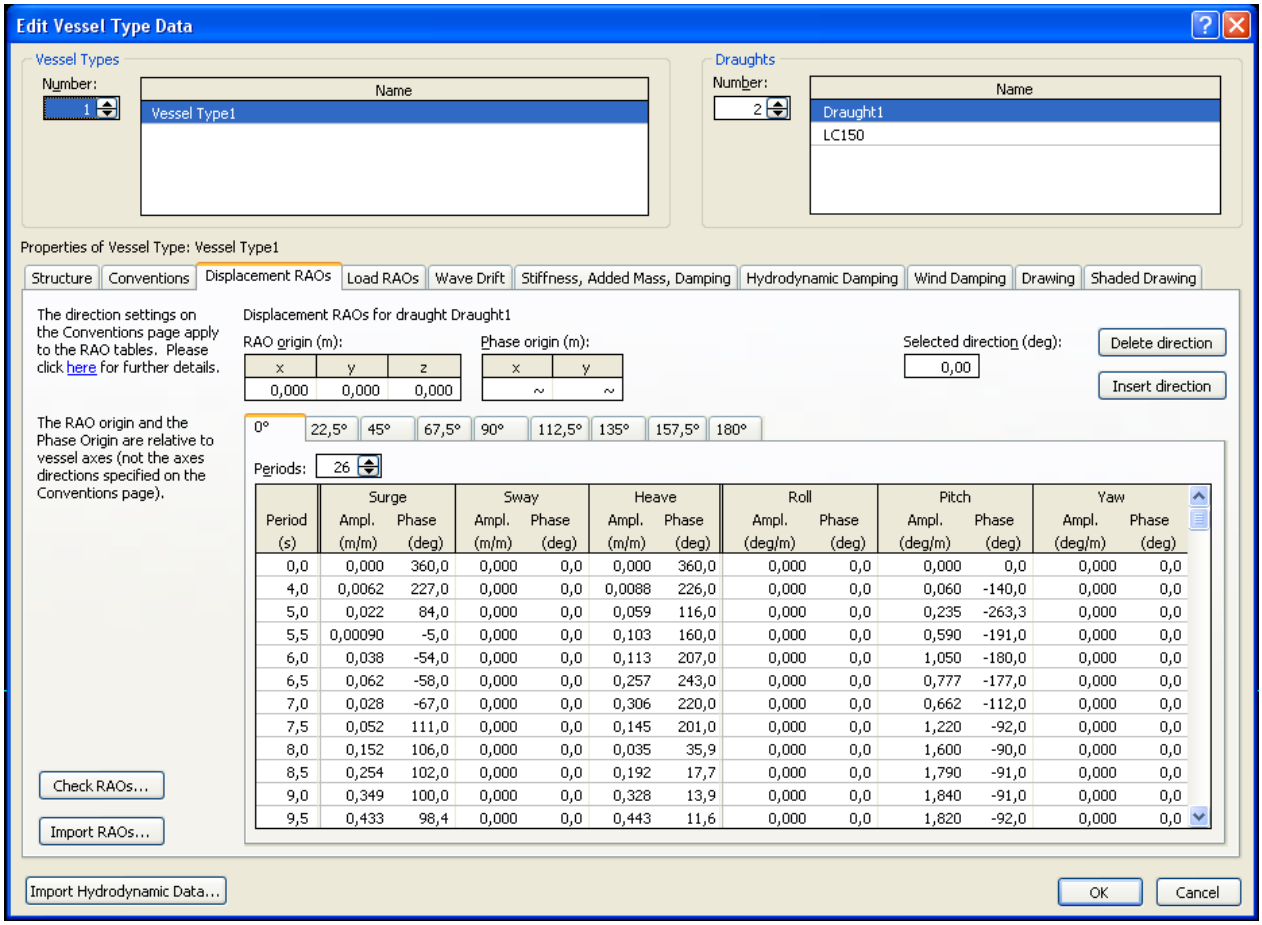

Figure 7 The Orcaflex Vessel Data Form

3.1.3 Lines

Orcaflex uses a finite element model for a line as illustrated in Figure 8. The line is divided into a series of line segments which are then modeled by straight massless model segments with a node at each end. The segments model the axial and torsional properties of the line, while the nodes include the other properties (mass, weight buoyancy etc.).

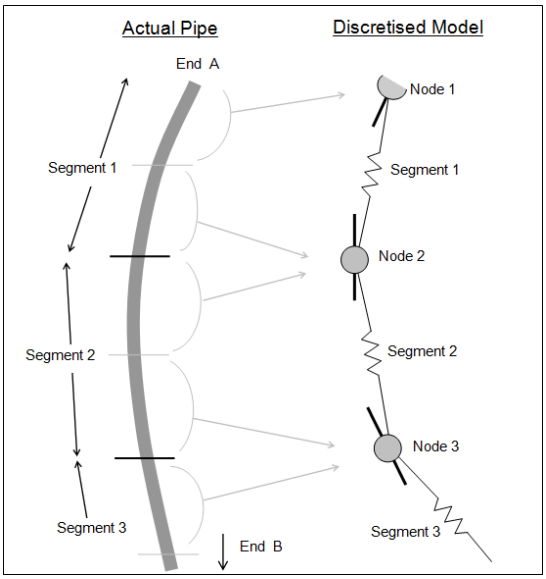

Figure 8 Line Finite Element Model

Orcaflex calculates the forces and moments on a mid-node in 5 stages (3):

1. The linear tension forces

$$T_e = T_w + (P_O A_O - P_i A_i) \tag{3.1}$$

Where T_e is the effective tension and T_w is the wall tension.

$$T_w = EA\varepsilon - 2\nu(P_O A_O - P_i A_i) + \frac{EAe\left(\frac{dL}{dt}\right)}{L_0} \tag{3.2}$$

$$\varepsilon = \frac{L - \lambda L_0}{\lambda L_0} \tag{3.3}$$

$$e = e(critical) \cdot \frac{Target\ Axial\ Damping}{100} \tag{3.4}$$

$$e(critical) = (2 \cdot Segment\ Mass \cdot \frac{L_0}{EA})^{\frac{1}{2}} \tag{3.5}$$

The wall tension consists of three parts, first the axial stiffness where EA is the axial stiffness of a line multiplied with the total mean axial strain ε. L is the instantaneous length, λ is the expansion factor and L_0 is the unstretched length of the segment. The second part is the contribution from external and internal pressure (via the Poisson ratio effect ν), where P_O, P_i , A_O and A_i is the external pressure, internal pressure, external cross section area and internal cross section area respectively. The last term is

the axial damping contribution where *e* is the damping coefficient of the line and *dL/dt* is the rate increase of length. This effective tension force vector is then applied to the nodes at each end of the segment (with opposite signs) (3).

2. Bend Moments

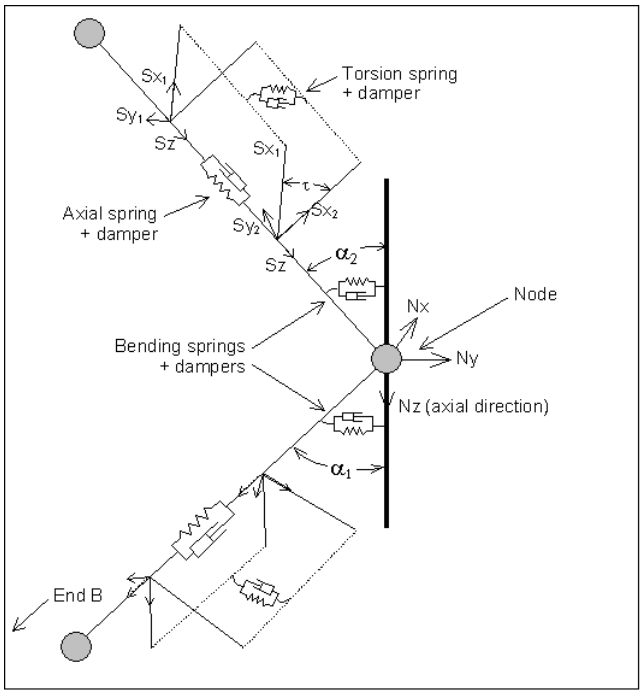

Figure 9 Bending Moments

When the tension forces are found, the bend moments are calculated. There are bending spring and dampers at each side of the node as shown in Figure 9. The node's frame of reference Nxyz is a Cartesian set of axes that is fixed to the node. The segment has Sxyz at each end with corresponding numbers 1 and 2. Because the two frames have the same Sz direction, it is possible to find the bend angle between the axial direction Nz and Sz. The effective curvature vector C, being orthogonal to the Nz and Sz direction, is then calculated with magnitude:

$$C_{1,2} = \frac{\alpha_{1,2}}{\left(\frac{1}{2}L_0\right)} \tag{3.6}$$

Each node will experience two bending moments in the binormal direction, M_1 and M_2, from forces in the upper and lower line segments meeting at the node:

$$M_{1,2} = EI\left|C_{1,2}\right| + D\frac{d\left|C_{1,2}\right|}{dt} \tag{3.7}$$

$$D = \frac{\lambda}{100}D_c \tag{3.8}$$

$$D_c = L_0(Segment\ Mass \cdot EI \cdot L_0)^{1/2} \tag{3.9}$$

where EI is the bending stiffness, D_c is the bending critical damping value for a segment and λ is the target bending damping. The target bending damping is often a value between 5 and 50 % of critical damping and the effect is usually to damp high frequency noise. It can be specified independently for tension, bending and torsion (3).

3. Shear Forces

The shear forces are found from the bend moments.

$$Shear\ Force\ Vector = \frac{M_2 - M_1}{L} \tag{3.10}$$

Both M_1 and M_2 are vectors, so this is a vector formula that defines both the magnitude and the direction of the shear force. The shear force is applied (with opposite signs) at each end of the segment.

4. Torsion Moments

If torsion is included the torsion moments are calculated. Then Sxyz at each end of the segment is calculated.

$$Torque = \frac{K\tau}{L_0} + C\frac{d\tau}{dt} \tag{3.11}$$

$$C = C(critical) \cdot \frac{Target\ Torsional\ Damping}{100} \tag{3.12}$$

$$C(critical) = \left(\frac{2I_z K}{L_0}\right)^{\frac{1}{2}} \tag{3.13}$$

Here, K is the torsional stiffness, τ is the segment twist angle between Sx_1 and Sx_2, $\frac{d\tau}{dt}$ is the rate of twist and C is the torsional damping coefficient of the line. The torsional damping coefficient C is based on the target torsional damping. The target torsional damping is almost the same as the target bending damping, only in torsional direction. $C(critical)$ is the critical damping value for a segment and I_z is the rotational moment of inertia of the segment about its axis.

The total force and moment on the node is found from these contributions along with the other non-structural loads. Orcaflex then calculates the resulting translational and rotational acceleration of the node, and integrates to obtain the node's velocity and position at the next time step (3).

3.1.4 Links

Links can be used when connecting parts in the model. There are two options, either a tether or a spring-damper as illustrated in Figure 10. The tethers are simple elastic ties that can take tension but not compression. Both the unstretched length and the stiffness of the tether need to be specified. The

spring-damper can take both compression and tension. Either a linear or a piecewise linear length-force relationship can be specified for both the spring and the damper. (3)

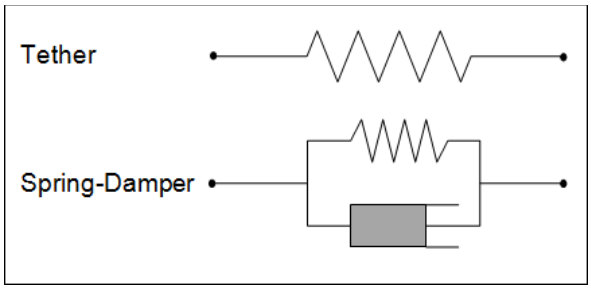

Figure 10 Links

3.1.4.1 Tethers

Linear force characteristics for a tether yields:

$$t = \frac{k(L - L_0)}{L_0} \tag{3.14}$$

where t is the tension, k is the specified stiffness, L is the current stretched length between the two ends and L_0 is the specified unstretched length (3).

3.1.4.2 Spring/Damper

For a linear spring in a spring-damper the following formula is applied:

$$t = k(L - L_0) \tag{3.15}$$

A linear damper exerts an extra tension:

$$t = c(rate\ of\ increase\ of\ L) \tag{3.16}$$

Where c is the specific damping. The rate of increase of L can be specified in a table of tension against length or velocity. This table can be either linear or non-linear damping (3).

3.1.5 Winch

As well as lines and links, it is possible to use winches in Orcaflex. A winch can lower or haul an object a given distance. In static analysis the tension is calculated as:

$$t = Wire\ Stiffness \cdot \frac{(L - L_0)}{L_0} \tag{3.17}$$

where the wire stiffness is specified in the data, L is the total length of the winch wire path, L_0 is the unstretched length of the wire paid out and the winch drive force f is set to equal t. In the dynamic analysis the following formula is used:

$$t = [(L - L_0) + (Wire\ damping)\left(\frac{dL}{dt} - \frac{dL_0}{dt}\right)] \cdot \frac{Wire\ Stiffness}{L_0} \tag{3.18}$$

The wire damping is specified in the data. The winch wire is not allowed to go into compression, it will then go slack and t is set to zero. (3)

3.1.6 Connections

Lines, links, winches and shapes are special objects in Orcaflex that makes connections possible. Each line has two ends that can either be free, fixed or connected to a vessel, 3D- or a 6D buoy. When an end of the line is connected to another object, the end becomes slave and the object master. Links and winches also have two ends but unlike lines they cannot be free. They can be connected to nodes on a line, vessel, 3D- or 6D buoy. Shapes only have one joint which can either be fixed or connected to a vessel, 3D- or a 6D buoy. (3)

3.1.7 Shapes

Shapes can be used in Orcaflex to create elastic solids. An elastic solid represents a physical barrier that can interact with lines and buoys. The user must specify the stiffness for the shape. The solid resists penetration by applying a reaction force proportional to the penetration depth of the buoy or line into the elastic solid. The normal contact stiffness, k_c, should then be specified as a reaction force, F_R, per unit depth of penetration per unit of contact area:

$$k_c = \frac{F_R}{dA_c} \tag{3.19}$$

where A_c is the contact area and d is the penetration depth into the elastic solid. (3)

When a solid interacts with a line in Orcaflex, the interaction is only felt in the line nodes. Between the nodes there will be no interaction. This is illustrated in Figure 11.

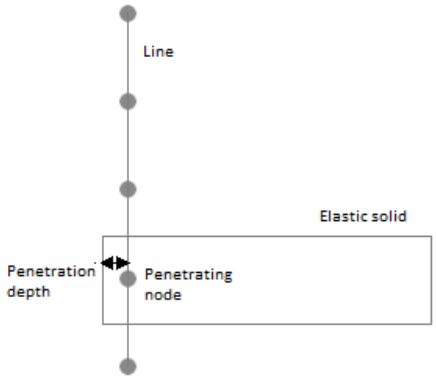

Figure 11 Line Penetrating an Elastic Solid Shape

3.2 Environment

One of Orcaflex benefits is the simple and easy way to model different wave and current scenarios. This chapter shows briefly how different input parameters can be implemented for the scenarios.

3.2.1 Waves

Each eave train can be a regular wave, a random wave or specified by a time history file. Different variables such as wave direction, significant wave height, wave period and spectra may easily be implemented. Orcaflex then simulates a wave train from the variables given. It is also possible to choose the different variables for the spectrum by choosing “Partially Specified” or “Fully Specified” spectral parameters. See Figure 12 for the input alternatives.

“Wave Preview” is a feature in Orcaflex where the generated sea profile can be analyzed for a given period of time. This makes it possible to search through a period of global time looking for an interesting wave event and then set time origin so that the simulation covers that event. The sea profile is based on the wave spectrum. With this feature it is possible to find the worst scenarios during a period of time, as illustrated in Figure 13.

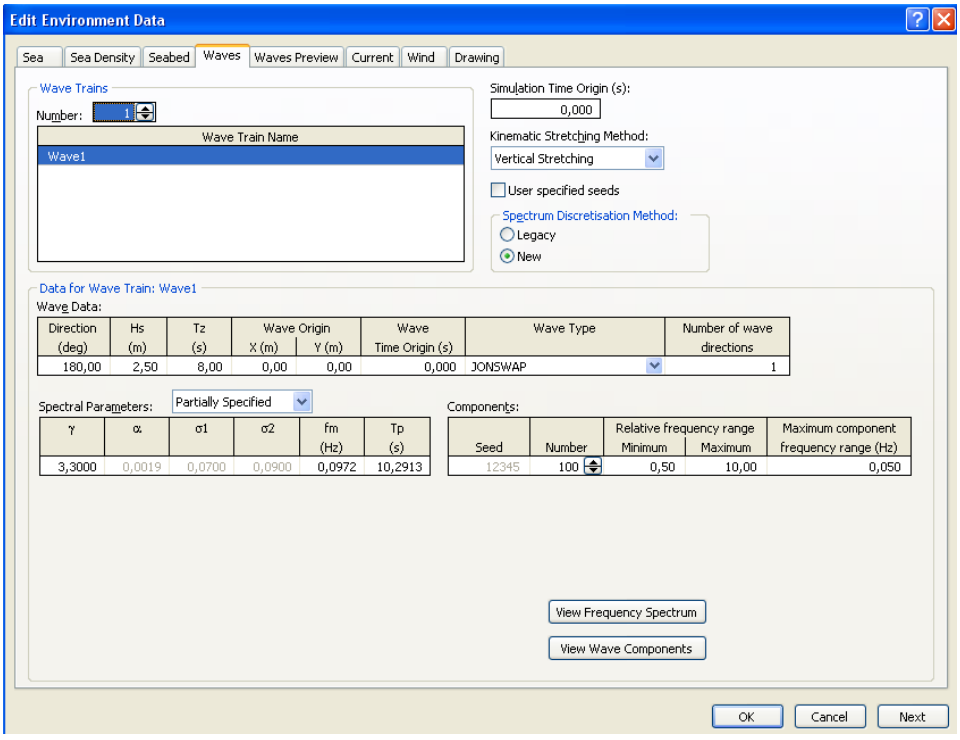

Figure 12 The Orcaflex Environment Data Form

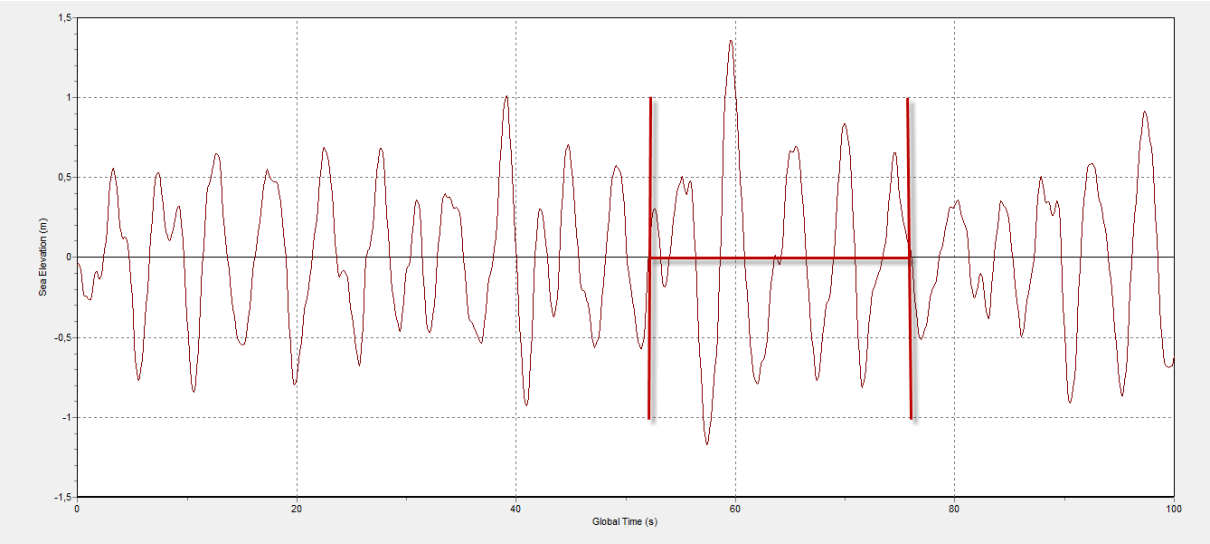

Figure 13 The Wave Preview Feature

3.2.2 Current

The horizontal current is specified as a full 3D profile, variable in magnitude and direction with depth. Orcaflex offers three methods, extrapolation, interpolated method and power law method.

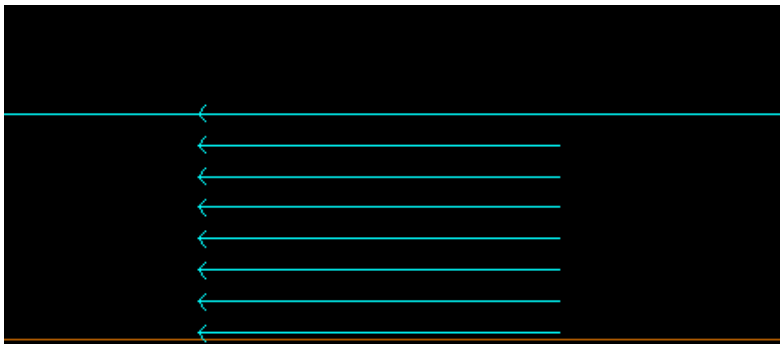

Figure 14 Uniform Current Profile

When waves are present, the current must be extrapolated above the still water level. In the interpolated method, the horizontal current is specified as a full 3D profile, variable in magnitude and direction with depth. This option is used for intermediate depths. In the power law method, one can choose the decay rate of the current. (3)

3.3 Loads

Orcaflex calculates the environmental loads for the problem, using input data specified by the user. This chapter describes how Orcaflex calculate the loads, and which data that needs to be specified. The forces and moments are calculated using the cross flow assumption. This means that the forces and moments are decomposed into six components acting in three directions. These directions are defined by the local coordinate system of the buoy, and the input parameters specified by the user should therefore be specified according to the buoy's local coordinate system.

3.3.1 Drag Forces

Orcaflex uses the extended version of Morison's equation to calculate wave drag and current forces on Buoys (see chapter 2.3.1).

The drag forces in x-, y-and z-direction are calculated as follows:

$$x\ Drag\ Force = (PW)\ {}^{1}/_{2}\ \rho\ C_{Dx}A_xV_{rx}|V_{rxy}| \tag{3.20}$$

$$y\ Drag\ Force = (PW)\ {}^{1}/_{2}\ \rho\ C_{Dy}A_yV_{ry}|V_{rxy}| \tag{3.21}$$

$$z\ Drag\ Force = (PW)\ {}^{1}/_{2}\ \rho\ C_{Dz}A_zV_{rz}|V_{rz}| \tag{3.22}$$

where C_{Di} is the drag coefficient and $V_{ri}$is the relative fluid velocity in i-direction. $|V_{rxy}|$ is the absolute magnitude of the relative velocity in the xy-plane. The drag coefficients must be specified by the user and should be given as the buoy was fully submerged. Orcaflex accounts for the portion wet through the (PW)-factor. A_i is the drag area for the indicated direction and must be specified by the user. This should be the projected area of the fully submerged buoy subjected to drag forces. Figure 15 shows how the drag area should be specified for flow in x-direction. (3)

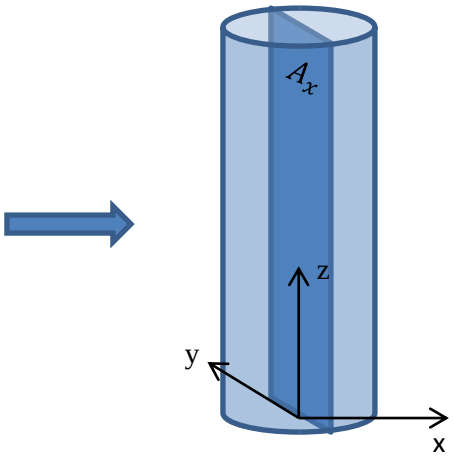

Figure 15 The Understanding of Specified Drag Area

The drag moments should be specified when using 6D Buoys for modeling. The drag moments about the local x-, y- and z-direction are given by:

$$x\ Drag\ Moment = (PW)\ {}^{1}/_{2}\ \rho\ C_{Dmx} A_{mx} w_{rx} |w_{rxy}| \tag{3.23}$$

$$y\ Drag\ Moment = (PW)\ {}^{1}/_{2}\ \rho\ C_{Dmx} A_{my} w_{ry} |w_{rxy}| \tag{3.24}$$

$$z\ Drag\ Moment = (PW)\ {}^{1}/_{2}\ \rho\ C_{Dmz} A_{mz} w_{rz} |w_{rz}| \tag{3.25}$$

where C_{Dmi} is the drag moment coefficient and w_{ri} is the fluid angular velocity of the local water isobar relative to the body in i-direction. $|w_{rxy}|$ is the absolute magnitude of the relative angular velocity in the xy-plane. A_{mi} is the projected drag area moment for the indicated direction and must also be specified by the user. The drag moment coefficients and corresponding drag areas must be specified by the user for the fully submerged buoy. (3)

An additional current Munk moment may be specified directly by the user. This should be calculated as described in chapter 2.3.4.

3.3.2 Inertia Forces

The fluid inertia forces are automatically calculated by Orcaflex using the extended version of Morrison's equation to calculate the drag forces on buoys, when the added mass coefficient, C_a, is specified. (3) (see chapter 2.3.1).

3.3.3 Added Mass

Orcaflex uses the following formulas to calculate added mass forces and moments on buoys:

$$F_{am,i} = C_{ai} (DM)_i a_{ri} \quad , \qquad i = 1{:}\,3 \tag{3.26}$$

$$F_{am,i} = (PW)(AI)_i \dot{w}_{ri} \quad , \qquad i = 4{:}\,6 \tag{3.27}$$

where $F_{am,i}$ are the added mass force and moments, C_{ai} is the added mass coefficient, $(DM)_i$ is the instantaneous displaced mass for flow in i-direction. $(AI)_i$ is the added inertia moment when the body is fully submerged, and a_{ri} and $\dot{w}_{ri}$ are normal and angular water particle accelerations relative to the body. $(AI)_i$ and C_{ai} are specified by the user. Orcaflex accounts for the wetted surface through the portion-wet-factor, PW. (3)

If the jacket buoy is hollow, it will be partly flooded by water, depending on the draught. According to DNV's recommended practice for marine operations (4), the mass of the water moving together with the structure should be included in the added mass calculations. The Orcaflex formulas for added mass forces will account for this through the instantaneous displaced mass, $(DM)_i$. For hollow cylinders and directions normal to the cylinder axis, 1 and 2, the $(DM)_i$ will denote the displaced mass of the cylinder and contents. In these directions the water mass inside the flooded cylinders will move with the structure. However, this is not the case for z-direction. $(DM)_3$ will then be the displacement of the wetted cylinder only, excluding the content mass. This is automatically interpreted by Orcaflex. Similarly,

the added inertia moments about x- and y-axes, will account for the displaced mass of the water inside the cylinder, but exclude the water mass when computing the axial added moment. This is based on the assumption that the water is free to rotate inside the cylinder about the axial cylinder axis, but restrained against normal rotations. (3)

3.3.4 Damping

Orcaflex uses the following formula to compute damping forces and moments (3):

$$F_{damp,i} = (PW)B_i V_{ri} \ , \qquad i = 1{:}3 \tag{3.28}$$

$$F_{damp,i} = (PW)B_i w_{ri} \ , \qquad i = 4{:}6 \tag{3.29}$$

Here, B_i are the unit damping forces and moments, when the relative velocity, V_{ri}, or angular velocity, w_{ri}, of the local fluid particle equals 1. B_i are specified by the user. Also in these calculations Orcaflex applies the force at the centroid of the wetted volume, and accounts for the wetted surface by a portion-wet-factor, so the damping coefficient, B_i, should be specified as if the cylinder is fully submerged.

3.3.5 Restoring Forces

For Buoys, Orcaflex calculates heave stiffness and righting moments in pitch and roll by calculating the intersection of the water surface, at instantaneous positions of the buoy (3). Hence stiffness properties do not need to be specified by the user.

3.4 Analysis in Orcaflex

This chapter mentions the methods available for dynamic analysis in Orcaflex, and the conditions for the choice of which method to use.

3.4.1 Time Domain Analysis

In Orcaflex it is possible to choose between explicit and implicit integration methods when performing a response analysis. Orcaflex uses the forward Euler method for explicit integration. For implicit integration method, the generalized α-method is used. (3) Both these methods are described in chapter 2.4.1.

3.4.2 Modal Analysis

When performing a modal analysis, Orcaflex uses one of two approaches to solve for the eigenfrequencies and mode shapes. The choice of method used is dependent on the modes extracted, n and the number of degrees of freedom, N. The Lanczos eigensolver algorithm (described in chapter 2.4.2.2), is used if

$$n \leq N/3 \tag{3.30}$$

$$n \leq 1000 \tag{3.31}$$

Otherwise a direct method based on tridiagonal matrix diagonalization is used. (3)

The Lanczos iterative algorithm is much faster and requires less memory for large systems, and should therefore be used if possible.

3.4.3 Batch Processing

The batch process allows the user to set up a list of jobs and run them simultaneously. This is a favorable feature if many scenarios are to be run, typically sea condition scenarios.

Script Table	Script.txt					
// Example script table. // The script generates separate data files for 4 wave directions, 2 wave heights and 9 wave periods. The Jacket is 3 meters above seabed						
// Case	LoadData	Select Environment Select WaveTrain "Wave1" WaveTrainDirection =	Select Environment Select WaveTrain "Wave1" WaveTrainHs =	Select Environment Select WaveTrain "Wave1" WaveTrainTz =	Select Environment Select WaveTrain "Wave1" SimulationTimeOrigin =	SaveData
1	"Jacket and Barge.dat"	180	2	4	5336,53	Case01.dat
2		195				Case02.dat
3		210				Case03.dat
4		225				Case04.dat
5		180	2	5	294,8	Case05.dat
6		195				Case06.dat
7		210				Case07.dat

Table 2 Script Table with Different Cases

Excel is one possible option to create a batch process. Orcaflex offers an excel spreadsheet where the different parameters can be implemented. First one has to create a base case, the model on which the scenarios are to be run. Excel then creates a script that can be run to create the different cases. When the different cases are created, Orcaflex can batch process them and run a dynamic analysis. The results are saved in a simulation file.

1									
Sheet Name	**Label Cell**	**Label**	**Output Cell**	**Command**	**Object Name**	**Additional Data**	**Simulation Period**	**Variable**	
1				Load K:\600 - Interne prosjekter\2009\09-609 vindturbininstallasjon\Masteroppgave Atle og Amund\Environment\Results\Case					1
Jacket	A2	Min X	A3	Min	1a		Whole Simulation	X	
Jacket	B2	Max X	B3	Max	1a		Whole Simulation	X	
Jacket	C2	Min Y	C3	Min	1a		Whole Simulation	Y	
Jacket	D2	Max Y	D3	Max	1a		Whole Simulation	Y	
Jacket	E2	Min Z	E3	Min	1a		Whole Simulation	Z	
Jacket	F2	Max Z	F3	Max	1a		Whole Simulation	Z	
Jacket	G2	Gx-Velocity	G3	Max	1a		Whole Simulation	GX-Velocity	
Jacket	H2	Gy-Velocity	H3	Max	1a		Whole Simulation	GY-Velocity	
Jacket	I2	Gz-Velocity	I3	Max	1a		Whole Simulation	GZ-Velocity	
Jacket	J2	Rotation 1	J3	Max	1a		Whole Simulation	Rotation 1	
Jacket	K2	Rotation 2	K3	Max	1a		Whole Simulation	Rotation 2	
Jacket	L2	Rotation 3	L3	Max	1a		Whole Simulation	Rotation 3	

Table 3 Excel Result Sheet Collecting Specified Result Information from Orcaflex

Instruction format	Instruction
Sheet Name	Specifies the name of the excel worksheet on which any output is produced
Label Cell	Specifies the cell, in the specified worksheet, to which the label will be written
Label	Specifies the label string to be written to the label cell
Output Cell	Specify the cell to which results or data should be written
Command	Specify different commands such as minimum, maximum and standard deviation values from the results.
Object Name	The name of the Orcaflex object whose results or data are output
Additional Data	This column is used when outputting results for certain types of Orcaflex object
Simulation Period	The period of simulation for which the results are wanted
Variable	The name of the output variable

Table 4 Batch Processing Tool

When the simulation files are created excel can be used to gather information from the different files. This is done by creating an instruction list (see Tables 3 and 4). Here different result parameters like displacements and velocities can be specified. The results are collected into a new spreadsheet. This makes it easy to compare results from different cases and scenarios.

4 Methods

4.1 Critical Scenarios

There will be several critical scenarios during lowering of the jacket. Two critical phases will be analyzed. The first critical scenario is contact with the support frame. Collision between jacket and the support frame may occur, and to look at the contact forces between these two structures is important. The second scenario is when landing the jacket on the seabed. It is important to look at the behavior of the jacket before and during landing. The different scenarios analyzed are presented in Table 5.

Scenario number	Description	Items	Jacket horizontal position from seabed
Scenario 1a	Collision with support frame. Simplified frame modeled with the barge. Lines used to get contact forces.	Jacket, Line and Vessel with support frame	10 meters
Scenario 2a	Landing of jacket. Finding behavior of jacket just above seabed. No frame	Jacket, Line and Vessel	3 meters
Scenario 1b	Same as scenario 1a, but with heave compensation	Jacket, Link and Vessel with support frame	10 meters
Scenario 2b	Same as scenario 2a, but with heave compensation	Jacket, Link and Vessel	3 meters
Scenario 3	Scenario 1a with bumper system attached to support frame	Jacket, Line and Vessel with support frame and bumper system	10 meters

Table 5 Identified Critical Scenarios to be Analyzed

4.1.1 Scenario 1a

A support frame will guide the jacket during lowering. The support frame will be modeled as a simple frame attached to the barge. The jacket will be approximately 10 meters above the seabed. This is when contact forces are most likely to happen because of the close distance between the lower jacket legs and the support frame (see Figure 16).

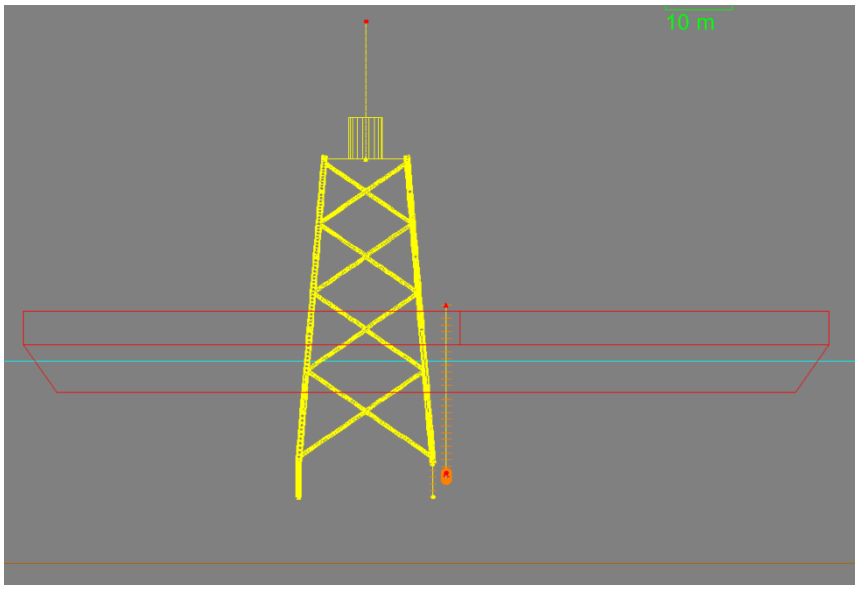

Figure 16 Scenario 1a

4.1.2 Scenario 2a

When landing the jacket on the seabed, the jacket is to be guided into a seabed support frame. Large fluctuations should therefore be avoided. To analyze the behavior for the different sea conditions is therefore important. The jacket is approximately 3 meters above seabed (see Figure 17).

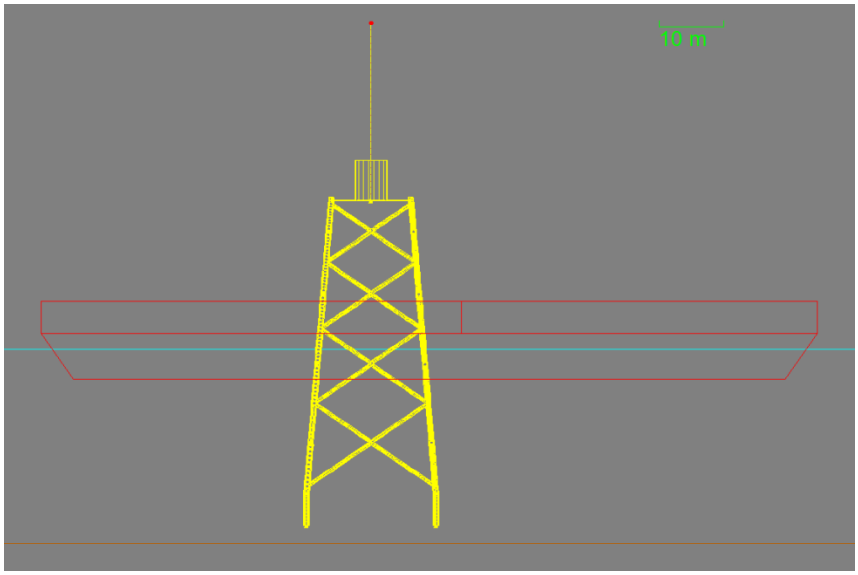

Figure 17 Scenario 2a

4.1.3 Scenario 1b and 2b

Scenario 1b and 2b are the same as Scenario 1a and 2b, respectively. The only difference is applying passive heave compensation to investigate the effect of damping on the vertical jacket motions. Heave compensation can be modeled as a link connection in Orcaflex (see chapter 4.2.5).

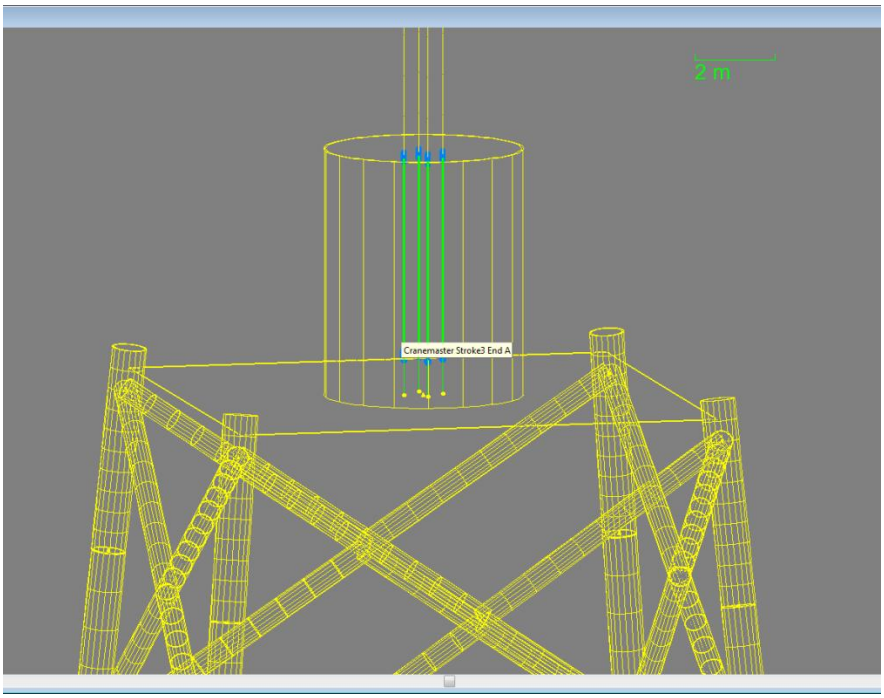

Figure 18 Scenario 1b and 2b with Heave Compensation System

4.1.4 Scenario 3

Scenario 3 is equal to Scenario 1a, only with a bumper system attached to the support frame. A bumper system will be important to damp the impact forces between the jacket and the support frame.

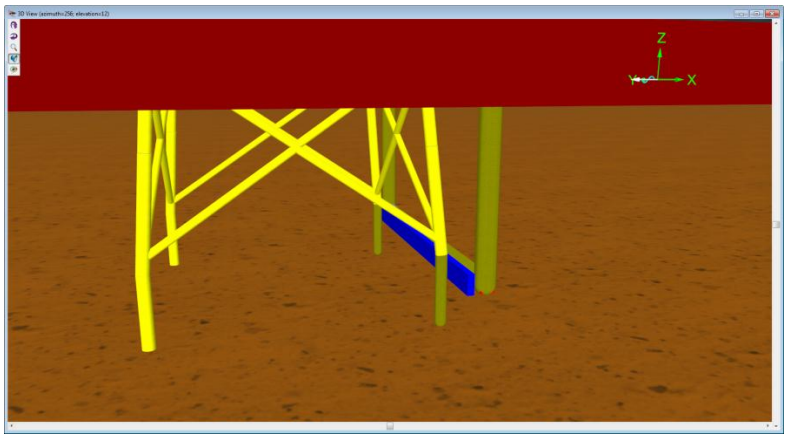

Figure 19 Scenario 3 With a Bumper System Attached to the Frame

4.2 Modeling the System

This chapter will describe how the jacket, barge and support frame are modeled and implemented in the system. The objects used as well as the parameters will be explained.

4.2.1 Jacket

The jacket is the most complicated structure to model in Orcaflex. Information about the jacket is provided by Ingenium. The jacket is designed with 6D spar buoys, split into 10 cylinder parts. For a spar buoy represented in several cylindrical sections, moments will be generated automatically as a result of the distribution of hydrodynamic forces along the buoy axis. Therefore no hydrodynamic moments have to be implemented. (See chapter 4.4.1)

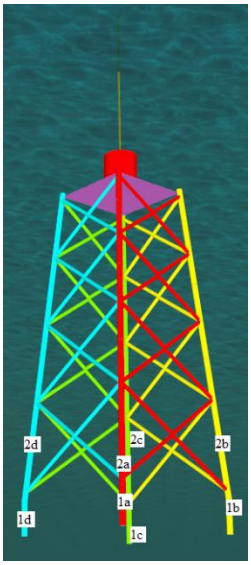

Figure 20 Jacket

Jacket Foundation parts								
		Coordinates						
Item	Part	x	y	z	rot1	rot2	rot3	Length
1	1a	10	10	-5,0000	0	0	0	5,0000
	1b	-10	10	-5,0000	0	0	0	5,0000
	1c	-10	-10	-5,0000	0	0	0	5,0000
	1d	10	-10	-5,0000	0	0	0	5,0000
2	2a	10	10	0	4,846477	-4,84648	0	7,6750
	2b	-10	10	0	4,846477	4,846477	0	7,6750
	2c	-10	-10	0	-4,84648	4,846477	0	7,6750
	2d	10	-10	0	-4,84648	-4,84648	0	7,6750
3	3a	9,351569	9,351569	7,647559	4,846477	-4,84648	0	12,1310
	3b	-9,35157	9,351569	7,647559	4,846477	4,846477	0	12,1310
	3c	-9,35157	-9,35157	7,647559	-4,84648	4,846477	0	12,1310
	3d	9,351569	-9,35157	7,647559	-4,84648	-4,84648	0	12,1310
4	4a	8,326667	8,326667	19,73519	4,846477	-4,84648	0	11,1250

Table 6 Jacket Foundation Parts

Excel is used to calculate the position and the different parameters for each part of the jacket (see Appendices 1 and 2).

In the excel worksheet the initial position, rotation and length of each jacket part is calculated and implemented in Orcaflex. Each item is given a number and a letter, the number referring to the identical parts, and the letter to all the symmetric counterparts. The first part “Xa” is in the positive xy-plane, and then the following parts will follow in a counterclockwise direction. This made it easy to use the symmetry of the jacket to find the positions and rotations of the parts. Figure 20 and Table 6 shows how the parts are divided and titled.

Main parts	Part title
Horizontal legs	1 to 7
Diagonal pipes	7 to 22
Topside	Topdeck, Topcylinder

Table 7 Numbering System of the Cylindrical Jacket Parts

Tables 7 show the different main parts and the consisting items. The main parts of the jacket are the horizontal legs, the diagonal pipes and the topside.

Lack of information on the topside led to some simplifications. Two parts are used to simulate the topside, a deck and a topside cylinder where the wind turbine will be installed. The simplified details can be found in Appendix 2.

When all the different parts are implemented they will be connected to the top deck. The jacket will then behave as a rigid system. All the loads on the different parts will be transferred to the top deck.

4.2.2 Barge

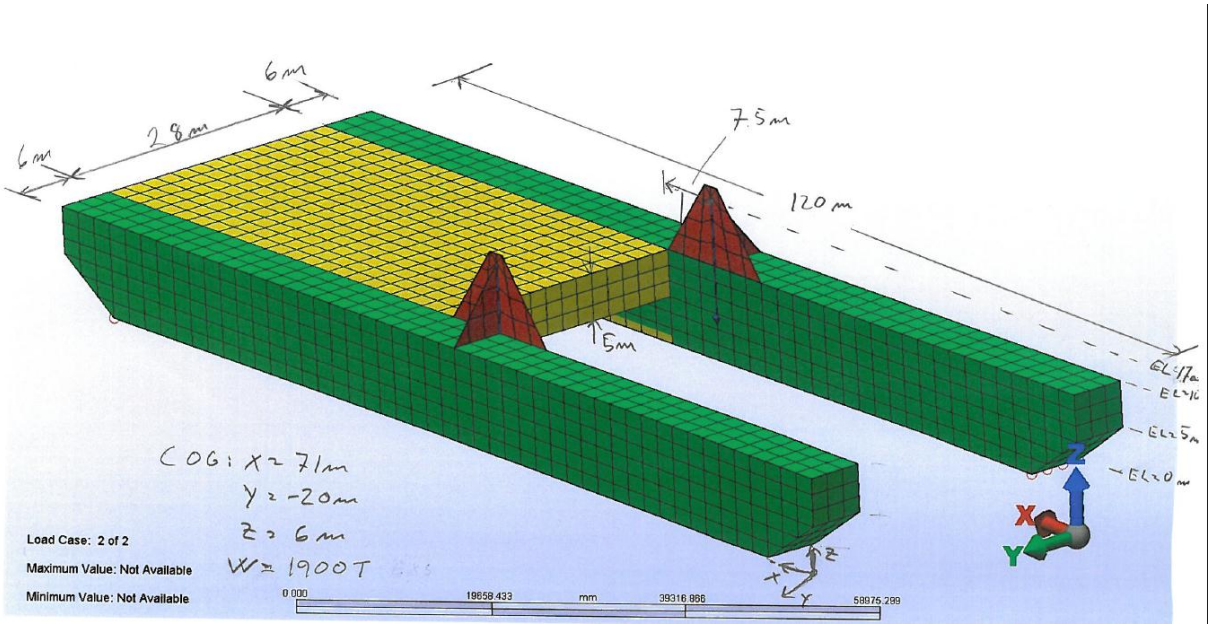

Figure 21 The Barge Provided by Ingenium

The displacement RAOs for the barge are provided by Noble Denton (see Appendix 7). Displacement RAOs are linear motions due to a unit wave elevation. To include second order effects, one should specify the load RAOs for the slow drift-, and high frequency forces. These need to be specified separately, and are not accounted for in the analysis. The barge is designed using the vessel feature in Orcaflex with the RAOs implemented. It is illustrated with measurements provided by Ingenium (see Figure 21). The modeled barge is only for visualization, the RAOs will define the motions for the given position.

4.2.3 Connection between Jacket and Barge

The connection between the barge and the jacket will be different in the different scenarios. For scenario 1a, 2a and 3 the connection will be a line, while scenario 1b and 2b will be with a link which will act as a heave compensation system. Because the jacket is perfectly symmetrical, the system will be statically underdefined. Two lines are therefore used to keep the jacket in the initial position. The lines are connected 1 meter apart in the y-direction to the barge and the jacket. The distance Z1 and X1 are used for the top connection point between the jacket and barge (see Figure 22). For Scenario 1b and 2b four lines with links are implemented due to the SWL for the passive heave compensation (see chapter 4.2.5).

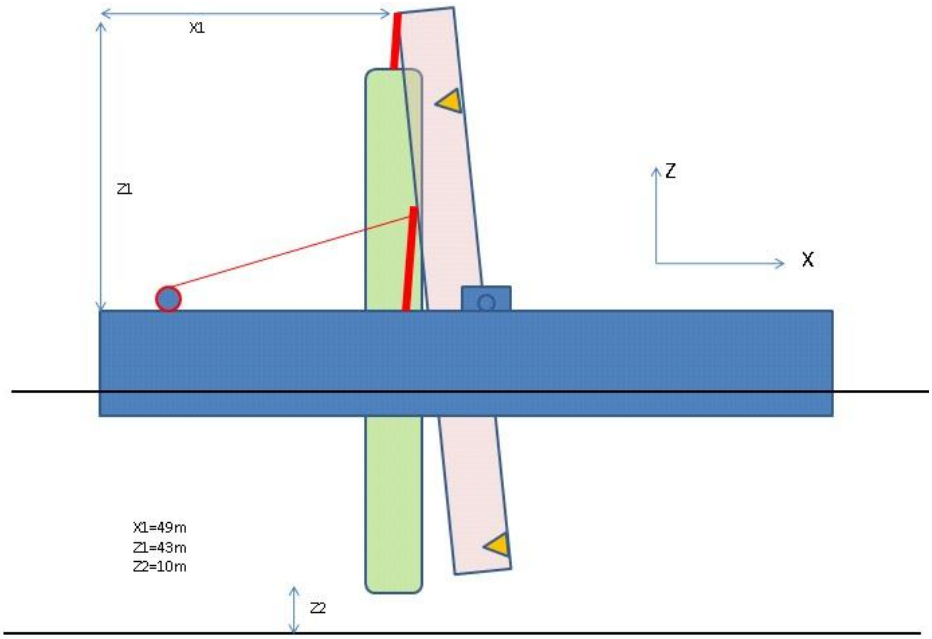

Figure 22 Connection Between Jacket and Barge

4.2.4 Support Frame

In Scenarios 1a and 1b, a frame is modeled to act as the support frame. The frame is modeled using lines, because buoys cannot experience contact forces. Therefore also the legs on the jacket that will experience contact will be replaced with lines. This is part 1a and 1d, from the excel sheet in Appendix 1.

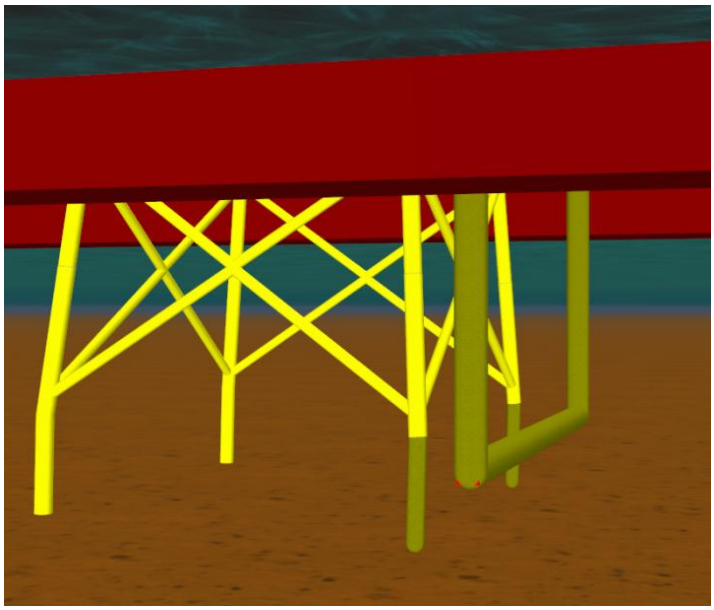

Figure 23 The Support Frame Modelled as Lines

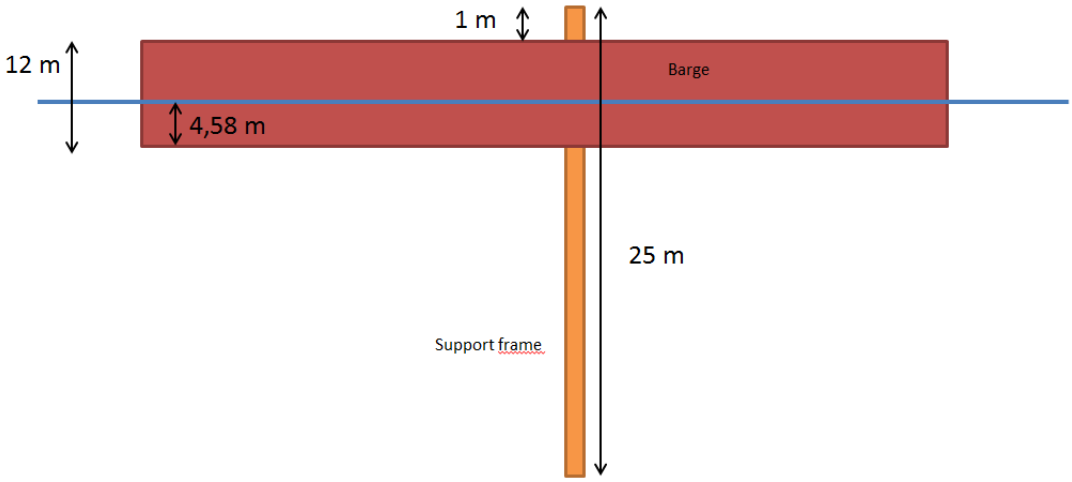

Figure 24 Support Frame Dimensions and Barge Connection

The support frame details are provided by Ingenium, see Figure 24. It is a simplified model consisting of 3 lines, using one horizontal line between the lower ends of two vertical lines connected to the barge. If collision is to happen during installation, the impact can be registered and analyzed.

4.2.5 Heave Compensation

Cranemaster offers an excel calculation sheet with output that can be implemented directly into Orcaflex. The input for this worksheet is operating water depth, temperature in air, water temperature, load needed to extend Cranemaster at zero stroke and oil reserve volume. The maximum pressure check shows if the Cranemaster system can handle the load (see Table 8).

Ernst-B. Johansen a.s				
N-3970 Langesund, NORWAY. Tel +4735963407, fax +4735972190				
Author: Ernst-B. Johansen. Email: post@cranemaster.no		Date: 16. Sept 2010		
CRANEMASTER DEEP SEA SWL400T, STROKE 4300mm				
Drawing no P05050				
Load and Pressure vs. piston rod stroke				
Project specific inputs:				
CRANEMASTER operating water depth:	0	meters		
CRANEMASTER temp in air when checked gas pressure	15	degrees Celcius		
Water temperature at operating depth	4	degrees Celcius		
Load needed to extend Cranemaster at zero stroke	**137,5**	Te	(The oil reserve volume changes	
Oil reserve volume (must be 25 litres or more)	25	Liters	the spring stiffness of Cranemaster)	
Outputs:				
Cranemaster pretension pressure	**92,0**	**bar**	NB! To be adjusted prior to deployme	
Maximum pressure check:	**OK**		"OK" or "Warning"	

Table 8 Input for Cranemaster Excel Sheet

Approximately 250 Te is the maximum handling load for a SWL400T (Safe Working Load), therefore four heave compensation systems is used to handle the jacket. Each system will handle 137.5 Te, which gives an “OK” maximum pressure check.

Output for three different gas states are present in the excel calculation sheet. It shows the relation between stroke, load and internal pressure for the Cranemaster. The “Orcaflex values” sheet shows the values that can be implemented in Orcaflex. For the “Link Stiffness Table” (see Appendix 17), the “Isotherm Compression and Adiabatic Cycling” values are used. These values assume an isotherm compression to the mid-stroke and with adiabatic retraction and extension. They are normally used for passive heave compensation, seabed landings and resonance reduction.

4.2.6 Bumper System

The bumper attached to the support frame in Scenario 3 (see Figure 19) is modeled as an elastic solid shape in Orcaflex (see chapter 3.1.7). To find the contact stiffness that needs to be specified, the shape is considered as a spring with linear stiffness, k where the spring force, F is proportional to the contraction length, x:

$$F = kx \tag{4.1}$$

Here, the spring force F and x is analogous to the reaction force, F_R and penetration depth, d of the elastic solid. If Hooke’s law is valid and transverse strain is neglected, the reaction force may be written as a function of the spring stiffness:

$$F_R = kd = EA_c\varepsilon \tag{4.2}$$

where E is Young’s modulus of the material, A_c is the contact area and ε is the elastic strain of the shape. Recall from chapter 3.1.7 that the contact stiffness is defined as:

$$k_c = \frac{F_R}{dA_c} = \frac{E\varepsilon}{d} \tag{4.3}$$

It is seen that the contact stiffness is proportional to Young's modulus.

The contact stiffness of a steel bumper is found by removing the bumper and let the jacket collide with the steel frame. A stress-time distribution at the fixed end of the jacket leg may then be provided by Orcaflex. When the bumper is implemented, an iteration procedure is then used to find a contact stiffness, $k_{c,steel}$, that gives the same stress-time distribution at the fixed end as for the frame collision (see Figure 25).

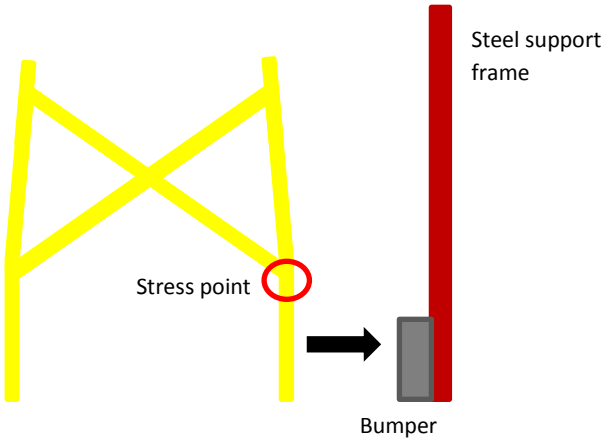

Figure 25 Modeling of Bumper System Using Stress in the Fixed End of the Jacket Leg

By using that the contact stiffness is proportional to Young's modulus, it is possible to obtain the contact stiffness for different bumper materials by the following relationship:

$$k_{c,x} = E_x \left(\frac{k_{c,steel}}{E_{steel}} \right) \tag{4.4}$$

The contact stiffness of several materials chosen for the bumper system is presented in Table 9. These values are specified for the bumper shape in Orcaflex for the different analyses.

Material	E [kPa]	Contact Stiffness [kN/m/m^2]
Rubber	100000	2,38E+01
Oak wood	1,10E+07	2,62E+03
Polypropylene	2,00E+06	4,76E+02
Steel	2,10E+08	5,00E+04

Table 9 Stiffness Properties of Different Materials Used for Bumper Analyses

4.3 Environment

Several environmental conditions need to be analyzed for this marine operation.

	Parameter	Values	Unit
Water depth	z_{seabed}	-30	[m]
Wave Directions	α_{wave}	0, 15, 30 and 40	[degrees]
Significant wave height	H_s	2 and 2.5	[m]
Wave periods	T_z	4 – 12	[s]
Current velocity	$v_{current}$	2	[knot]
Wind velocity	v_{wind}	12	[m/s]

Table 10 Environmental Conditions Used for Analysis

With four wave directions, two significant wave heights and nine different wave periods this made a total of 72 cases. All these cases were implemented into an excel file and batch processed through Orcaflex. This made it possible to run all the cases without separately implementing the different values into the program.

The JONSWAP spectrum is used, along with the mean values from Hasselmann. The same values are also specified in DNV Recommended Practice (4).

The wave spectrum specified in Orcaflex is used to generate a 3 hour long wave train. The wave preview feature is then used to find the time interval with the largest wave height during these three hours. Worst case intervals of 30 seconds are used, together with a build up period of 8 seconds. This build up period let the waves build up from calm water to the simulation origin.

4.4 Determining Loads

For Orcaflex to calculate the loads acting on the system, the input parameters and coefficients for Orcaflex must be found correctly. To determine the hydrodynamic force coefficients is not always straight forward. This chapter will therefore describe the methods used for calculating the coefficients of the jacket members (buoys).

4.4.1 Drag

The drag coefficients used for the calculations in Orcaflex are calculated according to DNV-RP-C205 (9). Both normal and tangential drag coefficients have to be specified for each of the ten cylinders of the buoy. The interaction between the jacket members is neglected.

The drag moments of inertia, A_{mi} , for each cylinder is set to zero, due to the cylinder discretization of the buoys when modeling the jacket members. Each buoy, representing one jacket member, is divided into 10 equal cylinders. The area moments of these cylinders is small, compared to the area moments of the whole buoy, and may be neglected. This approach hence implies that a discretized distribution of forces is applied over the whole buoy, instead of a smooth moment distribution, as illustrated in Figure 26. The Munk moment due to current forces are also not accounted for when determining drag moments.

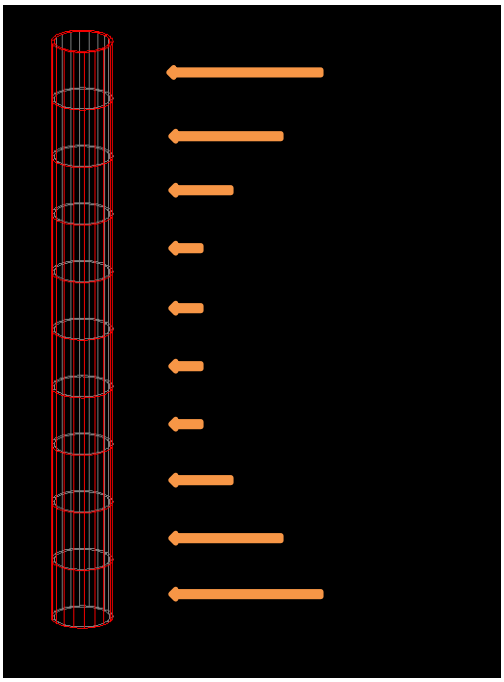

Figure 26 Discrete Force Distribution by Dividing the Buoy Into 10 Cylinders

4.4.1.1 Normal drag coefficients

The drag coefficients in x- and y- direction for a cylinder is equal, and are denoted the normal drag coefficient, C_{Dn}. It is assumed that the Reynolds number, R_n, is larger than 10^6, and that the KC-number is sufficiently large, so the flow can be described as post-critical. This assumption is reasonable as long as the cylinder is rough. Since the structure is to be installed, the only roughness on the jacket members will be due to fabrication imperfections, and marine growth is not taken into account. The roughness parameter for the jacket members is set to $\Delta = 3 \cdot 10^{-3}$ for highly corroded steel. This value is taken from DNV-RP-C205, chapter 6.7 (see Table 11). (9)

Table 6-1 Surface roughness

Material	*k (meters)*
Steel, new uncoated	5×10^{-5}
Steel, painted	5×10^{-6}
Steel, highly corroded	3×10^{-3}
Concrete	3×10^{-3}
Marine growth	5×10^{-3} - 5×10^{-2}

Table 11 Surface Roughness Constants from DNV

According to DNV the drag coefficient dependence of the surface roughness is then given as:

$$C_{DS}(\Delta) = \frac{29 + 4\log(\Delta)}{20} \tag{4.5}$$

The effect of the KC-number must be taken into account. However, the drag coefficient for steady current is equal to the asymptotic value for infinitely large KC-number. Hence, the effect of a steady in-line current added to the oscillatory pushes the drag coefficient C_D towards its asymptotic value, C_{DS}. Therefore, DNV states that when

$$v_c > 0.4\, v_m \tag{4.6}$$

C_D may be taken as the asymptotic value for steady current, C_{DS}. (9) Here, v_c is the current velocity and v_m is the maximum wave velocity for inflow on the cylinder. The current velocity for all scenarios is v_c = 2 knots = 1.029 m/s. This is sufficient to fulfill the stated condition above for all environmental conditions.

The bottom members of the jacket are not connected in the lower ends, and are free to move. According to DNV, the drag coefficients of the cylinders at the bottom of these buoys must then be corrected due to finite length. Table 12 shows the proposed correction factors for finite length.

Table 6-2 Values of reduction factor κ for member of finite length and slenderness.							
A - Circular cylinder – subcritical flow B - Circular cylinder – supercritical flow C - Flat plate perpendicular to flow							
l/d	*2*	*5*	*10*	*20*	*40*	*50*	*100*
A	0.58	0.62	0.68	0.74	0.82	0.87	0.98
B	0.80	0.80	0.82	0.90	0.98	0.99	1.00
C	0.62	0.66	0.69	0.81	0.87	0.90	0.95

Table 12 Reduction Factors by DNV due to Finite Length

In DNV-RP-C205 (9), it is stated that the l/d ratio should be doubled for member with one free end when determining the correction factor, κ. When both ends are connected to other members, the drag coefficient should be taken equal to the coefficient for an infinitely long member.

The drag area for each cylinder is determined as indicated in Figure 15. The full calculations for normal drag coefficients and drag areas are presented in Appendix 3.

4.4.1.2 Tangential drag coefficients

The tangential drag coefficients for the cylinders are calculated according to DNV-RP-C205 (9), as for the normal drag coefficients. In this DNV note, it is stated that a tangential drag coefficient, C_{Dt} , on an inclined cylinder may be calculated by use of the normal drag coefficient, C_{Dn}. The following formula is used for the calculation:

$$C_{Dt} = C_{Dn}\,(m + n\sin\alpha)\cos\alpha \qquad (4.7)$$

where m and n are coefficients based on published data, and α is the flow angle of attack on the inclined cylinder. For the jacket tubular members, $m = 0.03$ and $n = 0.05$ is used. These numbers are based on Table 13 from DNV, presented below (9).

	m	n
Bare cables, smooth cylinders	0.02-0.03	0.04-0.05
Faired cables	0.25-0.50	0.50-0.25
6-stranded wire	0.03	0.06

Table 13 Coefficients m and n for Calculation of Tangential Drag

The tangential drag area for one cylinder is taken as $A_z = \frac{\pi r^2}{2}$ where r is the cylinder radius. The full calculations for tangential drag coefficients and areas are presented in Appendix 4.

4.4.2 Added Mass

Like for the drag coefficients, the added mass coefficients and the added moments of inertia, $(AI)_i$, need to be calculated and specified in Orcaflex. The added moments are all set to zero, due to the same reason as for the drag moments (see chapter 4.4.1).

4.4.2.1 Normal added mass

The normal added mass coefficients for each cylinder are calculated according to DNV-RP-C205 (9). For cylinders far from the free surface, the added mass coefficient is found from:

$$C_A = \max\begin{cases}1.0 - 0.044(K_C - 3)\\ 0.6 - (C_{DS} - 0.65)\end{cases} \tag{4.8}$$

where K_C is the Keulegan Carpenter number and C_{DS} is the drag coefficient when the K_C number is accounted for. The K_C number is defined by:

$$K_C = \frac{VT}{D} \tag{4.9}$$

where V is the inflow velocity on the cylinder, T is the period of oscillation and D is the cylinder diameter (1).

Since the period of oscillation must be specified to find K_C it is obvious that the added mass coefficient will be frequency dependent. It is not possible to specify coefficients for different frequencies in Orcaflex. Since the frequencies of the incident waves hitting the jacket member are unknown and of different magnitudes at different time steps, a simplified approach is needed. A modal analysis is then performed in Orcaflex to get the oscillation period of the critical pendulum modes, for all scenarios. The critical periods obtained from these analyses are presented in Table 14. Using these periods of oscillation for the calculation of the added mass coefficients, assures that the added mass is correct when the jacket experience resonance and hence when the largest displacements take place.

Scenario	Period of critical modes
Scenario 1	5 s
Scenario 2	5,7 s
Scenario 3	5 s

Table 14 Periods of the Most Critical Modes Obtained from Modal Analysis

For cylinders close to or piercing the free surface the added mass coefficients will depend strongly on the frequency of oscillation, ω as illustrated in Figure 27 (9). The fully submerged cylinders that are close to the free surface are therefore checked for their h/r ratio, where h is the distance to the free surface and r is the radius of the cylinder.

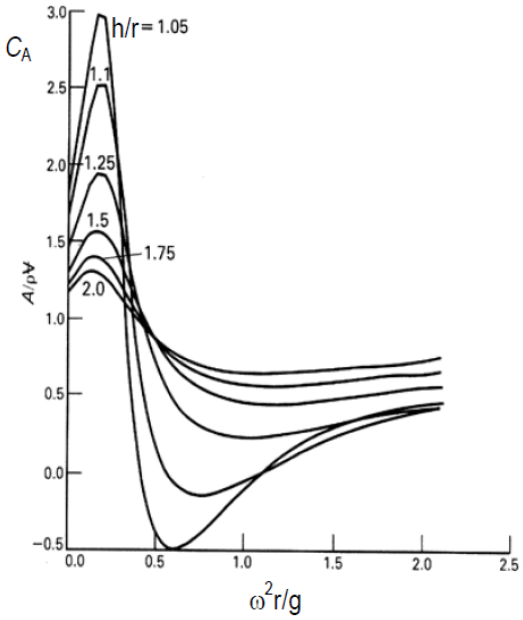

Figure 27 Added Mass Frequency Dependence for Cylinders Close to the Free Surface

Cylinders that are piercing the free surface have an added mass coefficient that can be calculated according to DNV by:

$$C_A = \frac{4}{\pi(kR)^2\sqrt{A_1(kR)}} - 1 \tag{4.10}$$

where k is the wave number, R is the cylinder radius and

$$A_1(kR) = J_1'^2(kR) + Y_1'^2(kR) \tag{4.11}$$

Here, J_1' and Y_1' are the first derivatives of the Bessel functions of first order. (9) The Bessel functions are defined as:

$$J_\alpha(x) = \sum_{m=0}^{\infty} \frac{(-1)^m}{m!\,\Gamma(m+\alpha+1)} \left(\frac{1}{2}x\right)^{2m+\alpha} \tag{4.12}$$

$$Y_\alpha(x) = \sum_{m=0}^{\infty} \frac{J_\alpha(x)\cos(\alpha\pi) - J_{-\alpha}(x)}{\sin(\alpha\pi)} \tag{4.13}$$

where $J_\alpha(x)$ and $Y_\alpha(x)$ are Bessel functions of first and second kind respectively. The gamma function, Γ is defined as $\Gamma(n) = (n-1)!$ if n is a positive integer (8).

In order to find the added mass coefficients, one needs to solve for k through the disperation relation given as

$$k = \frac{\omega^2}{g \tanh(kh)} \tag{4.14}$$

where h is the water depth. (1) This equation must be solved by iteration because it is an implicit equation with respect to k. This is done by a simple MATLAB program, *solvek.m*, presented in Appendix 9. k is then found for one specific wave frequency. Once again, the critical periods of Table 14 are used.

The full calculations of the normal added mass coefficients can be found in Appendices 5 and 6. The calculations of the Bessel functions derivatives for obtaining the added mass for the surface piercing cylinders are calculated in the MATLAB program *bessel.m* and may be found in Appendix 8.

4.4.2.2 Tangential added mass

The tangential added mass is calculated according to "DNV-RP-H103" (4). In chapter 4.6 of this recommended practice it is stated that a simplified approximation of added mass in heave of a three dimensional body with vertical sides may be applied:

$$A_{33} \approx \left[1 + \sqrt{\frac{1 - \lambda^2}{2(1 + \lambda^2)}}\right] \cdot A_{330} \tag{4.15}$$

where

$$\lambda = \frac{\sqrt{A_p}}{h + \sqrt{A_p}} \tag{4.16}$$

A_{330} is the added mass for a flat plate with a shape equal to the horizontal projected area of the object, A_p is the area of the submerged part of the object on a horizontal plane and h is the object height. The water moving with the structure is automatically included in Orcaflex, and does not need to be included manually. A_{330} is calculated from "DNV-RP-H103" – Appendix A (4).The full calculation procedure is here presented in Appendices 5 and 6.

4.4.3 Damping

The damping coefficients are like the added mass, strongly frequency dependent, and are difficult to calculate analytically. Figure 28 shows how added mass and damping in sway and heave depends on the frequency for a circular cylinder (1).

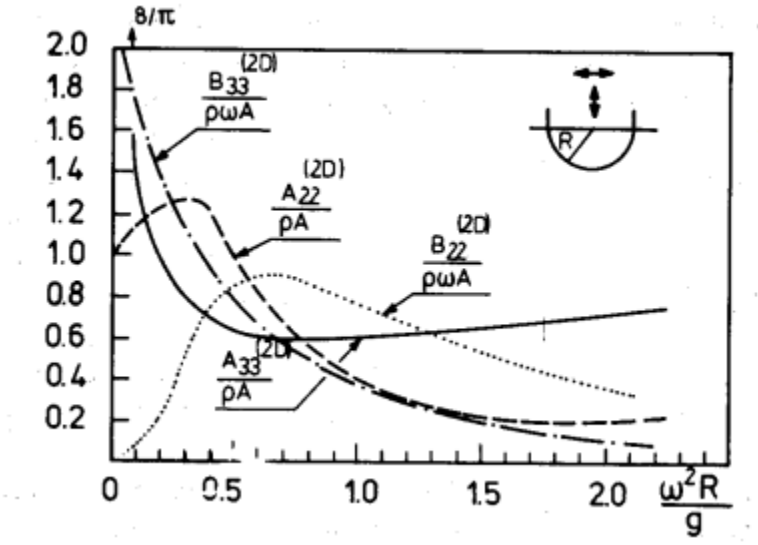

Figure 28 Addad Mass and Damping Coefficients for Varying Frequencies

The difficulty of the analytical calculation calls for a simplified consideration of the linear hydrodynamic damping. Since the drag force formally acts like a second order damping force, due to its dependency on the square velocity, this would arguably dominate the damping in general, especially for a jacket, which is a drag force dominated structure. Based on the assumption that this statement is valid, the remaining linear unit damping force is expressed as a percentage, ξ, of the critical damping of one jacket member, B_{cr}, where:

$$B_{cr} = 2\sqrt{(A+M)C} = 2(A+M)\omega_0 \tag{4.17}$$

such that

$$B = \xi B_{cr} \tag{4.18}$$

Here, A is the added mass and M is the mass of one member. C is the restoring force coefficient and ω_0 is the eigenfrequency of the system.

It is seen that the critical damping depends on the natural frequency as well as the damping and added mass. The simplified approach used for the added mass calculations (see chapter 4.4.2) will therefore be used, with the natural frequency values obtained from the modal analysis in Table 14. The calculation procedure is presented in Appendices 5 and 6.

4.5 Model Testing

Before running an analysis, it is important to validate that the jacket is modeled correctly. Some tests are run to ensure that the jacket has the right mass distribution and buoyancy properties.

4.5.1 Jacket Weight Test

To calculate the weight, the jacket is lifted above seawater and connected to a line with fixed end. By doing a static analysis the tension in the line is measured. The jacket rotates about 160 degrees around the vertical axis to equilibrium in the static analysis. Because the model is perfectly symmetrical it will be statically underdefined. There will be infinitely many equilibrium positions for the jacket. Orcaflex calculates the static position from iteration and then chooses an arbitrary equilibrium position. One option of solving this problem is to restrain the jacket against rotation about the z-axis by using two lines instead of one.

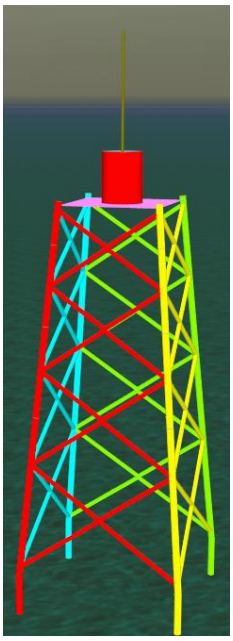

Figure 29 Jacket Buoyancy Test

	Jacket	Orcaflex
Mass	550 Te	552.5 Te
Difference		0,45 %

Table 15 Results of Jacket Weight Test

Table 15 shows the measured tension values versus the real jacket weight. A 0.45 % deviation from the actual weight is observed. No rotation in the horizontal plane implies a symmetric distribution of the weight. These results are satisfactory. One of the main reasons for the small difference in weight is the complex intersection between the different parts.

4.5.2 Buoyancy Test

The buoyancy also needs to be checked to ensure that the submerged jacket members are flooded. This is done by placing the jacket under water. The tension in the line is measured to ~500.5 Te. The buoyancy of the jacket is the displaced volume multiplied with the density of sea water ~50.5 Te. This is not very far from the buoyancy calculated by Orcaflex ~52.0 Te, so these results are satisfactory.

	Jacket calc	Orcaflex
Mass	550 Te	552.5 Te
Buoyancy	49.7 Te	51.8 Te
Tension in line	500.3 Te	500.7 Te
Difference	0,08 %	

Table 16 Results of Buoyancy Test

4.5.3 Center of Gravity Test

One of the ways to test the center of gravity is to measure the tension in two lines holding the jacket.

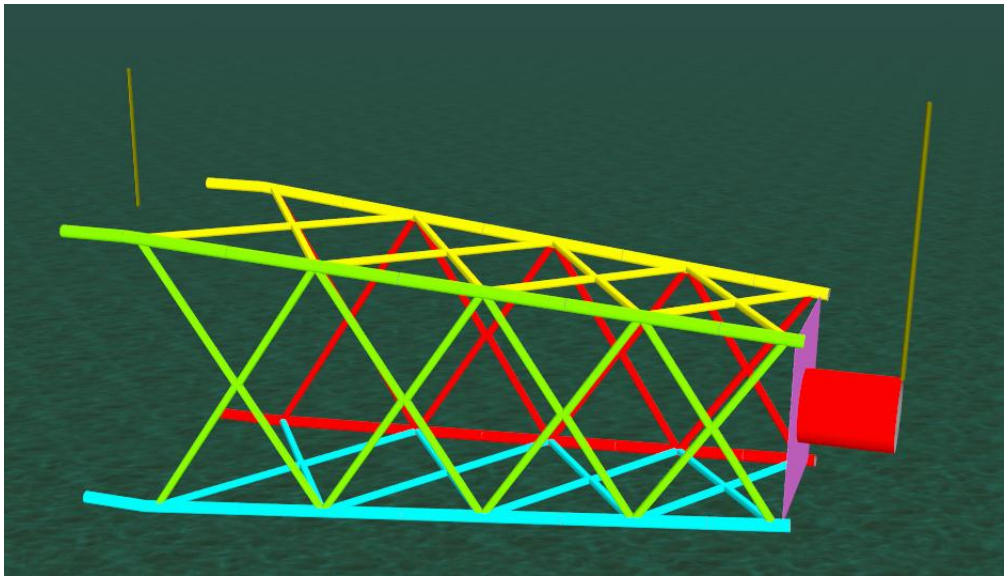

Figure 30 Center of Gravity Test

	Line bottom	Line Top
Tension	259,3 Te	294,2 Te
Length	0 m	56,7 m
Center of gravity	30,13 from bottom	

Table 17 Results of Center of Gravity Test

The center of gravity is found by moment considerations about the unknown moment equilibrium position. The calculations show that CoG is approximately 30 meters from the bottom of the jacket, which is reasonable.

4.6 Parameter Studies

A parameter study will show to what extent deviation in the different parameters will affect the behavior of the structure. Several studies of the hydrodynamic coefficients specified in Orcaflex are performed to get an indication of the uncertainty regarding the actual coefficients.

All of the parameter studies were done in the same wave conditions. The JONSWAP spectrum with a significant wave height of 2.5 meter and a period of 8 seconds is used. Also each test is done with a timescale of 32 seconds plus a build up time of 8 seconds.

4.6.1 Drag Coefficients

The calculated normal drag coefficients are in the region 0.95 to 1.00, while the axial are in the region 0.00 to 0.04. Because the axial drag coefficients are small, no parameter study is done with these numbers. The normal drag coefficients are set to 0.7, the calculated numbers from Appendix 3, and 1.3. Scenario 1a, with the bottom legs 10 m above sea level is used for the parameter analysis.

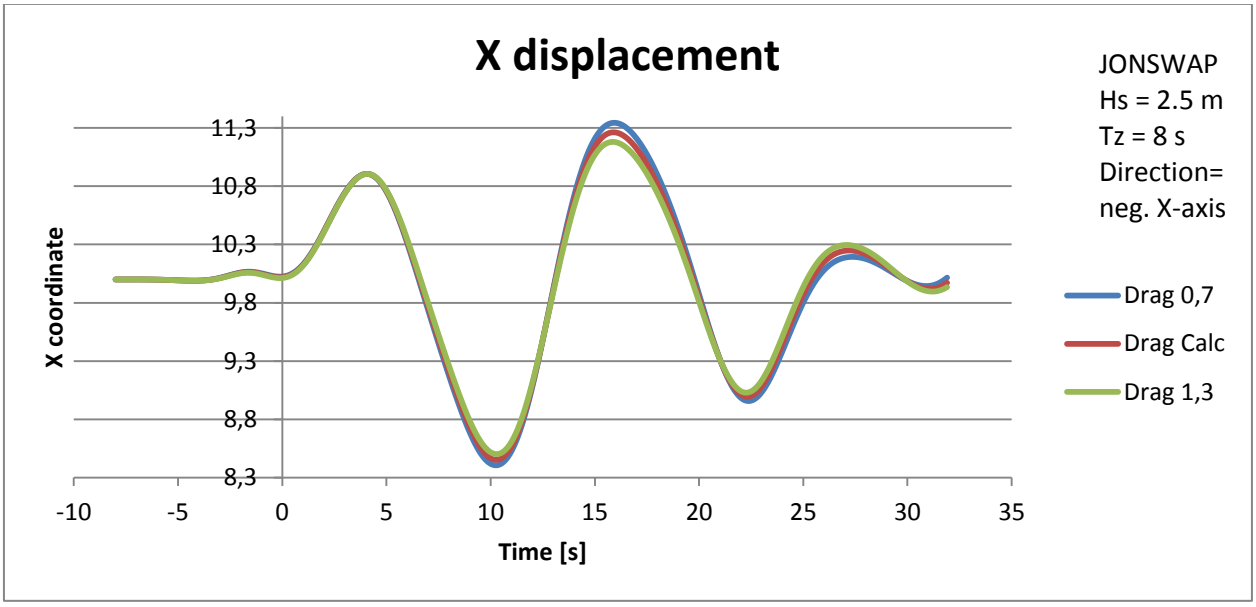

Figure 31 X Displacement for Varying Normal Drag

From Figure 31 one can see that the horizontal displacement of one of the bottom legs (1a). It is seen that lower drag coefficients results in larger amplitudes. However, the difference in amplitude is small for the various coefficients, so a change of drag coefficients in the indicated manner will not influence the behavior significantly. This is a good indication that even though the drag coefficients are not exact, the behavior is still reasonable.

4.6.2 Normal Added Mass Coefficient

As for the drag forces, a normal added mass coefficient study is done to see the effect it had on the behavior of the structure. With the same sea conditions, tests are done with Normal Added Mass coefficient respectively 0.7, 1 and 1.3.

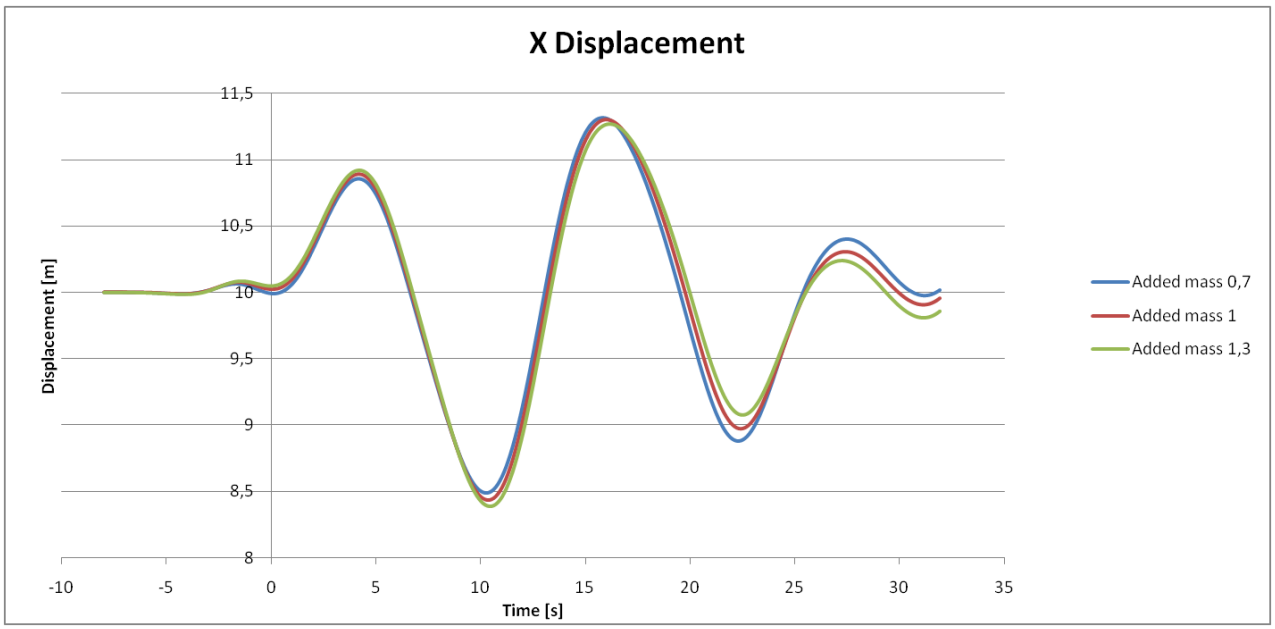

Figure 32 X Displacement for Varying Normal Added Mass

Figure 32 shows the horizontal displacement of the jacket for varying added mass. Deviation of ±0.2 meters can be observed in the horizontal direction with a normal added mass coefficient of 0.7 and 1.3. This is a quite narrow compared to the given coefficient interval. It should be noted that the difference in amplitude increases with time. This phenomenon can be explained by considering the inertia forces caused by the added mass. At the start of the simulation at -8 seconds, the system is in static equilibrium with no added mass. When the waves first hit the jacket structure, it will start moving as a cause of the wave forces. When the jacket starts oscillating, the system will get inertia as a consequence of the jacket mass, and the added mass. As the inertia starts to dominate the pendulum oscillation, the added mass radiation force will dissipate energy from the system to induce waves. The larger added mass coefficient, the larger the dissipation. That is why the larger added mass coefficient will result in lower displacements with time. This is a quite complicated manner, and the uncertainty of these coefficients may be of larger extent than indicated by Figure 32, due to the short time period.

The vertical motion of the structure is also important because the normal added mass coefficient affects the vertical behavior. It is seen from Figure 33 that the normal added mass coefficients have less effect on the z-displacement. This is logical, since the jacket is much more restrained against heave motion compared to the pendulum motion discussed above.

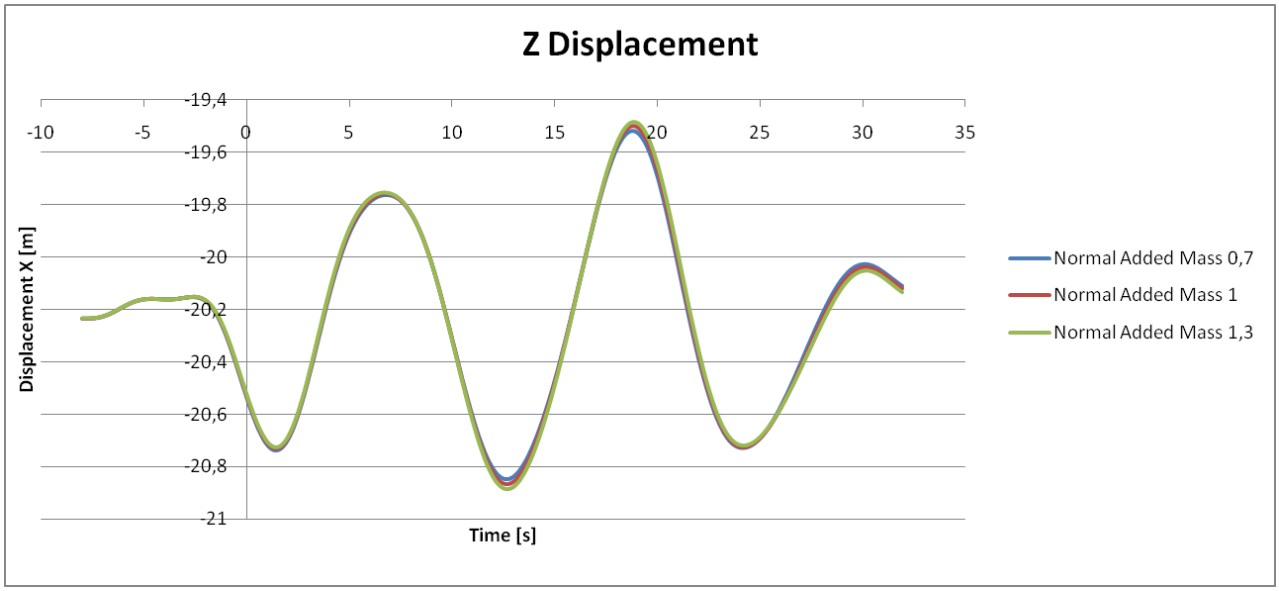

Figure 33 Z Displacement for Varying Normal Added Mass

4.6.3 Axial Added Mass Coefficient

When adjusting the axial added mass coefficient, there is virtually no change in behavior of the structure. This can be seen from Figures 34 and 35. As discussed above, the axial direction do not have much build up of inertia like the case for the normal directions (pendulum motion). This indicates that the uncertainty of the axial added mass coefficient specified is very small.

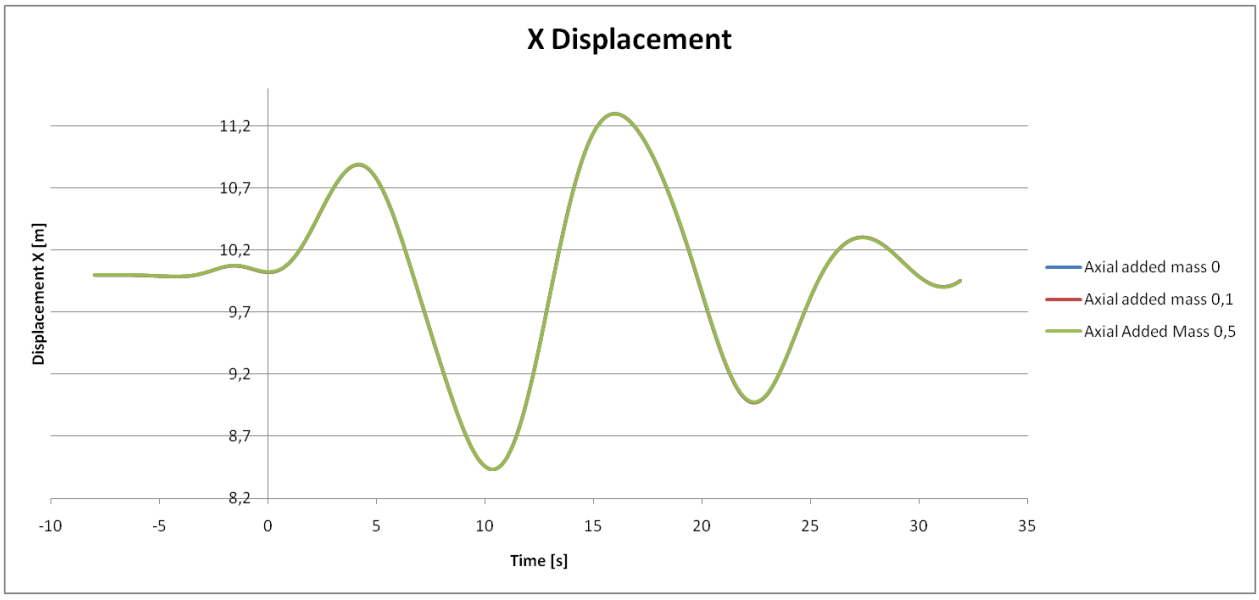

Figure 34 X Displacements for Varying Axial Added Mass

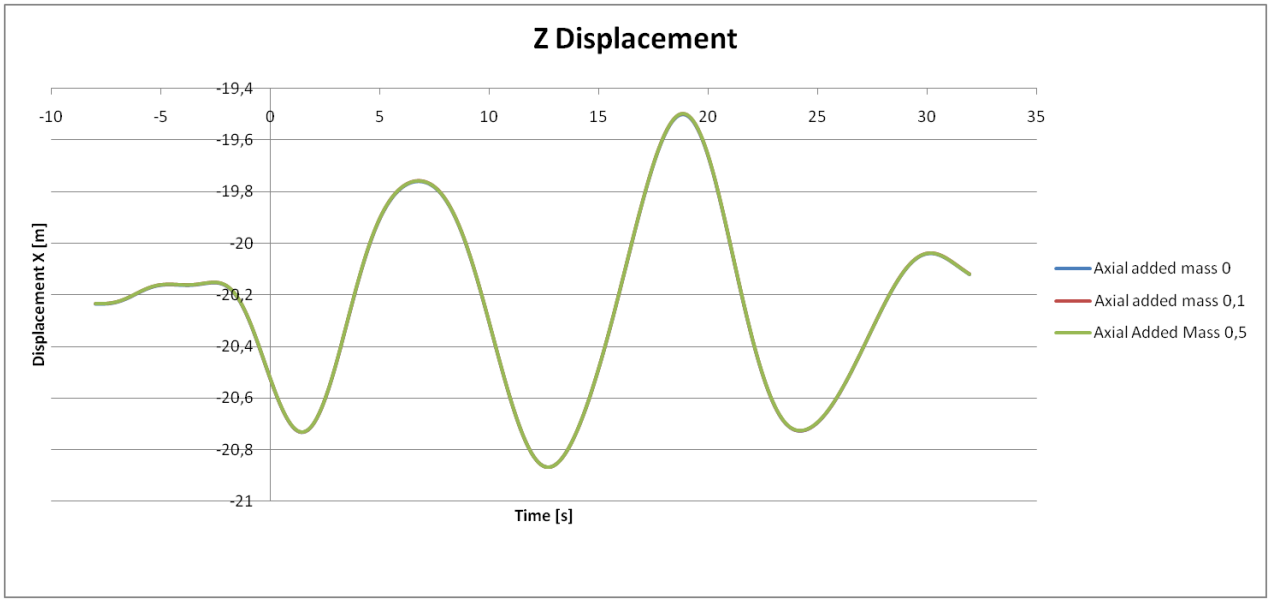

Figure 35 Z Displacements for Varying Axial Added Mass

4.6.4 Unit Damping Force

The hydrodynamic damping is an important parameter in the behavior of the jacket, but is difficult to determine analytically. Damping of respectively 0, 5 and 10 % of critical damping are used to see the effect of the specified damping force on the x-displacement. This parameter study shows that the unit damping force coefficients are of significant character considering the response. Compared to the other hydrodynamic forces, damping is probably the most uncertain parameter; it is hard to determine correctly from analytical considerations, and the motions are quite sensitive to changes in the damping parameter.

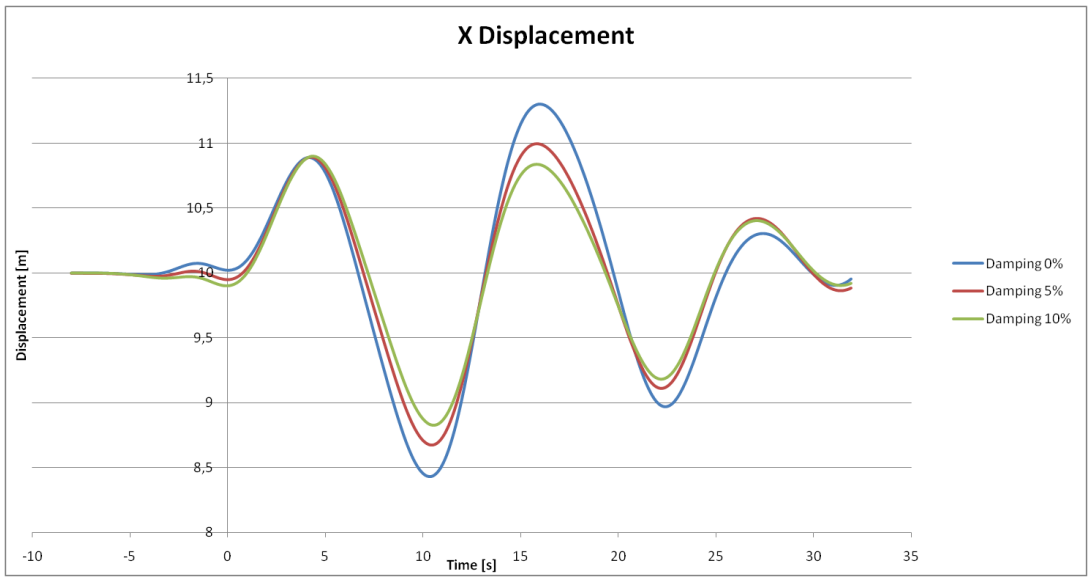

Figure 36 X Displacements for Varying Damping Coefficients

4.7 Analysis

The system to be analyzed consists of four subsystems; the barge, the jacket, the support frame and the connecting lines (see Figure 37).

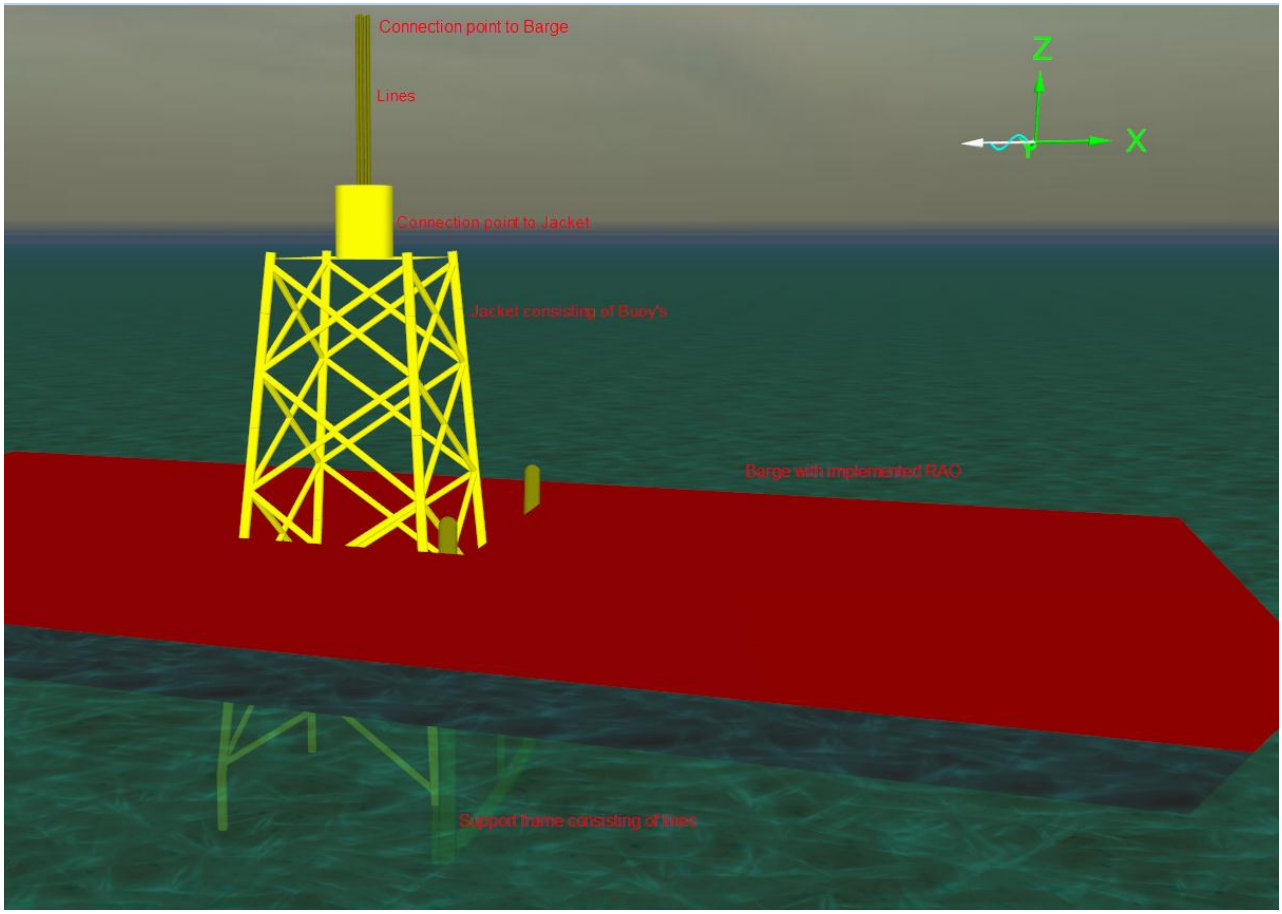

Figure 37 Overview of Methods Used for Modeling

Table 18 shows what objects are used in the different subsystems, where to find the theory surrounding the matter and how they are connected.

Subsystem	Objects used	Theory	Connected to
Jacket	6D Buoys	3.1.1 Buoys	Lines
Lines	Line	3.1.3 Lines	Jacket, Barge
Barge	Vessel	3.1.2 Vessels	Free
Support Frame	Line	3.1.3 Lines	Barge

Table 18 Overview of Methods Used for Modeling

4.7.1 Time Domain Response Analysis

Response analyses for the critical scenarios identified in chapter 4.1 are performed in Orcaflex using the generalized α-method described in chapter 2.4.1.2. The response analyses for the different scenarios are

performed for different environmental conditions. A matrix which defines the different cases of load parameters is established and presented in Table 19.

CASE	Wave dir. [deg]	Hs [m]	Tz [s]	Wind [m/s]	Current [knots]
1	180	2	4	12	2
2	195				
3	210				
4	225				
5	180	2	5	12	2
6	195				
7	210				
8	225				
9	180	2	6	12	2
10	195				
11	210				
12	225				
13	180	2	7	12	2
14	195				
15	210				
16	225				
17	180	2	8	12	2
18	195				
19	210				
20	225				
21	180	2	9	12	2
22	195				
23	210				
24	225				
25	180	2	10	12	2
26	195				
27	210				
28	225				
29	180	2	11	12	2
30	195				
31	210				
32	225				
33	180	2	12	12	2
34	195				
35	210				
36	225				

CASE	Wave dir. [deg]	Hs [m]	Tz [s]	Wind [m/s]	Current [knots]
37	180	2,5	4	12	2
38	195				
39	210				
40	225				
41	180	2,5	5	12	2
42	195				
43	210				
44	225				
45	180	2,5	6	12	2
46	195				
47	210				
48	225				
49	180	2,5	7	12	2
50	195				
51	210				
52	225				
53	180	2,5	8	12	2
54	195				
55	210				
56	225				
57	180	2,5	9	12	2
58	195				
59	210				
60	225				
61	180	2,5	10	12	2
62	195				
63	210				
64	225				
65	180	2,5	11	12	2
66	195				
67	210				
68	225				
69	180	2,5	12	12	2
70	195				
71	210				
72	225				

Table 19 Parameter Matrix Defining the Different Cases for Analysis of Scenarios 1 and 2

All the scenarios are analyzed with zero damping. Since the structure is drag dominant and Morison's equation is used for calculating the excitation loads, it is assumed that the drag forces will dominate the damping behavior, as a nonlinear damping force proportional to the velocity squared. The added mass coefficients are calculated customary for each scenario (see chapter 4.4.2).

4.7.1.1 Scenarios 1and 2

Analyses of Scenario 1a, 1b, 2a and 2b are each performed for all 72 cases in the parameter matrix in Table 19. The maximum displacements at the bottom of the jacket are collected from the analyses.

4.7.1.2 Scenario 3

Only cases with the most critical periods with respect to high excitation are analyzed for this scenario. The two worst cases with H_S = 2,5 m and T_Z = 5 and 8 s are used to examine the bumper effect for

different materials. The current velocity will damp the impact between the jacket and the support frame significantly when the barge maneuvers against the current during installation. To investigate the effect of a bumper system attached to the support frame, the current velocity is set to zero to get larger impacts which are easier to investigate. The cases are presented in a parameter matrix for Scenario 3 in Table 20 below.

CASE	Wave dir. [deg]	Hs [m]	Tz [s]	Wind [m/s]	Current [knots]
341	180	2,5	5	12	0
353	180	2,5	8	12	0

Table 20 Parameter Matrix Defining the Different Cases for Analysis of Scenario 3

It is important to note that the added mass and drag coefficients are unchanged from Scenarios 1a and 1b. These coefficients will therefore not be analytically correct according to DNV, due to the assumption of strong current when calculating the added mass and drag (see chapters 4.4.1 and 4.4.2). However, the effect of the bumper system may still be investigated, and the results will give a brief overview of the bumper properties of the different materials when compared with each other.

The stress-time distribution in the fixed end of the jacket leg is collected from the analyses. Each case is simulated first with no bumper, then with 3 bumper materials with different stiffness properties.

4.7.2 Modal Analysis

The natural frequencies of the pendulum motions of the system will change during lowering due to the change in line length and draught. Modal analyses are performed at different stages of the lowering to investigate this effect. The mode shapes and natural frequencies of the whole system are calculated by Orcaflex using the eigensolver algorithms described in chapter 2.4.1. These are calculated for each of the scenarios in Table 5.

Even though the parameter studies indicates that the jacket motions not are particularly sensitive to the added mass coefficients, the modal periods of the critical modes (pendulum motions) seems to be more affected. The added mass calculated for response analysis will change slightly with the critical frequencies from Table 14. This will again affect the critical periods. Investigation of the natural periods iteration is therefore required to find the correct values. This is done manually by running modal analysis in Orcaflex, use the new periods in the calculation for added mass and then run a new analysis with the new added mass values. The damping coefficients are set to zero due to drag dominance.

5 Results

The displacement of the jacket foundation under the different sea states are here presented with graphs covering the significant wave height, wave period and the incoming wave direction. The main focus is to describe the extremes of a chosen point on the jacket in all directions.

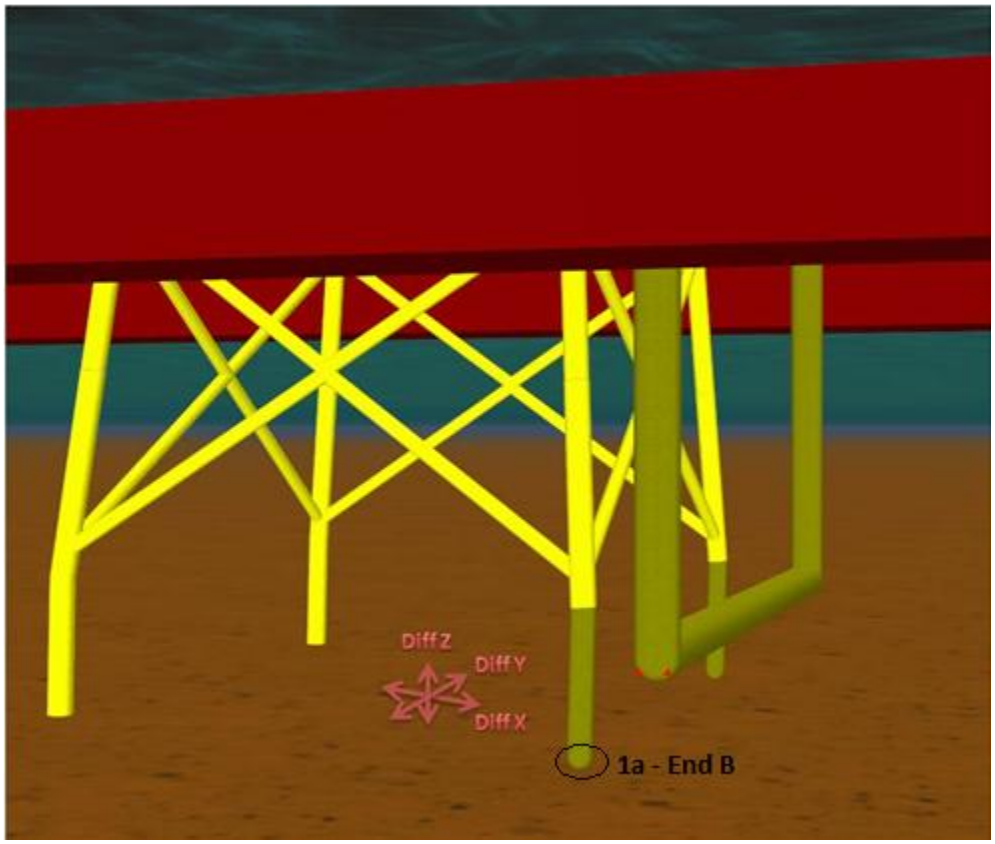

Figure 38 Points Used for Presentation of Results

The point used to describe the motion in the parametric results is the midpoint between the bottom jacket legs (1a -1d). This point is indicated in Figure 38 with a purple star. The displacements are described is by finding the maxima and minima in each direction over the time interval of the simulation. The difference between these points shows the most critical possible motion of the jacket.

For the two sea states with the most critical behavior, the displacements are presented as time history plots. The displacements used in these plots are the displacements at End B of element 1a (see Figure 38). This is Case 41 and 53, with wave period 5 and 8 seconds, significant wave height 2.5 meters and wave direction 0 degrees respectively. For these two cases plots and spectra are presented and shortly described.

In Scenario 1b and 2b only the vertical displacement is considered. This is because the effect of the heave compensation system is to be analyzed.

5.1 Scenario 1

Scenario 1a is considered a critical phase due to possible collision between the jacket and the support frame. Due to current in the negative x- direction this does not occur in any of the sea states (see Appendix 15). Therefore only the displacement of the jacket can be investigated.

In Scenario 1b, a heave compensation system is implemented. The main reason to use such a system is to damp and minimize the vertical motions of the structure. The results will therefore focus on the vertical displacements only.

Here plots with respect to the different sea states are presented. The motions in z-direction are plotted for Scenario 1a and 1b, without and with heave compensation respectively. All other plots are plotted only for Scenario 1a. The values for the plot along with x,y,z – velocities and accelerations can be found, together with the full results for Scenario 1a and 1b, in Appendix 10 and 11 respectively.

5.1.1 Displacement in X-direction

The motion in the x-direction is worst when the heading angle is zero degrees (see Figures 39 and 40). When the heading angle increase, the motions decrease. Two significant peaks are present at wave periods 5 and 8 seconds. Only an increase in displacement with an increase in significant wave height is present, no difference in the general shape of the plot.

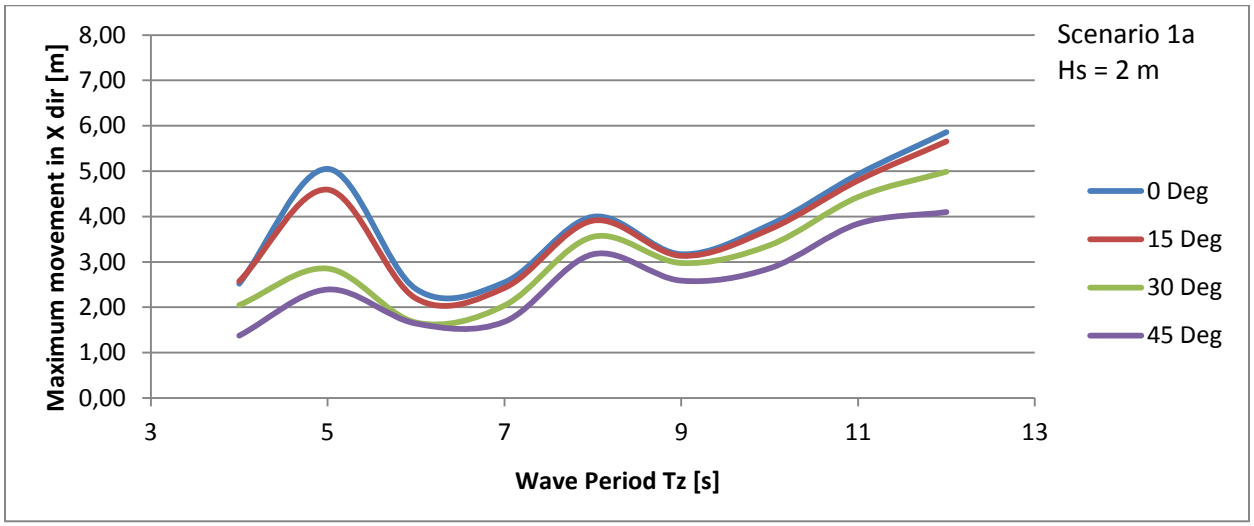

Figure 39 Scenario 1a: Maximum Displacements in X Direction for Various Wave Directions and Periods. Hs = 2 m

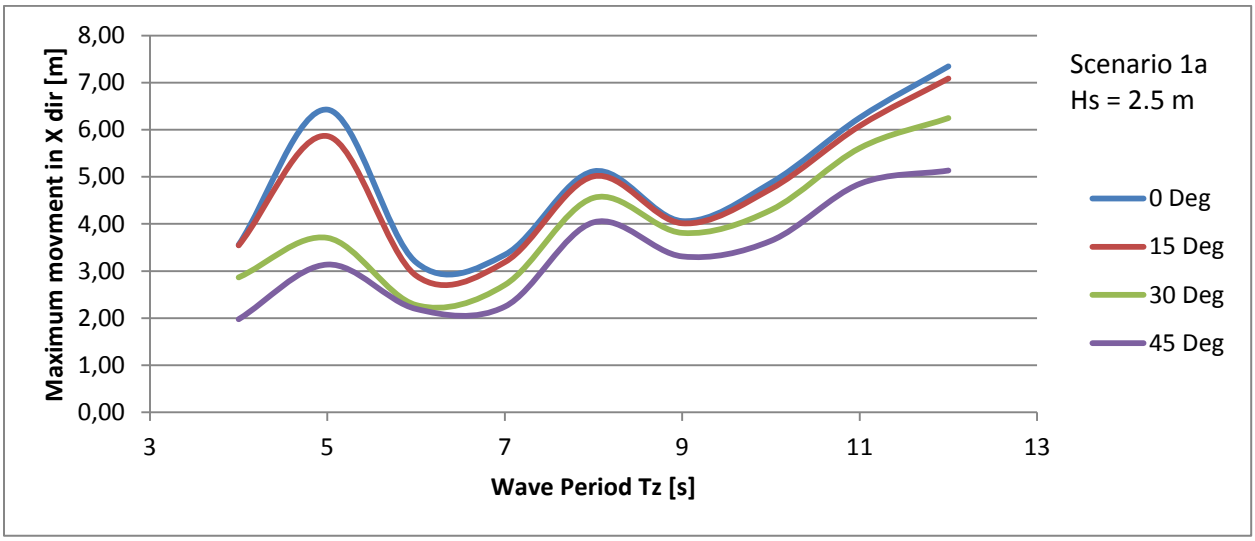

Figure 40 Scenario 1a: Maximum Displacements in X Direction for Various Wave Directions and Periods. Hs = 2,5 m

5.1.2 Displacement in Y-direction

Figures 41 and 42 show the displacements in y-direction for Scenario 1a. No displacement is present when the heading angle is zero, as expected. The displacement increases with heading angle. As in x-direction a peak at wave period 5 seconds is present, while the peak at 8 seconds is not that significant.

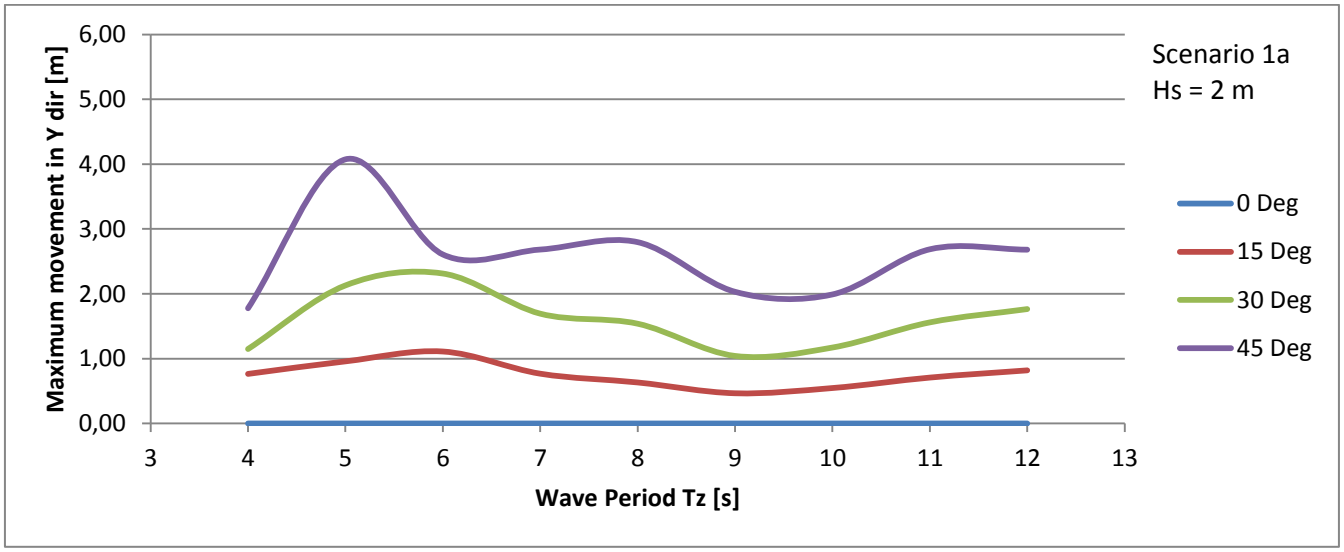

Figure 41 Scenario 1a: Maximum Displacements in Y Direction for Various Wave Directions and Periods. Hs = 2 m

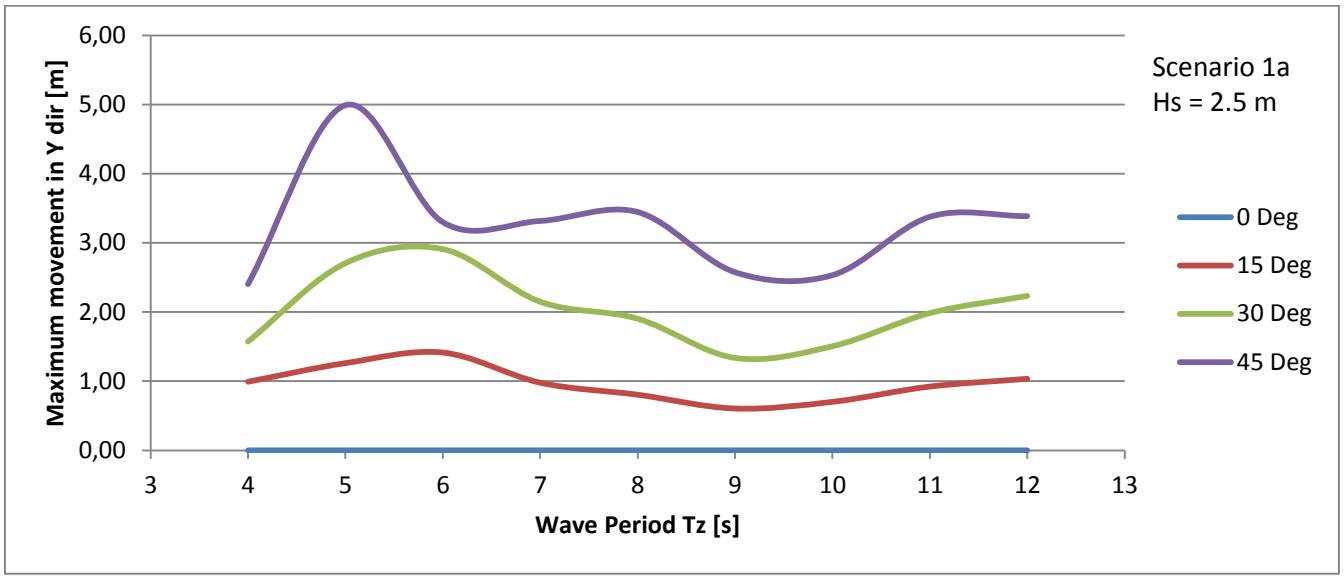

Figure 42 Scenario 1a: Maximum Displacements in Y Direction for Various Wave Directions and Periods. Hs = 2,5 m

5.1.3 Displacement in Z-direction

The vertical displacement increases with wave period, with two significant peaks at wave period 5 and 8 seconds (see Figures 43 and 44). The heading angle only affects the motion at small wave periods.

The vertical displacements are larger with heave compensation than without the system for all sea states. There seem to be little difference in the general shape of the graph when comparing the different scenarios.

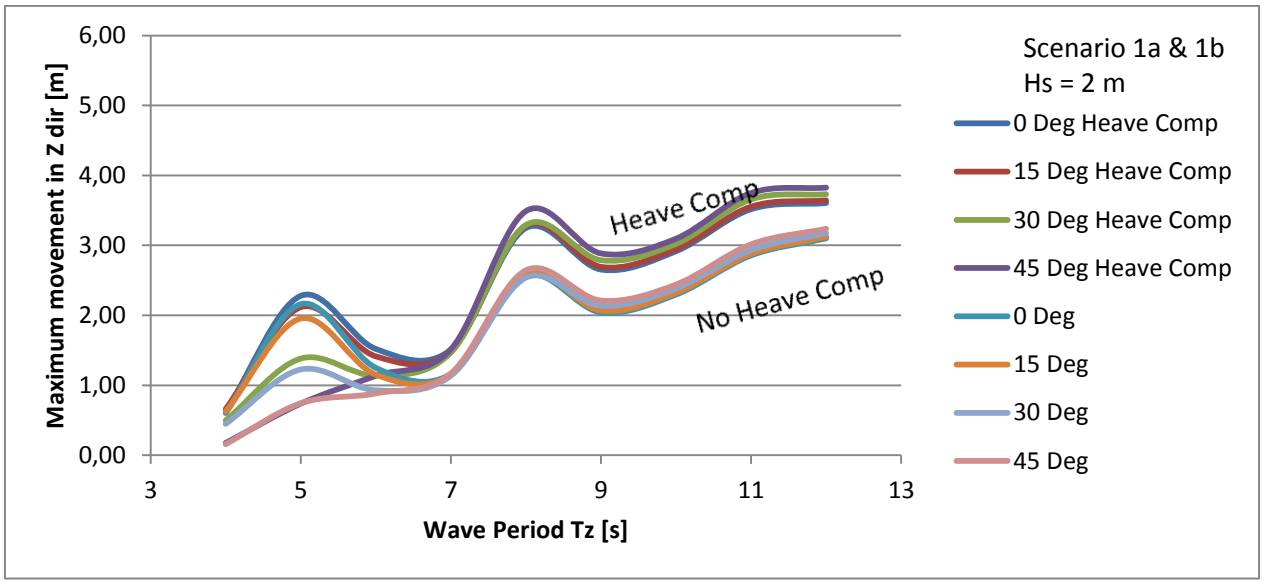

Figure 43 Scenario 1: Maximum Displacements in Z Direction with and without Heave Compensation. Hs = 2 m

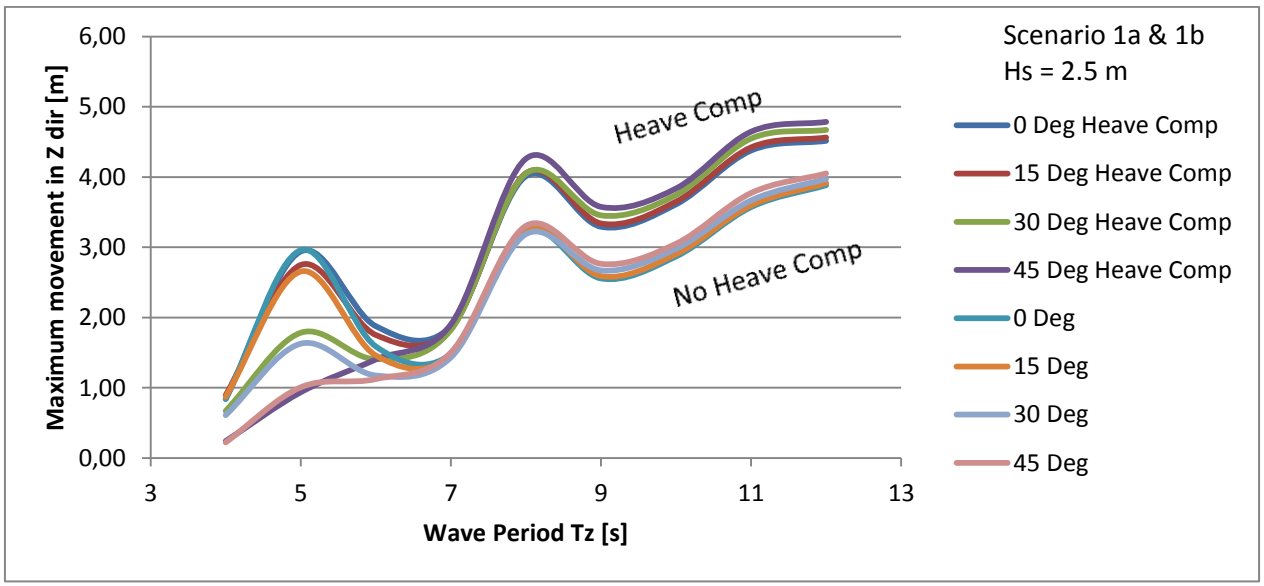

Figure 44 Scenario 1: Maximum Displacements in Z Direction with and without Heave Compensation. Hs = 2 m

5.1.4 Time Plot of Case 41

Case 41 is considered a critical case in the behavior of the jacket. A further analysis of the behavior is therefore to be performed. The spectral density is used to identify the different periodicities. There will be no displacement in y direction due to zero heading angle, therefore only the X-displacement is investigated.

5.1.4.1 Horizontal behavior

Figures 45 and 46 show the horizontal behavior of the jacket motion and the spectral density of the oscillations. The spectrum shows peaks at:

Peak	Period [s]
1	37,879
2	6,317

Table 21 Scenario 1a, Case 41: Peaks in Spectral Density of Horizontal Motions

The horizontal behavior is dominated by two periods, with one close to the incoming wave period and one low frequency oscillation.

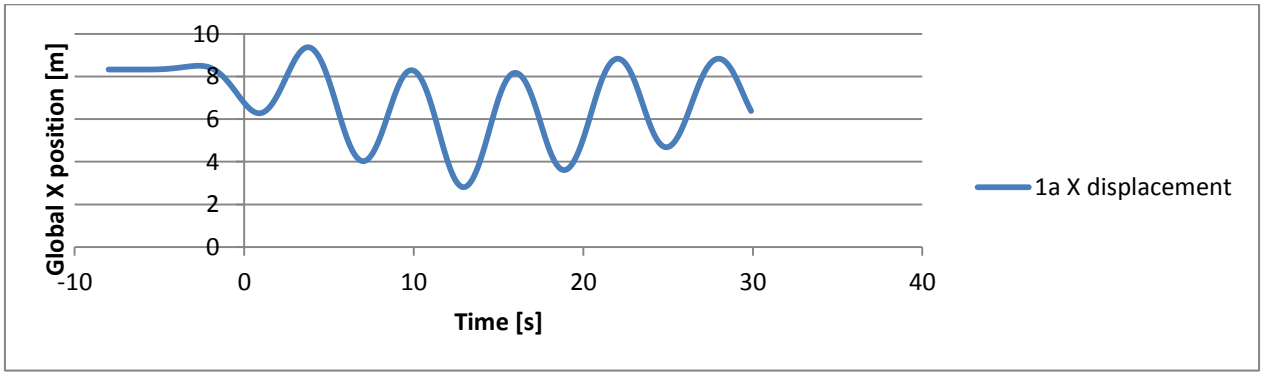

Figure 45 Scenario 1a, Case 41: Time History Plot of Global X Position at Jacket Member 1a

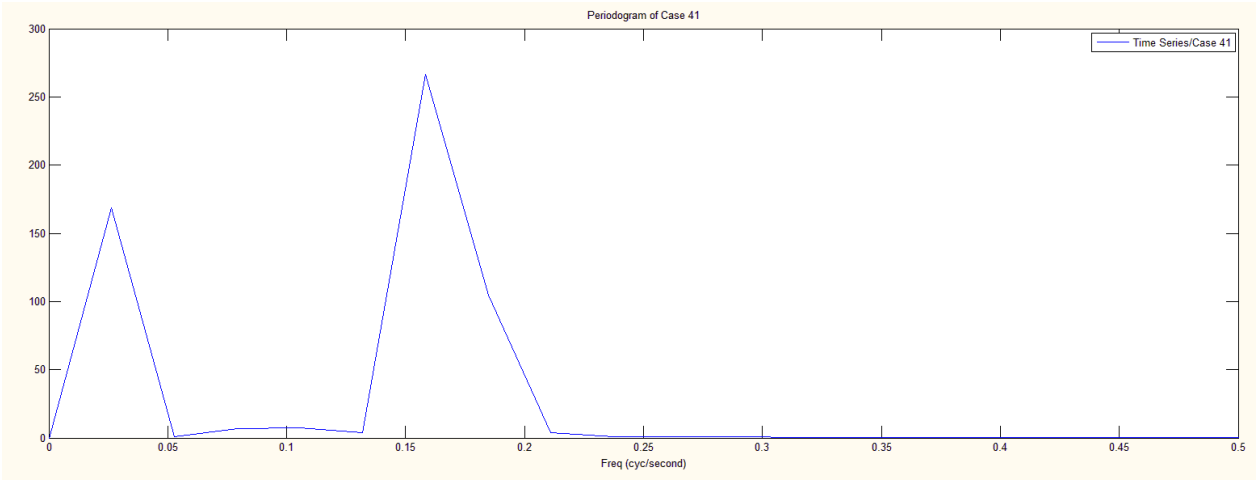

Figure 46 Scenario 1a, Case 41: Spectral Density of Horizontal Motions

5.1.4.2 Vertical behavior

The vertical behavior is a bit more complicated than the horizontal. One oscillation is dominant with period 5,336 and one high frequency is also notable at 2,915 seconds (see Figures 47 and 48).

Peak	Period [s]
1	7,582
2	5,336
3	2,915

Table 22 Scenario 1a, Case 41: Peaks in Spectral Density of Vertical Motions

The vertical displacement change when applying a heave compensation system. The jacket sinks approximately 1 meter due to initial stretching, and there seems to be some varying oscillations.

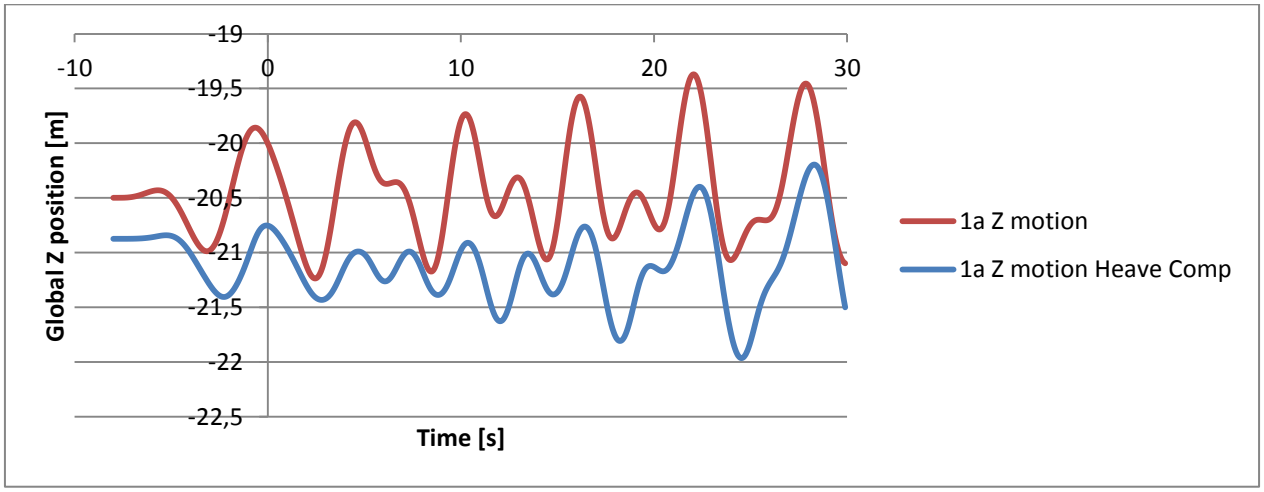

Figure 47 Scenario 1, Case 41: Time History Plot of Global Z Position at Jacket Member 1a with and without Heave Comp

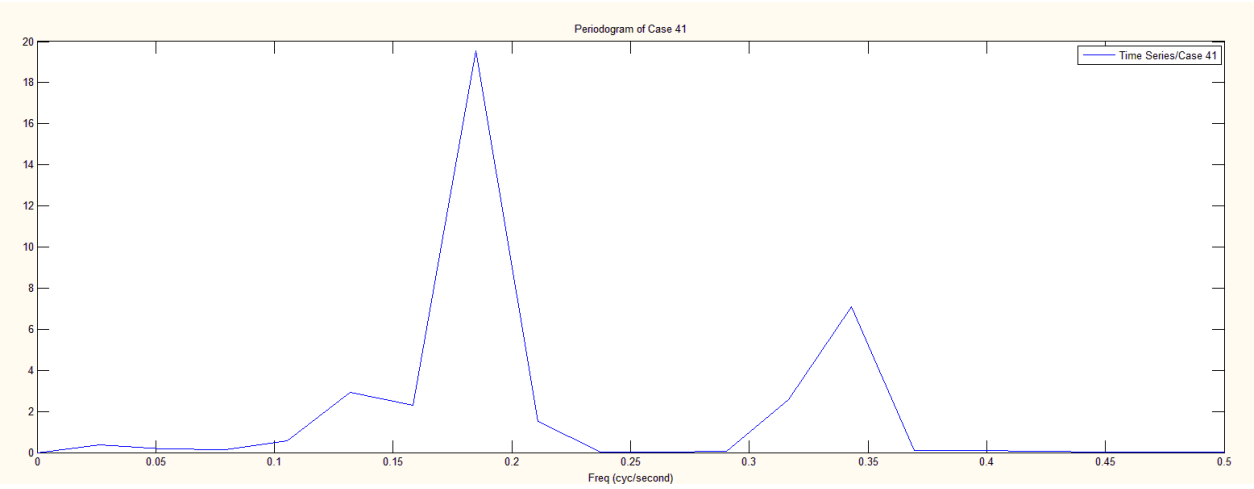

Figure 48 Scenario 1a, Case 41: Spectral Density of Vertical Motions

5.1.5 Time Plot of Case 53

Case 53 is also a critical case, covering the other peak visible in the different plots of displacement (Figures 39 and 40). Case 53 looks a bit more complicated than the behavior of Case 41 when considering the smoothness of the oscillations.

5.1.5.1 Horizontal behavior

The horizontal behavior in Case 53 is a bit more complicated than the behavior in Case 41 (see Figure 49). While Case 41 only is dominated by two significant periods, Case 53 has a wider spectrum of different periods with one dominating at 9,477 seconds. The low frequency oscillation at 37,879 seconds is both present in the horizontal behavior of Case 41 and Case 53.

Peak	Period [s]
1	37,879
2	9,477
3	5,414

Table 23 Scenario 1a, Case 53: Peaks in Spectral Density of Horizontal Motions

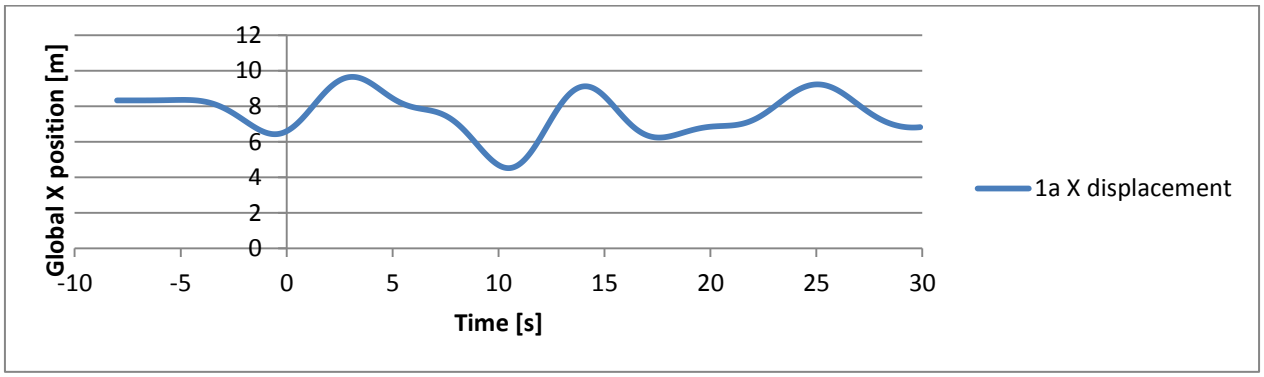

Figure 49 Scenario 1a, Case 53: Time History Plot of Global X Position at Jacket Member 1a

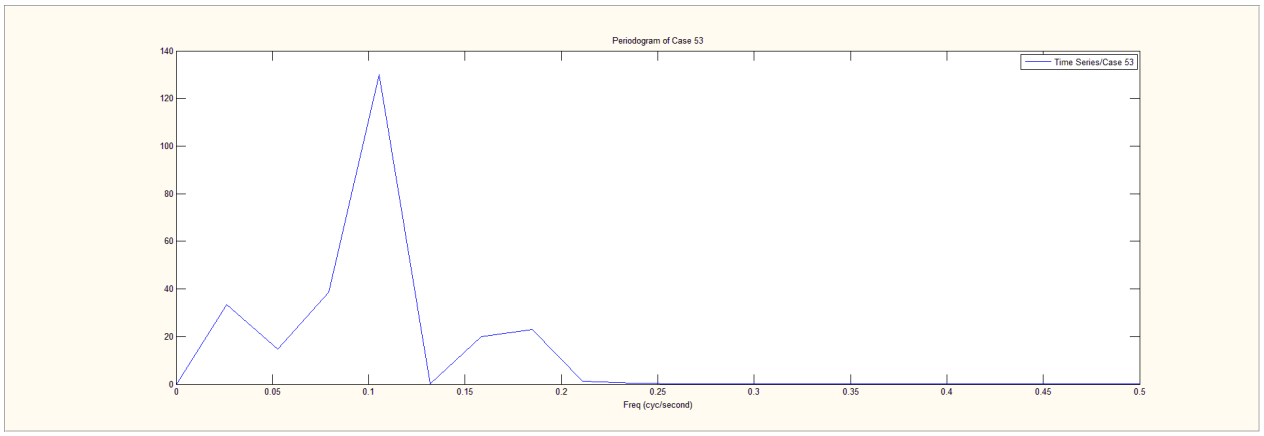

Figure 50 Scenario 1a, Case 53: Spectral Density of Horizontal Motions

5.1.5.2 Vertical behavior

The vertical behavior of Case 53 is very similar to the horizontal behavior. The only difference is the period of 9,477 seconds is more dominant (see Figures 51 and 52).

Peak	Period [s]
1	37,879
2	9,477
3	5,414

Table 24 Scenario 1a, Case 53: Peaks in Spectral Density of Vertical Motions

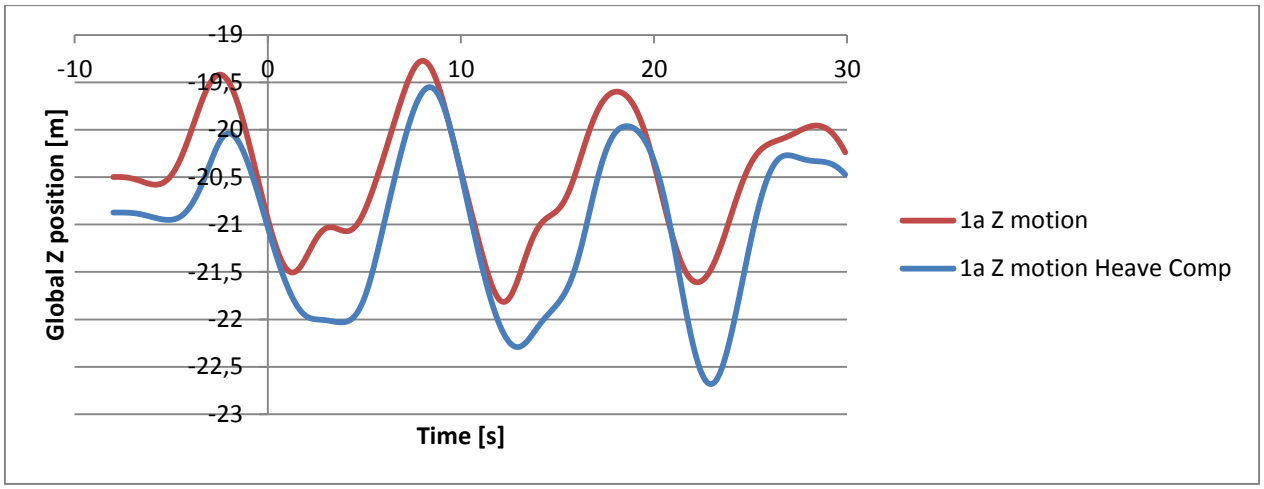

Figure 51 Scenario 1, Case 53: Time History Plot of Global Z Position at Jacket Member 1a with and without Heave Comp

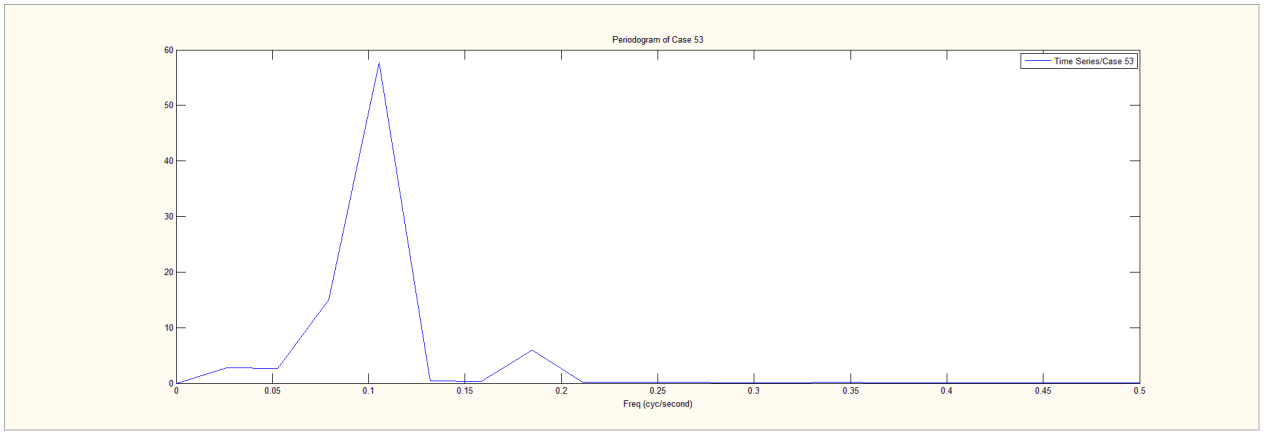

Figure 52 Scenario 1a, Case 53: Spectral Density of Vertical Motions

5.2 Scenario 2

In scenario 2a, the jacket is approximately 3 meters above the seabed. This is a critical phase of the installation when large motions of the jacket will make it difficult to place it on the seabed. Full results for this scenario may be found in Appendix 12.

In Scenario 2b, a heave compensation system is implemented. The results will therefore focus on the vertical displacements only. Full results for this scenario may be found in Appendix 13.

Here, the results from the different sea states are presented, together with time history plots for the worst cases, Case 41 and 53. The motions in z-direction are plotted for Scenario 2a and 2b, without and with heave compensation. All other plots are plotted only for Scenario 2a.

5.2.1 Displacement in X-direction

Figures 53 and 54 show the displacements in x-direction for Scenario 2a. As in scenario 1a, there are two peaks at wave period 5 and 8 seconds. The largest displacement is present when zero heading angle. Increasing significant wave height only increases the motion. No difference in the general shape of the graph is present.

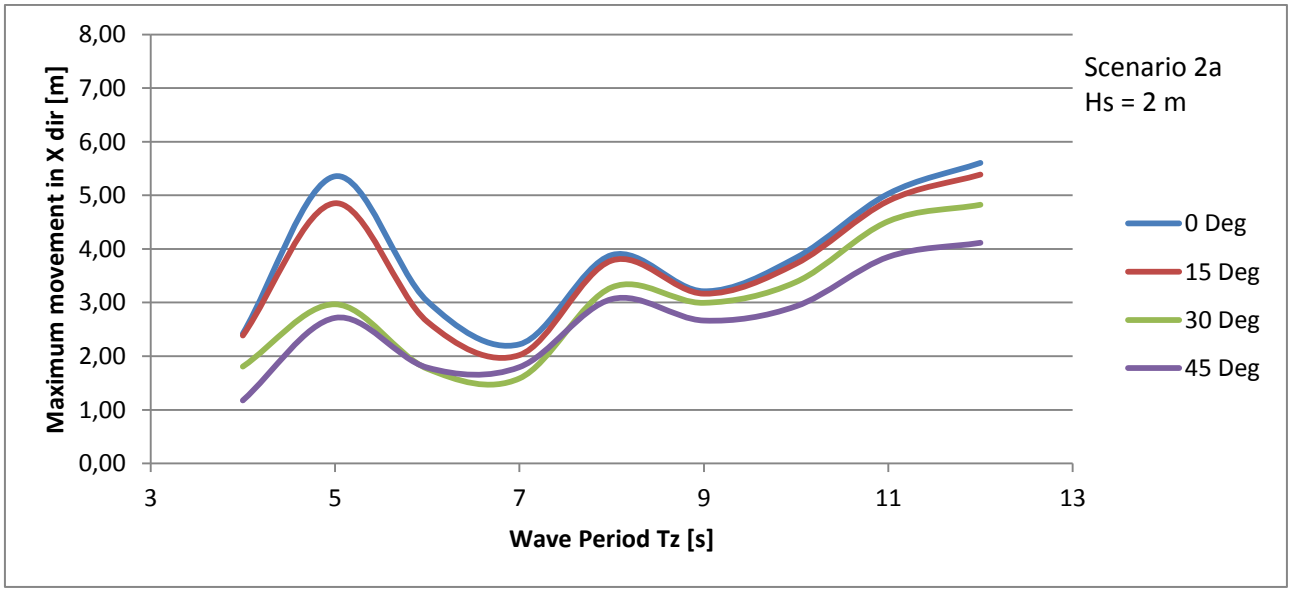

Figure 53 Scenario 2a: Maximum Displacements in X Direction for Various Wave Directions and Periods. Hs = 2 m

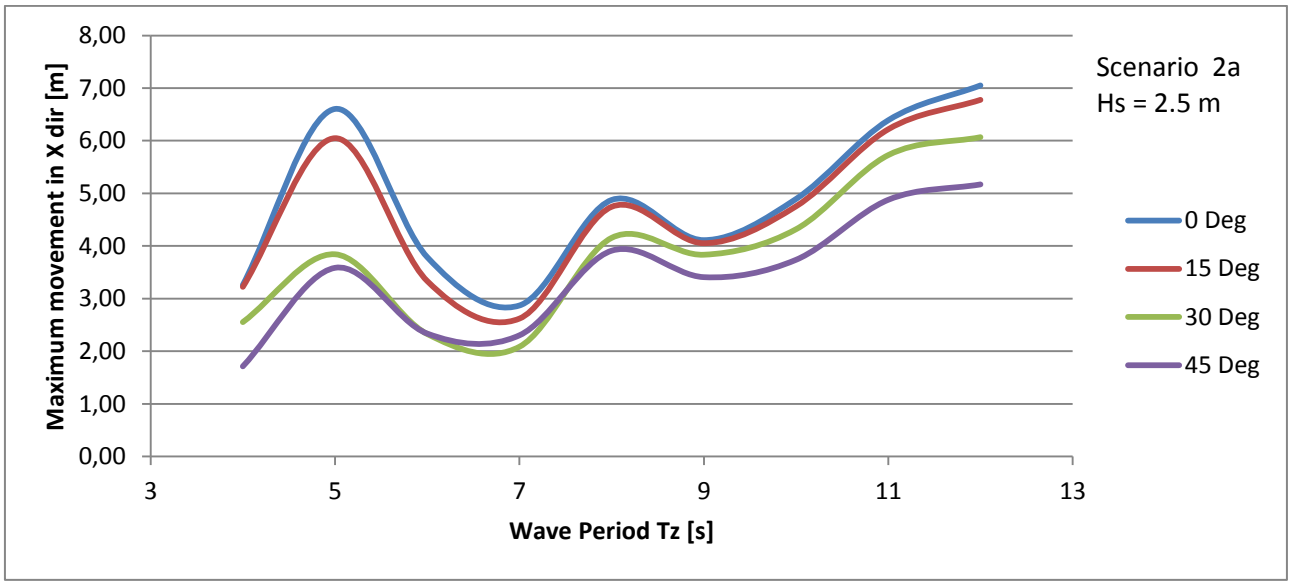

Figure 54 Scenario 2a: Maximum Displacements in X Direction for Various Wave Directions and Periods. Hs = 2,5 m

5.2.2 Displacement in Y-direction

The displacement in Y direction is very similar Scenario 1. Only one peak is present at wave period 5 seconds (see Figures 55 and 56).

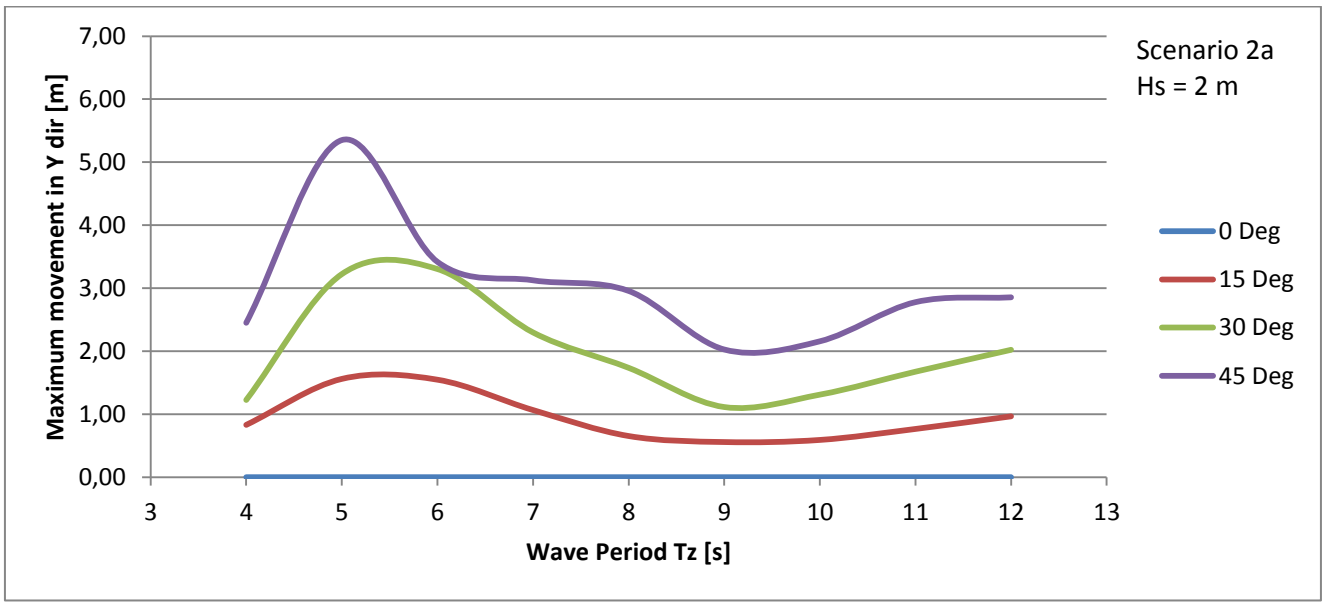

Figure 55 Scenario 2a: Maximum Displacements in Y Direction for Various Wave Directions and Periods. Hs = 2 m

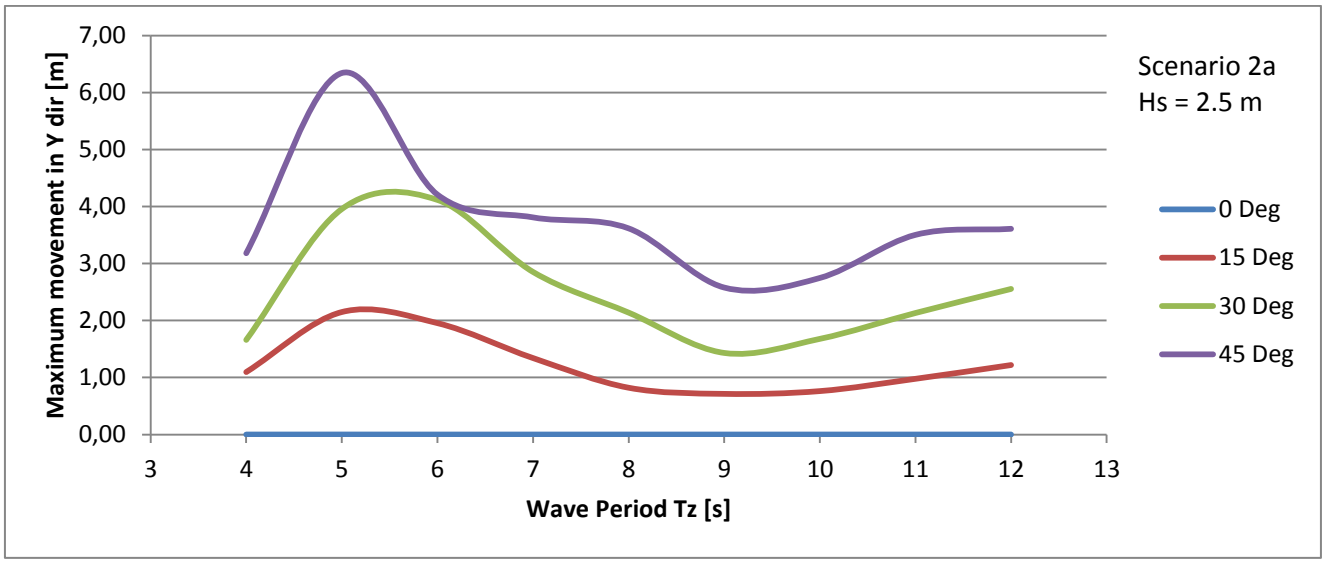

Figure 56 Scenario 2a: Maximum Displacements in Y Direction for Various Wave Directions and Periods. Hs = 2,5 m

5.2.3 Displacement in Z-direction

The vertical displacement has two significant peaks at wave periods 5 and 8 seconds (see Figures 57 and 58). The displacement increases with increasing wave period.

When applying a passive heave compensation system the displacement seems to increase. Lowering the jacket does not improve the heave compensation system.

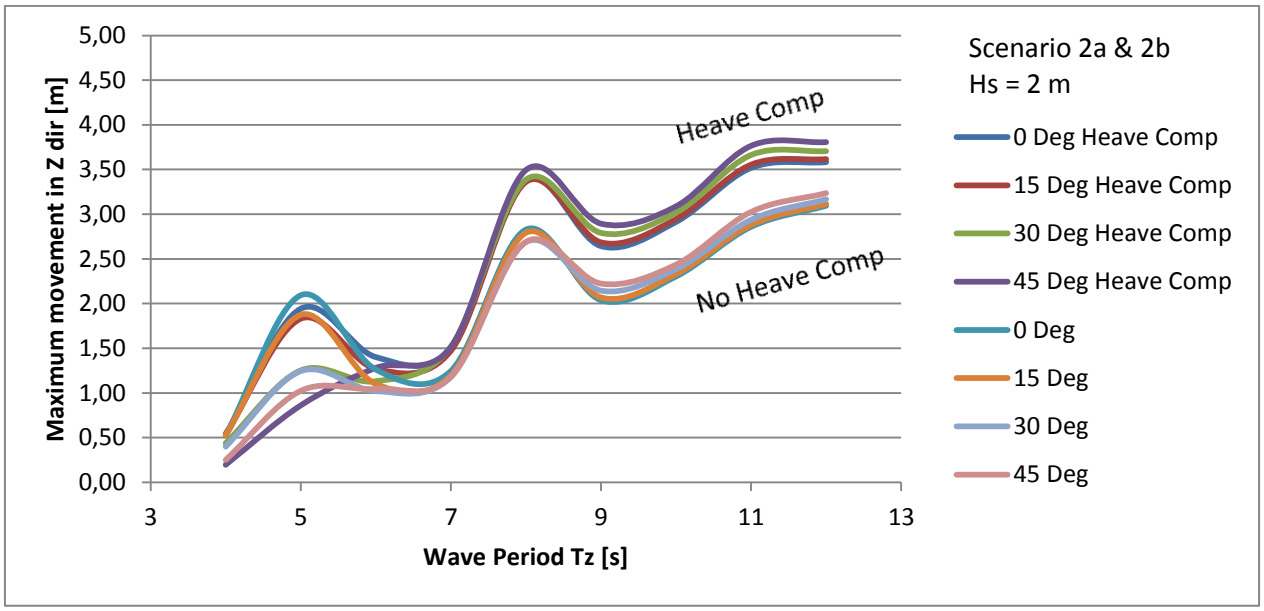

Figure 57 Scenario 2: Maximum Displacements in Z Direction with and without Heave Compensation. Hs = 2 m

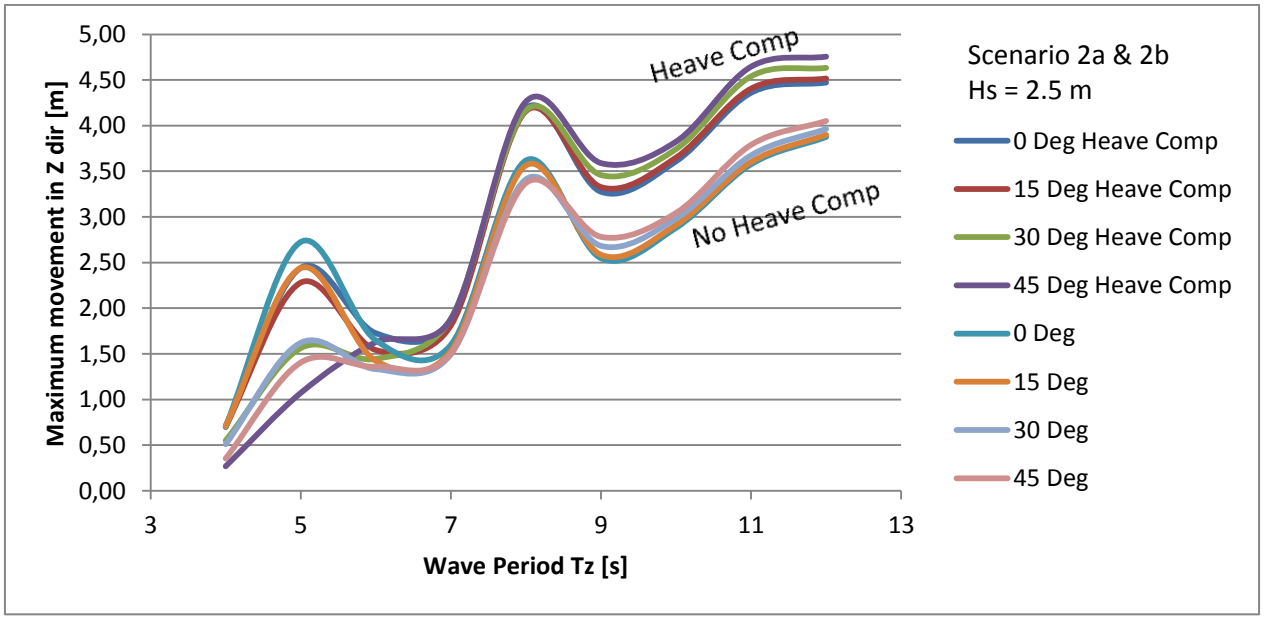

Figure 58 Scenario 2: Maximum Displacements in Z Direction with and without Heave Compensation. Hs = 2,5 m

5.2.4 Time Plot of Case 41

The displacement in Scenario 2a does not look very different from Scenario 1a. The differences compared to Scenario 1a are further considered.

5.2.4.1 Horizontal Behavior

The horizontal behavior in Scenario 2a is almost identical to Scenario 1a (see Figures 45 and 59). The draught of the jacket does not seem to influence the horizontal behavior significantly.

Peak	Period [s]
1	37,879
2	6,317

Table 25 Scenario 2a, Case 41: Peaks in Spectral Density of Horizontal Motions

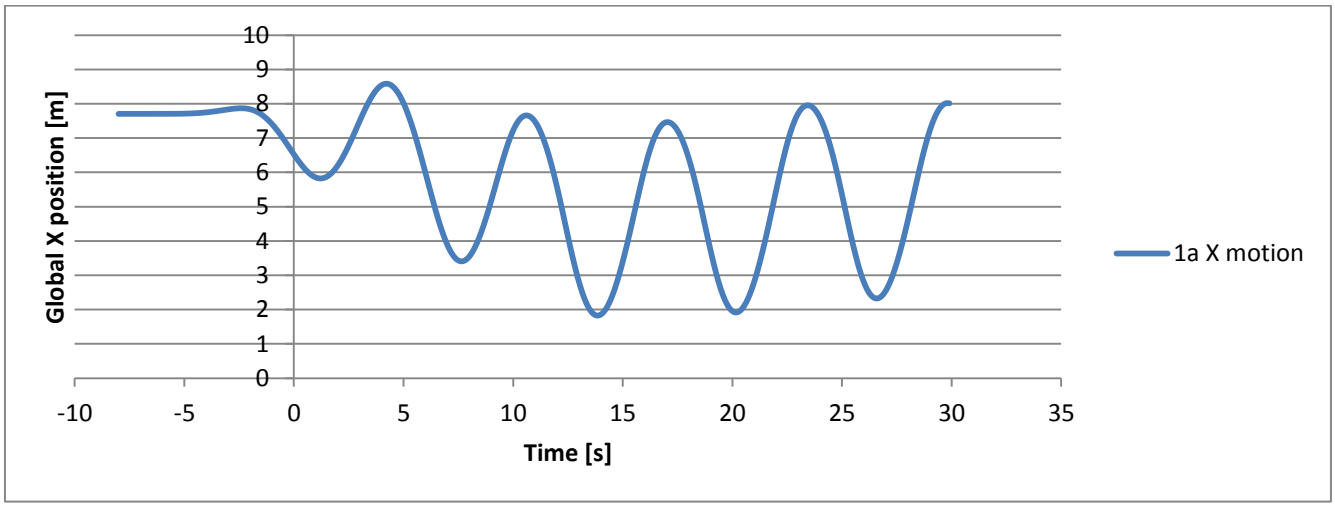

Figure 59 Scenario 2a, Case 41: Time History Plot of Global X Position at Jacket Member 1a

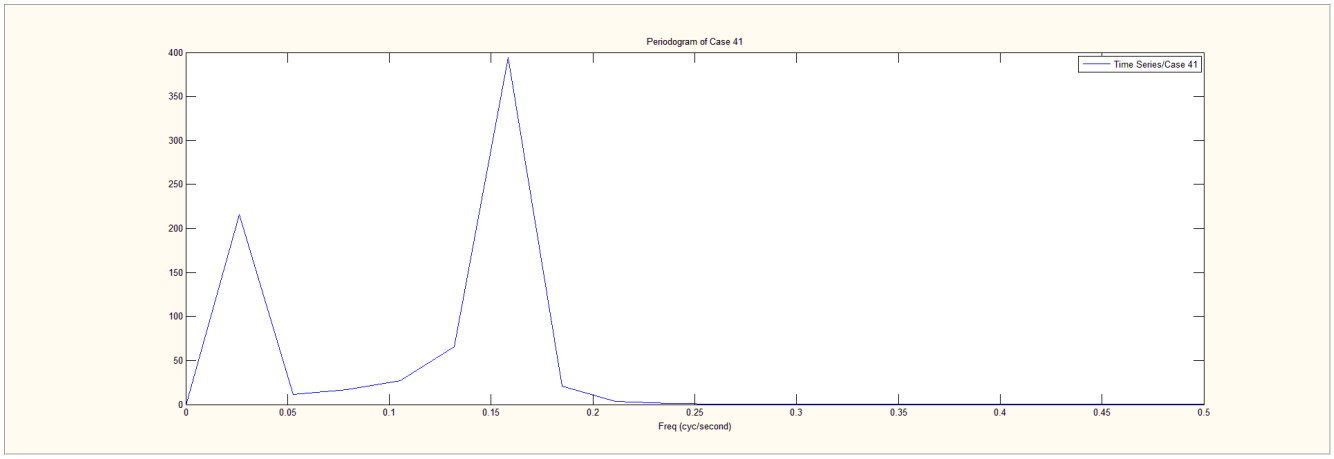

Figure 60 Scenario 2a, Case 41: Spectral Density of Horizontal Motions

5.2.4.2 Vertical Behavior

The vertical behavior of the jacket is different from Scenario 1a. The dominant wave period from the spectrum has increased from 5,336 to 6,317 seconds. Also the high frequency oscillation has increased from 2,915 to 3,159 seconds (see Table 26).

In this case there are some notable results. While the horizontal displacements are very similar with/without heave compensation, the vertical seems to be damped with the heave compensation (see Figure 61).

Peak	Period [s]
1	6,317
2	3,159

Table 26 Scenario 2a, Case 41: Peaks in Spectral Density of Vertical Motions

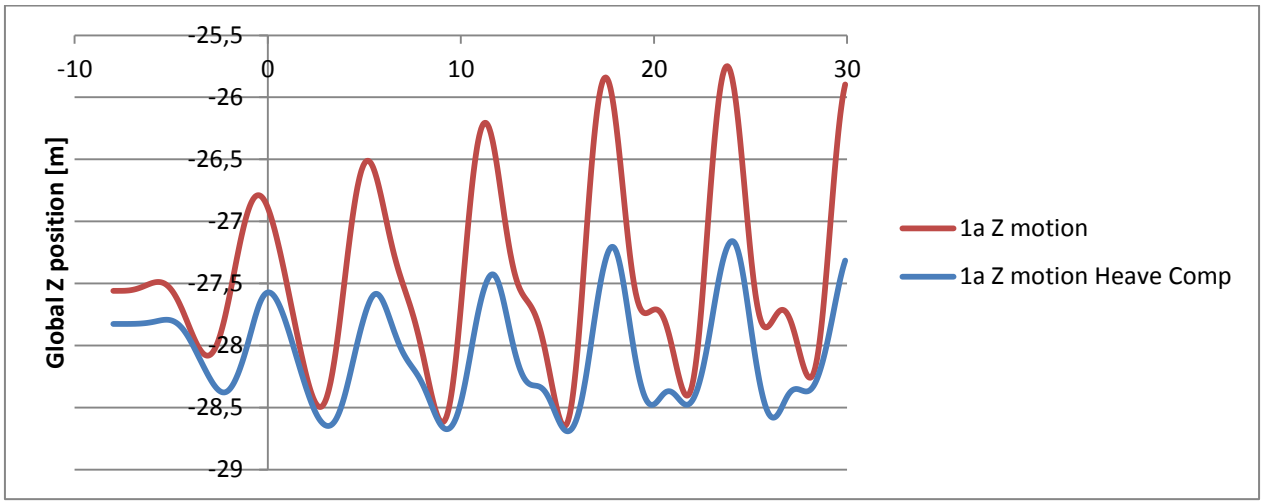

Figure 61 Scenario 2, Case 41: Time History Plot of Global Z Position at Jacket Member 1a with and without Heave Comp

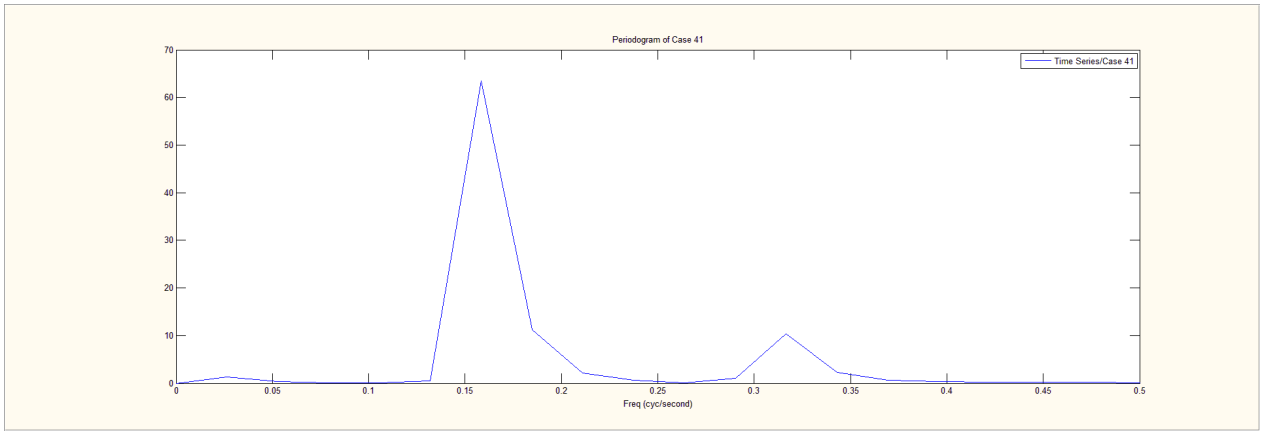

Figure 62 Scenario 2a, Case 41: Spectral Density of Vertical Motions

5.2.5 Time Plot of Case 53

The displacement in Case 53 is also very similar to those of Scenario 1a.

5.2.5.1 Horizontal Behavior

The horizontal behavior of the jacket as compared to Scenario 1a is very similar. Both periods of 37,879 and 9,477 seconds are equal to those of Scenario 1a. The high frequency oscillation has increased from 5,414 seconds to 6,317 seconds (see Table 27 and Figures 63 and 64).

Peak	Period [s]
1	37,879
2	9,477
3	6,317

Table 27 Scenario 2a, Case 53: Peaks in Spectral Density of Horizontal Motions

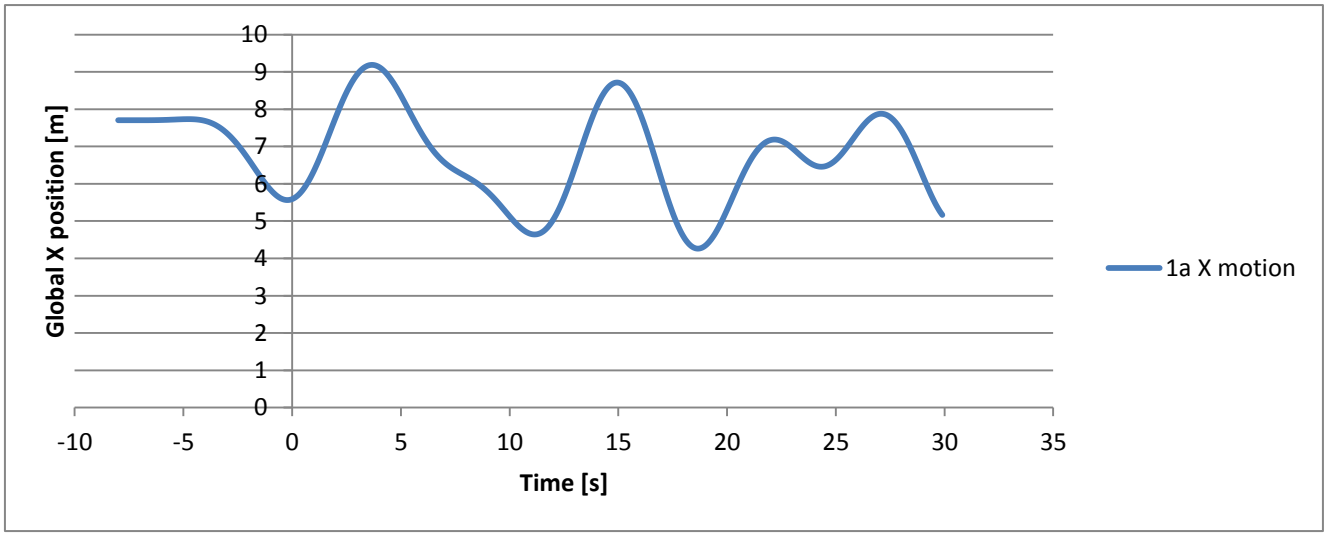

Figure 63 Scenario 2a, Case 53: Time History Plot of Global X Position at Jacket Member 1a

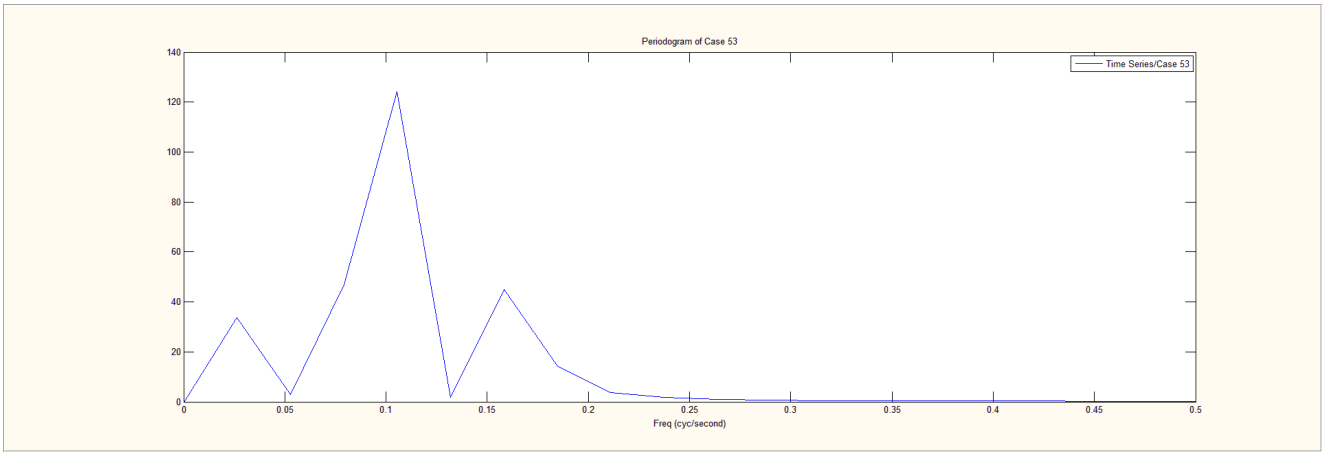

Figure 64 Scenario 1a, Case 53: Spectral Density of Horizontal Motions

5.2.5.2 Vertical Behavior

The vertical behavior is also very similar to Scenario 1a. The only difference being no low frequency peak in the spectrum. This does not mean that a low frequency oscillation is present, as we can see from the spectrum (Figure 66).

Case 53 is more similar to the general trend of the behavior of the jacket. Heave compensation does not seem to decrease the displacements notably (see Figure 65).

Peak	Period [s]
1	9,477
2	5,414

Table 28 Scenario 2a, Case 53: Peaks in Spectral Density of Vertical Motions

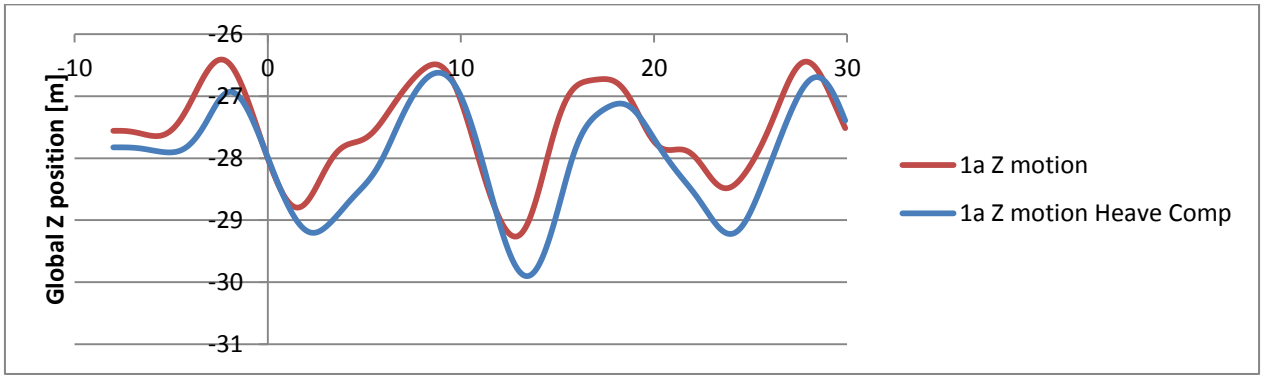

Figure 65 Scenario 2, Case 53: Time History Plot of Global Z Position at Jacket Member 1a with and without Heave Comp

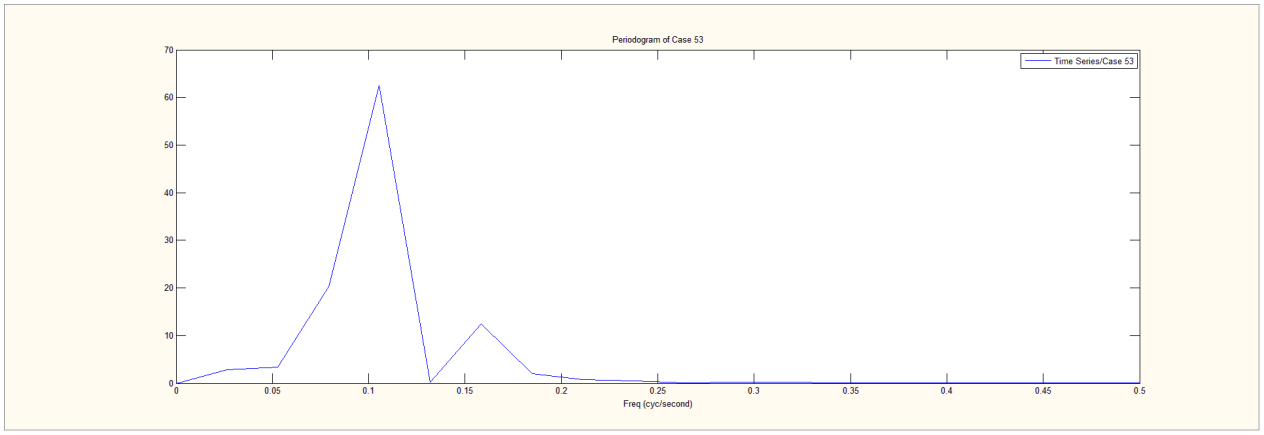

Figure 66 Scenario 2a, Case 53: Spectral Density of Vertical Motions

5.3 Scenario 3

In Scenario 3 a bumper system is added to Scenario 1a. Also no current is present so that contact will be achieved. The critical cases, Case 341 and 353 are analyzed. The materials used for the bumper system is shown in Table 9.

Von Mises stress is analyzed in jacket leg 1a, one of the two legs experiencing impact forces.

5.3.1 Case 341

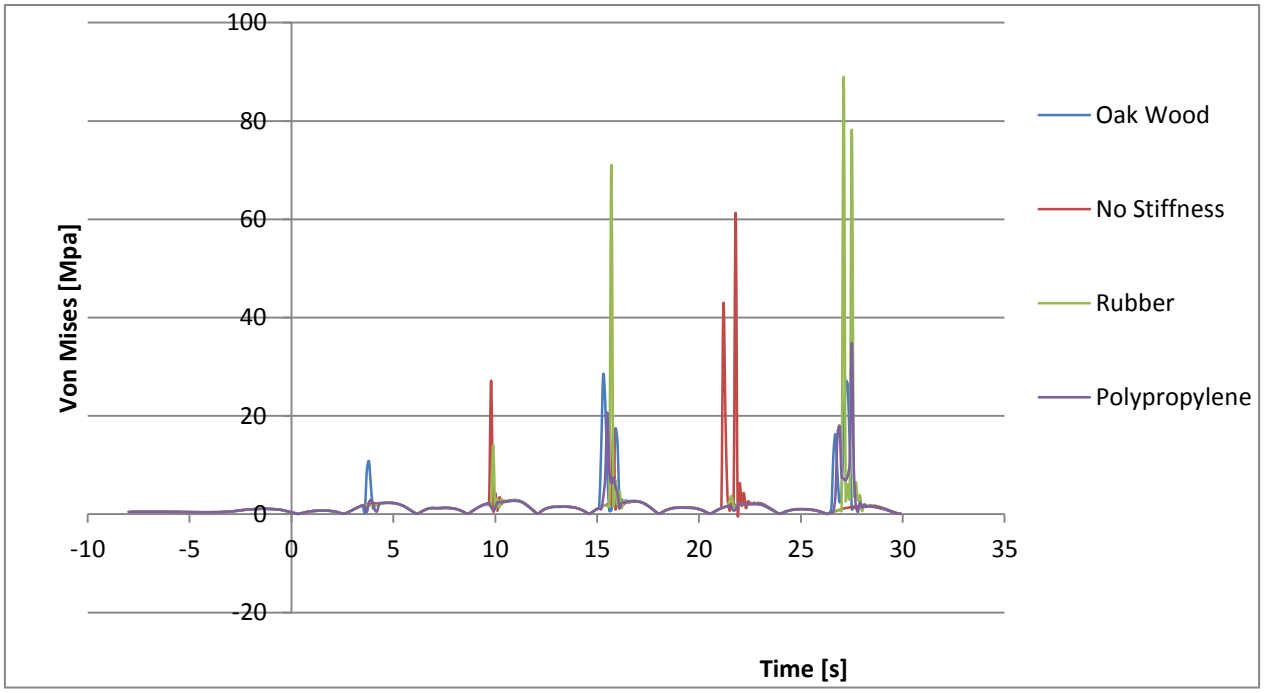

Figure 67 Case 341: Von Mises Stress at Fixed End of Jacket Member 1a for Different Bumpers

From Figure 67 both Oak Wood and Polypropylene give lower Von Mises stress in the jacket leg under impact. Rubber gives the highest stress in the jacket leg.

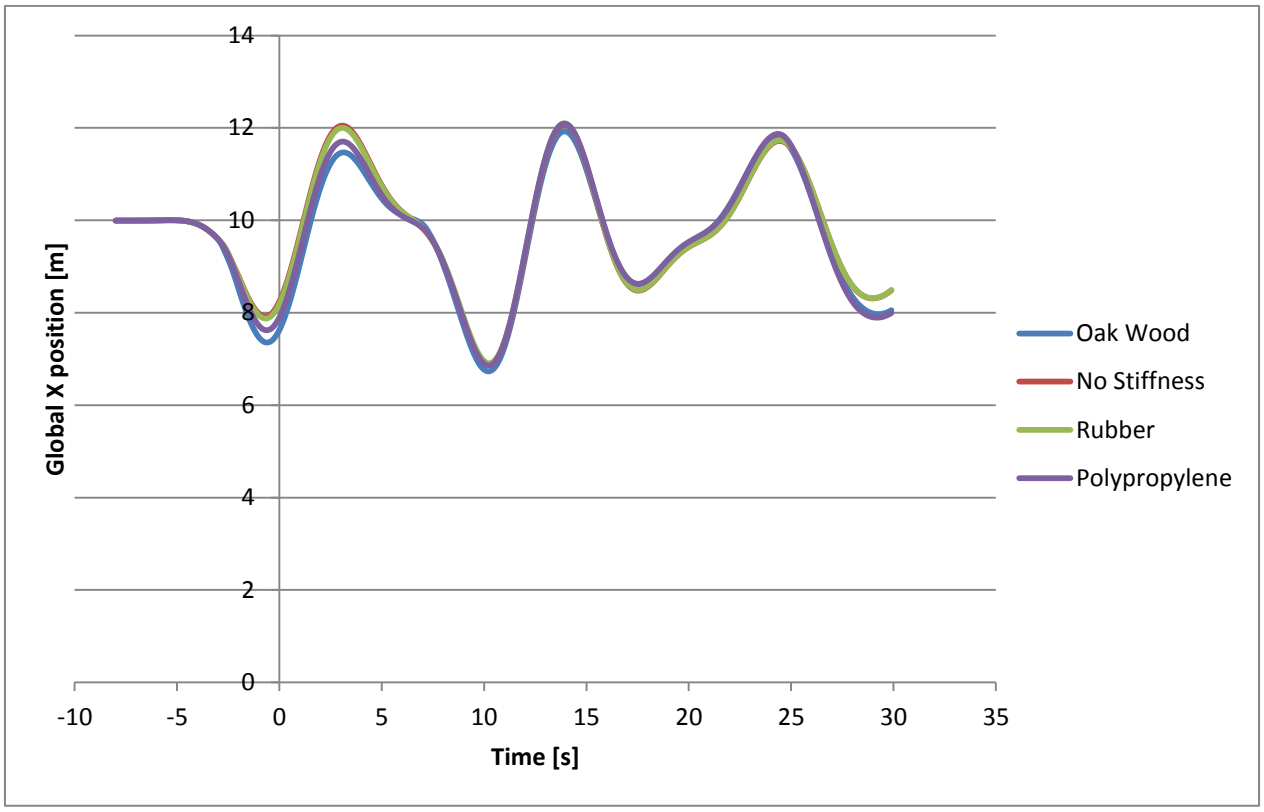

Figure 68 Case 341: Time History Plot of Global X position of Jacket Member 1a for Different Bumpers

The displacement using the different materials for a bumper system does not seem to change very much (see Figure 68). With no bumper system, the displacement starts to differ after approximately 15 seconds. Especially for “No Stiffness”, the system with no bumper attached, the vertical displacement starts to differ.

5.3.2 Case 353

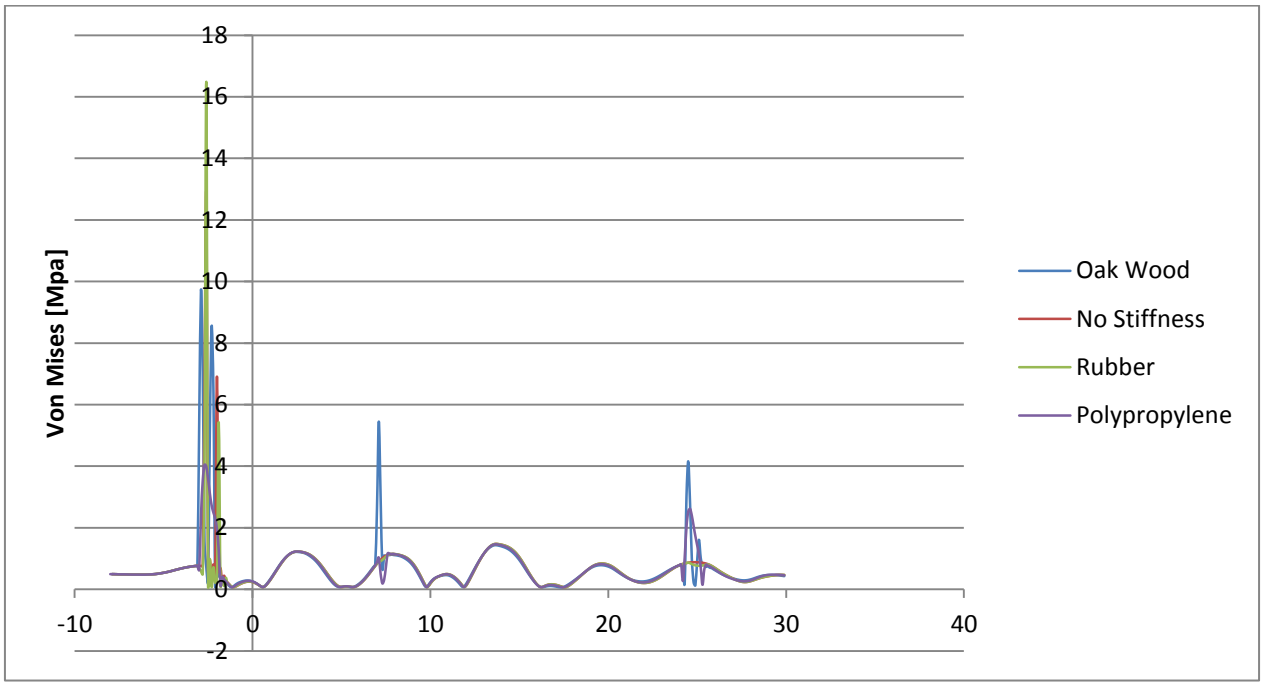

Figure 69 Case 353: Von Mises Stress at Fixed End of Jacket Member 1a for Different Bumpers

In Case 353 the jacket leg only experiences one major impact (see Figure 69). Because the first impact happens at the same time for all the different materials used as a bumper, this can give valuable information on what material to use. Figure 70 shows the first impact.

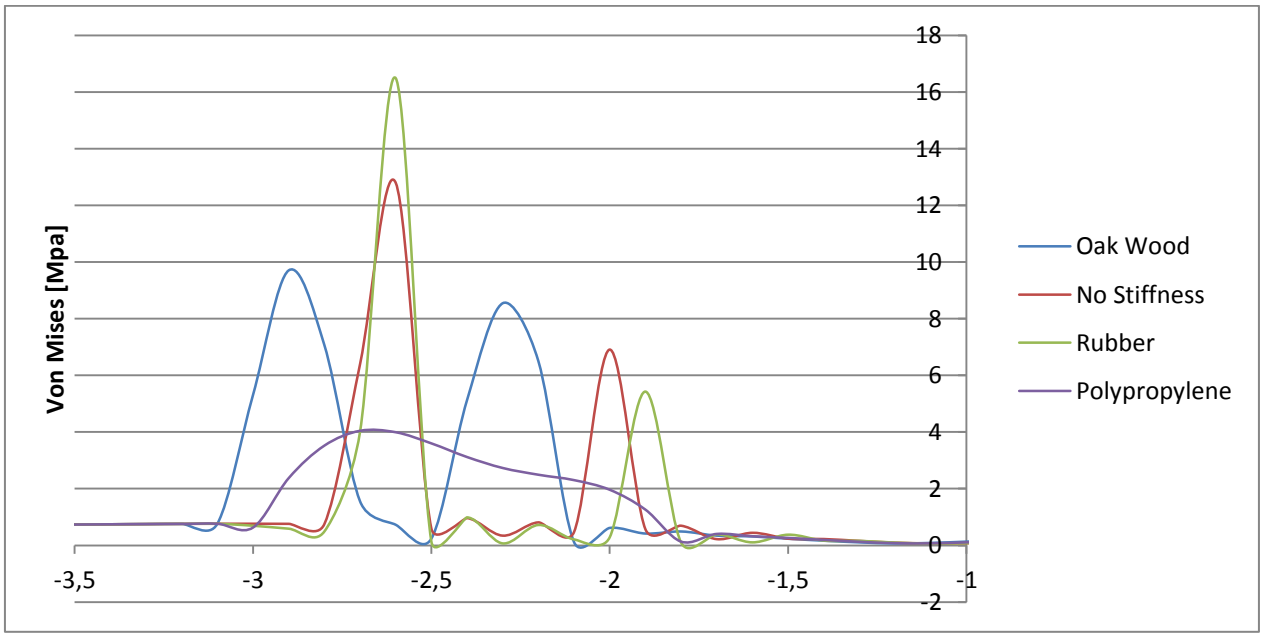

Figure 70 Case 353: Von Mises Stress at Fixed End of Jacket Member 1a for Different Bumpers. First Impact

Rubber gives the highest von Mises stress in the jacket leg. Polypropylene gives the lowest stress and opposed to the other materials only gives one impact.

The displacement for Case 353 is very similar to Case 341. No major difference with the different materials is present (see Figure 71).

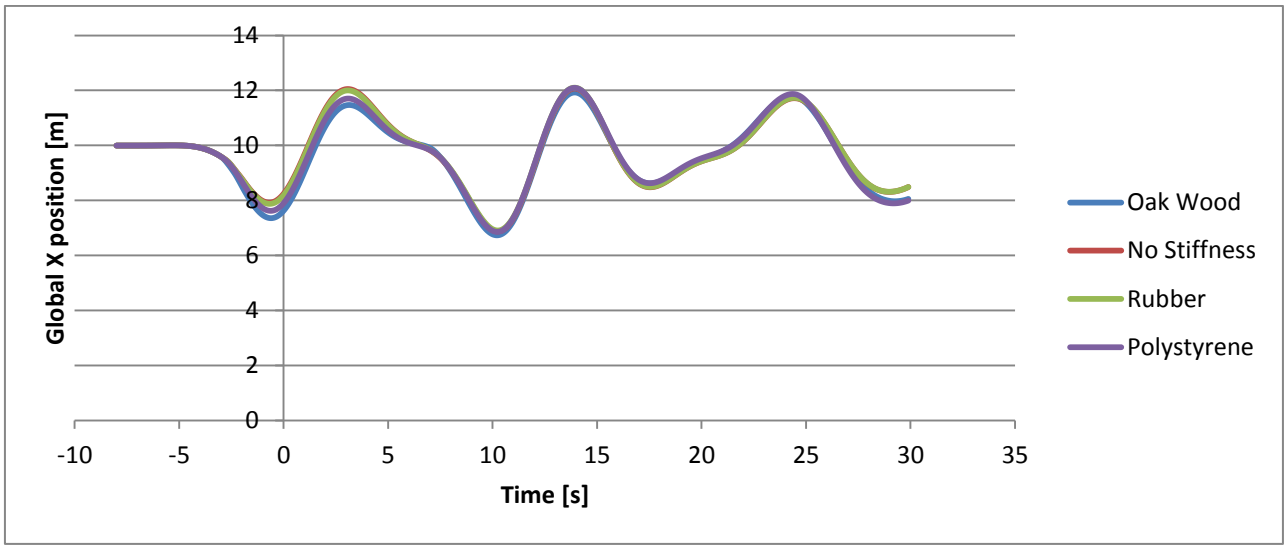

Figure 71 Case 353: Time History Plot of Global X position of Jacket Member 1a for Different Bumpers

5.4 Modal Analysis

A modal analysis is done for the whole system with the jacket at different draughts, to investigate the variation in natural frequency with changing line length (see Table 29).

Case	Dist below sealevel [m]	Dist to seabed [m]	Approximately [m]	Line length [m]
M10	-20,167	9,833	10	20,42
M7	-23,000	7,000	7	23,253
M5	-25,000	5,000	5	25,253
M3	-27,144	2,856	3	27,397

Table 29 Modal Analyses is Performed for Different Draughts of the Jacket

Case M10 and M3 are Scenario 1a and 2a respectively. Two other cases are created between these to see how the modes change with draught. All the mode periods can be found in Appendix 15. Here only the important modes are taken into account. These are the ones in the range that can be influenced by the incoming wave period.

Mode	M10 Period [s]	M7 Period [s]	M5 Period [s]	M3 Period [s]
2	17,889	18,636	18,956	19,460
3	16,895	17,744	18,111	18,676
4	5,363	5,644	5,822	6,010
5	5,244	5,520	5,692	5,877

Table 30 Natural Frequencies of the Critical Modeshapes for Different Line Lengths

All the mode periods increase with increasing draught (see Table 30). Pictures of the different modes are presented in Figures 73-76 below. Modes 4 and 5 have natural periods very close to the incoming wave period and is therefore important (see Figure 72).

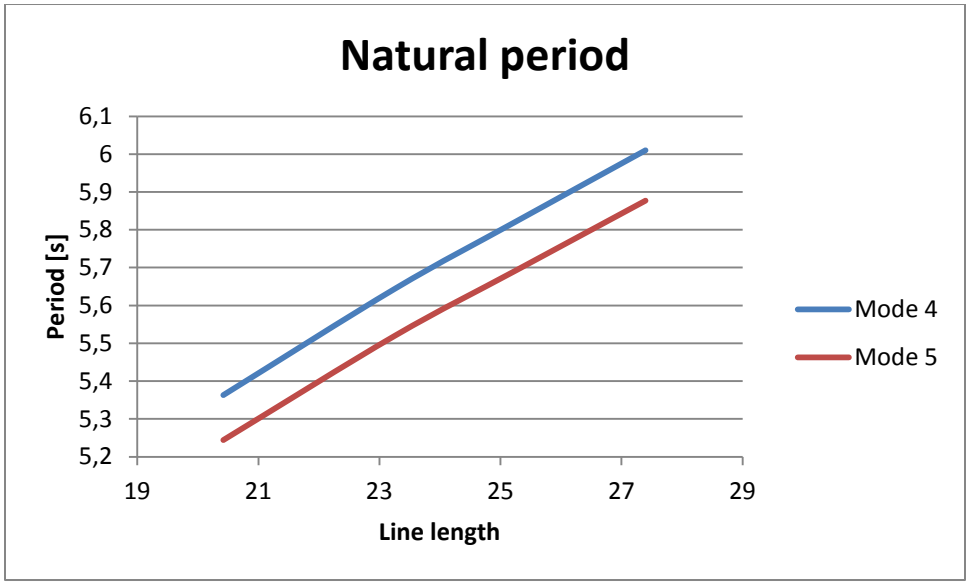

Figure 72 Natural Frequency Variation with Line Length

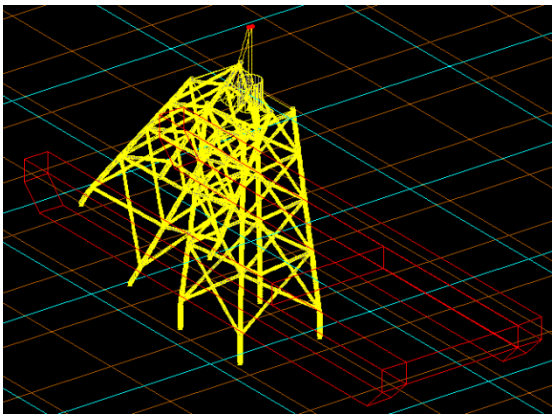

Figure 76 Mode 2

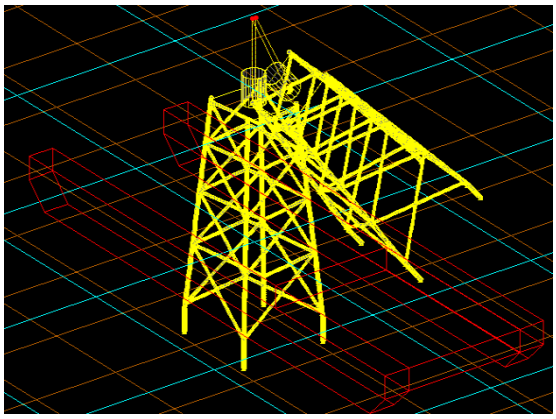

Figure 75 Mode 3

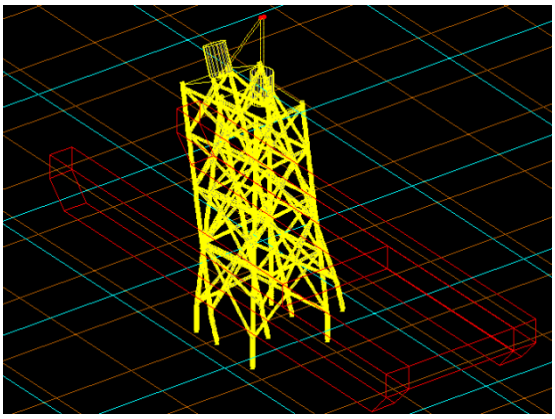

Figure 74 Mode 4

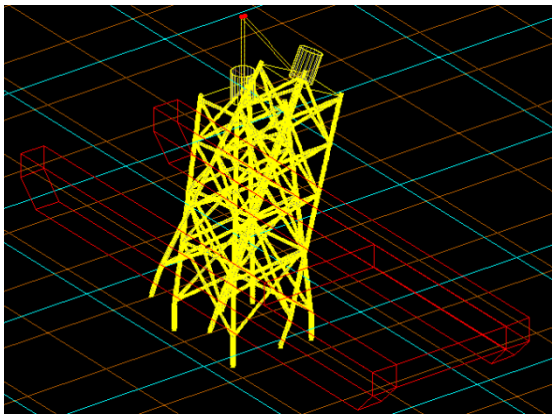

Figure 73 Mode 5

6 Discussion

This chapter will discuss the results presented in chapter 5. One thing that should be noticed before going into detail in the different scenarios is that the significant wave height only scales the motion amplitudes and does not have any other effect on the jacket behavior. This can easily be seen by examining Figures 39-44.

6.1 Scenario 1

6.1.1 Displacement in X-direction

When looking at Figures 39 and 40, peaks at periods 5 and 8 seconds can be found for displacements in x-direction. It is obvious that these peaks are due to dynamic amplification at the corresponding critical periods. It can therefore be interesting to compare these periods with the critical periods obtained from the modal analysis. Mode 4 (see Figure 75), which is a rotational mode rotating in the xz-plane, describes the behavior of the jacket very well, and plays an important role in the dynamic amplification. Since this is a rotational mode, the amplification will also affect motions in z-direction. The eigenperiod for this mode is $T_{04} = 5{,}36\ s$ for the line length corresponding to Scenario 1 (see Table 29). This means that wave periods of approximately 5 seconds are hitting the eigenperiod of the system which is 5.36 seconds, and hence the dynamic amplification. This explains the peak in the Figures 39 and 40 at $T_z = 5\ s$.

The presence of the peak at 8 seconds is not that obvious. This is most likely caused by a combination of mode shapes or by second order effects, described in chapter 2.3.5. It is worth noting that the presence of Mode 2 (see Figure 73), which is a straight pendulum mode in the xz-plane, seems to be more represented in Case 53 with $T_z = 8\ s$, than in Case 41 with $T_z = 5\ s$ when looking at the animations (see animation files from memory stick). Mode 2 has an eigenperiod $T_{02} = 17{,}89\ s$ (see Table 30). The dynamic amplification may then be caused by a combination of the two modes 2 and 4. This may be due to a sum frequency force, with frequency ≈ 2 · 8s which makes Mode 2 more critical for excitation than in Case 41, where the sum frequency force are too far from T_{02} to excite the mode.

The directions 0 and 15 degrees cause the most motions in the x-directions, as expected. The smaller the attacking angle is with respect to the x- axis the larger motions. It is also seen that the cases with 0 and 15 degrees attacking angle have larger peaks at $T_z = 5\ s$. This makes sense since these directions easier induce motions in the x-direction which can excite the critical mode (Mode 4).

6.1.2 Displacement in Y-direction

For the y-direction plots (Figures 41 and 42) only peaks at 5 seconds are noted. This is due to Mode 5 (Figure 76), which is a rotational mode such as Mode 4, only rotating in the yz-plane. The eigenperiod for this mode is $T_{05} = 5{,}24\ s$, so this mode will excite larger motions at 5 seconds in the same manner as Mode 4 does for the x- direction.

The directions 30 and 45 degrees cause the most motions in the y- direction, as expected. For incoming wave direction 45 degrees there is a small peak at $T_z = 8\ s$ in Figures 41 and 42. This peak is caused by the same reasons as the peak in the x-displacement plot (Figures 39 and 40). The straight pendulum mode in the yz-plane is Mode 3, with an eigeperiod of $T_{03} = 16{,}9$ s (see Figure 74 and Table 30). The reason why this peak is so small is most likely because of the strong current force in x- direction, which makes it harder for Mode 3 to be excited. This also explains why the peak is not present at other degrees than 45.

6.1.3 Displacement in Z-direction

When looking at the plots for motions in z-direction (Figures 43 and 44), the same tendencies as for the x-direction plots (Figures 39 and 40) can be seen. The motion peaks at 5 and 8 seconds, more or less for all attacking angles. Consider the point at the bottom of the jacket from Figure 38, which these plots are based on. It is quite easy to explain why the heave motion peaks at the same periods as the x-displacement. The heave motion to the point due to the pitch or pendulum motion of the jacket will be in addition to the heave motion of the barge. When the x-displacement of the jacket gets larger, caused by a rotation, the z-displacement also increases. This is easily understood intuitively by considering a pendulum, but may also be seen from Equation (2.1) in chapter 2.1.

One remarkable thing worth noticing is that the passive heave compensation system applied in Scenario 1b, tends to increase the heave motion, rather than decrease it. In fact, for all cases heave compensation seems to have an increasing effect on the heave motion. This implies that such a system does not serve its purpose at all in the case for Scenario 1. There may be several reasons for why such a system does not work in this case. One of the most important reasons can be that the jacket has too small hydrodynamic damping and added mass. The Cranemaster system is designed especially for subsea installations and splash zone problems for lifting items with large surface areas. Most of the jacket mass is above the water surface at this phase of the installation process. The added mass and drag damping in heave is small for the tubular jacket members due to the small cross section area. The forces acting in the opposite direction of the movement hence is small, and a passive heave compensation system may therefore be difficult to use. One other important thing to remember is that the linear hydrodynamic damping is set to zero for all analyses. This will of course affect the results in some way. Besides, the restoring force is a function of waterline area. The restoring force will therefore also be small due to the small waterline area of the tubular members.

6.1.4 Time Plot of Case 41

It is seen from Figure 45 that the motions in x-direction are large for Case 41. The stroke is approximately 4-5 meters, which probably is too large to continue the installation. Wire systems may be used to restrain the jacket from such large oscillations during the process. However, the motions are small enough to prevent collision with the support frame. The reason for this is the strong current, which continuously pushes the jacket in negative x-direction.

From the spectral density plot in Figure 46 one may see that a lot of energy is concentrated around the peak at 6.317 seconds (see Table 21). This is close to the eigenperiod of Mode 4 (see Table 30), which is the dominating mode.

From Figure 47 it is seen that the vertical motion oscillates in a more complicated manner than the horizontal motion. The most notable matter with this plot is that the heave compensation system seems to decrease the heave motion by first sight. This result is completely different from the plot in Figures 43 and 44. It is important to remember that this plot is for point P from Figure 38, and not the point between the jacket legs. If the heave and pitch motion of the jacket is out of phase, the point P may experience smaller vertical movement with larger heave motions, while the point in the middle of the jacket legs will experience larger vertical movement. This is illustrated in Figure 77, and can imply that the pitch and heave motions are out of phase in a similar manner.

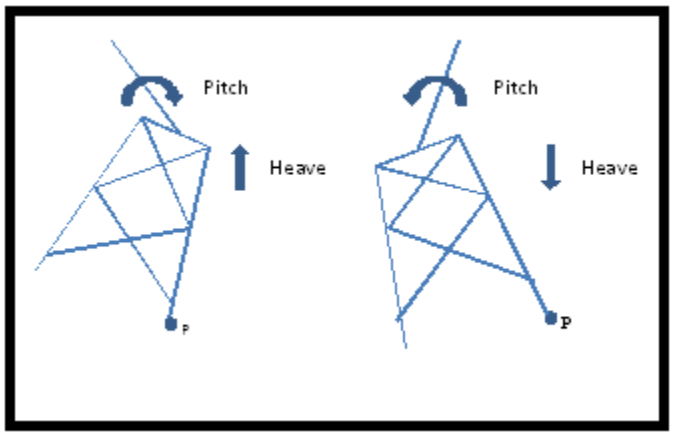

Figure 77 Small Vertical Motion of Point P When the Heave and Pitch Motions is Out of Phase

When looking at the spectral density of the vertical motion (Figure 48), it is seen that the largest peak is present at 5.33 seconds (see Table 22). This is almost exactly the same as the natural period for Mode 4, $T_{04} = 5{,}36\ s$. That explains why Case 41 is subjected to dynamic amplification.

6.1.5 Time Plot of Case 53

The oscillations of the horizontal motions in Figure 49 are pretty complex, but the max stroke is about 4-5 meters. Again, this is too large motions to continue installation, and wires should be used as discussed in chapter 6.1.4.

Also for this case, the motions are small enough to prevent contact with the support frame, as a consequence of the current (see Appendix 15 and 16). In fact, the current assures no contact in all the 72 cases for Scenario 1. This scenario should therefore be run for cases with no current to investigate all aspects of this critical scenario.

By looking at the spectral density for the horizontal motion (Figure 50), it is seen that there are three peaks at different periods. The majority of the energy is concentrated around the peak at 9.48 s, which

may be due to a combination of Mode 2 and 4. The peak may also be linked directly to the eigenperiod of Mode 2 through second order effects, since 2·9.48 is close to $T_{02} = 17{,}89\ s$. Another peak of importance in the spectral density plot is at 5.14 seconds, which is real close to $T_{04} = 5{,}36\ s$. One can see from the time history plot that the oscillations are complicated as a consequence of combination of modes with different mode shapes. Mode 2 then plays a larger role in Case 53 than in Case 41.

The vertical motion plot (Figure 51) indicates that the motions are larger with heave compensation than without. The first oscillation seems to have about the same amplitude for both cases. Further it looks like the heave compensation system gets worse with time. This emphasizes the allegation of lack of damping in the system, discussed in chapter 6.1.3.

The spectral density plot in Figure 52 shows that the energy is concentrated mainly around 9.48 seconds, the same dominating period as for the horizontal motion.

6.2 Scenario 2

6.2.1 Displacement in X-direction

The displacement plots for x-direction movement in Scenario 2a (Figures 53 and 54), are very similar to those for Scenario 1a (Figures 39 and 40). The graphs look almost the same and the same tendencies may be found as those discussed in chapter 6.1.1.

The plots have peaks at 5 and 8 seconds. The dynamic amplification at $T_z = 5\ s$ is caused by Mode 4, due to its natural period $T_{04} = 6\ s$ for Scenario 2 (see Table 30). The peak at 8 seconds is due to the same reasons as in Scenario 1; combinations of the Modes 2 and 4. It is noted that the peak at 5 seconds is slightly larger than for Scenario 1, while the peak at 8 seconds is slightly lower. This is a direct cause of the variation of the draught. The draught is larger in Scenario 2 than in Scenario 1. More draught means more resistance in the water, and makes it difficult for the straight pendulum motion of Mode 2 to take place. The peak at $T_z = 8\ s$ where Mode 2 plays an important role is then expected to decrease. However, Mode 4 becomes even more dominant for the motion, and the peak at $T_z = 5\ s$ will increase.

6.2.2 Displacement in Y-direction

The displacement plots for the y-direction (Figures 55 and 56) are also very similar to Scenario 1. The peak at 5 seconds may be explained with the eigenperiod of Mode 3, $T_{03} = 5{,}88\ s$, which is excited at $T_z = 5\ s$.

The motions at the different directions leave no surprises. A larger attacking angle with respect to the x-axis gives larger motions.

6.2.3 Displacement in Z-direction

When looking at Figures 57 and 58 peaks at 5 and 8 seconds are observed. The z-displacement seems to be dominated by Modes 2 and 4 in the same manner as for Scenario 1. Due to their rotational shape, these modes will dominate the z- as well as the x-displacement for the critical periods.

The heave compensation system leads to larger vertical motions than for the cases with no such system. Even though the resistance in the water is larger for Scenario 2 due to larger draught, the heave compensation does not seem to work. When comparing the two plots in Figures 50 and 58, the extra water resistance from Scenario 2 does not improve the heave compensation notably. It should again be noted that the linear hydrodynamic damping is zero. The added mass and drag for larger draught does not improve the heave compensation system properly. Analyses with linear hydrodynamic damping would be of interest for both Scenarios 1 and 2, to see if there is any change in the behavior for the cases with heave compensation.

It could also be interesting to run analyses with heave compensation different from the Cranemaster system. For example, tanks partly flooded with water could be attached to the jacket during lowering as illustrated in Figure 78. As the jacket heaves the water would create sloshing inside the tanks which would create a damping force on the structure that counteracts with the motions. If such a system is

considered, parameters like the tank inertia and water mass will be crucial, and should be investigated further.

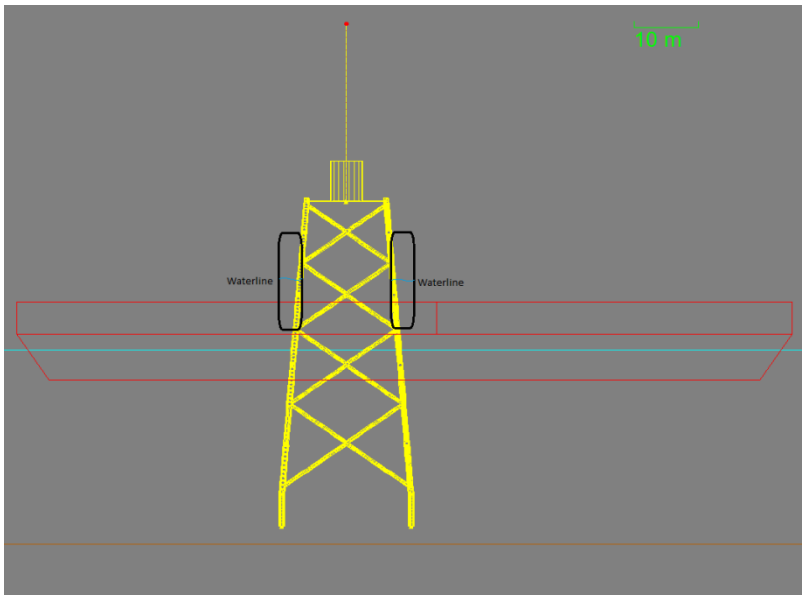

Figure 78 Alternative Heave Compensation System with Improved Resistance

6.2.4 Time Plot of Case 41

The motions for Case 41 are larger for Scenario 2 than Scenario 1. The largest stroke is approximately 6 meters, which is way too large for installation of the jacket (see Figure 59). Wire systems to restrain these large motions are strictly necessary.

The spectral density (See Figure 60) shows two peaks, one of them at 6.14 seconds. Here, a significant part of the energy is concentrated, and periods in this range dominates the motion. Comparing with the eigenperiod of the critical mode (Mode 4) $T_{04} = 6{,}01\ s$, it is easy to understand why Case 41 includes large dynamic amplification. A large peak at 37.88 seconds is also present, and it is seen by the time history plot in Figure 59 that the motion also oscillates with this frequency. This may be due to second order effects and combinations of higher order modes.

When considering the vertical motion in Figure 61, the heave compensation improves, just like in Case 41 of Scenario 1. The only difference from Scenario 1 is the draught. Since the environmental conditions are exactly the same for both cases the same modes will be dominating. The heave and pitch motions will therefore be out of phase in the same manner as illustrated in Figure 77, and the point P in Figure 38 experiences smaller vertical motions when using heave compensation.

The period dominating the vertical motion is the largest peak in the spectral density plot in Figure 62. The peak is located at 6.32 seconds which is close enough to $T_{04} = 6{,}01\ s$ to induce dynamic amplification.

6.2.5 Time Plot of Case 53

When looking at the horizontal motion time history plot for Case 53 in Figure 63, it is seen that the oscillations are more complicated than for Case 41. This is also the case for Scenario 1. The motions are much larger than an installation procedure allows. The spectral density in Figure 64 has three peaks with most of the energy concentrated around 6.32 seconds. This will excite the eigenperiod for Mode 4, $T_{04} = 6{,}01\ s$ and hence the dynamic amplification. In addition, the peak at 9.48 seconds seems to play a role when noticing the complicated behavior in the time history plot. This period may be linked to Mode 2 through second order effects.

From the vertical motion in Figure 65 one can see that the heave compensation system fails, like it does for the same case in Scenario 1. The motions in the z-direction increase when applying heave compensation. However it is noted that the increase in amplitude is slightly smaller than for Case 53 in Scenario 1 (Figure 51). This may be a consequence of the extra water resistance due to larger drag and added mass that follows from more draught in Scenario 2.

The spectral density plot in Figure 66 indicates that most of the energy is located around the peak of 9.47 seconds, and this period is also recognized as the dominating period in the time history plot.

6.3 Scenario 3

In Scenario 3, Case 341 and 353 are run with a bumper system attached to the frame. These cases are similar to Case 41 and 53 for Scenario 1, but without current. Figures 67 and 69 shows the von Mises stress in the jacket leg at different times. Not surprisingly, the cases with no bumper present give high stress in the jacket leg. What is rather surprising is that the Rubber bumper gives higher stress than for example the Oak Wood bumper. This indicates that Rubber has a stiffness that is too low, and the jacket leg would behave like colliding with the pure steel frame. In Case 353 there is a major impact early in the simulation, which are further investigated in Figure 70. Where the other materials have sharp and high stress peaks, the curve for Polypropylene is rather blunt, and distributes the stress smoothly over the impact. This indicates that the Polypropylene have a contact stiffness that is convenient and may be beneficial to use for a bumper.

It should be noted that the materials chosen for the bumper analysis are guidelines for what stiffness to use for the bumper. Some of the materials may have other properties which make them inconvenient to use. Properties like brittleness are not taken into account, neither is plasticity when the analysis is linear elastic and based on Hooke's law. Before deciding which material to use, this should be investigated further.

Another thing that is worth noticing is how the colliding elements are modeled. The jacket legs and the steel frame are modeled as lines, strictly spoken beams with few FEM elements. This causes much uncertainty regarding the bumper analysis and the results are likely to be inaccurate. For more accurate results a FEM-program is recommended, with a proper shell element mesh.

6.4 Modal Analysis

A modal analysis is performed to investigate how the natural frequencies change with the line length. From Table 30 it is seen that all natural periods increase when the line length increases. This means that the natural frequencies get smaller as the jacket is lowered to the seabed. Modes 2 and 3 are pendulum modes rotating about the hanging point where the line is connected to the barge (see Figures 73 and 74). Modes 4 and 5 are pendulum motions with two rotational points (see Figures 75 and 76). Figure 72 illustrates how the natural periods changes with the line length for Mode 4 and 5.

Consider the formula for the natural period of a simple pendulum:

$$T_0 = 2\pi\sqrt{\frac{L}{g}} \tag{6.1}$$

where L is the length of the pendulum line and g is the gravitational acceleration. This formula is only accurate for an ideal simple pendulum, but still gives an indication on the behavior of the eigenperiods of the pendulum modes. For the simplified pendulum problem the relation is linear. By looking at Figure 72, it is seen that this actually describes the relation very well, also for this complicated problem.

7 Conclusion

The two scenarios identified and chosen for the response analysis should describe the behavior of the jacket during two phases of installation. The results of the analyses show that the jacket motions are way too large to install, especially for the cases with high dynamic amplification. A system to prevent the motions is therefore strictly needed, for example by use of wires. In Scenario 1 the jacket does not collide with the support frame due to the strong current. With no current present, contact between the jacket leg and the support frame will happen. If the jacket is allowed to collide with the support frame, this would also help to keep the jacket in place. It must then be assured that the impact stress in the colliding jacket legs can be tolerated.

High dynamic amplification will occur for zero upcrossing periods at 5 and 8 seconds, for the motions in x- and z-directions. The wave frequencies will here be close to the eigenfrequency of the critical modes. Mode 4 is critical for both of these zero upcrossing periods, but for 8 seconds Mode 2 will also play an important role. The motions in y-direction is of less importance, since the jacket never will collide with the barge in the sideway direction.

The natural periods of the system change with the line length. A nearly linear relationship is discovered when considering the eigenperiods of the different critical modes. This relationship matches very well with the relationship of a simple pendulum model.

The passive heave compensation system provided for the analyses has a rather negative effect on the vertical motion of the jacket. The system is designed especially for subsea installations and splash zone problems when lifting items with large surface area. The compensation fail can then be due to little resistance from too small drag and added mass in heave. In addition, the restoring force is small due to small water line area. The fact that the linear hydrodynamic damping is zero may also cause problems.

From the bumper analysis Polypropylene is the material that gives the lowest stress in the jacket leg. Using the stiffness for this chosen material also assures that the stress are distributed smoothly and avoids large stress peaks in the stress-time plot. It should however be noted that Polypropylene only is an indication on the proper stiffness to use for the bumper. Other properties like brittleness are not taken into account in the analysis, and a plastic analysis with proper shell elements should be used for more accurate results.

8 Recommendations for Further Work

The results presented for Scenario 1a and 2a show that the jacket motions are too large to install. Wire systems to restrain the jacket from large movements may be a good solution to this problem and should be considered. A simplified wire system should then be implemented in the Orcaflex model for analysis.

Analyses should be run for other environmental conditions. Even though analyses are performed with many different cases, the effect of some parameters is still not investigated. The current has a large effect on the response of the jacket, and analyses with no current should be run as well as other velocities than 2 knots.

The passive heave compensation system tested in Scenario 1b and 2b does not work satisfactory. The effect of the damping parameters such as drag and added mass should be investigated further. The linear hydrodynamic damping is particularly interesting. It has large effects on the response according to the parameter studies, but is set to zero in the analyses.

The bumper analysis should be performed with a FEM program and a proper shell element mesh to get more accurate results. Orcaflex handles the colliding items like beam models with very few elements. The assumption of linear elastic material and neglecting brittleness will also give inaccurate results. Besides, the added mass and drag calculations are based on the assumption that the current is large enough to dominate the water particle motion, but no current is present in the analysis to assure impact.

As one reaches new stages of the design process, one could perform model tests of the system in different environmental conditions to determine the added mass, drag and damping more accurately for the jacket. In particular, damping is difficult to determine by analytical considerations. In this way, the effect of the heave compensation system is easier to investigate correctly because the system seems to be sensitive to the hydrodynamic parameters. The added mass for the bumper analysis will also be correct.

Flexibility in the support frame and jacket are not accounted for in the analyses, as the structures are modeled as rigid. The support frame is high and the distance is long between the connection point with the jacket and the connection with the barge. The flexibility in the frame will then induce motions caused by this alone, and this should at least be kept in mind, if not accounted for in a more detailed analysis.

A more detailed analysis should also consider second order effects related to the barge. These effects may cause larger barge motions, which may affect the behavior of the jacket. Load RAO’s for the barge should therefore be provided and implemented in further analyses.

It would also be an advantage to damp the motions of the barge. This would also reduce the magnitude of the jacket motions. Besides, if the natural period of the barge is critical for a certain sea state, damping would also reduce the dynamic amplification. One way to reduce roll motion is to attach bilge keels to the hull in the longitudinal direction.

9 Bibliography

1. **Faltinsen, Odd.** *Sea Loads on Ships and Offshore Structures.* New York : Cambridge University Press, 1990. ISBN: 0-521-45870-6.

2. **Myrhaug, Dag.** Marin Dynamikk, Uregelmessig sjø. *Kompendium.* Trondheim : Institutt for Marin Teknikk, 2007.

3. **Orcina Ltd.** Orcaflex Manual v. 9.4 a. *Orcaflex Manual.* UK : Orcina, 2010.

4. **DNV.** DNV-RP-H103 Modeling and Analysis of Marine Operations. *Recommended Practice .* April 2011.

5. **Kreyszig, Erwin.** *Advanced Engineering Mathematics, 9th edition.* Singapore : John Wiley & Sons, Inc, 2006. ISBN: 0-471-72897-7.

6. **Hulbert, G. M. and Chung, J.** A Time Integration Algorithm for Structural Dynamics With Improved Numerical Dissipation: The Generalized-α Method. *Journal of Applied Mechanics, Transactions ASME.* Ann Arbor, MI : The University of Michigan, June 1993. Vol. 60, 1.

7. **Langen, Ivar and Sigbjörnsson, Ragnar.** Dynamisk Analyse av Marine Konstruksjoner. *Kompendium.* Trondheim : Institutt for Marin Teknikk, 1999.

8. **Craig Jr., Roy R. and Kurdilla, Andrew J.** *Fundamentals of Structural Dynamics.* Hoboken, NJ : John Wiley & Sons, Inc., 2006. ISBN: 0-471-43044-7.

9. **DNV.** DNV-RP-C205 Environmental Conditions and Environmental Loads. *Recommended Practice.* April 2011.

Appendices

Appendix 1 – Jacket Foundation

Jacket foundation

		[m]				[deg]		
Item	Quantity	OD	WT	ID	Length	rot1	rot2	rot3
1	4	0,8840	0,0560	0,7720	5,0000	0,0000	0,0000	0,0000
2	4	0,8840	0,0560	0,7720	7,6750	4,846477	4,846477	0,0000
3	4	0,8640	0,0450	0,7740	12,1310	4,846477	4,846477	0,0000
4	4	0,8640	0,0450	0,7740	11,1250	4,846477	4,846477	0,0000
5	4	0,8640	0,0450	0,7740	9,7760	4,846477	4,846477	0,0000
6	4	0,8640	0,0450	0,7740	5,1680	4,846477	4,846477	0,0000
7	2	0,5590	0,0180	0,5230	10,7510	4,846477	55,77	0,0000
8	2	0,5590	0,0180	0,5230	10,1830	4,846477	124,23	0,0000
9	4	0,5590	0,0180	0,5230	9,4910	4,846477	214,23	0,0000
10	4	0,5590	0,0180	0,5230	11,4700	4,846477	235,77	0,0000
11	4	0,5590	0,0140	0,5310	9,4300			0,0000
12	2	0,5590	0,0140	0,5310	9,0030			0,0000
13	4	0,5590	0,0140	0,5310	8,3100			0,0000
14	4	0,5590	0,0140	0,5310	10,1490			0,0000
15	4	0,5590	0,0140	0,5310	8,2490			0,0000
16	2	0,5590	0,0140	0,5310	7,9510			0,0000
17	4	0,5590	0,0140	0,5310	7,2590			0,0000
18	4	0,5590	0,0140	0,5310	8,9680			0,0000
19	4	0,5590	0,0180	0,5230	7,1980			0,0000
20	4	0,5590	0,0180	0,5230	7,0140			0,0000
21	4	0,5590	0,0180	0,5230	6,3220			0,0000
22	4	0,5590	0,0180	0,5230	7,9170			0,0000
23	8	0,5870	0,0280	0,5310	1,6000			0,0000
24	8	0,5870	0,0320	0,5230	1,6000			0,0000
25	2	0,5590	0,0180	0,5230	7,8990			0,0000
26	4	0,5870	0,0320	0,5230	1,0000			0,0000
27	2	0,5590	0,0180	0,5230	1,9510			0,0000
28	2	0,5590	0,0180	0,5230	7,9710			0,0000
29	2	0,5590	0,0180	0,5230	1,6590			0,0000
30	2	0,5590	0,0140	0,5310	6,4260			0,0000
31	4	0,5870	0,0280	0,5310	1,0000			0,0000
32	4	0,5590	0,0140	0,5310	1,6590			0,0000
33	2	0,5590	0,0140	0,5310	5,3740			0,0000

Geometry of Jacket parts
OD - Outer Diameter
WT - Width
ID - Inner Diameter
x - x global coordinate
y - y global coordinate
z - z global coordinate
rot1 - Rotation about local x axis
rot2 - Rotation about local y axis
rot3 - Rotation about local z axis
Length - Length of part

Because of symmetry of the jacket items, the rotations did not have to be calculated.

The rest of the rotations consist of ±4,846477, ±55,77, ±124,23, ±214,23

Jacket Foundation parts

		Coordinates						
Item	Part	x	y	z	rot1	rot2	rot3	Length
1	1a	10	10	-5,0000	0	0	0	5,0000
	1b	-10	10	-5,0000	0	0	0	5,0000
	1c	-10	-10	-5,0000	0	0	0	5,0000
	1d	10	-10	-5,0000	0	0	0	5,0000
2	2a	10	10	0	4,846477	-4,84648	0	7,6750
	2b	-10	10	0	4,846477	4,846477	0	7,6750
	2c	-10	-10	0	-4,84648	4,846477	0	7,6750
	2d	10	-10	0	-4,84648	-4,84648	0	7,6750
3	3a	9,351569	9,351569	7,647559	4,846477	-4,84648	0	12,1310
	3b	-9,35157	9,351569	7,647559	4,846477	4,846477	0	12,1310
	3c	-9,35157	-9,35157	7,647559	-4,84648	4,846477	0	12,1310
	3d	9,351569	-9,35157	7,647559	-4,84648	-4,84648	0	12,1310
4	4a	8,326667	8,326667	19,73519	4,846477	-4,84648	0	11,1250
	4b	-8,32667	8,326667	19,73519	4,846477	4,846477	0	11,1250
	4c	-8,32667	-8,32667	19,73519	-4,84648	4,846477	0	11,1250
	4d	8,326667	-8,32667	19,73519	-4,84648	-4,84648	0	11,1250
5	5a	7,386759	7,386759	30,82041	4,846477	-4,84648	0	9,7760
	5b	-7,38676	7,386759	30,82041	4,846477	4,846477	0	9,7760
	5c	7,386759	-7,38676	30,82041	-4,84648	4,846477	0	9,7760
	5d	-7,38676	-7,38676	30,82041	-4,84648	-4,84648	0	9,7760
6	6a	6,560823	6,560823	40,56146	4,846477	-4,84648	0	5,1680
	6b	-6,56082	6,560823	40,56146	4,846477	4,846477	0	5,1680
	6c	6,560823	-6,56082	40,56146	-4,84648	4,846477	0	5,1680
	6d	-6,56082	-6,56082	40,56146	-4,84648	-4,84648	0	5,1680
7	7a	9,914922	9,914922	1,0034				10,7510
8	8a	8,826487	8,826487	13,84034				10,1830
9	9a	-8,82649	8,826487	13,84034				9,4910
10	10a	-9,91492	9,914922	1,0034				11,4700
11	11a	8,826487	8,826487	13,84034				9,4300
12	12a	7,850588	7,850588	25,35004				9,0030
13	13a	-7,85059	7,850588	25,35004				8,3100
14	14a	-8,82649	8,826487	13,84034				10,1490
15	15a	7,850588	7,850588	25,35004				8,2490
16	16a	6,981141	6,981141	35,60425				7,9510
17	17a	-6,98114	6,981141	35,60425				7,2590
18	18a	-7,85059	7,850588	25,35004				8,9680
19	19a	6,981141	6,981141	35,60425				7,1980
20	20a	6,213415	6,213415	44,65876				7,0140
21	21a	-6,21342	6,213415	44,65876				6,3220
22	22a	-6,98114	6,981141	35,60425				7,9170

Appendix 2 – Jacket Foundation Continued

Jacket foundation

[m]

Item	Quantity	OD	WT	ID	Length	New length	Mass	Ix,y	Iz	Drag area	local COG	Total mass
1	4	0,8840	0,0560	0,7720	5,0000	5,0000	8,055662	17,47614	1,387024	4,42	2,5	32,22265
2	4	0,8840	0,0560	0,7720	7,6750	7,6750	12,36544	61,76404	2,129082	6,7847	3,8375	49,46176
3	4	0,8640	0,0450	0,7740	12,1310	12,1310	15,53481	191,8165	2,6129	10,48118	6,0655	62,13923
4	4	0,8640	0,0450	0,7740	11,1250	11,1250	14,24654	148,1341	2,396218	9,612	5,5625	56,98615
5	4	0,8640	0,0450	0,7740	9,7760	9,7760	12,51902	100,7566	2,105656	8,446464	4,888	50,07609
6	4	0,8640	0,0450	0,7740	5,1680	5,1680	6,618076	15,28632	1,113137	4,465152	2,584	26,47231
7	4	0,5590	0,0180	0,5230	10,7510	12,0010	4,060692	39,26131	0,297451	6,708559	6,0005	16,24277
8	4	0,5590	0,0180	0,5230	10,1830	10,7330	3,631648	31,51453	0,266023	5,999747	5,3665	14,52659
9	4	0,5590	0,0180	0,5230	9,4910	10,7410	3,634355	27,41472	0,266221	6,004219	5,3705	14,53742
10	4	0,5590	0,0180	0,5230	11,4700	12,0200	4,067121	44,73847	0,297922	6,71918	6,01	16,26848
11	4	0,5590	0,0140	0,5310	9,4300	10,6800	2,831448	21,08738	0,210391	5,97012	5,34	11,32579
12	4	0,5590	0,0140	0,5310	9,0030	9,5530	2,532662	17,20096	0,18819	5,340127	4,7765	10,13065
13	4	0,5590	0,0140	0,5310	8,3100	9,5600	2,534517	14,67949	0,188328	5,34404	4,78	10,13807
14	4	0,5590	0,0140	0,5310	10,1490	10,6990	2,836486	24,4524	0,210766	5,980741	5,3495	11,34594
15	4	0,5590	0,0140	0,5310	8,2490	9,4990	2,518345	14,37384	0,187126	5,309941	4,7495	10,07338
16	4	0,5590	0,0140	0,5310	7,9510	8,5010	2,253759	11,95698	0,167466	4,752059	4,2505	9,015035
17	4	0,5590	0,0140	0,5310	7,2590	8,5090	2,25588	9,989582	0,167624	4,756531	4,2545	9,023518
18	4	0,5590	0,0140	0,5310	8,9680	9,5180	2,523383	17,00568	0,187501	5,320562	4,759	10,09353
19	4	0,5590	0,0180	0,5230	7,1980	8,4480	2,858489	12,44651	0,209388	4,722432	4,224	11,43396
20	4	0,5590	0,0180	0,5230	7,0140	7,5640	2,559376	10,58637	0,187478	4,228276	3,782	10,23751
21	4	0,5590	0,0180	0,5230	6,3220	7,5720	2,562083	8,627216	0,187676	4,232748	3,786	10,24833
22	4	0,5590	0,0180	0,5230	7,9170	8,4670	2,864918	15,06909	0,209859	4,733053	4,2335	11,45967
Topcylinder	1	5,0000	0,0500	4,9000	6,2000	6,2000	53,31872	334,1196	326,6438	31	3,1	53,31872
Topdeck	1	12,2560	0,0000	0,0000	0,0200	0,0200	33,22695	415,9182	831,8341	0,24512	0,01	33,22695
							Total Mass:					550,0045

	Density	
Steel	11,0602	[T/m^3]
Sea water	1,025	[T/m^3]

Mass - Mass of the part
Ix, Iy and Iz - Mass moment of inertia in the respective direction
Drag Area - Projected drag area

After designing the jacket, new lengths were used to get a continous and symmetric jacket. These are the "new length" column.
The Steel Denisty is corrected to get the right weight.

Appendix 3 – Normal Drag Area

Hydrodynamic coefficients of jacket members

Drag "DNV-RP-C205" — For Vc > 0.4*Vm, CD =CDS — Correction for finite length, FL corr.

Surface roughı 0,003

			Normal Drag Coefficients					Normal drag Area
Meml	Length	OD	Delta	CDS	Length/OD	Corr.factor	Normal CD	Drag area
1	5,0000	0,884	3,394E-03	0,956134	5,6561086	0,82264	0,956133798	4,42
2	7,6750	0,884	3,394E-03	0,956134		1	0,956133798	6,7847
3	12,1310	0,864	3,472E-03	0,958122		1	0,958121502	10,481184
4	11,1250	0,864	3,472E-03	0,958122		1	0,958121502	9,612
5	9,7760	0,864	3,472E-03	0,958122		1	0,958121502	8,446464
6	5,1680	0,864	3,472E-03	0,958122		1	0,958121502	4,465152
7	12,0010	0,559	5,367E-03	0,995942		1	0,995941889	6,708559
8	10,7330	0,559	5,367E-03	0,995942		1	0,995941889	5,999747
9	10,7410	0,559	5,367E-03	0,995942		1	0,995941889	6,004219
10	12,0200	0,559	5,367E-03	0,995942		1	0,995941889	6,71918
11	10,6800	0,559	5,367E-03	0,995942		1	0,995941889	5,97012
12	9,5530	0,559	5,367E-03	0,995942		1	0,995941889	5,340127
13	9,5600	0,559	5,367E-03	0,995942		1	0,995941889	5,34404
14	10,6990	0,559	5,367E-03	0,995942		1	0,995941889	5,980741
15	9,4990	0,559	5,367E-03	0,995942		1	0,995941889	5,309941
16	8,5010	0,559	5,367E-03	0,995942		1	0,995941889	4,752059
17	8,5090	0,559	5,367E-03	0,995942		1	0,995941889	4,756531
18	9,5180	0,559	5,367E-03	0,995942		1	0,995941889	5,320562
19	8,4480	0,559	5,367E-03	0,995942		1	0,995941889	4,722432
20	7,5640	0,559	5,367E-03	0,995942		1	0,995941889	4,228276
21	7,5720	0,559	5,367E-03	0,995942		1	0,995941889	4,232748
22	8,4670	0,559	5,367E-03	0,995942		1	0,995941889	4,733053
							CD	
	Corrected for loose ends at downer cylinders of element 1						0,786553908	

Appendix 4 – Tangential Drag Area

Tangential drag

"DNV-RP-C205"

m	0,03
n	0,05

					angle of attack [deg]				Tangential Drag Coefficient				Tangential drag area
Item	Part	Length	x-length	y-length	0	15	30	45	0 deg	15 deg	30 deg	45 deg	
1	1a	5	0	0	90	90	90	90	0,0000	0,0000	0,0000	0,0000	0,61375411
	1b	5	0	0	90	90	90	90	0,0000	0,0000	0,0000	0,0000	0,61375411
	1c	5	0	0	90	90	90	90	0,0000	0,0000	0,0000	0,0000	0,61375411
	1d	5	0	0	90	90	90	90	0,0000	0,0000	0,0000	0,0000	0,61375411
2	2a	7,675	0,648431	0,648431	85,1535244	84,9821283	84,4015387	85,1535244	0,0064	0,0067	0,0074	0,0064	0,61375411
	2b	7,675	0,648431	0,648431	85,1535244	84,9821283	84,4015387	85,1535244	0,0064	0,0067	0,0074	0,0064	0,61375411
	2c	7,675	0,648431	0,648431	85,1535244	84,9821283	84,4015387	85,1535244	0,0064	0,0067	0,0074	0,0064	0,61375411
	2d	7,675	0,648431	0,648431	85,1535244	84,9821283	84,4015387	85,1535244	0,0064	0,0067	0,0074	0,0064	0,61375411
3	3a	12,131	1,024899	1,024899	85,1535346	84,9823894	84,4015506	85,1535346	0,0065	0,0067	0,0075	0,0065	0,58629659
	3b	12,131	1,024899	1,024899	85,1535346	84,9823894	84,4015506	85,1535346	0,0065	0,0067	0,0075	0,0065	0,58629659
	3c	12,131	1,024899	1,024899	85,1535346	84,9823894	84,4015506	85,1535346	0,0065	0,0067	0,0075	0,0065	0,58629659
	3d	12,131	1,024899	1,024899	85,1535346	84,9823894	84,4015506	85,1535346	0,0065	0,0067	0,0075	0,0065	0,58629659
4	4a	11,125	0,939911	0,939911	85,1535095	84,9821292	84,4015215	85,1535095	0,0065	0,0067	0,0075	0,0065	0,58629659
	4b	11,125	0,939911	0,939911	85,1535095	84,9821292	84,4015215	85,1535095	0,0065	0,0067	0,0075	0,0065	0,58629659
	4c	11,125	0,939911	0,939911	85,1535095	84,9821292	84,4015215	85,1535095	0,0065	0,0067	0,0075	0,0065	0,58629659
	4d	11,125	0,939911	0,939911	85,1535095	84,9821292	84,4015215	85,1535095	0,0065	0,0067	0,0075	0,0065	0,58629659
5	5a	9,776	0,825936	0,825936	85,1535264	84,98213041	84,401541	85,1535264	0,0065	0,0067	0,0075	0,0065	0,58629659
	5b	9,776	0,825936	0,825936	85,1535264	84,98213041	84,401541	85,1535264	0,0065	0,0067	0,0075	0,0065	0,58629659
	5c	9,776	0,825936	0,825936	85,1535264	84,98213041	84,401541	85,1535264	0,0065	0,0067	0,0075	0,0065	0,58629659
	5d	9,776	0,825936	0,825936	85,1535264	84,98213041	84,401541	85,1535264	0,0065	0,0067	0,0075	0,0065	0,58629659
6	6a	5,168	0,432823	0,432823	85,1958178	85,02592488	84,450433	85,1958178	0,0064	0,0066	0,0074	0,0064	0,58629659
	6b	5,168	0,432823	0,432823	85,1958178	85,02592488	84,450433	85,1958178	0,0064	0,0066	0,0074	0,0064	0,58629659
	6c	5,168	0,432823	0,432823	85,1958178	85,02592488	84,450433	85,1958178	0,0064	0,0066	0,0074	0,0064	0,58629659
	6d	5,168	0,432823	0,432823	85,1958178	85,02592488	84,450433	85,1958178	0,0064	0,0066	0,0074	0,0064	0,58629659
7	7a	12,001	10	0,0844846	33,5645065	30,38362444	15,8100398	89,596646	0,0478	0,0475	0,0418	0,0006	0,245422
	7b	12,001	0,0844846	10	89,596646	89,58241699	89,5342457	33,5645065	0,0006	0,0006	0,0006	0,0478	0,245422
	7c	12,001	10	0,0844846	33,5645065	30,38362444	15,8100398	89,596646	0,0478	0,0475	0,0418	0,0006	0,245422
	7d	12,001	0,0844846	10	89,596646	89,58241699	89,5342457	33,5645065	0,0006	0,0006	0,0006	0,0478	0,245422
8	8a	10,733	8,826487	0,525082	34,6773474	31,63801514	18,269958	87,1958449	0,0479	0,0477	0,0432	0,0039	0,245422
	8b	10,733	0,525082	8,826487	87,1958449	87,09684177	86,7616092	34,6773474	0,0039	0,0040	0,0045	0,0479	0,245422
	8c	10,733	8,826487	0,525082	34,6773474	31,63801514	18,269958	87,1958449	0,0479	0,0477	0,0432	0,0039	0,245422
	8d	10,733	0,525082	8,826487	87,1958449	87,09684177	86,7616092	34,6773474	0,0039	0,0040	0,0045	0,0479	0,245422
9	9a	10,741	8,826487	0,525082	34,7389813	31,70721065	18,3987824	87,1979352	0,0479	0,0477	0,0433	0,0039	0,245422
	9b	10,741	0,525082	8,826487	87,1979352	87,09900592	86,7640237	34,7389813	0,0039	0,0040	0,0045	0,0479	0,245422
	9c	10,741	8,826487	0,525082	34,7389813	31,70721065	18,3987824	87,1979352	0,0479	0,0477	0,0433	0,0039	0,245422
	9d	10,741	0,525082	8,826487	87,1979352	87,09900592	86,7640237	34,7389813	0,0039	0,0040	0,0045	0,0479	0,245422
10	10a	12,02	10	0,0844846	33,7007607	30,53774059	16,1267937	89,5972836	0,0478	0,0475	0,0420	0,0006	0,245422
	10b	12,02	0,0844846	10	89,5972836	89,58307708	89,5349819	33,7007607	0,0006	0,0006	0,0006	0,0478	0,245422
	10c	12,02	10	0,0844846	33,7007607	30,53774059	16,1267937	89,5972836	0,0478	0,0475	0,0420	0,0006	0,245422
	10d	12,02	0,0844846	10	89,5972836	89,58307708	89,5349819	33,7007607	0,0006	0,0006	0,0006	0,0478	0,245422
11	11a	10,68	8,826487	0,499817	34,2642149	31,17346306	17,3881094	87,3176153	0,0479	0,0476	0,0427	0,0037	0,245422
	11b	10,68	0,499817	8,826487	87,3176153	87,22291813	86,9022714	34,2642149	0,0037	0,0039	0,0043	0,0479	0,245422
	11c	10,68	8,826487	0,499817	34,2642149	31,17346306	17,3881094	87,3176153	0,0479	0,0476	0,0427	0,0037	0,245422
	11d	10,68	0,499817	8,826487	87,3176153	87,22291813	86,9022714	34,2642149	0,0037	0,0039	0,0043	0,0479	0,245422
12	12a	9,553	7,850588	0,476079	34,7353208	31,70310181	18,3911501	87,1434501	0,0479	0,0477	0,0433	0,0040	0,245422
		9,553	0,476079	7,850588	87,1434501	87,0425939	86,7010842	34,7353208	0,0040	0,0041	0,0046	0,0479	0,245422
		9,553	7,850588	0,476079	34,7353208	31,70310181	18,3911501	87,1434501	0,0479	0,0477	0,0433	0,0040	0,245422
		9,553	0,476079	7,850588	87,1434501	87,0425939	86,7010842	34,7353208	0,0040	0,0041	0,0046	0,0479	0,245422
13	13a	9,56	7,850588	0,476079	34,7957828	31,77095621	18,5169154	87,1455435	0,0479	0,0477	0,0433	0,0040	0,245422
		9,56	0,476079	7,850588	87,1455435	87,04476129	86,7035024	34,7957828	0,0040	0,0041	0,0046	0,0479	0,245422
		9,56	7,850588	0,476079	34,7957828	31,77095621	18,5169154	87,1455435	0,0479	0,0477	0,0433	0,0040	0,245422
		9,56	0,476079	7,850588	87,1455435	87,04476129	86,7035024	34,7957828	0,0040	0,0041	0,0046	0,0479	0,245422
14	14a	10,699	8,826487	0,499817	34,4132901	31,34124169	17,7101411	87,3223823	0,0479	0,0476	0,0429	0,0037	0,245422
		10,699	0,499817	8,826487	87,3223823	87,22785371	86,9077779	34,4132901	0,0037	0,0039	0,0043	0,0479	0,245422
		10,699	8,826487	0,499817	34,4132901	31,34124169	17,7101411	87,3223823	0,0479	0,0476	0,0429	0,0037	0,245422
		10,699	0,499817	8,826487	87,3223823	87,22785371	86,9077779	34,4132901	0,0037	0,0039	0,0043	0,0479	0,245422
15	15a	9,499	7,850588	0,463829	34,2627304	31,17179146	17,3848798	87,2011774	0,0479	0,0476	0,0427	0,0039	0,245422
		9,499	0,463829	7,850588	87,2011774	87,10236279	86,767769	34,2627304	0,0039	0,0040	0,0045	0,0479	0,245422
		9,499	7,850588	0,463829	34,2627304	31,17179146	17,3848798	87,2011774	0,0479	0,0476	0,0427	0,0039	0,245422
		9,499	0,463829	7,850588	87,2011774	87,10236279	86,767769	34,2627304	0,0039	0,0040	0,0045	0,0479	0,245422
16	16a	8,501	6,981141	0,405618	34,7934856	31,76837862	18,5121486	87,2651421	0,0479	0,0477	0,0433	0,0038	0,245422
		8,501	0,405618	6,981141	87,2651421	87,16858952	86,8416579	34,7934856	0,0038	0,0039	0,0044	0,0479	0,245422
		8,501	6,981141	0,405618	34,7934856	31,76837862	18,5121486	87,2651421	0,0479	0,0477	0,0433	0,0038	0,245422
		8,501	0,405618	6,981141	87,2651421	87,16858952	86,8416579	34,7934856	0,0038	0,0039	0,0044	0,0479	0,245422
17	17a	8,509	6,981141	0,405618	34,8709356	31,85526028	18,6723622	87,2677153	0,0479	0,0477	0,0434	0,0038	0,245422
		8,509	0,405618	6,981141	87,2677153	87,17125372	86,8446303	34,8709356	0,0038	0,0039	0,0044	0,0479	0,245422
		8,509	6,981141	0,405618	34,8709356	31,85526028	18,6723622	87,2677153	0,0479	0,0477	0,0434	0,0038	0,245422
		8,509	0,405618	6,981141	87,2677153	87,17125372	86,8446303	34,8709356	0,0038	0,0039	0,0044	0,0479	0,245422
18	18a	9,518	7,850588	0,463829	34,4302728	31,36034428	17,7465448	87,2067689	0,0479	0,0476	0,0429	0,0039	0,245422
		9,518	0,463829	7,850588	87,2067689	87,10815202	86,7742281	34,4302728	0,0039	0,0040	0,0045	0,0479	0,245422
		9,518	7,850588	0,463829	34,4302728	31,36034428	17,7465448	87,2067689	0,0479	0,0476	0,0429	0,0039	0,245422
		9,518	0,463829	7,850588	87,2067689	87,10815202	86,7742281	34,4302728	0,0039	0,0040	0,0045	0,0479	0,245422
19	19a	8,448	6,981141	0,420318	34,2727595	31,18308428	17,4066898	87,1481541	0,0479	0,0476	0,0427	0,0040	0,245422
		8,448	0,420318	6,981141	87,1481541	87,04746424	86,7065181	34,2727595	0,0040	0,0041	0,0046	0,0479	0,245422
		8,448	6,981141	0,420318	34,2727595	31,18308428	17,4066898	87,1481541	0,0479	0,0476	0,0427	0,0040	0,245422
		8,448	0,420318	6,981141	87,1481541	87,04746424	86,7065181	34,2727595	0,0040	0,0041	0,0046	0,0479	0,245422
20	20a	7,564	6,213415	0,347408	34,7702268	31,7422789	18,4638347	87,3675282	0,0479	0,0477	0,0433	0,0037	0,245422
		7,564	0,347408	6,213415	87,3675282	87,2745957	86,9599264	34,7702268	0,0037	0,0038	0,0042	0,0479	0,245422
		7,564	6,213415	0,347408	34,7702268	31,7422789	18,4638347	87,3675282	0,0479	0,0477	0,0433	0,0037	0,245422
		7,564	0,347408	6,213415	87,3675282	87,2745957	86,9599264	34,7702268	0,0037	0,0038	0,0042	0,0479	0,245422
21	21a	7,572	6,213415	0,347408	34,8573257	31,83999617	18,6442824	87,3703114	0,0479	0,0477	0,0434	0,0037	0,245422
		7,572	0,347408	6,213415	87,3703114	87,27747732	86,9631414	34,8573257	0,0037	0,0038	0,0042	0,0479	0,245422
		7,572	6,213415	0,347408	34,8573257	31,83999617	18,6442824	87,3703114	0,0479	0,0477	0,0434	0,0037	0,245422
		7,572	0,347408	6,213415	87,3703114	87,27747732	86,9631414	34,8573257	0,0037	0,0038	0,0042	0,0479	0,245422
22	22a	8,467	6,981141	0,420318	34,4609784	31,39487724	17,8122217	87,1545589	0,0479	0,0476	0,0429	0,0040	0,245422
		8,467	0,420318	6,981141	87,1545589	87,0540956	86,7139169	34,4609784	0,0040	0,0041	0,0046	0,0479	0,245422
		8,467	6,981141	0,420318	34,4609784	31,39487724	17,8122217	87,1545589	0,0479	0,0476	0,0429	0,0040	0,245422
		8,467	0,420318	6,981141	87,1545589	87,0540956	86,7139169	34,4609784	0,0040	0,0041	0,0046	0,0479	0,245422

Appendix 5 – Added Mass and Damping Case 1a

Added mass coefficients
CASE 1a
For jacket in initial position,
Distance to sea bed 10 m

k is obtained from "solvek.m"
Run "bessel.m" with the right k to get the added mass coefficient for the different radii of the surface piercing elements

Critical period 5,3 sec (from modal analysis)
Current velocity 1,02888889 m/s
in x-direction
Water depth 30 m
omega 1,18550666 rad/s
k 0,1433 rad/m (from "solvek.m" - solves disperation relation)

Item	Member	Length	OD	Near freesurface	Surface piercing	Kc	Added mass coefficient CA	2d added mass	Ap	lamda	3d added mass	Axial added mass coefficient CA	Normal Damping Bcr	2% damp	5% damp	10 % damp
1	a	5,0000	0,884	-	-	6,14662255	0,8615	0,236025761	0,613754107	0,61041732	0,390902756	0,4852522	3,55557297	0,07111146	0,17777865	0,3555573
2	a	7,6750	0,884	-	-	6,14662255	0,8615	0,236025761	0,613754107	0,50513391	0,397396734	0,32137693	5,45780451	0,10915609	0,27289023	0,54578045
3	a	12,1310	0,864	YES	YES	6,28890548	1,0092	0,220365619	0,586296587	0,38695171	0,374431011	0,24102714	7,40053361	0,14801067	0,37002668	0,74005336
4	a	11,1250	0,864	-	-	6,28890548	0,8553	0,220365619	0,586296587	0,40767758	0,374020454	0,26253431	6,26692728	0,12533855	0,31334636	0,62669273
5	a	9,7760	0,864	-	-	6,28890548	0,8553	0,220365619	0,586296587	0,43922448	0,373260503	0,29815464	5,50700954	0,11014019	0,27535048	0,55070095
6	a	5,1680	0,864	-	-	6,28890548	0,8553	0,220365619	0,586296587	0,59703706	0,365952187	0,55295854	2,91123417	0,05822468	0,14556171	0,29112342
7	a	12,0010	0,559	-	-	9,72024031	0,7043	0,059681267	0,245422003	0,29218555	0,101728224	0,25051942	1,64090145	0,03281803	0,08204507	0,16409015
	b	12,0010	0,559	-	-	5,48741362	0,8906	0,059681267	0,245422003	0,29218555	0,101728224	0,25051942	1,8202167	0,03640433	0,09101083	0,18202167
	c	12,0010	0,559	-	-	9,72024031	0,7043	0,059681267	0,245422003	0,29218555	0,101728224	0,25051942	1,64090145	0,03281803	0,08204507	0,16409015
	d	12,0010	0,559	-	-	5,48741362	0,8906	0,059681267	0,245422003	0,29218555	0,101728224	0,25051942	1,8202167	0,03640433	0,09101083	0,18202167
8	a	10,7330	0,559	-	-	9,72024031	0,7043	0,059681267	0,245422003	0,31580327	0,101671897	0,27996077	1,46752731	0,02935055	0,07337637	0,14675273
	b	10,7330	0,559	-	-	5,48741362	0,8906	0,059681267	0,245422003	0,31580327	0,101671897	0,27996077	1,62789649	0,03255793	0,08139482	0,16278965
	c	10,7330	0,559	-	-	9,72024031	0,7043	0,059681267	0,245422003	0,31580327	0,101671897	0,27996077	1,46752731	0,02935055	0,07337637	0,14675273
	d	10,7330	0,559	-	-	5,48741362	0,8906	0,059681267	0,245422003	0,31580327	0,101671897	0,27996077	1,62789649	0,03255793	0,08139482	0,16278965
9	a	10,7410	0,559	-	-	9,72024031	0,7043	0,059681267	0,245422003	0,3156423	0,101672326	0,27975343	1,46862116	0,02937242	0,07343106	0,14686212
	b	10,7410	0,559	-	-	5,48741362	0,8906	0,059681267	0,245422003	0,3156423	0,101672326	0,27975343	1,62910987	0,0325822	0,08145549	0,16291099
	c	10,7410	0,559	-	-	9,72024031	0,7043	0,059681267	0,245422003	0,3156423	0,101672326	0,27975343	1,46862116	0,02937242	0,07343106	0,14686212
	d	10,7410	0,559	-	-	5,48741362	0,8906	0,059681267	0,245422003	0,3156423	0,101672326	0,27975343	1,62910987	0,0325822	0,08145549	0,16291099
10	a	12,0200	0,559	-	-	9,72024031	0,7043	0,059681267	0,245422003	0,29185849	0,101728914	0,25012513	1,64349933	0,03286999	0,08217497	0,16434993
	b	12,0200	0,559	-	-	5,48741362	0,8906	0,059681267	0,245422003	0,29185849	0,101728914	0,25012513	1,82309847	0,03646197	0,09115492	0,18230985
	c	12,0200	0,559	-	-	9,72024031	0,7043	0,059681267	0,245422003	0,29185849	0,101728914	0,25012513	1,64349933	0,03286999	0,08217497	0,16434993
	d	12,0200	0,559	-	-	5,48741362	0,8906	0,059681267	0,245422003	0,29185849	0,101728914	0,25012513	1,82309847	0,03646197	0,09115492	0,18230985
11	a	10,6800	0,559	YES	YES	9,72024031	1,0046	0,059681267	0,245422003	0,31687385	0,101669022	0,35907073	1,34576852	0,02691537	0,06728843	0,13457685
	b	10,6800	0,559	YES	YES	9,72024031	1,0046	0,059681267	0,245422003	0,31687385	0,101669022	0,35907073	1,34576852	0,02691537	0,06728843	0,13457685
	c	10,6800	0,559	YES	YES	9,72024031	1,0046	0,059681267	0,245422003	0,31687385	0,101669022	0,35907073	1,34576852	0,02691537	0,06728843	0,13457685
	d	10,6800	0,559	YES	YES	9,72024031	1,0046	0,059681267	0,245422003	0,31687385	0,101669022	0,35907073	1,34576852	0,02691537	0,06728843	0,13457685
12	a	9,5530	0,559	-	-	9,72024031	0,7043	0,059681267	0,245422003	0,3414907	0,101594362	0,40113674	1,02343345	0,02046867	0,05117167	0,10234335
	b	9,5530	0,559	-	-	5,48741362	0,8906	0,059681267	0,245422003	0,3414907	0,101594362	0,40113674	1,13527273	0,02270545	0,05676364	0,11352727
	c	9,5530	0,559	-	-	9,72024031	0,7043	0,059681267	0,245422003	0,3414907	0,101594362	0,40113674	1,02343345	0,02046867	0,05117167	0,10234335
	d	9,5530	0,559	-	-	5,48741362	0,8906	0,059681267	0,245422003	0,3414907	0,101594362	0,40113674	1,13527273	0,02270545	0,05676364	0,11352727
13	a	9,5600	0,559	-	-	9,72024031	0,7043	0,059681267	0,245422003	0,341326	0,101594919	0,40084522	1,02418338	0,02048367	0,05120917	0,10241834
	b	9,5600	0,559	-	-	5,48741362	0,8906	0,059681267	0,245422003	0,341326	0,101594919	0,40084522	1,1361046	0,02272209	0,05680523	0,11361046
	c	9,5600	0,559	-	-	9,72024031	0,7043	0,059681267	0,245422003	0,341326	0,101594919	0,40084522	1,02418338	0,02048367	0,05120917	0,10241834
	d	9,5600	0,559	-	-	5,48741362	0,8906	0,059681267	0,245422003	0,341326	0,101594919	0,40084522	1,1361046	0,02272209	0,05680523	0,11361046
14	a	10,6990	0,559	YES	YES	9,72024031	1,0046	0,059681267	0,245422003	0,31648922	0,101670058	0,35843672	1,34816267	0,02696325	0,06740813	0,13481627
	b	10,6990	0,559	YES	YES	5,48741362	1,0046	0,059681267	0,245422003	0,31648922	0,101670058	0,35843672	1,34816267	0,02696325	0,06740813	0,13481627
	c	10,6990	0,559	YES	YES	9,72024031	1,0046	0,059681267	0,245422003	0,31648922	0,101670058	0,35843672	1,34816267	0,02696325	0,06740813	0,13481627
	d	10,6990	0,559	YES	YES	5,48741362	1,0046	0,059681267	0,245422003	0,31648922	0,101670058	0,35843672	1,34816267	0,02696325	0,06740813	0,13481627
15	a	9,4990	0,559	-	-	9,72024031	0,7043	0,059681267	0,245422003	0,34276659	0,101590019	0,40339988	1,01764832	0,02035297	0,05088242	0,10176483
	b	9,4990	0,559	-	-	5,48741362	0,8906	0,059681267	0,245422003	0,34276659	0,101590019	0,40339988	1,1288554	0,02257711	0,05644277	0,11288554
	c	9,4990	0,559	-	-	9,72024031	0,7043	0,059681267	0,245422003	0,34276659	0,101590019	0,40339988	1,01764832	0,02035297	0,05088242	0,10176483
	d	9,4990	0,559	-	-	5,48741362	0,8906	0,059681267	0,245422003	0,34276659	0,101590019	0,40339988	1,1288554	0,02257711	0,05644277	0,11288554
16	a	8,5010	0,559	-	-	9,72024031	0,7043	0,059681267	0,245422003	0,36819066	0,101492719	0,45032647	0,91073043	0,01821461	0,04553652	0,09107304
	b	8,5010	0,559	-	-	5,48741362	0,8906	0,059681267	0,245422003	0,36819066	0,101492719	0,45032647	1,01025368	0,02020507	0,05051268	0,10102537
	c	8,5010	0,559	-	-	9,72024031	0,7043	0,059681267	0,245422003	0,36819066	0,101492719	0,45032647	0,91073043	0,01821461	0,04553652	0,09107304
	d	8,5010	0,559	-	-	5,48741362	0,8906	0,059681267	0,245422003	0,36819066	0,101492719	0,45032647	1,01025368	0,02020507	0,05051268	0,10102537
17	a	8,5090	0,559	-	-	9,72024031	0,7043	0,059681267	0,245422003	0,36797188	0,101493648	0,4499072	0,91158749	0,01823175	0,04557937	0,09115875
	b	8,5090	0,559	-	-	5,48741362	0,8906	0,059681267	0,245422003	0,36797188	0,101493648	0,4499072	1,0112044	0,02022409	0,05056022	0,10112044
	c	8,5090	0,559	-	-	9,72024031	0,7043	0,059681267	0,245422003	0,36797188	0,101493648	0,4499072	0,91158749	0,01823175	0,04557937	0,09115875
	d	8,5090	0,559	-	-	5,48741362	0,8906	0,059681267	0,245422003	0,36797188	0,101493648	0,4499072	1,0112044	0,02022409	0,05056022	0,10112044
18	a	9,5180	0,559	-	-	9,72024031	0,7043	0,059681267	0,245422003	0,34231658	0,101591557	0,4026007	1,01968383	0,02039368	0,05098419	0,10196838
	b	9,5180	0,559	-	-	5,48741362	0,8906	0,059681267	0,245422003	0,34231658	0,101591557	0,4026007	1,13111335	0,02262227	0,05655567	0,11311133
	c	9,5180	0,559	-	-	9,72024031	0,7043	0,059681267	0,245422003	0,34231658	0,101591557	0,4026007	1,01968383	0,02039368	0,05098419	0,10196838
	d	9,5180	0,559	-	-	5,48741362	0,8906	0,059681267	0,245422003	0,34231658	0,101591557	0,4026007	1,13111335	0,02262227	0,05655567	0,11311133
19	a	8,4480	0,559	-	-	9,72024031	0,7043	0,059681267	0,245422003	0,36964672	0,10148649	0,35503544	1,15509836	0,02310197	0,05775492	0,11550984
	b	8,4480	0,559	-	-	5,48741362	0,8906	0,059681267	0,245422003	0,36964672	0,10148649	0,35503544	1,28132578	0,02562652	0,06406629	0,12813258
	c	8,4480	0,559	-	-	9,72024031	0,7043	0,059681267	0,245422003	0,36964672	0,10148649	0,35503544	1,15509836	0,02310197	0,05775492	0,11550984
	d	8,4480	0,559	-	-	5,48741362	0,8906	0,059681267	0,245422003	0,36964672	0,10148649	0,35503544	1,28132578	0,02562652	0,06406629	0,12813258
20	a	7,5640	0,559	-	-	9,72024031	0,7043	0,059681267	0,245422003	0,39575053	0,1013615	0,39603985	1,0342287	0,02068457	0,05171143	0,10342287
	b	7,5640	0,559	-	-	5,48741362	0,8906	0,059681267	0,245422003	0,39575053	0,1013615	0,39603985	1,14724766	0,02294495	0,05736238	0,11472477
	c	7,5640	0,559	-	-	9,72024031	0,7043	0,059681267	0,245422003	0,39575053	0,1013615	0,39603985	1,0342287	0,02068457	0,05171143	0,10342287
	d	7,5640	0,559	-	-	5,48741362	0,8906	0,059681267	0,245422003	0,39575053	0,1013615	0,39603985	1,14724766	0,02294495	0,05736238	0,11472477
21	a	7,5720	0,559	-	-	9,72024031	0,7043	0,059681267	0,245422003	0,39549778	0,101362838	0,39562664	1,03532254	0,02070645	0,05176613	0,10353225
	b	7,5720	0,559	-	-	5,48741362	0,8906	0,059681267	0,245422003	0,39549778	0,101362838	0,39562664	1,14846103	0,02296922	0,05742305	0,1148461
	c	7,5720	0,559	-	-	9,72024031	0,7043	0,059681267	0,245422003	0,39549778	0,101362838	0,39562664	1,03532254	0,02070645	0,05176613	0,10353225
	d	7,5720	0,559	-	-	5,48741362	0,8906	0,059681267	0,245422003	0,39549778	0,101362838	0,39562664	1,14846103	0,02296922	0,05742305	0,1148461
22	a	8,4670	0,559	-	-	9,72024031	0,7043	0,059681267	0,245422003	0,36912342	0,101488737	0,35424658	1,15769624	0,02315392	0,05788481	0,11576962
	b	8,4670	0,559	-	-	5,48741362	0,8906	0,059681267	0,245422003	0,36912342	0,101488737	0,35424658	1,28420755	0,02568415	0,06421038	0,12842075
	c	8,4670	0,559	-	-	9,72024031	0,7043	0,059681267	0,245422003	0,36912342	0,101488737	0,35424658	1,15769624	0,02315392	0,05788481	0,11576962
	d	8,4670	0,559	-	-	5,48741362	0,8906	0,059681267	0,245422003	0,36912342	0,101488737	0,35424658	1,28420755	0,02568415	0,06421038	0,12842075

Appendix 6 – Added Mass and Damping Case 2a

Added mass coefficients
CASE 2a
For jacket in initial position,
Distance to sea bed 3 m

k is obtained from "solvek.m"
Run "bessel.m" with the right k to get the added mass coefficient for the different radii of the surface piercing elements

Critical perio	5,9	sec	(from modal analysis)
Current velo	1,02888889	m/s	
in x-direction			
Water depth	30	m	
omega	1,06494666	rad/s	
k	0,1158	rad/m	(from "solvek.m" - solves disperation relation)

Item	Member	Length	OD	Near freesurface	Surface piercing	Kc	Added mass coefficient CA	2d added mass	Ap	lamda	3d added ma	Axial added mass coefficient CA	Normal Damping Bcr	2% damp	5% damp	10 % damp
1	a	5,0000	0,884	-	-	6,84246661	0,8309	0,236025761	0,61375411	0,61041732	0,39090276	0,4852522	3,14145731	0,06282915	0,15707287	0,31414573
2	a	7,6750	0,884	-	-	6,84246661	0,8309	0,236025761	0,61375411	0,50513391	0,39739673	0,32137693	4,82213697	0,09644274	0,24110685	0,4822137
3	a	12,1310	0,864	-	-	7,00085704	0,8240	0,220365619	0,58629659	0,38695171	0,37443101	0,24102714	6,03503202	0,12070064	0,3017516	0,6035032
4	a	11,1250	0,864	YES	YES	7,00085704	1,0065	0,220365619	0,58629659	0,40767758	0,37402045	0,26253431	6,08844384	0,12176888	0,30442219	0,60884438
5	a	9,7760	0,864	-	-	7,00085704	0,8240	0,220365619	0,58629659	0,43922448	0,3732605	0,29815464	4,86344679	0,09726894	0,24317234	0,48634468
6	a	5,1680	0,864	-	-	7,00085704	0,8240	0,220365619	0,58629659	0,59703706	0,36595219	0,55295854	2,57102015	0,0514204	0,12855101	0,25710202
7	a	12,0010	0,559	-	-	10,8206449	0,6559	0,059681267	0,245422	0,29218555	0,10172822	0,25051942	1,43215433	0,02864309	0,07160772	0,14321543
	b	12,0010	0,559	-	-	6,10863025	0,8632	0,059681267	0,245422	0,29218555	0,10172822	0,25051942	1,61146958	0,03222939	0,08057348	0,16114696
	c	12,0010	0,559	-	-	10,8206449	0,6559	0,059681267	0,245422	0,29218555	0,10172822	0,25051942	1,43215433	0,02864309	0,07160772	0,14321543
	d	12,0010	0,559	-	-	6,10863025	0,8632	0,059681267	0,245422	0,29218555	0,10172822	0,25051942	1,61146958	0,03222939	0,08057348	0,16114696
8	a	10,7330	0,559	-	-	10,8206449	0,6559	0,059681267	0,245422	0,31580327	0,1016719	0,27996077	1,28083597	0,02561672	0,0640418	0,1280836
	b	10,7330	0,559	-	-	6,10863025	0,8632	0,059681267	0,245422	0,31580327	0,1016719	0,27996077	1,44120515	0,0288241	0,07206026	0,14412051
	c	10,7330	0,559	-	-	10,8206449	0,6559	0,059681267	0,245422	0,31580327	0,1016719	0,27996077	1,28083597	0,02561672	0,0640418	0,1280836
	d	10,7330	0,559	-	-	6,10863025	0,8632	0,059681267	0,245422	0,31580327	0,1016719	0,27996077	1,44120515	0,0288241	0,07206026	0,14412051
9	a	10,7410	0,559	-	-	10,8206449	0,6559	0,059681267	0,245422	0,3156423	0,10167233	0,27975343	1,28179066	0,02563581	0,06408953	0,12817907
	b	10,7410	0,559	-	-	6,10863025	0,8632	0,059681267	0,245422	0,3156423	0,10167233	0,27975343	1,44227937	0,02884559	0,07211397	0,14422794
	c	10,7410	0,559	-	-	10,8206449	0,6559	0,059681267	0,245422	0,3156423	0,10167233	0,27975343	1,28179066	0,02563581	0,06408953	0,12817907
	d	10,7410	0,559	-	-	6,10863025	0,8632	0,059681267	0,245422	0,3156423	0,10167233	0,27975343	1,44227937	0,02884559	0,07211397	0,14422794
10	a	12,0200	0,559	-	-	10,8206449	0,6559	0,059681267	0,245422	0,29185849	0,10172891	0,25012513	1,43442172	0,02868843	0,07172109	0,14344217
	b	12,0200	0,559	-	-	6,10863025	0,8632	0,059681267	0,245422	0,29185849	0,10172891	0,25012513	1,61402086	0,03228042	0,08070104	0,16140209
	c	12,0200	0,559	-	-	10,8206449	0,6559	0,059681267	0,245422	0,29185849	0,10172891	0,25012513	1,43442172	0,02868843	0,07172109	0,14344217
	d	12,0200	0,559	-	-	6,10863025	0,8632	0,059681267	0,245422	0,29185849	0,10172891	0,25012513	1,61402086	0,03228042	0,08070104	0,16140209
11	a	10,6800	0,559	-	-	10,8206449	0,6559	0,059681267	0,245422	0,31687385	0,10166902	0,35907073	0,99861574	0,01997231	0,04993079	0,09986157
	b	10,6800	0,559	-	-	6,10863025	0,8632	0,059681267	0,245422	0,31687385	0,10166902	0,35907073	1,12364907	0,02247298	0,05618245	0,11236491
	c	10,6800	0,559	-	-	10,8206449	0,6559	0,059681267	0,245422	0,31687385	0,10166902	0,35907073	0,99861574	0,01997231	0,04993079	0,09986157
	d	10,6800	0,559	-	-	6,10863025	0,8632	0,059681267	0,245422	0,31687385	0,10166902	0,35907073	1,12364907	0,02247298	0,05618245	0,11236491
12	a	9,5530	0,559	YES	YES	10,8206449	1,0032	0,059681267	0,245422	0,3414907	0,10159436	0,40113674	1,08058599	0,02161172	0,0540293	0,1080586
	b	9,5530	0,559	YES	YES	6,10863025	1,0032	0,059681267	0,245422	0,3414907	0,10159436	0,40113674	1,08058599	0,02161172	0,0540293	0,1080586
	c	9,5530	0,559	YES	YES	10,8206449	1,0032	0,059681267	0,245422	0,3414907	0,10159436	0,40113674	1,08058599	0,02161172	0,0540293	0,1080586
	d	9,5530	0,559	YES	YES	6,10863025	1,0032	0,059681267	0,245422	0,3414907	0,10159436	0,40113674	1,08058599	0,02161172	0,0540293	0,1080586
13	a	9,5600	0,559	YES	YES	10,8206449	1,0032	0,059681267	0,245422	0,341326	0,10159492	0,40084522	1,08137779	0,02162756	0,05406889	0,10813778
	b	9,5600	0,559	YES	YES	6,10863025	1,0032	0,059681267	0,245422	0,341326	0,10159492	0,40084522	1,08137779	0,02162756	0,05406889	0,10813778
	c	9,5600	0,559	YES	YES	10,8206449	1,0032	0,059681267	0,245422	0,341326	0,10159492	0,40084522	1,08137779	0,02162756	0,05406889	0,10813778
	d	9,5600	0,559	YES	YES	6,10863025	1,0032	0,059681267	0,245422	0,341326	0,10159492	0,40084522	1,08137779	0,02162756	0,05406889	0,10813778
14	a	10,6990	0,559	-	-	10,8206449	0,6559	0,059681267	0,245422	0,31648922	0,10167006	0,35843672	1,0003923	0,02000785	0,05001962	0,10003923
	b	10,6990	0,559	-	-	6,10863025	0,8632	0,059681267	0,245422	0,31648922	0,10167006	0,35843672	1,12564807	0,02251296	0,0562824	0,11256481
	c	10,6990	0,559	-	-	10,8206449	0,6559	0,059681267	0,245422	0,31648922	0,10167006	0,35843672	1,0003923	0,02000785	0,05001962	0,10003923
	d	10,6990	0,559	-	-	6,10863025	0,8632	0,059681267	0,245422	0,31648922	0,10167006	0,35843672	1,12564807	0,02251296	0,0562824	0,11256481
15	a	9,4990	0,559	-	-	10,8206449	0,6559	0,059681267	0,245422	0,34276659	0,10159002	0,40339988	0,88818829	0,01776377	0,04440941	0,08881883
	b	9,4990	0,559	-	-	6,10863025	0,8632	0,059681267	0,245422	0,34276659	0,10159002	0,40339988	0,99939537	0,01998791	0,04996977	0,09993954
	c	9,4990	0,559	-	-	10,8206449	0,6559	0,059681267	0,245422	0,34276659	0,10159002	0,40339988	0,88818829	0,01776377	0,04440941	0,08881883
	d	9,4990	0,559	-	-	6,10863025	0,8632	0,059681267	0,245422	0,34276659	0,10159002	0,40339988	0,99939537	0,01998791	0,04996977	0,09993954
16	a	8,5010	0,559	-	-	10,8206449	0,6559	0,059681267	0,245422	0,36819066	0,10149272	0,45032647	0,79487195	0,01589744	0,0397436	0,07948719
	b	8,5010	0,559	-	-	6,10863025	0,8632	0,059681267	0,245422	0,36819066	0,10149272	0,45032647	0,8943952	0,0178879	0,04471976	0,08943952
	c	8,5010	0,559	-	-	10,8206449	0,6559	0,059681267	0,245422	0,36819066	0,10149272	0,45032647	0,79487195	0,01589744	0,0397436	0,07948719
	d	8,5010	0,559	-	-	6,10863025	0,8632	0,059681267	0,245422	0,36819066	0,10149272	0,45032647	0,8943952	0,0178879	0,04471976	0,08943952
17	a	8,5090	0,559	-	-	10,8206449	0,6559	0,059681267	0,245422	0,36797188	0,10149365	0,4499072	0,79561997	0,0159124	0,039781	0,079562
	b	8,5090	0,559	-	-	6,10863025	0,8632	0,059681267	0,245422	0,36797188	0,10149365	0,4499072	0,89523688	0,01790474	0,04476184	0,08952369
	c	8,5090	0,559	-	-	10,8206449	0,6559	0,059681267	0,245422	0,36797188	0,10149365	0,4499072	0,79561997	0,0159124	0,039781	0,079562
	d	8,5090	0,559	-	-	6,10863025	0,8632	0,059681267	0,245422	0,36797188	0,10149365	0,4499072	0,89523688	0,01790474	0,04476184	0,08952369
18	a	9,5180	0,559	-	-	10,8206449	0,6559	0,059681267	0,245422	0,34231658	0,10159156	0,4026007	0,88996485	0,0177993	0,04449824	0,08899648
	b	9,5180	0,559	-	-	6,10863025	0,8632	0,059681267	0,245422	0,34231658	0,10159156	0,4026007	1,00139437	0,02002789	0,05006972	0,10013944
	c	9,5180	0,559	-	-	10,8206449	0,6559	0,059681267	0,245422	0,34231658	0,10159156	0,4026007	0,88996485	0,0177993	0,04449824	0,08899648
	d	9,5180	0,559	-	-	6,10863025	0,8632	0,059681267	0,245422	0,34231658	0,10159156	0,4026007	1,00139437	0,02002789	0,05006972	0,10013944
19	a	8,4480	0,559	-	-	10,8206449	0,6559	0,059681267	0,245422	0,36964672	0,10148649	0,35503544	1,00815264	0,02016305	0,05040763	0,10081526
	b	8,4480	0,559	-	-	6,10863025	0,8632	0,059681267	0,245422	0,36964672	0,10148649	0,35503544	1,13438005	0,0226876	0,056719	0,11343801
	c	8,4480	0,559	-	-	10,8206449	0,6559	0,059681267	0,245422	0,36964672	0,10148649	0,35503544	1,00815264	0,02016305	0,05040763	0,10081526
	d	8,4480	0,559	-	-	6,10863025	0,8632	0,059681267	0,245422	0,36964672	0,10148649	0,35503544	1,13438005	0,0226876	0,056719	0,11343801
20	a	7,5640	0,559	-	-	10,8206449	0,6559	0,059681267	0,245422	0,39575053	0,1013615	0,39603985	0,90265939	0,01805319	0,04513297	0,09026594
	b	7,5640	0,559	-	-	6,10863025	0,8632	0,059681267	0,245422	0,39575053	0,1013615	0,39603985	1,01567835	0,02031357	0,05078392	0,10156784
	c	7,5640	0,559	-	-	10,8206449	0,6559	0,059681267	0,245422	0,39575053	0,1013615	0,39603985	0,90265939	0,01805319	0,04513297	0,09026594
	d	7,5640	0,559	-	-	6,10863025	0,8632	0,059681267	0,245422	0,39575053	0,1013615	0,39603985	1,01567835	0,02031357	0,05078392	0,10156784
21	a	7,5720	0,559	-	-	10,8206449	0,6559	0,059681267	0,245422	0,39549778	0,10136284	0,39562664	0,90361408	0,01807228	0,0451807	0,09036141
	b	7,5720	0,559	-	-	6,10863025	0,8632	0,059681267	0,245422	0,39549778	0,10136284	0,39562664	1,01675257	0,02033505	0,05083763	0,10167526
	c	7,5720	0,559	-	-	10,8206449	0,6559	0,059681267	0,245422	0,39549778	0,10136284	0,39562664	0,90361408	0,01807228	0,0451807	0,09036141
	d	7,5720	0,559	-	-	6,10863025	0,8632	0,059681267	0,245422	0,39549778	0,10136284	0,39562664	1,01675257	0,02033505	0,05083763	0,10167526
22	a	8,4670	0,559	-	-	10,8206449	0,6559	0,059681267	0,245422	0,36912342	0,10148874	0,35424658	1,01042003	0,0202084	0,050521	0,101042
	b	8,4670	0,559	-	-	6,10863025	0,8632	0,059681267	0,245422	0,36912342	0,10148874	0,35424658	1,13693133	0,02273863	0,05684657	0,11369313
	c	8,4670	0,559	-	-	10,8206449	0,6559	0,059681267	0,245422	0,36912342	0,10148874	0,35424658	1,01042003	0,0202084	0,050521	0,101042
	d	8,4670	0,559	-	-	6,10863025	0,8632	0,059681267	0,245422	0,36912342	0,10148874	0,35424658	1,13693133	0,02273863	0,05684657	0,11369313

Appendix 7 – RAO Noble Denton

***OrcaFlex	RAO	Start	Data***										
Draught	LC150												
Direction	0,00												
	WP	XA	XP	YA	YP	ZA	ZP	RXA	RXP	RYA	RYP	RZA	RZP
	0.0	0.002	40573,00	0.000	-142.8	0.002	40753,00	0.000	-145.5	0.004	40813,00	0.000	-129.4
	2.0	0.002	40573,00	0.000	-142.8	0.002	40753,00	0.000	-145.5	0.004	40813,00	0.000	-129.4
	3.0	0.008	-74.0	0.000	40612,00	0.008	-73.2	0.000	22.0	0.019	-72.5	0.000	-19.8
	4.0	0.010	-35.0	0.000	166.5	0.024	-13.7	0.000	-123.8	0.048	-79.3	0.000	40681,00
	40667,00	0.015	131.8	0.000	-158.2	0.035	169.9	0.000	-175.7	0.058	153.8	0.000	-137.4
	5.0	0.019	91.5	0.000	92.8	0.072	40571,00	0.000	-10.9	0.069	-14.8	0.000	126.3
	40668,00	0.037	-73.6	0.000	69.0	0.231	-101.3	0.000	40804,00	0.184	-67.2	0.000	-17.1
	6.0	0.208	-9.7	0.000	85.4	0.219	-23.0	0.000	39.7	1.411	178.6	0.000	-45.2
	40669,00	0.281	92.0	0.000	40810,00	0.139	-165.2	0.000	91.2	1.373	-93.7	0.000	-133.5
	7.0	0.149	106.3	0.000	43.9	0.252	-159.6	0.000	143.2	0.172	-99.6	0.000	-156.6
	40670,00	0.072	93.0	0.000	55.6	0.171	-161.1	0.000	164.3	0.356	112.3	0.000	-164.9
	8.0	0.008	-44.3	0.000	55.4	0.082	173.4	0.000	178.3	0.679	97.1	0.000	-169.5
	40671,00	0.105	-92.1	0.000	49.1	0.049	92.2	0.000	-171.9	0.963	90.0	0.000	-171.6
	9.0	0.218	-93.9	0.000	40.7	0.101	36.7	0.000	-166.9	1.188	87.6	0.000	-177.9
	40672,00	0.328	-93.6	0.000	40755,00	0.177	40651,00	0.000	-164.9	1.334	87.3	0.000	157.8
	10.0	0.429	-92.8	0.000	40657,00	0.258	40553,00	0.000	-164.8	1.410	87.7	0.000	40770,00
	11.0	0.595	-91.5	0.000	40708,00	0.407	40666,00	0.000	-167.9	1.429	88.8	0.000	-1.8
	12.0	0.725	-90.8	0.000	40733,00	0.526	40603,00	0.000	-172.9	1.369	89.4	0.000	-4.4
	13.0	0.833	-90.4	0.000	40701,00	0.616	0.4	0.000	-178.9	1.286	89.7	0.000	-15.2
	14.0	0.928	-90.2	0.000	40609,00	0.684	0.1	0.000	173.5	1.203	89.8	0.000	-16.5
	15.0	1.015	-90.1	0.000	40700,00	0.735	0.0	0.000	169.3	1.125	89.9	0.000	-23.6
	18.0	1.252	-90.1	0.000	8.0	0.831	-0.1	0.000	159.7	0.934	90.0	0.000	-31.6
	20.0	1.401	-90.0	0.000	40702,00	0.868	0.0	0.000	153.1	0.837	90.0	0.000	-34.6
	25.0	1.762	-90.0	0.000	12.0	0.920	0.0	0.000	137.2	0.664	90.0	0.000	-46.7
	30.0	2.117	-90.0	0.000	40708,00	0.946	0.0	0.000	143.7	0.550	90.0	0.000	-46.2
Infinity	2.117	-90.0	0.000	40708,00	0.946	0.0	0.000	143.7	0.550	90.0	0.000	-46.2	
***OrcaFlex	RAO	End	Data***										
***OrcaFlex	RAO	Start	Data***										
Draught	LC150												
Direction	15,00												
	WP	XA	XP	YA	YP	ZA	ZP	RXA	RXP	RYA	RYP	RZA	RZP
	0.0	0.000	68.6	0.001	34.5	0.000	-154.0	0.007	11.0	0.000	64.0	0.001	123.0
	2.0	0.000	68.6	0.001	34.5	0.000	-154.0	0.007	11.0	0.000	64.0	0.001	123.0
	3.0	0.004	64.0	0.003	136.6	0.004	47.2	0.025	144.1	0.009	60.1	0.004	63.8
	4.0	0.005	-50.7	0.022	-71.4	0.007	-48.4	0.074	-111.3	0.018	-92.9	0.016	-70.3
	40667,00	0.013	122.7	0.045	138.5	0.015	129.6	0.156	96.7	0.039	137.9	0.055	141.9
	5.0	0.007	70.9	0.023	87.1	0.041	40797,00	0.105	40760,00	0.079	-28.1	0.087	98.0
	40668,00	0.038	-70.0	0.025	-45.4	0.228	-103.4	0.183	172.6	0.100	-93.0	0.049	40700,00
	6.0	0.203	-6.9	0.016	40686,00	0.142	-32.0	0.238	162.7	1.411	177.3	0.096	0.3
	40669,00	0.262	91.2	0.032	87.9	0.162	-169.0	0.183	91.8	1.195	-94.3	0.056	40547,00
	7.0	0.126	107.0	0.039	83.2	0.251	-161.4	0.368	74.8	0.057	-115.5	0.021	-172.2
	40670,00	0.046	98.3	0.036	79.0	0.156	-159.6	0.337	79.8	0.424	103.4	0.092	-173.0
	8.0	0.037	-93.5	0.020	72.5	0.056	172.8	0.218	81.5	0.745	93.1	0.144	-173.5
	40671,00	0.138	-94.7	0.008	-56.6	0.052	56.5	0.095	78.8	1.019	88.2	0.180	-174.7
	9.0	0.248	-94.7	0.034	-85.0	0.126	25.0	0.015	-44.4	1.225	86.8	0.202	-176.0
	40672,00	0.353	-93.9	0.061	-87.9	0.208	40707,00	0.090	-85.7	1.352	86.9	0.216	-177.2
	10.0	0.448	-92.9	0.086	-88.9	0.289	40762,00	0.147	-88.3	1.412	87.5	0.225	-178.1
	11.0	0.603	-91.5	0.129	-89.5	0.435	40757,00	0.213	-89.4	1.412	88.7	0.232	-179.2
	12.0	0.724	-90.8	0.164	-89.7	0.550	1.0	0.241	-89.7	1.343	89.4	0.232	-179.7
	13.0	0.824	-90.4	0.194	-89.8	0.636	0.3	0.249	-89.9	1.257	89.7	0.229	-179.9
	14.0	0.913	-90.2	0.221	-89.9	0.700	0.1	0.248	-89.9	1.172	89.8	0.225	180.0
	15.0	0.995	-90.1	0.245	-89.9	0.749	0.0	0.242	-90.0	1.094	89.9	0.222	179.9
	18.0	1.221	-90.1	0.310	-90.0	0.840	-0.1	0.216	-90.0	0.906	90.0	0.213	179.9
	20.0	1.363	-90.0	0.350	-90.0	0.875	0.0	0.199	-90.0	0.811	90.0	0.209	179.9
	25.0	1.709	-90.0	0.447	-90.0	0.924	0.0	0.163	-90.0	0.642	90.0	0.202	179.9
	30.0	2.051	-90.0	0.540	-90.0	0.949	0.0	0.138	-90.0	0.532	90.0	0.198	179.9
Infinity	2.051	-90.0	0.540	-90.0	0.949	0.0	0.138	-90.0	0.532	90.0	0.198	179.9	
***OrcaFlex	RAO	End	Data***										
***OrcaFlex	RAO	Start	Data***										
Draught	LC150												
Direction	30,00												
	WP	XA	XP	YA	YP	ZA	ZP	RXA	RXP	RYA	RYP	RZA	RZP
	0.0	0.001	117.0	0.001	86.0	0.001	104.0	0.002	150.5	0.002	115.4	0.002	56.9
	2.0	0.001	117.0	0.001	86.0	0.001	104.0	0.002	150.5	0.002	115.4	0.002	56.9
	3.0	0.004	-83.1	0.002	-49.3	0.005	-99.1	0.018	-172.1	0.010	-86.8	0.016	40746,00
	4.0	0.013	85.7	0.011	117.9	0.018	40568,00	0.071	118.1	0.010	-147.8	0.040	126.9
	40667,00	0.010	-96.8	0.028	-118.2	0.005	-66.3	0.174	-66.0	0.028	-83.9	0.027	77.5
	5.0	0.011	40728,00	0.008	-4.4	0.032	-102.7	0.193	-177.7	0.012	40570,00	0.166	18.0
	40668,00	0.018	-35.2	0.031	-33.6	0.062	-114.2	0.276	166.3	0.162	-174.9	0.101	-12.7
	6.0	0.108	-4.1	0.025	95.7	0.116	-127.1	0.269	97.7	0.816	173.5	0.093	-2.6
	40669,00	0.163	82.9	0.037	104.6	0.161	-171.6	0.676	56.2	0.604	-106.7	0.016	-123.3
	7.0	0.060	107.5	0.042	71.7	0.213	-167.3	0.809	67.7	0.197	99.0	0.131	-166.7
	40670,00	0.027	-127.9	0.032	57.7	0.103	-152.9	0.545	74.4	0.573	88.8	0.231	-169.6
	8.0	0.117	-102.4	0.017	-38.2	0.018	-12.3	0.245	71.9	0.891	84.4	0.302	-171.6
	40671,00	0.218	-98.5	0.061	-80.6	0.117	40553,00	0.045	-15.5	1.136	83.8	0.348	-173.6
	9.0	0.317	-96.2	0.112	-86.3	0.211	40670,00	0.198	-82.4	1.291	84.7	0.377	-175.4
	40672,00	0.407	-94.5	0.161	-88.1	0.299	5.0	0.326	-87.1	1.368	85.9	0.395	-176.9
	10.0	0.484	-93.2	0.205	-88.8	0.379	40546,00	0.413	-88.5	1.389	87.1	0.406	-178.0
	11.0	0.609	-91.5	0.282	-89.4	0.513	40544,00	0.503	-89.4	1.343	88.6	0.412	-179.2
	12.0	0.706	-90.8	0.345	-89.7	0.615	0.3	0.531	-89.7	1.255	89.3	0.409	-179.7
	13.0	0.787	-90.4	0.398	-89.8	0.689	0.0	0.530	-89.8	1.162	89.7	0.403	-179.9
	14.0	0.861	-90.2	0.446	-89.9	0.745	-0.1	0.515	-89.9	1.077	89.8	0.395	180.0
	15.0	0.929	-90.1	0.491	-89.9	0.786	-0.1	0.496	-89.9	1.000	89.9	0.388	179.9
	18.0	1.122	-90.1	0.612	-90.0	0.864	-0.1	0.432	-90.0	0.822	90.0	0.371	179.9
	20.0	1.245	-90.0	0.688	-90.0	0.894	-0.1	0.394	-90.0	0.734	90.0	0.363	179.9
	25.0	1.550	-90.0	0.871	-90.0	0.936	0.0	0.320	-90.0	0.579	90.0	0.351	179.9
	30.0	1.853	-90.0	1.050	-90.0	0.957	0.0	0.269	-90.0	0.478	90.0	0.344	179.9
Infinity	1.853	-90.0	1.050	-90.0	0.957	0.0	0.269	-90.0	0.478	90.0	0.344	179.9	
***OrcaFlex	RAO	End	Data***										
***OrcaFlex	RAO	Start	Data***										
Draught	LC150												
Direction	45,00												
	WP	XA	XP	YA	YP	ZA	ZP	RXA	RXP	RYA	RYP	RZA	RZP
	0.0	0.000	125.5	0.002	-137.2	0.001	102.9	0.001	-140.6	0.001	123.3	0.001	63.8
	2.0	0.000	125.5	0.002	-137.2	0.001	102.9	0.001	-140.6	0.001	123.3	0.001	63.8
	3.0	0.004	-153.1	0.004	156.5	0.006	-153.6	0.011	-54.6	0.011	-154.1	0.007	-46.3
	4.0	0.018	-53.1	0.024	-98.9	0.026	-107.4	0.051	-96.4	0.012	133.1	0.040	40704,00
	40667,00	0.010	133.9	0.081	65.6	0.030	161.5	0.156	69.3	0.059	138.8	0.118	-24.0
	5.0	0.022	67.1	0.034	-51.5	0.037	40715,00	0.184	-172.0	0.029	148.2	0.182	-82.1
	40668,00	0.027	99.4	0.029	168.8	0.153	114.2	0.246	39.5	0.191	-115.8	0.040	-100.7
	6.0	0.104	-141.8	0.060	169.0	0.219	-110.6	0.793	40571,00	0.586	37.3	0.082	-157.1
	40669,00	0.104	40665,00	0.031	-139.4	0.023	172.5	1.158	37.4	0.603	171.0	0.190	-158.3
	7.0	0.017	-0.3	0.033	-50.9	0.114	164.7	0.760	52.4	0.244	110.1	0.287	-161.3
	40670,00	0.087	-112.3	0.062	-66.9	0.029	-116.3	0.235	40815,00	0.611	73.9	0.362	-165.0
	8.0	0.194	-106.8	0.117	-80.2	0.118	-15.4	0.296	-67.7	0.965	74.7	0.413	-168.6
	40671,00	0.290	-101.4	0.184	-85.2	0.238	-7.0	0.544	-82.7	1.175	78.8	0.447	-171.8
	9.0	0.371	-97.7	0.250	-87.3	0.346	-3.7	0.713	-86.4	1.269	82.2	0.469	-174.4
	40672,00	0.437	-95.2	0.312	-88.3	0.436	-2.0	0.816	-87.9	1.291	84.7	0.483	-176.4
	10.0	0.491	-93.5	0.368	-88.8	0.511	-1.2	0.873	-88.7	1.272	86.4	0.490	-177.7
	11.0	0.575	-91.6	0.462	-89.4	0.625	-0.6	0.907	-89.4	1.183	88.4	0.491	-179.1
	12.0	0.640	-90.8	0.541	-89.6	0.706	-0.4	0.887	-89.6	1.081	89.3	0.484	-179.7
	13.0	0.697	-90.4	0.609	-89.8	0.764	-0.3	0.848	-89.8	0.988	89.7	0.473	-180.0
	14.0	0.750	-90.2	0.671	-89.8	0.806	-0.3	0.803	-89.9	0.907	89.8	0.463	179.9
	15.0	0.800	-90.1	0.729	-89.9	0.838	-0.2	0.758	-89.9	0.838	89.9	0.453	179.9
	18.0	0.946	-90.0	0.892	-90.0	0.897	-0.1	0.640	-90.0	0.681	90.0	0.431	179.9
	20.0	1.043	-90.0	0.995	-90.0	0.919	-0.1	0.578	-90.0	0.606	90.0	0.421	179.9
	25.0	1.285	-90.0	1.248	-90.0	0.951	0.0	0.463	-90.0	0.476	90.0	0.406	179.9
	30.0	1.528	-90.0	1.499	-90.0	0.967	0.0	0.385	-90.0	0.393	90.0	0.398	179.9
Infinity	1.528	-90.0	1.499	-90.0	0.967	0.0	0.385	-90.0	0.393	90.0	0.398	179.9	
***OrcaFlex	RAO	End	Data***										
***OrcaFlex	RAO	Start	Data***										

Draught	LC150												
Direction	60,00												
	WP	XA	XP	YA	YP	ZA	ZP	RXA	RXP	RYA	RYP	RZA	RZP
	0.0	0.000	62.4	0.003	40700,00	0.000	-82.7	0.003	40727,00	0.000	59.1	0.002	-130.2
	2.0	0.000	62.4	0.003	40700,00	0.000	-82.7	0.003	40727,00	0.000	59.1	0.002	-130.2
	3.0	0.003	-101.8	0.006	-105.8	0.007	-92.3	0.010	-158.9	0.011	-109.1	0.018	40569,00
	4.0	0.016	153.8	0.032	112.3	0.025	81.6	0.043	68.5	0.031	-68.5	0.058	-146.9
	40667,00	0.006	60.0	0.070	-79.7	0.038	40734,00	0.185	-86.8	0.078	-13.8	0.174	173.7
	5.0	0.017	-92.4	0.026	44.3	0.049	-140.9	0.711	40776,00	0.126	-63.2	0.293	-165.7
	40668,00	0.040	-110.3	0.064	-179.6	0.264	-143.9	0.415	40676,00	0.115	53.5	0.094	147.6
	6.0	0.227	-84.2	0.038	-149.1	0.136	-39.0	0.495	-19.7	1.429	98.5	0.158	-149.2
	40669,00	0.231	-0.4	0.046	-83.2	0.140	67.2	0.560	-71.0	1.343	-172.5	0.249	-146.9
	7.0	0.056	40751,00	0.100	-83.0	0.146	109.5	1.091	-87.2	0.229	-135.3	0.316	-152.2
	40670,00	0.086	-121.3	0.183	-85.4	0.022	40713,00	1.392	-86.2	0.434	50.5	0.360	-158.5
	8.0	0.202	-111.6	0.269	-86.4	0.192	-23.6	1.515	-86.4	0.823	64.8	0.388	-164.5
	40671,00	0.285	-103.9	0.350	-87.3	0.361	-16.9	1.559	-87.2	0.996	74.0	0.409	-169.6
	9.0	0.343	-99.0	0.424	-88.0	0.491	-10.8	1.558	-87.9	1.045	79.8	0.423	-173.3
	40672,00	0.385	-95.8	0.489	-88.5	0.584	-6.9	1.530	-88.4	1.033	83.4	0.433	-175.8
	10.0	0.416	-93.8	0.547	-88.9	0.651	-4.5	1.486	-88.8	0.994	85.8	0.437	-177.4
	11.0	0.462	-91.7	0.645	-89.3	0.742	-2.1	1.378	-89.3	0.896	88.2	0.436	-179.1
	12.0	0.499	-90.8	0.728	-89.6	0.800	-1.1	1.268	-89.6	0.804	89.2	0.427	-179.7
	13.0	0.532	-90.4	0.802	-89.7	0.840	-0.7	1.168	-89.8	0.726	89.7	0.416	-180.0
	14.0	0.564	-90.2	0.870	-89.8	0.869	-0.4	1.079	-89.9	0.662	89.8	0.406	179.9
	15.0	0.595	-90.1	0.936	-89.9	0.890	-0.3	1.001	-89.9	0.608	89.9	0.397	179.9
	18.0	0.691	-90.0	1.124	-90.0	0.930	-0.1	0.821	-90.0	0.489	90.0	0.376	179.9
	20.0	0.756	-90.0	1.246	-90.0	0.945	-0.1	0.733	-90.0	0.434	90.0	0.367	179.9
	25.0	0.922	-90.0	1.549	-90.0	0.967	0.0	0.579	-90.0	0.339	90.0	0.353	179.9
	30.0	1.092	-90.0	1.852	-90.0	0.977	0.0	0.478	-90.0	0.279	90.0	0.345	179.9
Infinity	1.092	-90.0	1.852	-90.0	0.977	0.0	0.478	-90.0	0.279	90.0	0.345	179.9	
***OrcaFlex	RAO	End	Data***										
***OrcaFlex	RAO	Start	Data***										
Draught	LC150												
Direction	75,00												
	WP	XA	XP	YA	YP	ZA	ZP	RXA	RXP	RYA	RYP	RZA	RZP
	0.0	0.000	-36.2	0.001	-81.7	0.000	148.5	0.002	-81.3	0.000	-34.0	0.003	154.1
	2.0	0.000	-36.2	0.001	-81.7	0.000	148.5	0.002	-81.3	0.000	-34.0	0.003	154.1
	3.0	0.001	120.3	0.003	77.4	0.002	-112.0	0.015	142.9	0.003	-92.2	0.026	99.1
	4.0	0.010	40766,00	0.031	-28.5	0.015	-80.6	0.034	124.7	0.038	159.9	0.107	47.9
	40667,00	0.017	-33.7	0.062	120.0	0.038	-159.0	0.203	106.8	0.137	171.0	0.299	40639,00
	5.0	0.038	-58.8	0.021	-98.5	0.054	56.2	0.744	-138.2	0.382	124.6	0.492	40672,00
	40668,00	0.120	-78.0	0.108	40602,00	0.556	33.8	1.208	-150.8	0.942	102.8	0.184	38.5
	6.0	0.404	-39.4	0.197	40627,00	0.840	116.3	2.360	-147.9	2.898	138.0	0.091	-67.2
	40669,00	0.255	40567,00	0.136	45.1	0.456	125.5	3.933	-128.1	1.577	-150.6	0.135	-116.9
	7.0	0.082	56.6	0.089	-99.7	0.269	123.3	4.098	-104.0	0.452	-109.6	0.180	-138.6
	40670,00	0.042	-144.3	0.271	-92.5	0.050	131.3	3.509	-93.1	0.225	40708,00	0.207	-151.0
	8.0	0.124	-116.5	0.396	-89.4	0.215	-35.3	3.025	-89.6	0.467	56.0	0.224	-160.6
	40671,00	0.176	-105.9	0.491	-88.5	0.443	-23.8	2.680	-88.6	0.572	70.3	0.237	-167.7
	9.0	0.207	-99.9	0.568	-88.5	0.598	-15.3	2.420	-88.5	0.594	78.0	0.246	-172.5
	40672,00	0.228	-96.3	0.632	-88.6	0.696	-9.8	2.214	-88.7	0.579	82.5	0.253	-175.5
	10.0	0.241	-94.1	0.689	-88.9	0.758	-6.5	2.044	-88.9	0.550	85.3	0.256	-177.4
	11.0	0.261	-91.7	0.784	-89.3	0.830	-3.0	1.776	-89.3	0.486	88.1	0.255	-179.2
	12.0	0.276	-90.8	0.865	-89.6	0.871	-1.6	1.573	-89.6	0.431	89.2	0.249	-179.9
	13.0	0.290	-90.4	0.940	-89.7	0.897	-0.9	1.413	-89.8	0.386	89.6	0.243	179.9
	14.0	0.304	-90.2	1.011	-89.8	0.916	-0.6	1.284	-89.8	0.350	89.8	0.236	179.8
	15.0	0.319	-90.1	1.079	-89.9	0.929	-0.4	1.178	-89.9	0.320	89.9	0.231	179.7
	18.0	0.366	-90.0	1.280	-90.0	0.954	-0.1	0.947	-90.0	0.256	90.0	0.218	179.7
	20.0	0.398	-90.0	1.412	-90.0	0.964	-0.1	0.839	-90.0	0.226	90.0	0.213	179.8
	25.0	0.483	-90.0	1.744	-90.0	0.978	0.0	0.655	-90.0	0.176	90.0	0.204	179.8
	30.0	0.569	-90.0	2.078	-90.0	0.985	0.0	0.539	-90.0	0.145	90.0	0.200	179.8
Infinity	0.569	-90.0	2.078	-90.0	0.985	0.0	0.539	-90.0	0.145	90.0	0.200	179.8	
***OrcaFlex	RAO	End	Data***										
***OrcaFlex	RAO	Start	Data***										
Draught	LC150												
Direction	90,00												
	WP	XA	XP	YA	YP	ZA	ZP	RXA	RXP	RYA	RYP	RZA	RZP
	0.0	0.000	91.1	0.023	168.3	0.000	40667,00	0.025	165.4	0.000	61.6	0.006	166.5
	2.0	0.000	91.1	0.023	168.3	0.000	40667,00	0.025	165.4	0.000	61.6	0.006	166.5
	3.0	0.000	143.1	0.107	45.5	0.002	40596,00	0.081	64.1	0.000	159.0	0.001	68.0
	4.0	0.000	163.3	0.225	160.7	0.072	138.1	0.072	-140.8	0.000	-28.7	0.000	40708,00
	40667,00	0.000	-104.5	0.498	114.2	0.205	72.1	0.760	118.4	0.001	86.2	0.002	-36.3
	5.0	0.000	-128.3	0.019	147.3	0.520	40.8	2.371	-142.3	0.002	58.6	0.003	103.2
	40668,00	0.001	-113.8	0.268	31.0	1.764	43.7	2.494	-152.3	0.007	71.2	0.001	32.4
	6.0	0.002	40798,00	0.380	31.2	1.696	124.3	4.163	-154.0	0.014	-164.0	0.003	40566,00
	40669,00	0.001	71.8	0.266	55.1	0.752	137.3	6.096	-132.0	0.004	-97.4	0.005	47.0
	7.0	0.000	116.6	0.062	-120.4	0.353	133.5	5.734	-106.2	0.002	-49.0	0.005	74.3
	40670,00	0.000	161.2	0.296	-95.3	0.094	148.1	4.563	-94.4	0.001	40606,00	0.004	87.1
	8.0	0.000	-147.6	0.442	-90.4	0.217	-42.1	3.733	-90.3	0.001	53.1	0.003	91.7
	40671,00	0.000	-107.6	0.545	-88.9	0.471	-26.5	3.183	-89.0	0.001	88.0	0.003	93.1
	9.0	0.000	-80.9	0.623	-88.6	0.638	-16.9	2.794	-88.7	0.001	111.5	0.003	93.3
	40672,00	0.000	-63.8	0.688	-88.7	0.737	-10.8	2.502	-88.8	0.001	127.6	0.002	93.1
	10.0	0.000	-53.6	0.743	-88.9	0.797	-7.1	2.274	-89.0	0.000	138.3	0.002	92.7
	11.0	0.000	-49.3	0.836	-89.3	0.863	-3.4	1.934	-89.3	0.000	150.3	0.002	92.0
	12.0	0.000	-60.1	0.916	-89.5	0.897	-1.7	1.691	-89.6	0.000	156.2	0.002	91.6
	13.0	0.000	-77.3	0.990	-89.7	0.918	-1.0	1.507	-89.7	0.000	159.6	0.001	91.3
	14.0	0.000	-89.5	1.061	-89.8	0.933	-0.6	1.361	-89.8	0.000	161.9	0.001	91.2
	15.0	0.000	-96.8	1.130	-89.9	0.944	-0.4	1.243	-89.9	0.000	163.4	0.001	91.0
	18.0	0.000	-106.4	1.335	-89.9	0.963	-0.1	0.992	-90.0	0.000	166.8	0.001	91.0
	20.0	0.000	-103.8	1.470	-90.0	0.971	-0.1	0.876	-90.0	0.000	168.3	0.001	91.0
	25.0	0.000	-105.6	1.812	-90.0	0.982	0.0	0.682	-90.0	0.000	170.7	0.001	91.2
	30.0	0.000	-100.9	2.157	-90.0	0.988	0.0	0.560	-90.0	0.000	171.2	0.001	91.4
Infinity	0.000	-100.9	2.157	-90.0	0.988	0.0	0.560	-90.0	0.000	171.2	0.001	91.4	
***OrcaFlex	RAO	End	Data***										

Appendix 8 - MATLAB code "bessel.m"

```
% Bessel funtions for calculation of Added Mass

k = 0.1158

R = [0.864/2; 0.559/2]

for i = 1:2  % for two radii

    J1(i) = 0;          %derivative of Bessel function J1(x)of first kind


    x(i)=k*R(i);


    for m = 0:1000 % Bessel function


        J1(i) = J1(i) + ((-1)^m/(factorial(m)*gamma(m+2)))*(2*m+1)*(1/2)*(k*R(i)/2)^(2*m);




    end

    %derivative of Bessel function Y1(x) of second kind:

    Ia(i)=0;
    theta = 0;
    for v=1:100

        dtheta = pi/100;
        theta = theta+dtheta;

        Ia(i) = Ia(i) + cos(x(i)*sin(theta) - theta)*sin(theta)*dtheta;

    end
    Ib(i) = 0;
    t=0;
    for w = 1:100000

        t = 0.001*w;
        dt = 0.001;

        Ib(i) = Ib(i) + (exp(t) + (-1)*exp(-t))*exp(-x(i)*sinh(t))*(-sinh(t))*dt;
    end

    Y1(i) = (Ia(i) - Ib(i))/pi;



A1(i) = (J1(i))^2 + (Y1(i))^2;
K(i) = sqrt(A1(i));
C(i) = 4/(pi()*(x(i))^2*K(i))-1;

end

J1
Y1
A1
K
C
```

Appendix 9 – MATLAB code "solvek.m"

```
% Iteration of disperation relation for finding k


T = 5.9;
w = 2*pi/T;
d = 30;
g = 9.81;

k=0.1;

for i = 1:10

    k = w^2/(g*tanh(k*d))
end


HS = w^2/(g*tanh(k*d))
```

Appendix 10 – Scenario 1a Results

Min X	Max X	Min Y	Max Y	Min Z	Max Z	Gx-Velocit	Gy-Velocit	Gz-Velocit	Gx-Accele	Gy-Accele	Gz-Accele
-3,86684	-1,34808	-1,2E-05	9,3E-05	-20,7507	-20,149	1,058943	4,07E-05	0,380544	1,087835	0,000143	0,408371
-3,87258	-1,29969	-0,50494	0,259781	-20,7699	-20,1438	1,051932	0,40139	0,339204	1,145721	0,546438	0,293223
-3,45661	-1,4074	-0,58496	0,563241	-20,7292	-20,2824	0,805627	0,53726	0,214051	0,851046	0,606141	0,262792
-2,88757	-1,51271	-1,23611	0,540522	-20,6112	-20,4541	0,42606	0,825631	0,119924	0,402239	1,019329	0,227603
-5,71442	-0,66482	-3,6E-05	0,000137	-21,2611	-19,1023	2,270691	0,000103	1,13684	2,268099	0,000119	1,561232
-5,35261	-0,76041	-0,6558	0,302013	-21,231	-19,277	2,062166	0,498454	0,969101	2,060702	0,539703	1,346978
-4,01683	-1,16394	-1,35607	0,773286	-21,0523	-19,8269	1,243312	1,006759	0,518282	1,303263	1,020331	0,751231
-3,67656	-1,28502	-2,25349	1,820201	-20,771	-20,0286	0,798758	2,157398	0,529663	1,038685	2,180192	0,974277
-3,65898	-1,2574	4,81E-06	6,11E-05	-21,1246	-19,8758	1,017521	2,58E-05	0,550306	0,959269	3,51E-05	0,393278
-3,43223	-1,23888	-0,61591	0,494142	-21,0886	-19,937	0,875706	0,550587	0,478684	0,806608	0,526912	0,391688
-2,97803	-1,31341	-1,19386	1,118935	-20,9688	-20,0408	0,689379	1,168997	0,348199	0,620278	1,113139	0,364855
-3,00051	-1,35972	-1,3823	1,223972	-20,9174	-20,0344	0,651825	1,310998	0,447021	0,609937	1,284365	0,459006
-3,42702	-0,87852	-7E-06	5,25E-05	-21,1125	-19,9518	1,108723	3,06E-05	0,571643	1,002143	3,65E-05	0,462057
-3,30907	-0,883	-0,47205	0,296068	-21,1194	-19,9653	1,008509	0,359149	0,540766	0,910936	0,330183	0,438843
-3,0303	-0,99245	-1,0189	0,674802	-21,1241	-19,9882	0,711651	0,806943	0,45488	0,585683	0,838378	0,447952
-2,85593	-1,17467	-1,53013	1,152431	-21,07	-19,9015	0,408462	1,409421	0,414079	0,383148	1,39381	0,630288
-4,47911	-0,48504	-9,1E-06	6,71E-05	-21,807	-19,248	1,639735	3,52E-05	1,00737	1,294082	4,17E-05	0,768223
-4,3676	-0,45917	-0,44019	0,192512	-21,8294	-19,2453	1,574513	0,230559	0,983376	1,211088	0,263577	0,747355
-4,01818	-0,4663	-1,02098	0,517859	-21,8456	-19,3074	1,265016	0,615113	0,912384	0,897176	0,553992	0,632416
-3,88154	-0,71441	-1,7192	1,07767	-21,8334	-19,1904	1,112293	1,112711	0,84681	0,899947	0,826703	0,647071
-3,81857	-0,6488	5,6E-06	3,67E-05	-21,6347	-19,5937	0,879715	1,4E-05	0,517549	0,738546	2,18E-05	0,356689
-3,77909	-0,64501	-0,27073	0,195496	-21,6384	-19,569	0,861349	0,173028	0,518267	0,743524	0,160917	0,346194
-3,5935	-0,61749	-0,61845	0,423303	-21,6588	-19,5227	0,792584	0,266761	0,532497	0,636143	0,227111	0,357666
-3,21146	-0,62443	-1,35119	0,679614	-21,6856	-19,4751	0,589838	0,717813	0,563387	0,390689	0,571751	0,357566
-4,16369	-0,34713	5,64E-06	3,85E-05	-21,7894	-19,4931	1,045522	1,53E-05	0,562567	0,782003	1,61E-05	0,402525
-4,07263	-0,3548	-0,32429	0,222225	-21,804	-19,4829	1,014221	0,100262	0,570279	0,742565	0,103806	0,399815
-3,77279	-0,40546	-0,77993	0,391486	-21,8269	-19,445	0,851448	0,339962	0,58439	0,558023	0,264157	0,389688
-3,45384	-0,59576	-1,37991	0,610227	-21,8133	-19,3737	0,610605	0,64227	0,565333	0,484947	0,446467	0,351832
-4,53586	0,392486	5,63E-06	4,03E-05	-21,8357	-18,9798	0,973365	1,81E-05	0,737165	0,783279	2,02E-05	0,343966
-4,4688	0,325144	-0,42433	0,28372	-21,8422	-18,966	0,933767	0,178698	0,742826	0,758023	0,109969	0,331839
-4,27347	0,156346	-0,88175	0,67766	-21,8899	-18,9574	0,858285	0,360247	0,75019	0,592967	0,249122	0,344693
-3,87065	-0,0297	-1,47944	1,207158	-21,9676	-18,9532	0,789843	0,560121	0,78728	0,483195	0,414801	0,396433
-4,74266	1,117336	5,43E-06	4,3E-05	-21,9026	-18,8029	1,107159	1,17E-05	0,796772	0,537514	1,12E-05	0,350243
-4,62746	1,027193	-0,4477	0,371827	-21,9165	-18,7931	1,080308	0,226932	0,803481	0,523416	0,122445	0,343893
-4,27273	0,714636	-0,90237	0,861906	-21,962	-18,788	0,939146	0,414595	0,807729	0,422641	0,223193	0,339079
-3,85842	0,239792	-1,27705	1,40343	-22,0269	-18,7903	0,842892	0,568662	0,812019	0,366464	0,209917	0,363707
-4,84282	-1,28732	-3,8E-05	0,000105	-20,7987	-19,9567	1,343537	7,03E-05	0,538226	1,385971	0,000268	0,623353
-4,79911	-1,25445	-0,6874	0,304589	-20,823	-19,952	1,33132	0,492241	0,472987	1,383987	0,698079	0,476025
-4,2313	-1,3664	-0,85896	0,714141	-20,7719	-20,1616	1,023895	0,664615	0,296753	1,057581	0,73225	0,364023
-3,4737	-1,49682	-1,68747	0,715682	-20,6234	-20,4015	0,563289	1,015482	0,167204	0,495804	1,288358	0,326583
-7,02504	-0,59847	-4,1E-05	0,000187	-21,4341	-18,4753	2,771337	0,000137	1,588449	2,6374	0,000146	2,539995
-6,56677	-0,70224	-0,90249	0,358694	-21,3949	-18,7396	2,521352	0,650642	1,341682	2,38472	0,690938	2,041466
-4,85457	-1,15002	-1,79946	0,907016	-21,1733	-19,5454	1,521114	1,291916	0,692625	1,557167	1,270421	1,079291
-4,40209	-1,26442	-2,85236	2,137445	-20,8085	-19,8012	0,982349	2,650349	0,739937	1,333218	2,628159	1,43652
-4,42983	-1,24466	4,63E-06	7,67E-05	-21,2538	-19,6651	1,275354	3,12E-05	0,708403	1,221495	5,1E-05	0,510481
-4,12122	-1,21809	-0,78899	0,624979	-21,2123	-19,7515	1,102679	0,691325	0,612973	1,024024	0,659394	0,517396
-3,51331	-1,23482	-1,52209	1,386772	-21,0641	-19,8889	0,84411	1,470255	0,460411	0,763745	1,379307	0,516664
-3,50005	-1,30423	-1,81288	1,485499	-21,0052	-19,881	0,810331	1,642999	0,593926	0,759566	1,58591	0,656025
-4,04401	-0,69851	-1,3E-05	6,43E-05	-21,2316	-19,7515	1,376162	3,87E-05	0,755386	1,236666	4,54E-05	0,635208
-3,88851	-0,69978	-0,62318	0,354846	-21,2424	-19,7855	1,252922	0,458073	0,708772	1,129593	0,42066	0,589592
-3,53228	-0,82786	-1,31893	0,829081	-21,2579	-19,8261	0,884279	1,013416	0,577655	0,742672	1,044883	0,58917
-3,2978	-1,05351	-1,94197	1,374627	-21,1966	-19,6945	0,511805	1,747115	0,552467	0,490231	1,707233	0,887432
-5,44111	-0,32375	-1,7E-05	8,44E-05	-22,1106	-18,8761	2,044834	4,6E-05	1,303983	1,614108	5,51E-05	1,071229
-5,29679	-0,28703	-0,5685	0,235811	-22,1412	-18,8771	1,964709	0,286106	1,266501	1,504756	0,324365	1,031401
-4,83475	-0,28119	-1,31292	0,590587	-22,1639	-18,9772	1,586849	0,750645	1,162234	1,130536	0,682879	0,843382
-4,60224	-0,56874	-2,18688	1,258667	-22,1441	-18,8399	1,384988	1,369524	1,073936	1,128964	1,020707	0,86821
-4,47449	-0,41444	1,72E-06	4,22E-05	-21,9016	-19,3449	1,096147	1,82E-05	0,649055	0,917587	2,81E-05	0,452313
-4,42351	-0,40971	-0,36367	0,24125	-21,9056	-19,3158	1,073286	0,218175	0,649887	0,930559	0,200236	0,43735
-4,18406	-0,3743	-0,81292	0,523128	-21,9313	-19,2605	0,991634	0,336109	0,668905	0,796389	0,2841	0,449152
-3,69249	-0,38146	-1,73304	0,842217	-21,9642	-19,1998	0,741568	0,885707	0,708876	0,491873	0,706568	0,447763
-4,90115	-0,03034	2,93E-06	4,39E-05	-22,0929	-19,2237	1,304664	1,93E-05	0,71004	0,982915	2,02E-05	0,518163
-4,78476	-0,04012	-0,42588	0,275343	-22,1123	-19,2113	1,266365	0,128705	0,719219	0,931111	0,128257	0,510721
-4,39924	-0,1036	-1,01258	0,49253	-22,1436	-19,1648	1,066109	0,42526	0,733903	0,700914	0,329207	0,487692
-3,98149	-0,34022	-1,77253	0,759992	-22,1255	-19,0755	0,764217	0,799959	0,708638	0,610654	0,553263	0,43598
-5,4182	0,835805	2,71E-06	4,69E-05	-22,152	-18,5802	1,246787	2,33E-05	0,921728	0,980837	2,65E-05	0,428033
-5,32628	0,75361	-0,56026	0,361915	-22,16	-18,5635	1,197715	0,229429	0,929522	0,950584	0,144425	0,417601
-5,05832	0,550884	-1,15687	0,827379	-22,2208	-18,554	1,06571	0,461426	0,940781	0,746364	0,317384	0,435045
-4,52282	0,328015	-1,89418	1,48222	-22,3193	-18,5475	0,981087	0,698682	0,986212	0,604744	0,519221	0,504261
-5,61922	1,725544	2,41E-06	5,03E-05	-22,2431	-18,3596	1,394504	1,46E-05	0,99414	0,666614	1,38E-05	0,4454
-5,4707	1,615775	-0,58054	0,453757	-22,2601	-18,3472	1,360547	0,289527	1,00423	0,649318	0,155778	0,436197
-5,01279	1,23456	-1,17205	1,060151	-22,3163	-18,3425	1,1854	0,520436	1,012541	0,526593	0,281957	0,428705
-4,47671	0,656905	-1,65529	1,730556	-22,396	-18,3452	1,047589	0,714123	1,015855	0,457606	0,266276	0,45751

CASE	Degrees	Hs	Tz	Diff X	Diff Y	Diff Z
1	180	2	4	2,52	0,00	0,60
2	195			2,57	0,76	0,63
3	210			2,05	1,15	0,45
4	225			1,37	1,78	0,16
5	180	2	5	5,05	0,00	2,16
6	195			4,59	0,96	1,95
7	210			2,85	2,13	1,23
8	225			2,39	4,07	0,74
9	180	2	6	2,40	0,00	1,25
10	195			2,19	1,11	1,15
11	210			1,66	2,31	0,93
12	225			1,64	2,61	0,88
13	180	2	7	2,55	0,00	1,16
14	195			2,43	0,77	1,15
15	210			2,04	1,69	1,14
16	225			1,68	2,68	1,17
17	180	2	8	3,99	0,00	2,56
18	195			3,91	0,63	2,58
19	210			3,55	1,54	2,54
20	225			3,17	2,80	2,64
21	180	2	9	3,17	0,00	2,04
22	195			3,13	0,47	2,07
23	210			2,98	1,04	2,14
24	225			2,59	2,03	2,21
25	180	2	10	3,82	0,00	2,30
26	195			3,72	0,55	2,32
27	210			3,37	1,17	2,38
28	225			2,86	1,99	2,44
29	180	2	11	4,93	0,00	2,86
30	195			4,79	0,71	2,88
31	210			4,43	1,56	2,93
32	225			3,84	2,69	3,01
33	180	2	12	5,86	0,00	3,10
34	195			5,65	0,82	3,12
35	210			4,99	1,76	3,17
36	225			4,10	2,68	3,24
37	180	2,5	4	3,56	0,00	0,84
38	195			3,54	0,99	0,87
39	210			2,86	1,57	0,61
40	225			1,98	2,40	0,22
41	180	2,5	5	6,43	0,00	2,96
42	195			5,86	1,26	2,66
43	210			3,70	2,71	1,63
44	225			3,14	4,99	1,01
45	180	2,5	6	3,19	0,00	1,59
46	195			2,90	1,41	1,46
47	210			2,28	2,91	1,18
48	225			2,20	3,30	1,12
49	180	2,5	7	3,35	0,00	1,48
50	195			3,19	0,98	1,46
51	210			2,70	2,15	1,43
52	225			2,24	3,32	1,50
53	180	2,5	8	5,12	0,00	3,23
54	195			5,01	0,80	3,26
55	210			4,55	1,90	3,19
56	225			4,03	3,45	3,30
57	180	2,5	9	4,06	0,00	2,56
58	195			4,01	0,60	2,59
59	210			3,81	1,34	2,67
60	225			3,31	2,58	2,76
61	180	2,5	10	4,87	0,00	2,87
62	195			4,74	0,70	2,90
63	210			4,30	1,51	2,98
64	225			3,64	2,53	3,05
65	180	2,5	11	6,25	0,00	3,57
66	195			6,08	0,92	3,60
67	210			5,61	1,98	3,67
68	225			4,85	3,38	3,77
69	180	2,5	12	7,34	0,00	3,88
70	195			7,09	1,03	3,91
71	210			6,25	2,23	3,97
72	225			5,13	3,39	4,05
						2,18

Hs = 2 — **Diff X**

Tz	180	195	210	225
4	2,52	2,57	2,05	1,37
5	5,05	4,59	2,85	2,39
6	2,40	2,19	1,66	1,64
7	2,55	2,43	2,04	1,68
8	3,99	3,91	3,55	3,17
9	3,17	3,13	2,98	2,59
10	3,82	3,72	3,37	2,86
11	4,93	4,79	4,43	3,84
12	5,86	5,65	4,99	4,10

Hs = 2 — **Diff Y**

Tz	180	195	210	225
4	0,00	0,76	1,15	1,78
5	0,00	0,96	2,13	4,07
6	0,00	1,11	2,31	2,61
7	0,00	0,77	1,69	2,68
8	0,00	0,63	1,54	2,80
9	0,00	0,47	1,04	2,03
10	0,00	0,55	1,17	1,99
11	0,00	0,71	1,56	2,69
12	0,00	0,82	1,76	2,68

Hs = 2 — **Diff Z**

Tz	180	195	210	225
4	0,60	0,63	0,45	0,16
5	2,16	1,95	1,23	0,74
6	1,25	1,15	0,93	0,88
7	1,16	1,15	1,14	1,17
8	2,56	2,58	2,54	2,64
9	2,04	2,07	2,14	2,21
10	2,30	2,32	2,38	2,44
11	2,86	2,88	2,93	3,01
12	3,10	3,12	3,17	3,24

Hs = 2.5 — **Diff X**

Tz	180	195	210	225
4	3,56	3,54	2,86	1,98
5	6,43	5,86	3,70	3,14
6	3,19	2,90	2,28	2,20
7	3,35	3,19	2,70	2,24
8	5,12	5,01	4,55	4,03
9	4,06	4,01	3,81	3,31
10	4,87	4,74	4,30	3,64
11	6,25	6,08	5,61	4,85
12	7,34	7,09	6,25	5,13

Hs = 2.5 — **Diff Y**

Tz	180	195	210	225
4	0,00	0,99	1,57	2,40
5	0,00	1,26	2,71	4,99
6	0,00	1,41	2,91	3,30
7	0,00	0,98	2,15	3,32
8	0,00	0,80	1,90	3,45
9	0,00	0,60	1,34	2,58
10	0,00	0,70	1,51	2,53
11	0,00	0,92	1,98	3,38
12	0,00	1,03	2,23	3,39

Hs = 2.5 — **Diff Z**

Tz	180	195	210	225
4	0,84	0,87	0,61	0,22
5	2,96	2,66	1,63	1,01
6	1,59	1,46	1,18	1,12
7	1,48	1,46	1,43	1,50
8	3,23	3,26	3,19	3,30
9	2,56	2,59	2,67	2,76
10	2,87	2,90	2,98	3,05
11	3,57	3,60	3,67	3,77
12	3,88	3,91	3,97	4,05

Appendix 11 – Scenario 1b Results

Min X	Max X	Min Y	Max Y	Min Z	Max Z	Gx-Velocity	Gy-Velocity	Gz-Velocity	Gx-Acceleration	Gy-Acceleration	Gz-Acceleration
-4,01891	-1,26469	1,55E-05	4,09E-05	-21,239	-20,6177	1,140671	1,74E-05	0,386253	1,20587	0,000154	0,374151
-4,02455	-1,26016	-0,50024	0,368263	-21,2574	-20,5993	1,145943	0,413127	0,402639	1,287331	0,458664	0,370578
-3,58056	-1,36421	-0,66586	0,699754	-21,2145	-20,7175	0,871471	0,639017	0,284453	0,940786	0,701967	0,2575
-2,96036	-1,63171	-1,35859	1,062551	-20,998	-20,8233	0,423532	1,008061	0,116082	0,427698	1,139617	0,141847
-6,15852	-0,69332	8,89E-06	8,31E-05	-21,8684	-19,5903	2,382538	1,94E-05	1,213317	2,544366	4,39E-05	1,014598
-5,82125	-0,79031	-0,74784	0,403157	-21,8433	-19,7269	2,218788	0,541033	1,090061	2,296265	0,53377	0,885764
-4,35906	-1,19821	-1,73666	1,063096	-21,6133	-20,2321	1,410444	1,333302	0,651786	1,478846	1,326373	0,559721
-4,03817	-1,28428	-2,67898	2,033324	-21,2209	-20,4838	1,109798	2,386731	0,409671	1,188572	2,54916	0,589659
-3,77328	-1,13954	1,25E-05	4,8E-05	-21,8033	-20,2845	1,115416	1,17E-05	0,7376	1,068998	2,84E-05	0,580063
-3,51534	-1,13953	-0,83174	0,580881	-21,7418	-20,3283	1,039747	0,633087	0,656489	1,018889	0,613093	0,524623
-3,03219	-1,19771	-1,59643	1,37787	-21,5381	-20,3985	0,861643	1,353464	0,466894	0,783888	1,2724	0,408503
-3,08175	-1,35981	-1,79949	1,406137	-21,4654	-20,3308	0,664216	1,423967	0,549641	0,602075	1,449551	0,380941
-3,471	-1,11242	1,31E-05	4,24E-05	-21,8052	-20,297	1,133813	6,21E-06	0,751875	1,008741	8,11E-06	0,581985
-3,34154	-1,0953	-0,58633	0,373914	-21,8073	-20,3144	1,021477	0,456869	0,722164	0,950056	0,410655	0,571913
-3,06223	-1,17769	-1,23783	0,850856	-21,7728	-20,3059	0,698066	1,041473	0,618746	0,649134	1,011874	0,548427
-2,98804	-1,25799	-1,6606	1,432602	-21,6816	-20,1674	0,457923	1,597728	0,49047	0,425913	1,520324	0,558202
-4,57623	-0,42109	6,64E-06	5,09E-05	-22,664	-19,4162	1,727245	1,09E-05	1,299095	1,300616	9,63E-06	0,765371
-4,45545	-0,39955	-0,52619	0,196729	-22,6991	-19,4156	1,647497	0,284971	1,267334	1,208566	0,295384	0,78824
-4,10029	-0,41984	-1,17503	0,604373	-22,7519	-19,4609	1,29913	0,791904	1,190105	0,84651	0,668421	0,784419
-3,99666	-0,69257	-1,80133	1,228088	-22,791	-19,3017	1,148575	1,293777	1,079663	0,843632	0,922038	0,829172
-3,90431	-0,63246	1,55E-05	2,64E-05	-22,4774	-19,8238	0,95762	3,77E-06	0,744581	0,751917	4,04E-06	0,590254
-3,86348	-0,63177	-0,31716	0,219209	-22,4868	-19,794	0,932475	0,204158	0,739885	0,745514	0,22189	0,588872
-3,67192	-0,60585	-0,68066	0,480077	-22,5205	-19,733	0,837298	0,350524	0,746013	0,626581	0,295638	0,592232
-3,30854	-0,62018	-1,41333	0,776666	-22,5483	-19,6641	0,591513	0,801381	0,782503	0,400483	0,596322	0,588467
-4,23013	-0,32846	1,33E-05	2,62E-05	-22,6512	-19,7351	1,118219	5,07E-06	0,787258	0,789764	3,45E-06	0,601113
-4,13472	-0,33806	-0,37461	0,207604	-22,667	-19,7205	1,077113	0,139881	0,793611	0,742869	0,122318	0,604267
-3,82909	-0,39654	-0,87033	0,438752	-22,684	-19,6639	0,886011	0,423402	0,800324	0,54481	0,307083	0,59696
-3,53818	-0,60554	-1,49953	0,702147	-22,6699	-19,575	0,64414	0,751246	0,749924	0,49547	0,487855	0,555967
-4,67847	0,417641	1,54E-05	2,86E-05	-22,6123	-19,0954	1,035749	3,86E-06	0,929628	0,789405	4,33E-06	0,521434
-4,60885	0,345988	-0,45878	0,274374	-22,6344	-19,0817	1,013334	0,210613	0,923507	0,766985	0,117646	0,5125
-4,40442	0,173964	-0,93742	0,732384	-22,7307	-19,074	0,887213	0,440422	0,927983	0,572718	0,242461	0,524272
-3,97732	-0,01792	-1,58458	1,326166	-22,8039	-19,0564	0,821821	0,586606	0,99245	0,486572	0,401816	0,565613
-4,77279	1,07023	9,86E-06	3,14E-05	-22,5084	-18,9041	1,158788	4E-06	0,944535	0,534098	3,18E-06	0,404503
-4,64605	0,967321	-0,49991	0,411477	-22,5382	-18,8959	1,124397	0,190195	0,94581	0,510999	0,115689	0,404639
-4,30014	0,629888	-0,99238	0,946745	-22,6245	-18,8941	0,949016	0,40814	0,947433	0,4489	0,216006	0,43473
-3,95194	0,182105	-1,36827	1,486453	-22,7213	-18,8965	0,866627	0,564005	0,97251	0,387749	0,251261	0,488086
-5,0104	-1,26442	-1,3E-05	8,55E-05	-21,3048	-20,4647	1,430369	4,05E-05	0,533565	1,517818	0,000321	0,51158
-4,99419	-1,24885	-0,69731	0,46736	-21,3345	-20,44	1,437855	0,499638	0,550608	1,584436	0,584101	0,49539
-4,38546	-1,32919	-0,97762	0,889774	-21,2831	-20,6123	1,106541	0,799916	0,372297	1,165375	0,85847	0,327941
-3,5536	-1,62104	-1,85249	1,322029	-21,0146	-20,7734	0,557634	1,265542	0,169811	0,53011	1,372121	0,217569
-7,44375	-0,62293	1,07E-05	8,1E-05	-22,0589	-19,1186	2,788673	1,99E-05	1,547527	3,041569	7,94E-05	1,599991
-7,0477	-0,72721	-1,01693	0,505578	-22,026	-19,2777	2,615312	0,711417	1,393006	2,726642	0,700032	1,356069
-5,25986	-1,17836	-2,25921	1,271915	-21,7445	-19,961	1,707145	1,656645	0,81651	1,788894	1,608508	0,784434
-4,86032	-1,26254	-3,34258	2,38209	-21,2627	-20,3258	1,399767	2,833118	0,555122	1,551997	3,064528	0,863608
-4,55996	-1,12147	6,43E-06	6,4E-05	-21,9798	-20,1027	1,388098	2,08E-05	0,920261	1,310992	3,34E-05	0,69414
-4,22083	-1,10836	-1,08016	0,708611	-21,9072	-20,155	1,272189	0,793544	0,816845	1,242467	0,760816	0,633446
-3,58958	-1,22331	-2,03756	1,686732	-21,6545	-20,2464	1,053113	1,683117	0,573048	0,964548	1,558863	0,494434
-3,59455	-1,30455	-2,30088	1,687963	-21,5929	-20,1896	0,825376	1,765339	0,70118	0,731299	1,769423	0,517952
-4,09469	-1,00498	1,36E-05	5,07E-05	-21,9865	-20,1126	1,403664	7,93E-06	0,955769	1,24596	1,24E-05	0,704618
-3,92427	-0,97605	-0,77127	0,441171	-21,9914	-20,1455	1,263691	0,57772	0,912921	1,163711	0,515559	0,691925
-3,56812	-1,06519	-1,59123	1,00131	-21,9537	-20,1307	0,867123	1,294519	0,760472	0,800562	1,252422	0,703446
-3,44779	-1,16933	-2,0944	1,688314	-21,8384	-19,936	0,567398	1,958355	0,598373	0,506977	1,868656	0,744437
-5,55705	-0,25359	7,23E-06	6,27E-05	-23,0283	-19,0175	2,134381	1,33E-05	1,627587	1,63362	1,16E-05	1,012525
-5,40093	-0,22084	-0,67939	0,218517	-23,0789	-19,0252	2,039203	0,341668	1,580718	1,508728	0,361685	1,031006
-4,93662	-0,22728	-1,50569	0,694932	-23,16	-19,111	1,620735	0,966187	1,470191	1,067408	0,827062	0,993962
-4,74603	-0,54184	-2,29002	1,434309	-23,1968	-18,9364	1,422767	1,584098	1,319971	1,061105	1,138545	1,042703
-4,57935	-0,39106	1,45E-05	2,99E-05	-22,8292	-19,5372	1,189562	5,03E-06	0,928572	0,935116	5,4E-06	0,713895
-4,5283	-0,3906	-0,42534	0,270341	-22,8399	-19,501	1,158727	0,260654	0,922333	0,935174	0,281604	0,710774
-4,28424	-0,35802	-0,89715	0,593099	-22,8811	-19,4265	1,04455	0,441792	0,929112	0,784738	0,371987	0,710339
-3,81605	-0,37419	-1,81567	0,961591	-22,9141	-19,3387	0,743485	0,989827	0,975412	0,50314	0,741018	0,701692
-4,98643	-0,00548	1,24E-05	2,86E-05	-23,043	-19,4319	1,390547	6,46E-06	0,983722	0,994394	4,01E-06	0,720477
-4,86225	-0,01738	-0,49145	0,258148	-23,0633	-19,4135	1,341305	0,174691	0,990365	0,933308	0,152111	0,723648
-4,47167	-0,09002	-1,12882	0,545971	-23,0868	-19,3431	1,107651	0,527866	0,996869	0,684299	0,383232	0,718017
-4,08675	-0,34945	-1,92533	0,873374	-23,0672	-19,2307	0,80385	0,932416	0,935559	0,623406	0,604694	0,663787
-5,61045	0,864557	1,59E-05	3,22E-05	-23,0093	-18,6322	1,28749	4,72E-06	1,157775	0,988245	5,42E-06	0,628072
-5,51403	0,77808	-0,60886	0,331053	-23,035	-18,6138	1,259873	0,271097	1,151286	0,960119	0,154893	0,615978
-5,23095	0,570421	-1,23337	0,893438	-23,1521	-18,6057	1,099205	0,563154	1,157331	0,720522	0,316838	0,62444
-4,66228	0,340032	-2,02643	1,625668	-23,2528	-18,6079	1,024901	0,734544	1,230927	0,610691	0,499794	0,66879
-5,67495	1,665125	7,95E-06	3,62E-05	-22,9061	-18,3911	1,457373	5,16E-06	1,182596	0,662038	4E-06	0,513563
-5,51208	1,538794	-0,65204	0,5013	-22,943	-18,3808	1,414074	0,237969	1,18517	0,633489	0,149171	0,51329
-5,06564	1,125102	-1,29495	1,162967	-23,0485	-18,3784	1,197818	0,512049	1,187765	0,55934	0,278135	0,547789
-4,60597	0,580689	-1,7743	1,828573	-23,1655	-18,3809	1,075558	0,710371	1,214943	0,483467	0,301469	0,608435

CASE	Degrees	Hs	Tz	Diff X	Diff Y	Diff Z
1	180	2	4	2,75	0,00	0,62
2	195			2,76	0,87	0,66
3	210			2,22	1,37	0,50
4	225			1,33	2,42	0,17
5	180	2	5	5,47	0,00	2,28
6	195			5,03	1,15	2,12
7	210			3,16	2,80	1,38
8	225			2,75	4,71	0,74
9	180	2	6	2,63	0,00	1,52
10	195			2,38	1,41	1,41
11	210			1,83	2,97	1,14
12	225			1,72	3,21	1,13
13	180	2	7	2,36	0,00	1,51
14	195			2,25	0,96	1,49
15	210			1,88	2,09	1,47
16	225			1,73	3,09	1,51
17	180	2	8	4,16	0,00	3,25
18	195			4,06	0,72	3,28
19	210			3,68	1,78	3,29
20	225			3,30	3,03	3,49
21	180	2	9	3,27	0,00	2,65
22	195			3,23	0,54	2,69
23	210			3,07	1,16	2,79
24	225			2,69	2,19	2,88
25	180	2	10	3,90	0,00	2,92
26	195			3,80	0,58	2,95
27	210			3,43	1,31	3,02
28	225			2,93	2,20	3,09
29	180	2	11	5,10	0,00	3,52
30	195			4,95	0,73	3,55
31	210			4,58	1,67	3,66
32	225			3,96	2,91	3,75
33	180	2	12	5,84	0,00	3,60
34	195			5,61	0,91	3,64
35	210			4,93	1,94	3,73
36	225			4,13	2,85	3,82
37	180	2,5	4	3,75	0,00	0,84
38	195			3,75	1,16	0,89
39	210			3,06	1,87	0,67
40	225			1,93	3,17	0,24
41	180	2,5	5	6,82	0,00	2,94
42	195			6,32	1,52	2,75
43	210			4,08	3,53	1,78
44	225			3,60	5,72	0,94
45	180	2,5	6	3,44	0,00	1,88
46	195			3,11	1,79	1,75
47	210			2,37	3,72	1,41
48	225			2,29	3,99	1,40
49	180	2,5	7	3,09	0,00	1,87
50	195			2,95	1,21	1,85
51	210			2,50	2,59	1,82
52	225			2,28	3,78	1,90
53	180	2,5	8	5,30	0,00	4,01
54	195			5,18	0,90	4,05
55	210			4,71	2,20	4,05
56	225			4,20	3,72	4,26
57	180	2,5	9	4,19	0,00	3,29
58	195			4,14	0,70	3,34
59	210			3,93	1,49	3,45
60	225			3,44	2,78	3,58
61	180	2,5	10	4,98	0,00	3,61
62	195			4,84	0,75	3,65
63	210			4,38	1,67	3,74
64	225			3,74	2,80	3,84
65	180	2,5	11	6,48	0,00	4,38
66	195			6,29	0,94	4,42
67	210			5,80	2,13	4,55
68	225			5,00	3,65	4,64
69	180	2,5	12	7,34	0,00	4,52
70	195			7,05	1,15	4,56
71	210			6,19	2,46	4,67
72	225			5,19	3,60	4,78
						2,66

Hs = 2	Diff X			
Tz	180	195	210	225
4	2,75	2,76	2,22	1,33
5	5,47	5,03	3,16	2,75
6	2,63	2,38	1,83	1,72
7	2,36	2,25	1,88	1,73
8	4,16	4,06	3,68	3,30
9	3,27	3,23	3,07	2,69
10	3,90	3,80	3,43	2,93
11	5,10	4,95	4,58	3,96
12	5,84	5,61	4,93	4,13

Hs = 2	Diff Y			
Tz	180	195	210	225
4	0,00	0,87	1,37	2,42
5	0,00	1,15	2,80	4,71
6	0,00	1,41	2,97	3,21
7	0,00	0,96	2,09	3,09
8	0,00	0,72	1,78	3,03
9	0,00	0,54	1,16	2,19
10	0,00	0,58	1,31	2,20
11	0,00	0,73	1,67	2,91
12	0,00	0,91	1,94	2,85

Hs = 2	Diff Z			
Tz	180	195	210	225
4	0,62	0,66	0,50	0,17
5	2,28	2,12	1,38	0,74
6	1,52	1,41	1,14	1,13
7	1,51	1,49	1,47	1,51
8	3,25	3,28	3,29	3,49
9	2,65	2,69	2,79	2,88
10	2,92	2,95	3,02	3,09
11	3,52	3,55	3,66	3,75
12	3,60	3,64	3,73	3,82

Hs = 2.5	Diff X			
Tz	180	195	210	225
4	3,75	3,75	3,06	1,93
5	6,82	6,32	4,08	3,60
6	3,44	3,11	2,37	2,29
7	3,09	2,95	2,50	2,28
8	5,30	5,18	4,71	4,20
9	4,19	4,14	3,93	3,44
10	4,98	4,84	4,38	3,74
11	6,48	6,29	5,80	5,00
12	7,34	7,05	6,19	5,19

Hs = 2.5	Diff Y			
Tz	180	195	210	225
4	0,00	1,16	1,87	3,17
5	0,00	1,52	3,53	5,72
6	0,00	1,79	3,72	3,99
7	0,00	1,21	2,59	3,78
8	0,00	0,90	2,20	3,72
9	0,00	0,70	1,49	2,78
10	0,00	0,75	1,67	2,80
11	0,00	0,94	2,13	3,65
12	0,00	1,15	2,46	3,60

Hs = 2.5	Diff Z			
Tz	180	195	210	225
4	0,84	0,89	0,67	0,24
5	2,94	2,75	1,78	0,94
6	1,88	1,75	1,41	1,40
7	1,87	1,85	1,82	1,90
8	4,01	4,05	4,05	4,26
9	3,29	3,34	3,45	3,58
10	3,61	3,65	3,74	3,84
11	4,38	4,42	4,55	4,64
12	4,52	4,56	4,67	4,78

Appendix 12 – Scenario 2a Results

Min X	Max X	Min Y	Max Y	Min Z	Max Z	Gx-Velocity	Gy-Velocity	Gz-Velocity	Gx-Accele	Gy-Accele	Gz-Accele
-4,33483	-1,91348	1,62E-05	0,000134	-27,7402	-27,2157	0,897787	6,12E-05	0,205132	0,932323	9,22E-05	0,397581
-4,32281	-1,93762	-0,41113	0,419525	-27,7592	-27,2317	0,882346	0,362842	0,210011	0,931624	0,452637	0,404687
-3,90142	-2,09488	-0,6129	0,613127	-27,7231	-27,3224	0,636598	0,573829	0,199267	0,663641	0,623043	0,266776
-3,40647	-2,23063	-1,20915	1,241348	-27,5989	-27,3472	0,292661	1,179877	0,214585	0,320464	1,26161	0,406714
-6,79197	-1,43725	-7,9E-05	0,000439	-28,2748	-26,1811	2,502371	0,000262	0,979928	2,355329	0,000287	2,105243
-6,37973	-1,5272	-0,97211	0,588205	-28,238	-26,3627	2,29089	0,763836	0,804138	2,191645	0,747749	1,78603
-4,84043	-1,87179	-1,92138	1,302166	-28,0451	-26,8001	1,280107	1,661336	0,59819	1,290345	1,581636	1,221741
-4,64192	-1,92683	-2,80462	2,546065	-27,7319	-26,708	1,086813	2,673729	0,790521	1,169313	2,490352	1,594272
-4,67376	-1,6474	6,14E-06	0,000192	-28,1385	-26,8761	1,537619	9,7E-05	0,456768	1,42852	9,29E-05	0,807535
-4,36666	-1,72208	-0,92111	0,626576	-28,0728	-26,9714	1,403235	0,684785	0,404995	1,30118	0,676835	0,734032
-3,64074	-1,87322	-1,84427	1,459548	-27,9519	-26,931	0,91696	1,578878	0,505073	0,771353	1,451644	0,660937
-3,7267	-1,93894	-1,93558	1,482049	-27,9129	-26,8661	0,798217	1,648584	0,507518	0,723083	1,526143	0,625461
-3,96298	-1,74051	1,07E-07	0,00012	-28,1524	-26,9065	0,989594	6,31E-05	0,42573	0,987704	6,56E-05	0,516744
-3,83719	-1,81565	-0,60385	0,462017	-28,1402	-26,9409	0,89494	0,510835	0,449287	0,874999	0,454962	0,471072
-3,59438	-2,0083	-1,24857	1,0488	-28,098	-26,9168	0,64495	1,126916	0,522746	0,613606	1,031255	0,510312
-3,62248	-1,82599	-1,65975	1,465025	-28,0293	-26,85	0,594246	1,510294	0,561248	0,530568	1,496351	0,640099
-4,84856	-0,96275	-2,1E-05	0,000162	-28,8642	-26,0358	1,397081	9,12E-05	0,840329	1,175731	9,51E-05	0,809178
-4,72242	-0,93865	-0,47852	0,174908	-28,8683	-26,0757	1,31478	0,281422	0,852406	1,11969	0,265073	0,77351
-4,22846	-0,94533	-1,0674	0,668547	-28,8643	-26,1764	1,106018	0,812905	0,825074	0,79136	0,655527	0,705935
-4,25995	-1,19569	-1,67549	1,281116	-28,8617	-26,1712	0,929242	1,21402	0,836789	0,609447	1,125631	0,696795
-4,32583	-1,11454	3,49E-05	7,7E-05	-28,6294	-26,591	0,906497	1,96E-05	0,549083	0,636815	2E-05	0,389252
-4,28612	-1,11967	-0,33228	0,225516	-28,6326	-26,5635	0,877749	0,222084	0,547093	0,618308	0,223446	0,389392
-4,11526	-1,11978	-0,63597	0,477528	-28,6538	-26,5079	0,771081	0,363822	0,542998	0,523639	0,357139	0,39066
-3,83962	-1,17415	-1,25319	0,773828	-28,6836	-26,4592	0,547967	0,728194	0,566224	0,426365	0,505067	0,420546
-4,65293	-0,81731	2,19E-05	8,89E-05	-28,7876	-26,4835	1,078395	3,6E-05	0,572459	0,667617	3,79E-05	0,446047
-4,55858	-0,83313	-0,38011	0,21143	-28,7994	-26,4705	1,029817	0,154538	0,572159	0,616494	0,119316	0,437404
-4,29375	-0,90946	-0,86068	0,449908	-28,8129	-26,4284	0,832866	0,437963	0,589314	0,450759	0,306941	0,408013
-4,07005	-1,13845	-1,43274	0,72428	-28,8006	-26,364	0,636022	0,743569	0,580611	0,46713	0,46783	0,384028
-5,06437	-0,03619	3,79E-05	8,17E-05	-28,8171	-25,9574	0,97955	1,32E-05	0,739618	0,625522	9,48E-06	0,379024
-5,00258	-0,10711	-0,47273	0,293061	-28,8256	-25,9453	0,951452	0,22056	0,746767	0,586622	0,1211	0,365786
-4,80539	-0,2898	-0,91815	0,756453	-28,8718	-25,9338	0,893869	0,459912	0,750465	0,485157	0,241183	0,373004
-4,37269	-0,52093	-1,43318	1,345026	-28,9438	-25,9182	0,840639	0,583438	0,774926	0,484811	0,303486	0,424629
-5,23091	0,374185	3,13E-05	8,86E-05	-28,8965	-25,8016	1,077626	1,41E-05	0,810317	0,434361	1,58E-05	0,347293
-5,12176	0,265566	-0,51955	0,446525	-28,9102	-25,7951	1,040341	0,190551	0,813424	0,449454	0,095578	0,345361
-4,88759	-0,06317	-1,0197	1,002253	-28,9539	-25,787	0,996439	0,40708	0,807385	0,473903	0,232116	0,350546
-4,55658	-0,44136	-1,32755	1,527548	-29,0159	-25,78	0,922754	0,599544	0,81816	0,419578	0,261728	0,374415
-5,20326	-1,94464	7E-06	0,000196	-27,7893	-27,0831	1,117048	5,6E-05	0,263929	1,183505	0,000109	0,597837
-5,17451	-1,95108	-0,57023	0,525591	-27,813	-27,1067	1,099902	0,443075	0,263734	1,178281	0,555228	0,537342
-4,61247	-2,05869	-0,8837	0,776354	-27,7652	-27,2557	0,800898	0,714515	0,249106	0,853265	0,769377	0,387445
-3,93133	-2,21823	-1,65506	1,525324	-27,6105	-27,257	0,367602	1,417559	0,306061	0,402987	1,495298	0,599097
-8,0018	-1,39777	-9,8E-05	0,000473	-28,4578	-25,7319	2,884429	0,00029	1,27014	2,682419	0,000315	2,923399
-7,54613	-1,49749	-1,36987	0,778712	-28,4101	-25,97	2,629108	1,092281	1,113092	2,507129	1,003797	2,466994
-5,71708	-1,87401	-2,39187	1,563682	-28,1684	-26,5472	1,49699	2,051308	0,828955	1,577404	1,879337	1,72386
-5,49435	-1,90903	-3,43889	2,90277	-27,7597	-26,3546	1,527744	3,059006	1,113363	1,552715	2,892972	2,176022
-5,46209	-1,67387	-1,5E-06	0,000239	-28,2813	-26,6321	1,875483	0,000124	0,602505	1,719077	0,000123	1,174991
-5,0607	-1,72662	-1,19011	0,7639	-28,1973	-26,774	1,717809	0,844543	0,500312	1,585272	0,836229	1,050031
-4,10504	-1,77733	-2,33746	1,777683	-28,0502	-26,7176	1,125301	1,945376	0,681326	0,946424	1,760647	0,940816
-4,19548	-1,85972	-2,46256	1,745889	-27,9969	-26,637	0,956852	2,030659	0,679369	0,888049	1,854337	0,884753
-4,55256	-1,68266	-8,3E-06	0,000146	-28,2994	-26,7005	1,227168	7,89E-05	0,526387	1,215659	8,3E-05	0,677245
-4,38772	-1,76675	-0,78517	0,556039	-28,2813	-26,7509	1,109981	0,643472	0,558066	1,079609	0,572511	0,607192
-4,07636	-1,99086	-1,59116	1,260793	-28,2224	-26,7279	0,803271	1,402008	0,67746	0,768297	1,274313	0,678295
-4,08728	-1,78441	-2,07156	1,737445	-28,1338	-26,6302	0,73688	1,855193	0,752342	0,654857	1,785494	0,891573
-5,66507	-0,78999	-4E-05	0,000204	-29,2004	-25,582	1,744244	0,000116	1,055988	1,390407	0,000122	1,079482
-5,50067	-0,75523	-0,63077	0,190075	-29,2051	-25,6413	1,648604	0,348587	1,069682	1,330769	0,331998	1,027509
-4,89945	-0,74449	-1,38479	0,753768	-29,2001	-25,7883	1,36601	1,009828	1,025517	0,95172	0,818483	0,930053
-4,93707	-1,02654	-2,12253	1,493688	-29,1912	-25,8202	1,160954	1,506395	1,059759	0,774908	1,350898	0,916667
-4,95489	-0,84378	3,09E-05	8,4E-05	-28,8976	-26,3503	1,130448	2,46E-05	0,692723	0,79991	2,55E-05	0,49821
-4,90388	-0,85027	-0,44123	0,271983	-28,9014	-26,3163	1,094803	0,284327	0,689167	0,77623	0,281361	0,497258
-4,68469	-0,85028	-0,84116	0,589743	-28,9293	-26,2466	0,965006	0,463053	0,682063	0,659749	0,447877	0,496605
-4,32515	-0,91689	-1,62012	0,958163	-28,9663	-26,1841	0,687688	0,907487	0,713116	0,53409	0,626441	0,537144
-5,36262	-0,46884	1,63E-05	9,97E-05	-29,0972	-26,2171	1,349408	4,56E-05	0,722438	0,838684	4,81E-05	0,57947
-5,24197	-0,488	-0,49932	0,262502	-29,1126	-26,2011	1,289547	0,196219	0,720155	0,776518	0,150895	0,565211
-4,90103	-0,58249	-1,11867	0,559408	-29,1291	-26,1478	1,046278	0,550505	0,74073	0,569288	0,387089	0,519428
-4,60447	-0,86631	-1,84526	0,901072	-29,1114	-26,0678	0,79576	0,930131	0,731315	0,587581	0,586124	0,489133
-5,94755	0,442024	3,72E-05	9,28E-05	-29,1313	-25,5544	1,212953	1,66E-05	0,922353	0,772902	1,17E-05	0,484304
-5,8618	0,356104	-0,62483	0,352662	-29,1417	-25,5401	1,178423	0,2846	0,932322	0,725431	0,158369	0,46654
-5,59128	0,135778	-1,20926	0,922472	-29,2001	-25,5259	1,107649	0,590219	0,938418	0,60638	0,313708	0,475775
-5,02039	-0,14228	-1,85183	1,650618	-29,2917	-25,5027	1,056396	0,734632	0,964833	0,596423	0,377891	0,542987
-6,11275	0,938215	2,81E-05	0,000102	-29,2389	-25,3636	1,356029	1,71E-05	1,014789	0,540649	1,96E-05	0,440774
-5,97224	0,804716	-0,67608	0,542779	-29,2557	-25,3559	1,292808	0,238056	1,019301	0,559625	0,124528	0,438297
-5,66368	0,403833	-1,32492	1,228765	-29,3087	-25,345	1,237732	0,510277	1,011438	0,590589	0,295586	0,443591
-5,223	-0,05284	-1,73008	1,878678	-29,3856	-25,3345	1,146644	0,76229	1,023913	0,524445	0,331129	0,471961

CASE	Degrees	Hs	Tz	Diff X	Diff Y	Diff Z
1	180	2	4	2,42	0,00	0,52
2	195			2,39	0,83	0,53
3	210			1,81	1,23	0,40
4	225			1,18	2,45	0,25
5	180	2	5	5,35	0,00	2,09
6	195			4,85	1,56	1,88
7	210			2,97	3,22	1,25
8	225			2,72	5,35	1,02
9	180	2	6	3,03	0,00	1,26
10	195			2,64	1,55	1,10
11	210			1,77	3,30	1,02
12	225			1,79	3,42	1,05
13	180	2	7	2,22	0,00	1,25
14	195			2,02	1,07	1,20
15	210			1,59	2,30	1,18
16	225			1,80	3,12	1,18
17	180	2	8	3,89	0,00	2,83
18	195			3,78	0,65	2,79
19	210			3,28	1,74	2,69
20	225			3,06	2,96	2,69
21	180	2	9	3,21	0,00	2,04
22	195			3,17	0,56	2,07
23	210			3,00	1,11	2,15
24	225			2,67	2,03	2,22
25	180	2	10	3,84	0,00	2,30
26	195			3,73	0,59	2,33
27	210			3,38	1,31	2,38
28	225			2,93	2,16	2,44
29	180	2	11	5,03	0,00	2,86
30	195			4,90	0,77	2,88
31	210			4,52	1,67	2,94
32	225			3,85	2,78	3,03
33	180	2	12	5,61	0,00	3,09
34	195			5,39	0,97	3,12
35	210			4,82	2,02	3,17
36	225			4,12	2,86	3,24
37	180	2,5	4	3,26	0,00	0,71
38	195			3,22	1,10	0,71
39	210			2,55	1,66	0,51
40	225			1,71	3,18	0,35
41	180	2,5	5	6,60	0,00	2,73
42	195			6,05	2,15	2,44
43	210			3,84	3,96	1,62
44	225			3,59	6,34	1,41
45	180	2,5	6	3,79	0,00	1,65
46	195			3,33	1,95	1,42
47	210			2,33	4,12	1,33
48	225			2,34	4,21	1,36
49	180	2,5	7	2,87	0,00	1,60
50	195			2,62	1,34	1,53
51	210			2,09	2,85	1,49
52	225			2,30	3,81	1,50
53	180	2,5	8	4,88	0,00	3,62
54	195			4,75	0,82	3,56
55	210			4,15	2,14	3,41
56	225			3,91	3,62	3,37
57	180	2,5	9	4,11	0,00	2,55
58	195			4,05	0,71	2,59
59	210			3,83	1,43	2,68
60	225			3,41	2,58	2,78
61	180	2,5	10	4,89	0,00	2,88
62	195			4,75	0,76	2,91
63	210			4,32	1,68	2,98
64	225			3,74	2,75	3,04
65	180	2,5	11	6,39	0,00	3,58
66	195			6,22	0,98	3,60
67	210			5,73	2,13	3,67
68	225			4,88	3,50	3,79
69	180	2,5	12	7,05	0,00	3,88
70	195			6,78	1,22	3,90
71	210			6,07	2,55	3,96
72	225			5,17	3,61	4,05
						2,22

Hs = 2 — **Diff X**

Tz	180	195	210	225
4	2,42	2,39	1,81	1,18
5	5,35	4,85	2,97	2,72
6	3,03	2,64	1,77	1,79
7	2,22	2,02	1,59	1,80
8	3,89	3,78	3,28	3,06
9	3,21	3,17	3,00	2,67
10	3,84	3,73	3,38	2,93
11	5,03	4,90	4,52	3,85
12	5,61	5,39	4,82	4,12

Hs = 2 — **Diff Y**

Tz	180	195	210	225
4	0,00	0,83	1,23	2,45
5	0,00	1,56	3,22	5,35
6	0,00	1,55	3,30	3,42
7	0,00	1,07	2,30	3,12
8	0,00	0,65	1,74	2,96
9	0,00	0,56	1,11	2,03
10	0,00	0,59	1,31	2,16
11	0,00	0,77	1,67	2,78
12	0,00	0,97	2,02	2,86

Hs = 2 — **Diff Z**

Tz	180	195	210	225
4	0,52	0,53	0,40	0,25
5	2,09	1,88	1,25	1,02
6	1,26	1,10	1,02	1,05
7	1,25	1,20	1,18	1,18
8	2,83	2,79	2,69	2,69
9	2,04	2,07	2,15	2,22
10	2,30	2,33	2,38	2,44
11	2,86	2,88	2,94	3,03
12	3,09	3,12	3,17	3,24

Hs = 2.5 — **Diff X**

Tz	180	195	210	225
4	3,26	3,22	2,55	1,71
5	6,60	6,05	3,84	3,59
6	3,79	3,33	2,33	2,34
7	2,87	2,62	2,09	2,30
8	4,88	4,75	4,15	3,91
9	4,11	4,05	3,83	3,41
10	4,89	4,75	4,32	3,74
11	6,39	6,22	5,73	4,88
12	7,05	6,78	6,07	5,17

Hs = 2.5 — **Diff Y**

Tz	180	195	210	225
4	0,00	1,10	1,66	3,18
5	0,00	2,15	3,96	6,34
6	0,00	1,95	4,12	4,21
7	0,00	1,34	2,85	3,81
8	0,00	0,82	2,14	3,62
9	0,00	0,71	1,43	2,58
10	0,00	0,76	1,68	2,75
11	0,00	0,98	2,13	3,50
12	0,00	1,22	2,55	3,61

Hs = 2.5 — **Diff Z**

Tz	180	195	210	225
4	0,71	0,71	0,51	0,35
5	2,73	2,44	1,62	1,41
6	1,65	1,42	1,33	1,36
7	1,60	1,53	1,49	1,50
8	3,62	3,56	3,41	3,37
9	2,55	2,59	2,68	2,78
10	2,88	2,91	2,98	3,04
11	3,58	3,60	3,67	3,79
12	3,88	3,90	3,96	4,05

Appendix 13 – Scenario 2b Results

Min X	Max X	Min Y	Max Y	Min Z	Max Z	Gx-Velocit	Gy-Velocit	Gz-Velocit	Gx-Accele	Gy-Accele	Gz-Accele
-4,27648	-1,94206	3,68E-05	0,000105	-28,1114	-27,5857	0,823801	1,49E-05	0,261694	0,845548	5,11E-05	0,272192
-4,27156	-1,96413	-0,36371	0,376807	-28,1375	-27,5937	0,825382	0,322515	0,280112	0,848392	0,356365	0,284012
-3,8566	-2,08879	-0,60315	0,508555	-28,089	-27,6501	0,584751	0,465922	0,236627	0,628498	0,505149	0,245432
-3,4008	-2,22947	-1,20617	1,191671	-27,8903	-27,6933	0,283907	1,100991	0,119564	0,310571	1,142346	0,158271
-6,69704	-1,52223	4,17E-05	0,000135	-28,7573	-26,8139	2,278611	3E-05	0,796014	2,405646	4,27E-05	1,226419
-6,34091	-1,60568	-0,82977	0,68036	-28,7253	-26,8939	2,158404	0,742237	0,79165	2,240822	0,71841	1,024023
-4,90732	-1,93417	-1,89164	1,295313	-28,4805	-27,2276	1,38214	1,5728	0,591803	1,424022	1,522858	0,674795
-4,82322	-1,93312	-2,79765	2,517632	-28,1171	-27,2556	1,251819	2,581611	0,460128	1,229226	2,633039	0,756713
-4,74887	-1,75913	3,57E-05	0,000114	-28,6427	-27,2406	1,540755	2,56E-05	0,631235	1,457316	2,75E-05	0,548812
-4,39676	-1,87505	-1,02327	0,669145	-28,5537	-27,2843	1,367039	0,784491	0,54499	1,276106	0,729342	0,478976
-3,72912	-1,86124	-1,97126	1,734751	-28,3002	-27,1685	0,860517	1,756404	0,458801	0,712694	1,590161	0,496685
-4,0306	-1,92837	-2,03216	1,785612	-28,3594	-27,0784	0,954392	1,803573	0,512812	0,841265	1,765701	0,465444
-3,99396	-1,59362	3,93E-05	9,65E-05	-28,6811	-27,1816	0,973417	1,7E-05	0,632107	0,941346	1,13E-05	0,523722
-3,89201	-1,68212	-0,64176	0,550885	-28,6813	-27,2095	0,88112	0,563222	0,651824	0,838487	0,512728	0,540909
-3,74027	-1,96185	-1,27474	1,213834	-28,6516	-27,1321	0,691375	1,198412	0,707329	0,621486	1,105452	0,589093
-3,74165	-1,77478	-1,70446	1,490763	-28,5701	-27,056	0,657902	1,522942	0,664619	0,60514	1,475956	0,527713
-5,06963	-0,9331	4,14E-05	0,000116	-29,6259	-26,2474	1,246878	1,95E-05	1,162987	1,216236	1,26E-05	0,866685
-4,93224	-0,91204	-0,48379	0,206599	-29,6423	-26,2809	1,216982	0,299002	1,170649	1,147933	0,250173	0,8595
-4,42298	-0,92751	-1,13061	0,753853	-29,6633	-26,2768	1,112541	0,834638	1,143875	0,798669	0,750313	0,830048
-4,39332	-1,18205	-1,93126	1,289054	-29,6882	-26,1933	0,864051	1,350549	1,142906	0,55695	1,249126	0,833771
-4,3374	-1,07817	4,16E-05	6,28E-05	-29,3577	-26,7144	0,878365	5,03E-06	0,74953	0,588706	6,38E-06	0,579321
-4,30668	-1,08516	-0,33236	0,286672	-29,3678	-26,6826	0,850254	0,252533	0,746486	0,573958	0,170519	0,580157
-4,16597	-1,09149	-0,59563	0,513692	-29,4037	-26,6124	0,744581	0,37566	0,747855	0,500902	0,303447	0,590454
-3,94927	-1,15792	-1,19021	0,835888	-29,4418	-26,5467	0,553826	0,677029	0,771468	0,464676	0,403969	0,598028
-4,64022	-0,79083	3,76E-05	6,49E-05	-29,5339	-26,62	1,053916	6,35E-06	0,773766	0,606472	5,93E-06	0,604244
-4,54927	-0,80811	-0,37998	0,228232	-29,5485	-26,6019	1,002214	0,172247	0,781094	0,552944	0,112672	0,607327
-4,3164	-0,88954	-0,85123	0,486977	-29,5619	-26,5429	0,802206	0,455781	0,796172	0,411877	0,324582	0,591863
-4,12219	-1,12981	-1,42253	0,778338	-29,5548	-26,4665	0,637785	0,755972	0,754916	0,466694	0,447974	0,560142
-5,13497	-0,01189	4,39E-05	6,8E-05	-29,4841	-25,9651	0,997418	5,07E-06	0,936735	0,632701	4,67E-06	0,525033
-5,07117	-0,0858	-0,47239	0,306927	-29,5083	-25,9539	0,957997	0,233116	0,932504	0,581071	0,118159	0,515583
-4,85879	-0,27473	-0,88813	0,782137	-29,6043	-25,9415	0,897347	0,484198	0,93394	0,474906	0,229427	0,526308
-4,41025	-0,51637	-1,45023	1,407554	-29,6768	-25,9115	0,858275	0,588607	0,991206	0,555159	0,372321	0,569087
-5,31414	0,342129	3,59E-05	7,57E-05	-29,3973	-25,8147	1,093461	7,62E-06	0,959446	0,453206	5,01E-06	0,413523
-5,21901	0,227448	-0,49961	0,445874	-29,4252	-25,8082	1,067974	0,201566	0,959656	0,466567	0,091241	0,413633
-5,00716	-0,09607	-0,97177	1,002805	-29,5062	-25,8003	1,030232	0,466525	0,959946	0,487615	0,24134	0,441813
-4,6512	-0,44155	-1,34681	1,536375	-29,5975	-25,7912	0,943049	0,626439	0,986671	0,426681	0,308305	0,490348
-5,1099	-1,95994	2,08E-05	0,000155	-28,1864	-27,4886	1,008899	2,91E-05	0,326991	1,082071	7,73E-05	0,362443
-5,096	-1,96786	-0,51188	0,480746	-28,2146	-27,5039	1,021835	0,399114	0,347556	1,074413	0,437563	0,349498
-4,54629	-2,07248	-0,88808	0,64479	-28,1583	-27,6073	0,734472	0,597241	0,297912	0,796704	0,622851	0,316887
-3,92338	-2,2168	-1,66664	1,450107	-27,9133	-27,6447	0,356318	1,329245	0,158698	0,386491	1,36202	0,210478
-7,94846	-1,4852	4,3E-05	0,000215	-28,9513	-26,5089	2,579346	3,21E-05	0,97055	2,760471	5,55E-05	1,698906
-7,52829	-1,58208	-1,09415	0,863765	-28,9129	-26,6324	2,474196	0,975289	0,963844	2,585067	0,935476	1,42136
-5,79675	-1,94314	-2,3286	1,494393	-28,6164	-27,0533	1,64103	1,864971	0,727919	1,681658	1,75127	0,92256
-5,67028	-1,92216	-3,41208	2,804477	-28,1708	-27,0985	1,605692	2,92417	0,661755	1,596325	3,033638	0,994132
-5,52885	-1,79342	3,35E-05	0,000125	-28,8026	-27,0761	1,861005	3,26E-05	0,759765	1,756559	3,41E-05	0,674697
-5,06769	-1,77843	-1,31424	0,815728	-28,6981	-27,156	1,657144	0,963907	0,656328	1,551948	0,899357	0,600785
-4,20191	-1,76247	-2,45432	2,022802	-28,4153	-26,9703	1,062229	2,115839	0,599633	0,893311	1,930641	0,678851
-4,58415	-1,84629	-2,45796	2,079108	-28,4801	-26,8514	1,188393	2,139	0,660314	1,070013	2,081261	0,614561
-4,58352	-1,52035	3,98E-05	0,000114	-28,8708	-27,0163	1,193798	2,19E-05	0,772935	1,16708	1,43E-05	0,659305
-4,45658	-1,61971	-0,83048	0,665272	-28,8687	-27,0583	1,094199	0,707728	0,806479	1,045719	0,631755	0,664812
-4,26646	-1,94591	-1,61602	1,456824	-28,8194	-26,9337	0,871912	1,483787	0,892474	0,787801	1,333346	0,732926
-4,23342	-1,71922	-2,06843	1,76986	-28,7109	-26,8305	0,798494	1,817142	0,83898	0,73544	1,762165	0,661226
-5,92384	-0,76352	4,28E-05	0,000142	-30,0479	-25,8583	1,559361	2,47E-05	1,424067	1,433557	1,54E-05	1,099689
-5,74824	-0,73239	-0,64168	0,230224	-30,0676	-25,9096	1,49256	0,375479	1,434655	1,360185	0,315117	1,091004
-5,09377	-0,7339	-1,43016	0,868117	-30,0856	-25,9176	1,368578	1,040093	1,402522	0,96189	0,89343	1,053697
-5,10886	-1,01748	-2,42302	1,509462	-30,1009	-25,8377	1,080075	1,6091	1,414953	0,694682	1,48582	1,021382
-4,97803	-0,80484	4,14E-05	7,08E-05	-29,7095	-26,4338	1,092122	6,42E-06	0,931839	0,739136	8,59E-06	0,696167
-4,93764	-0,81357	-0,44128	0,35149	-29,721	-26,394	1,057681	0,323469	0,92749	0,71947	0,218541	0,696828
-4,75756	-0,8209	-0,79353	0,634031	-29,7645	-26,3055	0,929442	0,480429	0,927792	0,629196	0,379763	0,709944
-4,47379	-0,90131	-1,54499	1,034148	-29,8111	-26,2214	0,691502	0,845662	0,952766	0,579113	0,50261	0,717842
-5,35483	-0,44138	3,64E-05	7,21E-05	-29,928	-26,3194	1,315967	7,74E-06	0,958167	0,76117	7,54E-06	0,72854
-5,23876	-0,46271	-0,50073	0,283356	-29,9462	-26,2964	1,253739	0,219514	0,964347	0,694846	0,143117	0,732456
-4,93845	-0,56237	-1,1086	0,605262	-29,9636	-26,2212	1,007036	0,573698	0,986948	0,51905	0,407584	0,712383
-4,67767	-0,8588	-1,8357	0,967272	-29,9511	-26,1266	0,795808	0,945428	0,93799	0,584857	0,560892	0,673381
-6,05828	0,46237	4,55E-05	7,9E-05	-29,8718	-25,5125	1,22745	6,83E-06	1,162239	0,776198	7,13E-06	0,633171
-5,96928	0,373085	-0,62762	0,370987	-29,9007	-25,4955	1,183302	0,302637	1,158948	0,712385	0,154448	0,622603
-5,67872	0,145865	-1,17803	0,954682	-30,0151	-25,4752	1,109382	0,624599	1,160831	0,591521	0,300409	0,632774
-5,08483	-0,14516	-1,86577	1,727136	-30,1085	-25,463	1,08737	0,751789	1,218922	0,683892	0,45978	0,679871
-6,24408	0,890751	3,52E-05	8,39E-05	-29,7957	-25,3239	1,357442	9,61E-06	1,205406	0,564502	6,13E-06	0,527503
-6,11934	0,750466	-0,65641	0,541381	-29,83	-25,3138	1,325283	0,256368	1,205664	0,581047	0,116406	0,526373
-5,83491	0,354526	-1,27416	1,228883	-29,9286	-25,2955	1,277233	0,593941	1,204499	0,607778	0,304858	0,557065
-5,36022	-0,06163	-1,74578	1,88691	-30,0396	-25,2841	1,169405	0,798327	1,233668	0,532336	0,374379	0,611812

CASE	Degrees	Hs	Tz	Diff X	Diff Y	Diff Z
1	180	2	4	2,33	0,00	0,53
2	195			2,31	0,74	0,54
3	210			1,77	1,11	0,44
4	225			1,17	2,40	0,20
5	180	2	5	5,17	0,00	1,94
6	195			4,74	1,51	1,83
7	210			2,97	3,19	1,25
8	225			2,89	5,32	0,86
9	180	2	6	2,99	0,00	1,40
10	195			2,52	1,69	1,27
11	210			1,87	3,71	1,13
12	225			2,10	3,82	1,28
13	180	2	7	2,40	0,00	1,50
14	195			2,21	1,19	1,47
15	210			1,78	2,49	1,52
16	225			1,97	3,20	1,51
17	180	2	8	4,14	0,00	3,38
18	195			4,02	0,69	3,36
19	210			3,50	1,88	3,39
20	225			3,21	3,22	3,49
21	180	2	9	3,26	0,00	2,64
22	195			3,22	0,62	2,69
23	210			3,07	1,11	2,79
24	225			2,79	2,03	2,90
25	180	2	10	3,85	0,00	2,91
26	195			3,74	0,61	2,95
27	210			3,43	1,34	3,02
28	225			2,99	2,20	3,09
29	180	2	11	5,12	0,00	3,52
30	195			4,99	0,78	3,55
31	210			4,58	1,67	3,66
32	225			3,89	2,86	3,77
33	180	2	12	5,66	0,00	3,58
34	195			5,45	0,95	3,62
35	210			4,91	1,97	3,71
36	225			4,21	2,88	3,81
37	180	2,5	4	3,15	0,00	0,70
38	195			3,13	0,99	0,71
39	210			2,47	1,53	0,55
40	225			1,71	3,12	0,27
41	180	2,5	5	6,46	0,00	2,44
42	195			5,95	1,96	2,28
43	210			3,85	3,82	1,56
44	225			3,75	6,22	1,07
45	180	2,5	6	3,74	0,00	1,73
46	195			3,29	2,13	1,54
47	210			2,44	4,48	1,45
48	225			2,74	4,54	1,63
49	180	2,5	7	3,06	0,00	1,85
50	195			2,84	1,50	1,81
51	210			2,32	3,07	1,89
52	225			2,51	3,84	1,88
53	180	2,5	8	5,16	0,00	4,19
54	195			5,02	0,87	4,16
55	210			4,36	2,30	4,17
56	225			4,09	3,93	4,26
57	180	2,5	9	4,17	0,00	3,28
58	195			4,12	0,79	3,33
59	210			3,94	1,43	3,46
60	225			3,57	2,58	3,59
61	180	2,5	10	4,91	0,00	3,61
62	195			4,78	0,78	3,65
63	210			4,38	1,71	3,74
64	225			3,82	2,80	3,82
65	180	2,5	11	6,52	0,00	4,36
66	195			6,34	1,00	4,41
67	210			5,82	2,13	4,54
68	225			4,94	3,59	4,65
69	180	2,5	12	7,13	0,00	4,47
70	195			6,87	1,20	4,52
71	210			6,19	2,50	4,63
72	225			5,30	3,63	4,76
						2,63

Hs = 2	Diff X			
Tz	180	195	210	225
4	2,33	2,31	1,77	1,17
5	5,17	4,74	2,97	2,89
6	2,99	2,52	1,87	2,10
7	2,40	2,21	1,78	1,97
8	4,14	4,02	3,50	3,21
9	3,26	3,22	3,07	2,79
10	3,85	3,74	3,43	2,99
11	5,12	4,99	4,58	3,89
12	5,66	5,45	4,91	4,21

Hs = 2	Diff Y			
Tz	180	195	210	225
4	0,00	0,74	1,11	2,40
5	0,00	1,51	3,19	5,32
6	0,00	1,69	3,71	3,82
7	0,00	1,19	2,49	3,20
8	0,00	0,69	1,88	3,22
9	0,00	0,62	1,11	2,03
10	0,00	0,61	1,34	2,20
11	0,00	0,78	1,67	2,86
12	0,00	0,95	1,97	2,88

Hs = 2	Diff Z			
Tz	180	195	210	225
4	0,53	0,54	0,44	0,20
5	1,94	1,83	1,25	0,86
6	1,40	1,27	1,13	1,28
7	1,50	1,47	1,52	1,51
8	3,38	3,36	3,39	3,49
9	2,64	2,69	2,79	2,90
10	2,91	2,95	3,02	3,09
11	3,52	3,55	3,66	3,77
12	3,58	3,62	3,71	3,81

Hs = 2.5	Diff X			
Tz	180	195	210	225
4	3,15	3,13	2,47	1,71
5	6,46	5,95	3,85	3,75
6	3,74	3,29	2,44	2,74
7	3,06	2,84	2,32	2,51
8	5,16	5,02	4,36	4,09
9	4,17	4,12	3,94	3,57
10	4,91	4,78	4,38	3,82
11	6,52	6,34	5,82	4,94
12	7,13	6,87	6,19	5,30

Hs = 2.5	Diff Y			
Tz	180	195	210	225
4	0,00	0,99	1,53	3,12
5	0,00	1,96	3,82	6,22
6	0,00	2,13	4,48	4,54
7	0,00	1,50	3,07	3,84
8	0,00	0,87	2,30	3,93
9	0,00	0,79	1,43	2,58
10	0,00	0,78	1,71	2,80
11	0,00	1,00	2,13	3,59
12	0,00	1,20	2,50	3,63

Hs = 2.5	Diff Z			
Tz	180	195	210	225
4	0,70	0,71	0,55	0,27
5	2,44	2,28	1,56	1,07
6	1,73	1,54	1,45	1,63
7	1,85	1,81	1,89	1,88
8	4,19	4,16	4,17	4,26
9	3,28	3,33	3,46	3,59
10	3,61	3,65	3,74	3,82
11	4,36	4,41	4,54	4,65
12	4,47	4,52	4,63	4,76

Appendix 14 – Modal Analysis

Modal analysis

					Mode	M10	M7	M5	M3
Number	Dist below sealevel	Dist seabed - 1a	Approx	Line length	4	5,363029	5,64391	5,821562	6,010142
M10	-20,167	9,833	10	20,42	5	5,24416	5,519733	5,692295	5,877042
M7	-23	7	7	23,253					
M5	-25	5	5	25,253					
M3	-27,144	2,856	3	27,397					

M10 — **Modal analysis for whole system**

Mode	Period (s)	Frequency (Hz)
1	237,8795009	0,004203809
2	17,88941078	0,05589899
3	16,89510161	0,059188753
4	5,363028959	0,186461794
5	5,244160471	0,190688291
6	0,596062636	1,677676034
7	0,338700969	2,952456862
8	0,338700121	2,952464251
9	0,337684625	2,961342994
10	0,337684337	2,961345529
11	0,1696036	5,896101258
12	0,169603501	5,896104693
13	0,169477493	5,900488515
14	0,169477437	5,900490444
15	0,113358093	8,821602146
16	0,113358064	8,821604398
17	0,113321388	8,824459517
18	0,113321373	8,82446069
19	0,085334062	11,71864987
20	0,085334051	11,71865149
21	0,085318977	11,72072193
22	0,08531897	11,72072281
23	0,068607981	14,57556382
24	0,068607975	14,57556506
25	0,068600518	14,57714932
26	0,068600515	14,57714998
27	0,057540653	17,37901731
28	0,05754065	17,37901829
29	0,057536518	17,38026629
30	0,057536516	17,38026681
31	0,049716872	20,11389633
32	0,04971687	20,11389711
33	0,049714402	20,11489531
34	0,049714401	20,11489573
35	0,043930356	22,76330269
36	0,043930355	22,76330332
37	0,043928805	22,76410661
38	0,043928804	22,76410695
39	0,039512103	25,30870109
40	0,039512102	25,3087016
41	0,039511094	25,30934752
42	0,039511093	25,30934779
43	0,036061767	27,7301997
44	0,036061766	27,7302001
45	0,036061096	27,73071598
46	0,036061095	27,7307162
47	0,033325617	30,00694627
48	0,033325617	30,00694659
49	0,033325165	30,00735342
50	0,033325165	30,00735359
51	0,031135561	32,11761579
52	0,031135561	32,11761604
53	0,031135256	32,11793075
54	0,031135256	32,11793088
55	0,029376373	34,04096229
56	0,029376373	34,04096247
57	0,029376168	34,04119937
58	0,029376168	34,04119946
59	0,027967017	35,75640557
60	0,027967017	35,7564057
61	0,027966883	35,75657732
62	0,027966883	35,75657739
63	0,026849513	37,24462305
64	0,026849513	37,24462314
65	0,026849428	37,24474088
66	0,026849428	37,24474093
67	0,025982046	38,48811613
68	0,025982046	38,48811619
69	0,025981996	38,48819074
70	0,025981996	38,48819077
71	0,025334594	39,4717197
72	0,025334594	39,47171973
73	0,025334567	39,47176144
74	0,025334567	39,47176145
75	0,024886075	40,18311507
76	0,024886075	40,18311508
77	0,024886062	40,18313469
78	0,024886062	40,18313469
79	0,024618799	40,61936602
80	0,024618799	40,61936602
81	0,024618792	40,61937663
82	0,024618792	40,61937663
83	0,020730949	48,23705782
84	0,020706008	48,29516198
85	0,010397533	96,17665819
86	0,010394439	96,20528911
87	0,006967509	143,523311
88	0,006966607	143,5419095
89	0,005263571	189,9850983
90	0,005263198	189,9985401
91	0,004250335	235,2755657
92	0,00425015	235,2858087
93	0,003582746	279,1154817
94	0,003582643	279,1235125
95	0,00311299	321,2345583
96	0,003112928	321,2409482
97	0,002767223	361,3731174
98	0,002767184	361,3782312
99	0,002504485	399,2836912
100	0,002504459	399,2877801

M7 — **Modal analysis for whole syst**

Mode	Period (s)	equency (Hz)
1	270,3753	0,003699
2	18,63627	0,053659
3	17,74472	0,056355
4	5,64391	0,177182
5	5,519733	0,181168
6	0,643355	1,554352
7	0,386306	2,588619
8	0,386305	2,588626
9	0,384995	2,597439
10	0,384994	2,597442
11	0,193365	5,171566
12	0,193365	5,171569
13	0,193202	5,175936
14	0,193202	5,175938
15	0,129151	7,742892
16	0,129151	7,742894
17	0,129103	7,745755
18	0,129103	7,745756
19	0,097124	10,29614
20	0,097124	10,29614
21	0,097104	10,29823
22	0,097104	10,29823
23	0,077978	12,82412
24	0,077978	12,82412
25	0,077968	12,82574
26	0,077968	12,82574
27	0,06528	15,31872
28	0,06528	15,31872
29	0,065274	15,32002
30	0,065274	15,32002
31	0,056272	17,77084
32	0,056272	17,77084
33	0,056269	17,7719
34	0,056269	17,7719
35	0,049578	20,17028
36	0,049578	20,17028
37	0,049576	20,17115
38	0,049576	20,17115
39	0,044433	22,50579
40	0,044433	22,50579
41	0,044432	22,50651
42	0,044432	22,50651
43	0,040379	24,76513
44	0,040379	24,76513
45	0,040378	24,76573
46	0,040378	24,76573
47	0,037126	26,93523
48	0,037126	26,93523
49	0,037125	26,93572
50	0,037125	26,93572
51	0,03448	29,00233
52	0,03448	29,00233
53	0,03448	29,00274
54	0,03448	29,00274
55	0,032308	30,95229
56	0,032308	30,95229
57	0,032307	30,95262
58	0,032307	30,95262
59	0,030515	32,77079
60	0,030515	32,77079
61	0,030515	32,77105
62	0,030515	32,77105
63	0,029033	34,44365
64	0,029033	34,44365
65	0,029033	34,44385
66	0,029033	34,44385
67	0,027811	35,95713
68	0,027811	35,95713
69	0,027811	35,95729
70	0,027811	35,95729
71	0,026811	37,29824
72	0,026811	37,29824
73	0,026811	37,29836
74	0,026811	37,29836
75	0,026004	38,45502
76	0,026004	38,45502
77	0,026004	38,4551
78	0,026004	38,4551
79	0,02537	39,41677
80	0,02537	39,41677
81	0,02537	39,41683
82	0,02537	39,41683
83	0,024892	40,17434
84	0,024892	40,17434
85	0,024891	40,17438
86	0,024891	40,17438
87	0,024558	40,72037
88	0,024558	40,72037
89	0,024558	40,7204
90	0,024558	40,7204
91	0,024355	41,0599
92	0,024355	41,0599
93	0,024355	41,05993
94	0,024355	41,05993
95	0,023601	42,37079
96	0,02357	42,42767
97	0,011828	84,54396
98	0,011824	84,5721
99	0,007916	126,323
100	0,007915	126,3414

M5 — **Modal analysis for whole syst**

Mode	Period (s)	equency (Hz)
1	287,8112	0,003474
2	18,95563	0,052755
3	18,11067	0,055216
4	5,821562	0,171775
5	5,692295	0,175676
6	0,672899	1,486106
7	0,419998	2,380962
8	0,419997	2,380969
9	0,418457	2,38973
10	0,418455	2,38974
11	0,210193	4,757538
12	0,210193	4,757541
13	0,210001	4,761889
14	0,21	4,761895
15	0,140348	7,125155
16	0,140348	7,125157
17	0,140292	7,128013
18	0,140291	7,128017
19	0,105497	9,478901
20	0,105497	9,478903
21	0,105474	9,481
22	0,105474	9,481003
23	0,08465	11,81337
24	0,08465	11,81337
25	0,084638	11,815
26	0,084638	11,81501
27	0,070809	14,12254
28	0,070809	14,12254
29	0,070802	14,12386
30	0,070802	14,12386
31	0,060977	16,39968
32	0,060977	16,39968
33	0,060973	16,40076
34	0,060973	16,40076
35	0,053656	18,63729
36	0,053656	18,63729
37	0,053653	18,63819
38	0,053653	18,63819
39	0,048014	20,82711
40	0,048014	20,82711
41	0,048013	20,82786
42	0,048013	20,82786
43	0,043554	22,96011
44	0,043554	22,96011
45	0,043553	22,96075
46	0,043553	22,96075
47	0,039957	25,0266
48	0,039957	25,0266
49	0,039957	25,02713
50	0,039957	25,02713
51	0,037015	27,01627
52	0,037015	27,01627
53	0,037014	27,01672
54	0,037014	27,01672
55	0,03458	28,91839
56	0,03458	28,91839
57	0,03458	28,91877
58	0,03458	28,91877
59	0,03255	30,72191
60	0,03255	30,72191
61	0,03255	30,72222
62	0,03255	30,72222
63	0,030849	32,41566
64	0,030849	32,41566
65	0,030849	32,41591
66	0,030849	32,41591
67	0,029422	33,98854
68	0,029422	33,98854
69	0,029422	33,98875
70	0,029422	33,98875
71	0,028225	35,42974
72	0,028225	35,42974
73	0,028225	35,4299
74	0,028225	35,4299
75	0,027227	36,72889
76	0,027227	36,72889
77	0,027226	36,72902
78	0,027226	36,72902
79	0,026402	37,87632
80	0,026402	37,87632
81	0,026402	37,87642
82	0,026402	37,87642
83	0,025731	38,86316
84	0,025731	38,86316
85	0,025731	38,86324
86	0,025731	38,86324
87	0,025628	39,01975
88	0,025591	39,07626
89	0,025201	39,68158
90	0,025201	39,68158
91	0,025201	39,68165
92	0,025201	39,68165
93	0,024799	40,32481
94	0,024799	40,32481
95	0,024799	40,32488
96	0,024799	40,32488
97	0,024517	40,78758
98	0,024517	40,78758
99	0,024517	40,78764
100	0,024517	40,78764

M3 — **Modal analysis for who**

Mode	Period (s)	equency (H
1	313,4437	0,00319
2	19,46032	0,051387
3	18,67566	0,053546
4	6,010142	0,166385
5	5,877042	0,170154
6	0,706718	1,414991
7	0,45623	2,191879
8	0,456228	2,191886
9	0,454433	2,200545
10	0,454431	2,200555
11	0,228296	4,380277
12	0,228296	4,38028
13	0,228072	4,384584
14	0,228072	4,384589
15	0,152402	6,561584
16	0,152402	6,561587
17	0,152336	6,56442
18	0,152336	6,564423
19	0,114522	8,731965
20	0,114522	8,731966
21	0,114494	8,734053
22	0,114494	8,734056
23	0,091851	10,88724
24	0,091851	10,88725
25	0,091837	10,88888
26	0,091837	10,88888
27	0,076788	13,02283
28	0,076788	13,02283
29	0,07678	13,02415
30	0,07678	13,02415
31	0,066078	15,13362
32	0,066078	15,13362
33	0,066073	15,13472
34	0,066073	15,13472
35	0,058092	17,214
36	0,058092	17,214
37	0,058089	17,21492
38	0,058089	17,21492
39	0,051927	19,25778
40	0,051927	19,25778
41	0,051925	19,25856
42	0,051925	19,25856
43	0,047041	21,25821
44	0,047041	21,25821
45	0,047039	21,25887
46	0,047039	21,25887
47	0,043089	23,20801
48	0,043089	23,20801
49	0,043088	23,20857
50	0,043088	23,20857
51	0,039842	25,09942
52	0,039842	25,09942
53	0,039841	25,0999
54	0,039841	25,0999
55	0,037141	26,92427
56	0,037141	26,92427
57	0,037141	26,92468
58	0,037141	26,92468
59	0,034875	28,67407
60	0,034875	28,67407
61	0,034874	28,67442
62	0,034874	28,67442
63	0,03296	30,34013
64	0,03296	30,34013
65	0,032959	30,34042
66	0,032959	30,34042
67	0,031335	31,91365
68	0,031335	31,91365
69	0,031334	31,9139
70	0,031334	31,9139
71	0,029953	33,38589
72	0,029953	33,38589
73	0,029953	33,3861
74	0,029953	33,3861
75	0,028778	34,74826
76	0,028778	34,74826
77	0,028778	34,74844
78	0,028778	34,74844
79	0,027801	35,96957
80	0,027784	35,99249
81	0,027784	35,99249
82	0,027783	35,99264
83	0,027783	35,99264
84	0,027758	36,02519
85	0,026946	37,11074
86	0,026946	37,11074
87	0,026946	37,11086
88	0,026946	37,11086
89	0,02625	38,09573
90	0,02625	38,09573
91	0,02625	38,09584
92	0,02625	38,09584
93	0,02568	38,94086
94	0,02568	38,94086
95	0,02568	38,94096
96	0,02568	38,94096
97	0,025227	39,64027
98	0,025227	39,64027
99	0,025227	39,64036
100	0,025227	39,64036

Appendix 15 – Scenario 1a Contact

Line Contact Clearance 1a Top	Line Contact Clearance 1a Bottom	Line Contact Clearance 1d Top	Line Contact Clearance 1d Bottom	Line Clash Force 1a	Line Clash Force 1d
2,125061889	4,472213574	2,125953932	4,472690593	0	0
2,129575631	4,457114774	2,092685331	4,359786053	0	0
2,208695927	4,708591081	2,078035235	4,375230586	0	0
2,203756649	4,807993631	2,26873003	4,60481255	0	0
2,243871093	4,001253052	2,244670285	4,00188551	0	0
2,243602067	4,20933176	2,079429327	4,011923309	0	0
2,277509631	4,376654824	2,131338601	4,618048986	0	0
2,014124983	4,302533611	2,177176836	4,368410344	0	0
2,14002203	4,53104399	2,140819922	4,531507173	0	0
1,959502863	4,538963273	2,120124436	4,503287865	0	0
1,79775179	4,508458279	2,144993748	4,426351569	0	0
2,173249563	4,720966752	2,204480175	4,43604821	0	0
1,865077475	4,302719582	1,865939632	4,303160237	0	0
1,858395232	4,330284722	1,960641656	4,379643145	0	0
1,958015812	4,500071783	2,024346517	4,637192348	0	0
2,127302023	4,599897931	2,050380975	4,537348306	0	0
1,662364217	4,424848919	1,663198987	4,425251566	0	0
1,681500232	4,453625072	1,623593875	4,392946376	0	0
1,713252302	4,502903972	1,607085161	4,393379684	0	0
1,787848697	4,562884277	1,652841762	4,467403169	0	0
1,692260873	4,389238502	1,693057335	4,389633021	0	0
1,764990649	4,451941268	1,692318666	4,3848234	0	0
1,878724041	4,516349717	1,790026744	4,498502011	0	0
1,972634364	4,659735567	1,959523474	4,672105038	0	0
1,60056565	4,298789755	1,601376747	4,299176108	0	0
1,621462411	4,33371055	1,638844372	4,336502198	0	0
1,746007857	4,451377345	1,741426467	4,524171271	0	0
1,901894023	4,579697589	1,898077671	4,604469991	0	0
1,467179139	4,217521701	1,468035674	4,217935017	0	0
1,495834597	4,221933126	1,518750727	4,259771632	0	0
1,623518495	4,332920452	1,648213217	4,358080366	0	0
1,746864636	4,418243474	1,711960605	4,523658983	0	0
1,319191983	4,110778948	1,32004619	4,111154992	0	0
1,33684256	4,13006299	1,394716394	4,132987245	0	0
1,477972274	4,241879014	1,496154873	4,246225639	0	0
1,747743315	4,422882597	1,686316766	4,409875793	0	0
2,122735117	4,361690467	2,123614379	4,362148472	0	0
2,122587222	4,376901754	2,071447764	4,214245428	0	0
2,196230495	4,65937751	2,054920701	4,258519312	0	0
2,212154192	4,783228638	2,262557896	4,527093115	0	0
2,221974354	3,838896914	2,222778872	3,839630314	0	0
2,221641006	4,138990757	2,181796723	3,826237697	0	0
2,263985102	4,332009655	2,070619306	4,617750353	0	0
1,861538635	4,239049198	2,205762102	4,239696793	0	0
2,11596321	4,490273014	2,116763103	4,490774844	0	0
1,932414836	4,480784513	2,094090169	4,467847547	0	0
1,68044431	4,424815457	2,138573551	4,307884004	0	0
2,182460699	4,693404634	2,172610703	4,317604043	0	0
1,767527647	4,144813996	1,768427564	4,145267953	0	0
1,751591635	4,17494408	1,888799975	4,24550974	0	0
1,86674418	4,390615272	1,952930688	4,563752569	0	0
2,081007714	4,513355819	1,990349185	4,433859267	0	0
1,513518248	4,311445466	1,514366778	4,311838818	0	0
1,537171702	4,346453386	1,465602399	4,272466213	0	0
1,577179037	4,407576299	1,446191937	4,273852844	0	0
1,669528595	4,479728443	1,502271893	4,365603092	0	0
1,589925113	4,295025963	1,590728137	4,295415886	0	0
1,677657112	4,373867603	1,591566123	4,287078954	0	0
1,791633724	4,428345027	1,71270389	4,425874789	0	0
1,885263853	4,592037748	1,869000493	4,6085707	0	0
1,466914218	4,175331159	1,46774018	4,175711445	0	0
1,481304857	4,211239534	1,517755764	4,225713889	0	0
1,62071867	4,346509543	1,636334321	4,457557907	0	0
1,796846047	4,492567195	1,8132302	4,544562441	0	0
1,269728529	4,049126719	1,270619453	4,049539671	0	0
1,291327777	4,045176611	1,345496468	4,108171327	0	0
1,436180651	4,172229431	1,508437607	4,277140907	0	0
1,607410616	4,295592691	1,562625128	4,437578318	0	0
1,083294712	3,927552054	1,08417882	3,927913322	0	0
1,094312373	3,943052272	1,187042621	3,958194392	0	0
1,259053189	4,070036954	1,378068453	4,095946291	0	0
1,589957542	4,283735541	1,603269606	4,32680864	0	0

Appendix 16 – Scenario 1b Contact

Line Contact Clearance 1a Top	Line Contact Clearance 1a Bottom	Line Contact Clearance 1d Top	Line Contact Clearance 1d Bottom	Line Clash Force 1a	Line Clash Force 1d
2,08285772	4,760487382	2,083771002	4,760980377	0	0
2,178926144	4,916377584	1,975587398	4,527246027	0	0
2,236101713	4,969595214	1,9823537	4,577725317	0	0
2,276224868	5,13529004	2,284431141	4,729500736	0	0
2,243732744	4,475016195	2,244476831	4,475952848	0	0
2,272009105	4,533706314	2,232230986	4,559538536	0	0
2,096037557	4,471817008	2,309880895	4,919061598	0	0
2,2720721	4,828786073	2,167181728	4,419508055	0	0
2,102838645	4,641283576	2,103656156	4,641733033	0	0
1,830730305	4,572109009	2,104290684	4,794973529	0	0
1,76233339	4,633236666	2,100693095	4,767788339	0	0
2,11335611	4,759621452	2,224412681	4,752291428	0	0
1,897369548	4,792219531	1,898306531	4,792726322	0	0
1,828142139	4,790850989	2,025621917	4,925333991	0	0
1,917141447	4,847002754	2,033197059	4,94330384	0	0
2,164858717	4,9005308	2,047602535	4,815460801	0	0
1,676654505	4,783539672	1,677471959	4,784079461	0	0
1,699243985	4,822165561	1,634196221	4,745611625	0	0
1,734017035	4,777801435	1,616536851	4,765854057	0	0
1,81266979	4,761767458	1,670629443	4,743064692	0	0
1,757239694	4,719863323	1,758033496	4,720280875	0	0
1,827119218	4,714634744	1,758160151	4,750664415	0	0
1,921300031	4,705373272	1,868137055	4,87637081	0	0
1,990147435	4,75730011	1,97845311	4,935009897	0	0
1,641726211	4,491617789	1,642548896	4,492012021	0	0
1,667643554	4,502790291	1,688474827	4,548966255	0	0
1,798469511	4,600021757	1,831436515	4,774092131	0	0
1,912939292	4,78717369	1,935120543	4,89749114	0	0
1,574371802	4,572323353	1,57525699	4,572732554	0	0
1,616049151	4,595078607	1,623806019	4,614774769	0	0
1,701714826	4,691852249	1,69220158	4,659345283	0	0
1,729740008	4,669402351	1,728411231	4,740492012	0	0
1,276026966	4,335387555	1,276902221	4,335758379	0	0
1,315173189	4,390736031	1,332743612	4,346606828	0	0
1,480805506	4,525101784	1,510102199	4,509649257	0	0
1,75840066	4,699132413	1,754502055	4,56727497	0	0
2,079552615	4,694315432	2,08059487	4,694867602	0	0
2,153999595	4,914954106	1,917818448	4,396476437	0	0
2,223002753	4,936004606	1,919031014	4,435413343	0	0
2,265783199	5,115758562	2,274495931	4,628216394	0	0
2,250756785	4,493207418	2,251556582	4,494323481	0	0
2,249603125	4,603101647	2,259132419	4,579401216	0	0
2,227919299	4,462470713	2,29673452	4,942394512	0	0
2,341563961	4,78465143	2,184292095	4,197993477	0	0
2,105184152	4,598511854	2,10596859	4,599018292	0	0
1,777349562	4,487461848	2,063993772	4,785519755	0	0
1,649669982	4,529193568	2,069067353	4,652893784	0	0
2,124655461	4,711635513	2,195240501	4,631825592	0	0
1,816535367	4,813980588	1,817547655	4,814539104	0	0
1,720424546	4,794916752	1,949229614	4,975638277	0	0
1,81984759	4,805730765	1,95573833	4,866553582	0	0
2,119730762	4,852248467	1,978852471	4,703916076	0	0
1,521952776	4,712956026	1,522773084	4,713567891	0	0
1,551652871	4,74490631	1,468885867	4,679713182	0	0
1,596465517	4,800075724	1,449329358	4,683504824	0	0
1,694931802	4,774514768	1,518342183	4,665928504	0	0
1,670733821	4,629877595	1,671533413	4,630310831	0	0
1,754096397	4,614114807	1,674609914	4,672947353	0	0
1,84634871	4,589013481	1,812394564	4,815229045	0	0
1,900334711	4,64314501	1,885633227	4,857346294	0	0
1,528732514	4,348393242	1,529577299	4,348792294	0	0
1,546714789	4,352070174	1,591137301	4,42311751	0	0
1,689152882	4,456304881	1,759032531	4,69912902	0	0
1,804366044	4,680722792	1,830498002	4,838551595	0	0
1,405360991	4,423949243	1,406300201	4,424369186	0	0
1,444542469	4,445678624	1,475585623	4,479847762	0	0
1,550027858	4,56196543	1,529794152	4,584653937	0	0
1,569079635	4,531089321	1,576048285	4,65781188	0	0
1,026436814	4,136161987	1,027352465	4,136522121	0	0
1,067980687	4,200913646	1,102579534	4,149937307	0	0
1,261911679	4,354399033	1,322583215	4,349307037	0	0
1,596802737	4,553176406	1,698095775	4,451604568	0	0

Appendix 17 – Passive Heave Compensation Values

For Orcaflex simulations, Cranemaster is modelled as a "Link".

Cranemaster stroke: 4,3 meters

Copy the values inside the bolded line box and paste into Orcaflex "Link Stiffness Table"

If the link length is SHORTER than Cranemaster stroke, the Pretension must be decreased.

If the link length is LONGER than Cranemaster stroke x 2 (max stroke), the Pretension must be increased.

	ADIABATIC GAS COMPRESSION		**ISOTERM GAS COMPRESSION**		**ISOTERM COMPRESSION AND ADIABATIC CYCLING**		**Damping Values**	
		0		0		0		
		Load		Load		Load		
Stroke (cm)	Link length (m)	(kN)	Link length (m)	(kN)	Link length (m)	(kN)	Speed (m/s)	Damping Force (kN)
0	4,3	1297,4	4,3	1297,4	4,3	1226,9	-3	-8829
10	4,4	1310,8	4,4	1307,7	4,4	1239,7	-2,75	-7418,8125
20	4,5	1324,5	4,5	1318,2	4,5	1252,6	-2,5	-6131,25
30	4,6	1338,4	4,6	1328,8	4,6	1265,8	-2,25	-4966,3125
40	4,7	1352,6	4,7	1339,7	4,7	1279,2	-2	-3924
50	4,8	1367,1	4,8	1350,7	4,8	1292,9	-1,75	-3004,3125
60	4,9	1381,8	4,9	1361,9	4,9	1306,8	-1,5	-2207,25
70	5,0	1396,9	5,0	1373,2	5,0	1321,0	-1,25	-1532,8125
80	5,1	1412,2	5,1	1384,8	5,1	1335,5	-1	-981
90	5,2	1427,8	5,2	1396,6	5,2	1350,3	-0,75	-551,8125
100	5,3	1443,7	5,3	1408,6	5,3	1365,4	-0,5	-245,25
110	5,4	1460,0	5,4	1420,7	5,4	1380,7	-0,25	-61,3125
120	5,5	1476,6	5,5	1433,1	5,5	1396,4	0	0
130	5,6	1493,5	5,6	1445,7	5,6	1412,4	0,25	10,4375
140	5,7	1510,7	5,7	1458,6	5,7	1428,7	0,5	41,75
150	5,8	1528,3	5,8	1471,6	5,8	1445,4	0,75	93,9375
160	5,9	1546,3	5,9	1484,9	5,9	1462,4	1	167
170	6,0	1564,7	6,0	1498,5	6,0	1479,7	1,25	260,9375
180	6,1	1583,4	6,1	1512,2	6,1	1497,5	1,5	375,75
190	6,2	1602,5	6,2	1526,3	6,2	1515,6	1,75	511,4375
200	6,3	1622,1	6,3	1540,6	6,3	1534,1	2	668
210	6,4	1642,1	6,4	1555,2	6,4	1553,0	2,25	845,4375
220	6,5	1662,5	6,5	1570,0	6,5	1572,3	2,5	1043,75
230	6,6	1683,4	6,6	1585,2	6,6	1592,0	2,75	1262,9375
240	6,7	1704,7	6,7	1600,6	6,7	1612,2	3	1503
250	6,8	1726,6	6,8	1616,4	6,8	1632,9	3,25	1763,9375
260	6,9	1748,9	6,9	1632,4	6,9	1654,0	3,5	2045,75
270	7,0	1771,7	7,0	1648,8	7,0	1675,6		
280	7,1	1795,1	7,1	1665,5	7,1	1697,7		
290	7,2	1819,0	7,2	1682,5	7,2	1720,3		
300	7,3	1843,5	7,3	1700,0	7,3	1743,5		
310	7,4	1868,6	7,4	1717,7	7,4	1767,2		
320	7,5	1894,3	7,5	1735,9	7,5	1791,5		
330	7,6	1920,7	7,6	1754,4	7,6	1816,4		
340	7,7	1947,6	7,7	1773,3	7,7	1841,9		
350	7,8	1975,3	7,8	1792,7	7,8	1868,1		
360	7,9	2003,7	7,9	1812,4	7,9	1894,9		
370	8,0	2032,8	8,0	1832,7	8,0	1922,4		
380	8,1	2062,6	8,1	1853,3	8,1	1950,7		
390	8,2	2093,3	8,2	1874,5	8,2	1979,6		
400	8,3	2124,7	8,3	1896,1	8,3	2009,4		
410	8,4	2157,0	8,4	1918,2	8,4	2039,9		
420	8,5	2190,2	8,5	1940,9	8,5	2071,3		
430	8,6	2224,3	8,6	1964,1	8,6	2103,5		